Systems-Level Analysis of Rootstock–Scion Interactions in Apple Reveals Mechanisms of Cold Tolerance Under Field Frost Events

Amolpreet Kaur Saini

Dissertation submitted to the faculty of the Virginia Polytechnic Institute and State University in partial fulfilment of the requirements for the degree of

Doctor of Philosophy

In

Horticulture

Sherif M. Sherif, Chair

Srdjan G. Acimovic

R. Clay Wright

Timothy S. Artlip

July 18, 2025

Winchester, VA

Keywords: *Malus* × *domestica*, spring frost, transcriptome, metabolome, soluble sugars, rootstock, apple, grafting

Systems-Level Analysis of Rootstock–Scion Interactions in Apple Reveals Mechanisms of Cold Tolerance Under Field Frost Events

Amolpreet Kaur Saini

ACADEMIC ABSTRACT

Late spring frosts threaten apple (*Malus* × *domestica* Borkh.) productivity by damaging developing floral buds, yet the mechanisms underlying rootstock-dependent cold tolerance in orchard conditions remain poorly understood. In this study, we investigated frost tolerance in two apple (Malus domestica Borkh.) cultivars, 'Fuji' and 'Gala', grafted onto ten different rootstocks over the springs of 2021–2023, to elucidate cold-responsive genes and regulatory mechanisms. Trees on the 'B.9' rootstock exhibited superior frost tolerance, with lower floral bud mortality compared to the sensitive 'M.26' rootstock. To uncover the mechanisms underlying this tolerance, we integrated RNA sequencing, untargeted metabolomics, and soluble sugar profiling across floral buds ('Gala'), scion leaves ('Gala'), and rootstock sucker leaves (B.9, M.26), sampled 12 hours before and 6 hours after a naturally occurring frost in April 2021. Transcriptomic analysis identified cold-responsive gene networks involving transcription factors (MdCBF4, MdHSFC1), ABA signaling, ROS detoxification, and membrane remodeling. Co-expression network analysis revealed frost-associated hub genes and regulatory modules.

Carbohydrate profiling showed that B.9 maintained more stable soluble sugars—such as sucrose, glucose, and sorbitol—during frost-sensitive stages, suggesting improved osmoprotection and energy balance. Metabolomic profiling revealed tissue-specific shifts in B.9, including increased ascorbate metabolism, arginine biosynthesis, and protective sugars like trehalose and melibiose. Lipid remodeling and signaling metabolites, such as colnelenic acid and LysoPA, were also enriched, pointing to dynamic membrane adaptation. Interestingly, despite exhibiting higher levels of reactive oxygen species (ROS), particularly superoxide and hydrogen peroxide, B.9 appeared to sustain redox homeostasis through coordinated antioxidant pathways, suggesting that ROS may function as protective signals rather than causing damage. In contrast, M.26 displayed higher bud mortality, weaker activation of cold-responsive genes, and metabolite profiles consistent with stress susceptibility, including elevated glutathione metabolism.

Together, these results provide the first systems-level insight into tissue-specific natural frost responses in apple under orchard conditions. By identifying key candidate genes, metabolites, and regulatory pathways associated with frost resilience, this work lays the groundwork for future efforts in rootstock improvement and molecular breeding. These findings offer promising targets for developing cold-tolerant apple germplasm and improving orchard management, while more broadly providing a framework to understand how rootstock–scion interactions modulate complex abiotic stress responses.

Systems-Level Analysis of Rootstock–Scion Interactions in Apple Reveals Mechanisms of Cold Tolerance Under Field Frost Events

Amolpreet Kaur Saini

GENERAL AUDIENCE ABSTRACT

Spring frost events often damage apple flower buds and reduce fruit harvests, especially as changing climates cause unpredictable cold snaps. My research studied how different apple tree roots (called rootstocks) help trees survive natural frost events in Virginia orchards. We worked with two apple varieties, 'Gala' and 'Fuji', grafted onto two rootstocks: Budagovsky 9 (B.9), which our three-year study showed to be frost-tolerant, and Malling 26 (M.26), which showed higher flower damage and frost susceptibility. By analyzing thousands of genes and hundreds of natural chemicals (metabolites) in flower buds, leaves, and stems, we found that trees on the tolerant B.9 rootstock seemed to prepare themselves better for frost. They had higher levels of protective sugars, antioxidants, and stress-response signals. Interestingly, the tolerant trees also had more reactive oxygen species (ROS)—molecules that can cause damage—but our data suggest that they might have balanced these with strong antioxidant defenses, using ROS as a protective signal rather than letting them cause harm. In contrast, the susceptible M.26 trees may have failed to activate these protective responses efficiently, possibly explaining their greater frost injury—but this is something future studies will need to confirm. Overall, our work suggests that the roots of apple trees play a much bigger role in frost survival than we once thought. By helping trees manage their sugars, stress chemicals, and protective genes, the right rootstocks may help farmers reduce frost damage and keep their orchards productive, even in a changing climate.

DEDICATION

To my parents, for their unwavering support and belief in me, your little Molu loves you.

Acknowledgement

As I sit down to write this, I’m overwhelmed with a mix of gratitude, happiness, and a touch of disbelief that this moment has finally arrived after 4 years. A Ph.D. is often described as a solo journey, but in truth, it’s anything but. It genuinely takes a village to complete a Ph.D. — no cap (though ironically, there are many caps). It’s a beautifully chaotic team effort — full of very late nights, existential spirals, good coffee (and very bad coffee), unexpected breakthroughs, and, most importantly, the people who walk alongside you through it all. This section is for them.

First and foremost, my deepest thanks (no amount of Thank yous will ever be enough but here I try) go to my advisor, Dr. Sherif M. Sherif. You are more than a mentor — you are an OG teacher! You taught me not just what a gene *is*, but how to think like a scientist. Your patience never wavered, even when I needed things explained… more than once, maybe a bunch of times. You sat with me, guided me step by step — from how to pipette RNA to full molecular workflows — and made time for me when I know your schedule barely allowed it. You never gave up on me, and I’ll never forget that. You were the best advisor I could have asked for — equal parts brilliant, somehow able to sense exactly when my brain was on the verge of going blank and saying “take it easy” at just the right moments, usually when I was trying to juggle six things and doing none of them perfectly.

To Dr. Srdjan Acimovic, thank you for being a constant source of thoughtful guidance. You read through my thesis drafts with a level of detail that still amazes me, and your feedback made me better every time. You and Dana made me feel welcome from day one, and our lunchroom conversations are memories I’ll carry with me. Thank you for always being there, for making space for me in your lab and in your time, and for always standing by my side. To Dr. Clay Wright, thank you for your encouragement and for helping shape the direction of my work with such care. I will never forget the days of us dealing with transcriptome for the first time, how you were so patient and calm trying to troubleshoot everything! To Dr. Timothy Artlip — thank you for your understanding, even when I kept sending you Google links that absolutely refused to work in your office. I genuinely hope I get the chance to work with you again in the future — there’s still so much I want to learn from you.

To my amazing Post Docs— Dr. Khalil Jahed and Dr. Mohammad Zarrabian— you were never just lab mates, you were family first. The sarcasm, the dark humor, the unfiltered honesty — I didn’t realize how much I would miss all of it until I was wrapping up my stuff from my desk alone. You made even the most stressful days feel lighter, and our inside jokes somehow made 30 plates of gene expression sound entertaining. Thank you for teaching me everything so patiently! Tipu, Gerald, Kenny, Katie, Naina, Jay, Tabibul, and Protiva, we could talk about anything — experiments gone wrong, life drama, completely random nonsense apart from sense and antisense strands — and it always felt safe, funny, and real. Nate, Andy, Andrew, and Debbie — I’ve been watching and learning from you since day one. I’ll never forget your kindness, and how much you shaped the environment around me. I really do hope we stay in touch, no matter how hectic life gets.

To my friends and family — thank you for being my foundation. My grandparents' prayers have kept me safe and sound. To my niece, Vani: I didn't realize how deeply someone could matter until the day you arrived. I wish I could watch you grow up in front of my eyes, but the price we pay…..To my baby nephews, Aadvik and Hunar, and to all my cousins — thank you for keeping my life joyful even when my brain was buried deep in data. To my mom and dad, my brother and sister-in-law: thank you for your endless love, praying for me every time I used to call and say, "I am so scared please ardaas kreyo", and belief in me from across the miles. And to my dearest friends — Raavi, Diksha, Neha, Rajdeep— you were my therapy, my haven, my people.

And most importantly, to my lifeline — my fiancé, Ajay. "cliché enough?" hehe!! from the moment you entered my life, everything shifted for the better. This degree may have my name on it, but your love made it possible. Thank you for being my home, you are my favourite rootstock!

Your Truly

Amol

Table of Contents

Chapter 1: Introduction

The cultivated apple (*Malus* × *domestica* Borkh), a member of the Rosaceae family and Maloideae sub-family, is among the most significant fruit crops globally, both economically and culturally. Its origins trace back to Central Asia, where it was domesticated from the wild species *Malus sieversii*, native to the Tian Shan mountains. From there, apples spread westward along ancient trade routes such as the Silk Road, undergoing extensive hybridization with other wild species, particularly *Malus sylvestris*, the European wild apple. This long and complex process of natural and human-mediated hybridization, selection, and propagation gave rise to the rich genetic diversity seen in modern cultivars (Cornille et al., 2014). Today, the apple ranks as the third most widely produced fruit worldwide (Fruit: World production by type 2023) and stands 17th among all agricultural commodities in terms of economic value (Volk et al., 2015; Aoun, 2024), illustrating its global importance not only as a dietary staple but also as a driver of agricultural economies. However, despite its global significance, apple production is highly susceptible to environmental challenges. For instance, in the 2022/2023 growing season, global apple production declined by approximately 4.3 million metric tons, falling to 78.4 million metric tons due to severe weather-induced losses (USDA, 2023), emphasizing the crop's vulnerability to climatic variability. In the United States, apples are a cornerstone of fruit production, with the state of Virginia consistently ranking sixth nationally in terms of yield. Virginia's favorable temperate climate and fertile soils support an average annual harvest of 5 to 6 million bushels. The region is home to a broad range of commercially grown cultivars including Red Delicious, Golden Delicious, Rome, Stayman, Gala, Winesap, York, Granny Smith, Jonathan, Fuji, and Ginger Gold, all of which are valued for their unique flavors, storage qualities, and market appeal (Virginia Apples, 2025).

Globally, the commercial apple market is dominated by a relatively small group of cultivars, each selected for their distinctive taste, texture, and ability to withstand post-harvest storage and transport. These include popular varieties such as 'Delicious', 'Granny Smith', 'Fuji', 'Gala', 'Honeycrisp' (also marketed in Europe as 'Honeycrunch'®), and 'Cripps Pink' (marketed as 'Pink Lady'®), which collectively shape consumer preferences and influence orchard management decisions across major production regions (Sapkota et al., 2021). Beyond their agronomic and commercial value, apples are also widely celebrated for their nutritional and health-promoting properties. The fruit is an abundant source of bioactive compounds including phytochemicals, dietary fiber, vitamins, and essential minerals, many of which are concentrated in the peel but also present in the flesh. These compounds contribute to a variety of physiological benefits and have attracted significant attention in nutritional and biomedical research (Francini et al., 2013). Epidemiological and experimental studies have reinforced apples' potential role in disease prevention. For instance, Gallus et al. (2005) demonstrated that individuals who consumed two apples per day exhibited a reduced risk of cancer, suggesting a protective effect linked to apple-derived phytochemicals. In support of this, Gosse et al. (2005) conducted a controlled animal study in which rats received apple extract mixed into drinking water over a six-week period. This intervention, which delivered approximately 6 mg/kg body weight of procyanidins (PCs), resulted in a notable reduction in neoplastic lesions. The authors extrapolated these findings to humans, proposing that a daily intake of two apples could provide an estimated 4–10 mg/kg body weight of PCs—an amount potentially sufficient to confer similar anticancer benefits (Gosse et al., 2005; Mierczak et al., 2024). Taken together, these findings underscore not only the apple's historical and cultural significance but also its continued relevance as a staple of global agriculture and a functional food with compelling health implications.

Apple production is frequently challenged by a wide range of biotic and abiotic stresses, among which drought, high salinity, and cold stress are recognized as the predominant abiotic factors affecting orchards worldwide (Lee et al., 2023; Li et al., 2019). The increasing incidence of extreme weather events, largely attributed to global climate change, poses an escalating threat to sustainable apple cultivation across major growing regions. Among the abiotic stressors, rising global temperatures and elevated atmospheric CO_2 concentrations are projected to adversely affect apple phenology and yield potential, as indicated by multiple modeling and field-based studies (Augspurger, 2013). Climatic irregularities, particularly periods of unseasonably warm temperatures occurring during late winter and early spring, are becoming more frequent (Pfleiderer et al., 2019), further compounding the complexity of maintaining optimal flowering and fruit set in temperate-adapted fruit trees such as apples. One of the major physiological consequences of these warm winters is the incomplete fulfillment of chilling requirements—an essential process for the timely and synchronized breaking of dormancy. Failure to meet these chilling thresholds not only delays or disrupts flowering but can also negatively influence fruit set and final yield. Moreover, an increasingly observed phenomenon across both hemispheres is the advancement of bud phenology, particularly the timing of full bloom, as a result of warmer winter and spring conditions. This phenological shift has been well documented in apple cultivars growing in the Southern Hemisphere (e.g., South Africa and South America) (Darbyshire et al., 2013, 2014; Grab & Craparo, 2011), as well as in the Northern Hemisphere, including diverse regions such as Asia, North Africa, Europe, and Eastern North America (Augspurger, 2013; Ellwood et al., 2013; Fujisawa & Kobayashi, 2010; Hoffmann & Rath, 2013; Kaya, 2020; Vitasse et al., 2018; Wolfe et al., 2018). The cumulative impact of recent climatic changes, particularly warming trends during winter and spring, threatens the physiological synchronization required for successful flowering and fruit development in perennial species such as apple. Seasonal bud dormancy is a critical adaptive response in perennial plants, enabling survival during adverse winter conditions. This complex physiological process involves two distinct phases: endodormancy, controlled by internal factors, and ecodormancy, influenced by environmental cues, primarily temperature. Endodormancy requires the accumulation of chilling units for release, while ecodormancy progresses with increasing temperatures (Jahed and Sherif, 2025). The changing climatic trends can disrupt essential phenological stages, including the timing and progression of endodormancy controlled by internal factors and requires the accumulation of chilling units for release, the rate of chilling accumulation, and the precision of budburst and bloom onset. Consequently, such disruptions elevate the risk of spring frost damage, ultimately leading to significant reductions in yield and fruit quality (Augspurger, 2013; Ma et al., 2019; Fadón et al., 2020).

Spring frost has emerged as a significant limiting factor in apple production and is increasingly recognized as a major economic threat to the tree fruit industry worldwide (Rodrigo, 2000; Hoffmann & Rath, 2013; Zhu et al., 2021). Frost damage in spring typically occurs in two forms—advective and radiative frost—based on the meteorological conditions under which freezing temperatures occur (Liu & Sherif, 2019). Advective frost is more severe and results from the influx of cold, dry air masses, often accompanied by strong winds, whereas radiative frost, which is more common, occurs on calm, clear nights when thermal energy from the soil radiates into the atmosphere, resulting in surface temperatures that drop below freezing due to temperature inversion. Importantly, the damage mechanisms of both frost types converge at the cellular level: the formation of extracellular ice leads to dehydration and eventual rupture of cell membranes, particularly when dehydration exceeds cellular tolerance (Pearce, 2001). The extent of freeze damage is influenced by species, genotype, developmental stage, pre-frost environmental conditions, dewpoint, and duration of exposure (Centinari et al., 2016). In apples, one of the most vulnerable periods is during floral development. As climate change accelerates the onset of spring phenology, apple buds are increasingly exposed to frost events during critical stages like ecodormancy release, tight cluster, and bloom (Augspurger, 2013; Ma et al., 2019). The sensitivity of reproductive organs increases as flowers progress toward full bloom (Rodrigo, 2000; Salazar-Gutiérrez et al., 2016). Economic implications are substantial: a single 2017 frost event in Europe caused $3.3 billion in losses to fruit and wine grape industries (Lamichhane, 2021), and in 2012, spring frost in the eastern U.S. destroyed half of the apple crop, resulting in millions of dollars in damage (Wolfe et al., 2018). Although "frost" and "freeze" damage are often used interchangeably, frost damage refers to injuries from dewpoints below 0°C, while freeze damage is strictly temperature-based (Perry, 1998). Regardless of terminology, flowering is the most frost-sensitive stage in most tree crops (Centinari et al., 2016). Critical temperatures for 90% floral bud damage vary widely—from -17.6°C in silver-tip stage to as high as -3°C post-bloom (Snyder et al., 2005) in apple. Observations from our multi-year experiments reflect this sensitivity. In 2023, a 1.5-hour frost event caused 87% floral bud mortality in 'Gala' cultivar in the tight cluster stage. Interestingly, a longer 2.5-hour frost in 2022 caused only 15–35% floral bud damage, as it coincided with earlier floral stages, with 'Gala' at tight cluster and 'Honeycrisp' at half-inch green and tight cluster stages which are more tolerant (Sherif, 2022). These findings reinforce that both the intensity and timing of frost events determine the extent of injury. As global temperatures continue to rise, phenological shifts such as shortened dormancy and earlier budburst will further elevate the frequency and severity of spring frost damage in apples, making this a pressing concern for sustainable fruit production (Augspurger, 2013; Fadón et al., 2020).

Frost protection strategies for plants are broadly classified into passive and active methods. Passive methods are preventive in nature, implemented prior to the onset of frost events to enhance long-term resilience (Liu & Sherif, 2019). These approaches are generally more cost-effective compared to active methods and are aimed at reducing vulnerability over extended periods. Examples include strategic site selection, the use of growth regulators and cryoprotectant compounds to enhance plant cold tolerance, and the cultivation of cold-hardy or late-blooming cultivars that are less susceptible to frost injury. In contrast, active frost protection methods are employed during or immediately before a frost event and are designed to prevent ambient temperatures from falling below freezing. These methods encompass a range of interventions, including heaters (e.g., solid fuel or propane-powered), wind machines, helicopters, and various irrigation systems such as over-tree and under-tree sprinklers. The effectiveness of both passive and active methods is significantly influenced by environmental conditions, including wind speed, humidity, and the severity and duration of the frost event (Unterberger et al., 2018). For instance, wind machines are particularly effective in combating radiative frost but are largely ineffective against advective frost, which is driven by strong cold air masses. Furthermore, active methods often entail substantial operational costs, including the purchase, maintenance, and energy requirements of equipment. Heaters, though efficient, require consistent fuel input and upkeep, while helicopter use can incur especially high operating expenses. Additionally, certain methods may not be feasible in all agricultural settings due to practical limitations, such as water scarcity hindering the use of irrigation or sprinkler systems. These challenges underscore the importance of evaluating not only economic viability but also environmental sustainability, particularly regarding water and energy consumption. A thorough understanding of the strengths and constraints associated with each method is crucial for developing context-specific frost protection strategies tailored to the needs and limitations of individual agricultural systems.

The plant stress response is a complex and dynamic physiological process that aims to restore cellular homeostasis under adverse environmental conditions (Lamers et al., 2020). Horticultural crops, including apples, are often cultivated under suboptimal conditions due to limited arable land, exposing them to a variety of abiotic stresses such as drought, temperature extremes, flooding, salinity, and nutrient deficiencies (Manzoor et al., 2023; Benavides-Mendoza et al., 2024). These stressors are becoming increasingly severe and unpredictable in the face of climate change, particularly with respect to fluctuations in water availability and temperature (Rosińska et al., 2024; NOAA, 2024). To survive and adapt to such challenges, plants engage a diverse array of stress-responsive mechanisms. These include the regulation of hormone signaling pathways, activation of protein kinases, gene expression modulation, reactive oxygen species (ROS) scavenging, osmolyte accumulation, modification of cellular structure, ion channel activation, as well as shifts in carbohydrate and energy metabolism, nitrogen assimilation, and fatty acid biosynthesis (Zhang et al., 2023; Jing et al., 2024). Plant tolerance is influenced not only by stress acclimation mechanisms but also by their capacity for recovery following the removal of stressors (Charng et al., 2022; Yeung et al., 2018). In this context, the utilization of genetically diverse rootstock genotypes for temperate fruit crops offers a sustainable strategy to enhance tolerance against abiotic stress while also supporting food security by improving yield potential, closing the yield gap under stress-prone environments, and optimizing water and nutrient use efficiency (Saini et al., 2020; Razi et al., 2024; Ferreira et al., 2024; Saini et al., 2025).

One of the most effective and ancient tools in this regard is grafting, a practice that dates back to 1800 BCE and marked a 'second wave' of woody perennial domestication, leading to the widespread cultivation of Rosaceae fruits such as apple, pear, plum, and cherry (Warschefsky et al., 2016). Grafting involves inosculation, the physical and physiological union between a genetically distinct scion and rootstock, made possible through the abrasion of their cambial layers and subsequent vascular integration (Feng et al., 2024). This method provides a suite of horticultural advantages including canopy structure modification, repair of damaged trunks, promotion of early fruiting, and the enhancement of tree vigor or dwarfing traits conducive to high-density orchard systems (Baron et al., 2019; Rasool et al., 2020; Albacete et al., 2015). In simpler terms, grafting process is natural or artificial fusion of plant tissues, by aligning the vascular systems of woody plant stems. It occurs when the cambium layers of two stems, branches, or roots come into contact, allowing them to grow together and share water and nutrient flow. Critically, rootstocks with strong ecological adaptability can confer increased resilience to external stressors. Such stress tolerance is often attributed to long-distance signal transduction between the rootstock and scion, including hydraulic and biochemical signaling via the phloem (Li et al., 2022). These signals can regulate growth, development, and stress resistance in distal tissues, ultimately modifying the scion phenotype. Rootstocks have been shown to influence traits such as stomatal conductance, intercellular CO_2 concentration, water and nutrient uptake efficiency, hormone synthesis, and root pressure, thereby enhancing scion vigor and productivity under challenging environmental conditions (Prinsi et al., 2021; Labarga et al., 2023; Opazo et al., 2020; Xu & Ediger, 2021; Gautier et al., 2019). This capacity to modulate the performance of commercial scion varieties through strategic rootstock selection represents a powerful tool for adapting fruit crops like apple to the stresses imposed by a changing climate.

Building upon the concept of grafting and rootstock-scion communication, it is now well recognized that rootstocks influence not only the structural and nutritional dynamics of a grafted plant but also significantly modulate the physiological and molecular responses of the scion under stress. Through the integration of hydraulic and molecular signals, rootstocks can regulate scion water potential, stomatal conductance, and hydraulic conductance, thereby enhancing resistance to abiotic stress conditions such as drought, salinity, and cold (Jaimez et al., 2023; Labarga et al., 2023). Grafting is thus widely employed in horticulture to confer desirable traits to elite scion cultivars, including enhanced nutrient and water uptake, resistance to soilborne and other diseases and pests, improved anchorage, regulated plant size, and increased yield (Gregory et al., 2013; Kumar et al., 2024). The combination of genetically distinct rootstock and scion genotypes within a single composite plant creates a unique biological model that enables the rapid induction of advantageous physiological traits—often mimicking genetic modifications. These effects are thought to be mediated by diverse signaling agents, including hormones, RNAs, proteins, and metabolites, that travel across the graft union. Indeed, recent studies have highlighted the movement of RNA molecules, gene expression reprogramming, and protein activity changes as central mechanisms underlying scion modulation (Takahashi et al., 2020; Hernández-Elvira et al., 2022; Kumar et al., 2025). These interactions can activate post-transcriptional gene regulation networks, allowing the scion to implement targeted responses against environmental stressors (Furnas & Strader, 2022; Khan, 2025). Additionally, hormonal crosstalk between rootstock and scion plays a vital role in stress adaptation, with studies in herbaceous systems emphasizing both the physical and biochemical nature of rootstock-scion communication (Martinez-Ballesta et al., 2010; Mauro et al., 2022; Aloni et al., 2010). Among various abiotic stressors, cold stress has particularly detrimental effects on plant metabolism, inducing oxidative stress, osmotic imbalance, membrane damage, and impaired cellular function due to the accumulation of toxic compounds (Shi et al., 2018; Wu et al., 2022). The plant's capacity to acclimate to cold is closely tied to rootstock-regulated processes such as gene expression, cryoprotectant biosynthesis, changes in membrane lipid composition, and hormonal adjustments (Hayat et al., 2021; Zhou et al., 2021). Notably, several studies have demonstrated that the genotype of the rootstock can influence flowering time and phenological traits, which are critical for avoiding spring frost. For instance, when ‘Rootpac 20’ was used instead of ‘Garnem’ in almond, bloom was delayed by several days in the late-flowering cultivar 'Marinade', offering protection from frost events (Vargas et al., 2008, 2011; Lordan et al., 2019). Similar rootstock-induced bloom delays have been observed in apples (Lordan et al., 2017).

Hormonal regulation plays a central role in cold tolerance. Brassinosteroids (BRs) have been shown to promote cold resistance by activating COLD-RESPONSIVE (COR) genes (Ramirez & Poppenberger, 2020; He et al., 2024), while salicylic acid (SA) can enhance chilling tolerance by regulating ROS levels, reducing ion leakage, and mitigating oxidative stress (Sendon et al., 2011; Dong et al., 2014; Shin et al., 2018; Fu et al., 2021). In grafted watermelon, antioxidant enzyme activities such as catalase (CAT) and glutathione peroxidase (GPX) were significantly elevated in cold-stressed scions grafted onto tolerant rootstocks (Lu et al., 2021). Likewise, the cold response in kiwifruit was associated with the activation of phosphatidylinositol signaling, inositol phosphate metabolism, and hormone-related pathways (Sun et al., 2021a). Specific transcription factors such as PtrWRKY2, which is cold-induced in the cold-hardy rootstock *Poncirus trifoliata* but repressed in the cold-sensitive Citrus species *pummelo*, further illustrate how transcriptional responses differ between rootstock genotypes and scion backgrounds (Banerjee & Choudhury, 2015). In citrus, the tolerant rootstock *Carrizo citrange* enhanced ABA accumulation and transport to the scion during cold stress, maintaining stable ABA concentrations in the leaves of 'Valencia' seedless orange, in contrast to the sensitive *C. macrophylla* which failed to upregulate ABA pathways (Primo-Capella et al., 2021, 2022). Furthermore, graft combinations in Japanese apricot demonstrated that the cold-sensitive rootstock *P. armeniaca* negatively influenced scion morphology, reducing shoot length, leaf area, and biomass, compared to the more resilient *P. mume* rootstock (Hayat et al., 2021). These findings collectively underscore that cold tolerance is not solely a function of the scion genotype, but is strongly influenced by the physiological, hormonal, and molecular contributions of the rootstock. Increasingly, evidence also points to rootstocks modulating scion responses at deeper biological levels, including the regulation of carbohydrate metabolism, transcriptional activity, and metabolite accumulation—processes that play a pivotal role in shaping the scion's resilience to cold and other abiotic stresses.

1.1 Molecular Responses to Abiotic Stress: The Role of Rootstock-Induced Gene Expression

Rootstock–scion relationships are governed by complex transcriptional regulation, influencing numerous traits related to growth, physiology, and stress resilience (Gregory et al., 2013). Dwarfing and invigorating rootstocks modulate gene expression in the scion, thereby affecting hormone biosynthesis, signal transduction, and stress responses (Aloni et al., 2010; Tworkoski & Fazio, 2016). This dynamic "molecular dialogue" can vary markedly, even within a single species like *Malus pumila*, and is shaped by both the rootstock's genetic background and prevailing environmental conditions, including cold stress. A foundational example in an herbaceous system was provided by Ntatsi et al. (2017), who showed that tomato scions grafted onto the cold-tolerant *Solanum habrochaites* rootstock upregulated genes linked to cellulose biosynthesis under low root-zone temperatures, contrasting with the transcriptomic profile of the cold-sensitive 'Moneymaker' rootstock. Among orchard crops, recent work by Kaur et al. (2023) in pecan (*Carya illinoensis*) found that rootstock–scion combinations differ in freeze tolerance through transcriptionally guided carbohydrate reallocation, as evidenced by reduced post-cold sugar accumulation in tolerant ('Maramec'/'Colby') vs. susceptible ('Kanza'/'Giles') combination. In *Prunus*, Klumb et al. (2019) demonstrated that the flood-tolerant 'Marianna 2624' rootstock invoked faster and more efficient transcriptional activation of anaerobic metabolism genes (*ADH1*, *PDC*, and *LDH1*) under flooding stress, while Yu et al. (2020) linked *early light-induced protein 1* and *glutamate dehydrogenase 2* expression patterns to cold acclimation and deacclimation in peach (*P. persica*). Focusing on rootstock-induced dwarf phenotypes, Zhou and Underhill (2021) showed that marang (*Artocarpus odoratissimus*) suppressed breadfruit scion growth by downregulating genes involved in sucrose metabolism and cell expansion. Several studies in grapevine emphasize a similarly intricate interplay: Harris et al. (2023) found scion transcriptional responses to be tissue- and year-specific, Zombardo et al. (2020) identified enhanced phenylpropanoid pathway gene expression (including *MYB14*) in berry skins grafted onto '1103 Paulsen,' and Corso et al. (2016) reported rootstock-driven modulation of auxin-related genes (*ARF*, *Aux/IAA*) affecting ripening. For cold tolerance in wild vs. cultivated grape, Gu et al. (2020) observed that *Vitis amurensis* ('Shuangyou') mounted an early, robust transcriptional response (>3,000 DEGs) including peroxiredoxin-mediated ROS scavenging, whereas the cold-sensitive 'Red Globe' lagged behind. In citrus, Liu et al. (2017) linked dwarfing rootstocks to auxin and gibberellin signaling gene expression changes, while Huang et al. (2011) identified altered *GH3*, nitrate transporter, and UDP-glycosyltransferase expression in cold-acclimated Satsuma mandarins grafted onto *Poncirus trifoliata*.

Moreover, Mahmoud et al. (2024) demonstrated that overexpression of *VvmybA1* in citrus enhanced anthocyanin-based ROS scavenging and ABA biosynthesis, reinforcing the role of transcriptionally driven secondary metabolism in cold acclimation. Shifting to *Malus sieversii*, Zhou et al. (2021) found over 24,000 DEGs tied to hormone signaling, carbohydrate metabolism, and antioxidative defense during freezing, while in apple scions, Saini et al. (2025) showed that the dwarfing rootstock 'B.9' enhanced frost tolerance by modulating key genes like *MdCBF4*, *MdAFP*, *MdHSFC1*, and *MdEXP8*. Wang et al. (2019) similarly identified 226 differentially expressed transcription factors across 32 families in the cold-resistant apple rootstock ‘71-3-150.’ Finally, in pear (*Pyrus betulifolia*), transcriptome analyses by Wang et al. (2025) under cold and drought revealed thousands of DEGs, with a core of 389 overlapping genes for hormone signaling and secondary metabolism, suggesting molecular cross-talk that underpins multiple abiotic stress tolerances. Among the molecular components implicated in rootstock-induced stress tolerance are protease inhibitors and antioxidant defenses, as demonstrated in apple by Tan et al. (2017). Overexpression of the *MpCYS4* gene (*Malus prunifolia*) in the ‘M26’ rootstock delayed leaf senescence and upregulated antioxidant enzymes (APX, CAT, POD), effectively maintaining ROS homeostasis under stress. In a complementary approach, Li et al. (2019) performed transcriptome profiling on in vitro-grown apple (*Malus* × *domestica*) plants exposed to drought, cold, and salinity, identifying 588 common differentially expressed genes (DEGs) across all stress conditions. Many of these DEGs regulated transcription factors such as *DREB6* and *CBF1*, suggesting a shared regulatory network for abiotic stress tolerance. Beyond conventional gene expression, the movement of small RNAs (miRNAs) across the graft union is increasingly recognized as a key mechanism of inter-partner communication. In grafted avocado, Ahsan et al. (2019) found that *miR156* and *miR172* levels were linked to scion maturity, with scion identity largely dictating the molecular “age” of the grafted plant. Similarly, in sweet cherry, Zhao et al. (2020) detected the transfer of endogenous small RNAs, including miRNAs, from scion to rootstock, indicating that mobile RNA signals can influence gene expression in distant tissues. This phenomenon also extends to mRNA mobility, as shown by Duan et al. (2015), who discovered that *PbWoxT1* transcripts in pear (*Pyrus betulaefolia*) are transported from rootstock to scion via the polypyrimidine tract binding protein *PbPTB3*. Such protein-facilitated phloem transport underscores the complexity of non-cell-autonomous gene regulation in woody plants. Furthermore, Sharma and Zheng (2019) emphasized the role of protein trafficking, demonstrating that the cyclophilin protein *SlCyp1*—essential for shoot-to-root ratio maintenance—moves from scion to rootstock in the phloem and is stimulated by auxin, ultimately promoting root growth. Collectively, these findings illustrate how rootstocks orchestrate transcriptional networks in scions, driving key metabolic and signaling pathways that improve cold tolerance and other stress-related traits—thus offering fertile ground for targeted breeding and grafting strategies across diverse fruit species.

1.2 Carbohydrate Metabolism and Partitioning under Abiotic Stress: Influence of Rootstock–Scion Interactions

Carbohydrate metabolism stands out as a key physiological mechanism through which rootstocks can modulate cold tolerance, vigor, and overall performance in grafted fruit crops. In apple, Foster et al. (2017) demonstrated that dwarfing rootstocks such as M.9 and M.27 shifted sugar partitioning by elevating starch reserves while simultaneously lowering fructose and glucose levels, ultimately curbing growth yet potentially bolstering freeze resilience. Zhou et al. (2020a) observed that ‘Red Fuji’ apples on M.9 and B.9 rootstocks showed reduced photosynthetic capacity, hydraulic conductance, and sorbitol/glucose concentrations but accumulated more starch, hastening flowering and hinting at a trade-off between carbohydrate availability for vegetative growth versus reproductive development. In apple, Foster et al. (2017) demonstrated that dwarfing rootstocks such as M.9 and M.27 caused an imbalance in carbohydrate allocation. They exhibited elevated starch reserves, with concentrations in M.9 roots, stems, and scions doubling those of vigorous rootstocks, while fructose and glucose levels were simultaneously much lower in these tissues. These findings indicated a state of sugar depletion and reduced cellular activity in dwarfing rootstocks, ultimately contributing to reduced growth and earlier shoot termination. Samuolienė et al. (2016) further highlighted the nuanced interplay of carbohydrate and nutrient dynamics in 'Ligol' apples on super-dwarfing P 22, where intensive crop-load conditions led to increased leaf sugars but also induced nitrogen deficiency, underscoring the impact of rootstock genotype on both metabolic and nutritional equilibria. At the orchard scale, Baldassi et al. (2023) reported that 'Honeycrisp' apples grafted onto G.935 attained greater photosynthetic rates and electron use efficiency than those on G.41 or M.9-T337, along with higher fructose, glucose, and sorbitol concentrations—particularly under low crop-load scenarios. Yang et al. (2021) likewise found that 'Gala' trees on M.26 responded to varied crop loads by accumulating non-structural carbohydrates such as starch, driven by enhanced enzyme activities for sucrose and sorbitol synthesis, thus highlighting a rootstock-mediated capacity to adjust carbon partitioning in response to shifting sink demands.

Beyond apple, Jamshidi Goharrizi et al. (2021) in pistachio revealed that cold-tolerant genotypes like 'Badami' experienced not only reduced chlorophyll loss and oxidative damage but also heightened proline and soluble sugar accumulation, reinforcing the notion that carbohydrates and compatible solutes help stabilize cellular structures under chilling. In peach (*Prunus persica*), Muthuramalingam et al. (2022) tied stronger stress tolerance to decreased sucrose degradation, while additional work in *Malus domestica* linked dormancy-associated sugar buildup to enhanced cold hardiness (Xu et al., 2023a). Mechanistically, starch catabolism emerges as a widespread strategy for generating protective soluble sugars when temperatures drop. Wang et al. (2018) found that *Jatropha curcas* seedlings subjected to chilling stress markedly increased leaf soluble sugar content in tandem with starch depletion, paralleling observations in sugar maple (*Acer saccharum*), where twig wood showed a reduction in starch alongside rising sucrose, glucose, and fructose during early autumn (Wong et al., 2009). Poplar (*Populus* spp.) follows a similar pattern, utilizing starch as a primary reserve that is hydrolyzed into simpler sugars during dormancy, supporting cold acclimation (Regier et al., 2010). Across a range of deciduous fruit species, cold-induced sugar accumulation is a consistent hallmark of acclimation: peach (*Prunus persica*), blueberry (*Vaccinium corymbosum*), and red raspberry (*Rubus idaeus*) all exhibit notable sucrose accumulation under chilling (Palonen et al., 2000; Lee et al., 2013; Yu et al., 2017). In Rosaceae, sorbitol is of particular importance, with Jia et al. (2015) documenting its seasonal buildup in apple and Ito et al. (2013) noting similar patterns in pear, where sorbitol evidently contributes to both osmotic adjustment and cryoprotection. Haagenson et al. (2003) proposed that hardier genotypes initiate sugar buildup earlier and reach higher concentrations than do cold-susceptible varieties, a notion corroborated by multiple orchard-focused studies. For instance, Wisniewski et al. (2003) discovered that cold-hardy apple rootstocks contained greater sorbitol and sucrose concentrations in bark tissues during acclimation than sensitive lines, while Kalberer et al. (2006) found elevated raffinose and stachyose in hardy pear cultivars. Beyond simply boosting cold tolerance, carbohydrate dynamics can profoundly affect yield, fruit quality, and plant architecture, often interacting with horticultural practices such as crop-load management. Mesa et al. (2016) confirmed that in pear ('Abbé Fétel'), soluble sugar concentrations varied by rootstock (Sydo® vs. Quince C) and correlated with fruit weight and flesh firmness. Shahkoomahally et al. (2020) showed that peach scions on 'MP-29' not only displayed higher soluble solids but also accumulated more anthocyanins and phenolic compounds, emphasizing that rootstock choice can simultaneously modulate carbohydrate pools and secondary metabolite synthesis. Even so, carbohydrate storage capacity alone does not fully explain vigor differences among rootstocks: Plavcová et al. (2023) determined that while vigorous apple and pear trees accumulated greater absolute levels of non-structural carbohydrates (NSC) due to higher biomass, the relative seasonal fluctuations were comparable across dwarfing and vigorous types.

Under water-limited or freezing conditions, certain rootstocks promote more strategic carbohydrate partitioning to critical tissues. In sweet cherry, Toro et al. (2023) reported that drought-tolerant pairings, such as ‘Lapins/Colt’ and self-rooted ‘Colt,’ accumulated higher sucrose and sorbitol levels in both leaves and roots, translating to superior water use efficiency and biomass retention, whereas Morandi et al. (2019) found that semi-dwarfing Gisela™6 rootstocks maintained lower stem and fruit water potential but increased osmotic accumulation in fruits, enhancing yield efficiency and sweetness. In citrus, Forner-Giner et al. (2014) investigated dwarfing rootstocks (Forner-Alcaide 517, 418) and observed restricted ^13C-photoassimilate flow and diminished sugar/starch buildup below the graft union, offering a mechanistic explanation for reduced vigor. Contrastingly, more vigorous stocks often facilitate stronger carbohydrate fluxes to roots and stems, as Iglesias et al. (2019) found in nectarines, where Krimsk-1 and PS rootstocks boosted fructose, glucose, sucrose, and antioxidant activity in ‘Big Top’ fruits, even under high temperatures. Karabulut and Çelik (2022) reported comparable outcomes in grapevine, showing that the American rootstock SO4 enhanced carbohydrate distribution at the graft junction in *Vitis labrusca*, thereby improving graft compatibility and sapling vigor. Finally, Vittal et al. (2023) demonstrated how mango rootstocks shape both carbohydrate and nutrient concentrations in leaves and buds, with ‘Kurukkan’ increasing starch and protein contents and ‘Olour’ raising reducing sugars and micronutrient levels, thereby modifying stress resilience and floral induction potential. Taken as a whole, these findings confirm that rootstock–scion interactions profoundly influence carbohydrate management—whether through sugar allocation, starch breakdown, or interplay with hormonal and mineral pathways—ultimately impacting cold tolerance, growth, fruit quality, and orchard productivity across a wide range of perennial fruit species.

1.3 Metabolite Accumulation and Stress Signaling in Fruit Crops

Recent metabolomic investigations have illuminated the importance of rootstock–scion interactions in regulating cold tolerance, fruit quality, and graft compatibility across diverse horticultural crops. In peach (*Prunus persica*), Li et al. (2023a) found that the cold-hardy cultivar ‘Donghe No.1’ accumulated more saccharides, phenolic acids, and flavones—particularly via galactose and flavonoid biosynthetic pathways—than the cold-sensitive ‘21st Century’ under cold conditions, correlating with the upregulation of *COMT*, *CCR*, *CAD*, *PER*, and *F3’H*. Another metabolomic study by Brizzolara et al. (2020) in peach revealed that cultivars tolerant to chilling injury, such as ‘Red Haven,’ amassed osmoprotective compounds (sorbitol, maltitol, myo-inositol, sucrose, putrescine) plus amino acids and urea, resulting in fewer symptoms like browning and bleeding. Similarly, trifoliate orange (*Poncirus trifoliata*), a commonly used cold-hardy rootstock, relies on the ethylene-responsive factor *PtrERF108*, which directly regulates raffinose synthase (*PtrRafS*) to boost raffinose accumulation and mitigate cold stress. Overexpression of *PtrERF108* in lemon enhanced cold tolerance, whereas silencing it diminished raffinose content—an effect reversed by exogenous raffinose application (Khan et al., 2021). In Chinese jujube (*Ziziphus jujuba*), Zhou et al. (2020) identified more than 20,000 expressed genes in the cold-tolerant cultivar ‘Jinsixiaozao’, including numerous DEGs related to sucrose metabolism, calcium signaling, ROS detoxification, antifreeze proteins, and key transcription factor families (WRKY, AP2/ERF, NAC, bZIP), highlighting cultivar-specific metabolic responses to chilling and freezing. Kiwifruit (*Actinidia arguta*) genotypes also display contrasting freezing responses: the tolerant KL genotype upregulates flavonoid biosynthesis genes (*chalcone* *isomerase*, *anthocyanin acyltransferase*) to reinforce ROS scavenging, while both tolerant and sensitive lines accumulate lipid-derived metabolites (LPCs, LPEs, FFAs) potentially indicative of frost damage (Sun et al., 2023b). In peach fruit, Wang et al. (2017) demonstrated that low-temperature conditioning (LTC) stimulates a coordinated transcriptomic and metabolomic shift—elevating ethylene production, fatty acid desaturation, phospholipid synthesis, and glucosylceramide biosynthesis—thereby alleviating chilling injury through an ERF-regulated signaling network. Grape rootstocks exert similar metabolic influences on scions: Chitarra et al. (2021) reported that grafting ‘Gaglioppo’ onto specific stocks (e.g., 41B) boosted stilbene accumulation and defense gene expression while downregulating ABA metabolism, whereas Prodhomme et al. (2019) showed that the graft interface itself undergoes major metabolic remodeling, with elevated branched-chain amino acids, increased PAL and neutral invertase activities, and enhanced stilbene biosynthesis. Moreover, graft incompatibility in *Prunus* (cherry, almond, apricot) has been tied to abnormal accumulations of phenolics (catechins, proanthocyanidins) that leak from vacuoles, disrupt lignin biosynthesis, and weaken vascular tissues, underscoring the centrality of metabolic homeostasis for successful grafting (Gainza et al.). In pear, Hudina et al. (2014) traced the accumulation of phenolic compounds, particularly arbutin, procyanidin B1, and chlorogenic acid, in phloem tissues above and below the graft union, linking higher arbutin levels in combinations like ‘Williams’/Quince MA or Fox 11 to incompatibility. Similarly focusing on phenolics, Tříska et al. (2017) analyzed trans-resveratrol, trans-ε-viniferin, and r2-viniferin in grape canes from seven *Vitis vinifera* cultivars over three years. They found that varietal genetics outweighed environmental factors for stilbene accumulation, with ‘Hibernal’ consistently producing the highest levels, underscoring its potential for metabolite-driven breeding or rootstock selection.

In grafted apples, Lee et al. (2023) revealed that ‘Gala’ scions on the cold-hardy rootstock ‘G202’ accumulated higher levels of polyphenol metabolites (including chlorogenic acid, eriodictyol, and phloretin derivatives) and upregulated lignin- and flavonoid-related genes, in contrast to scions on the sensitive ‘M9’—suggesting upward movement of cold-associated mRNAs and metabolites enhances seasonal cold resilience. Grape studies also underscore metabolite shifts at the rootstock–scion interface: Tedesco et al. (2021) found that heterografted grapevines (vs. homografted) showed increased defense-related metabolites in rootstock tissues, especially distant from the graft union, with leaf samples proving most sensitive for detecting these metabolic changes. Beyond graft unions, cultivar-specific cold tolerance is often reflected in metabolite accumulation, as evidenced by Xu et al. (2022), who compared apple cultivars ‘Hanfu’ (HF, cold-tolerant) and ‘Changfuji No. 2’ (CF, cold-sensitive) under freezing. HF upregulated *galactinol synthase*, *raffinose synthase*, and *stachyose synthetase*, accumulating raffinose, stachyose, GABA, spermidine, and ascorbic acid—key in osmotic balance and ROS scavenging—whereas CF exhibited weaker metabolic responses. Similar mechanisms operate in non-woody species: Song et al. (2024) showed that cold stress in tobacco (4 °C) disrupted membrane integrity, photosynthesis, and chlorophyll stability, but induced 178 differentially expressed metabolites (e.g., sucrose, proline, glutamate, phenylalanine) and over 16,000 DEGs, boosting antioxidant and osmolyte defenses. In wild grape, *Vitis amurensis* likewise displayed superior cold acclimation relative to *V. vinifera* ‘Muscat of Hamburg’, accumulating galactinol, raffinose, putrescine, glycine, proline, and ascorbate in tandem with the upregulation of *BAMY*, *GolS*, and *RafS*, demonstrating its potential as a rootstock donor for freezing tolerance (Chai et al., 2019). Meanwhile, further apple research by Xu et al. (2023b) compared the cold-tolerant ‘Hanfu’ and cold-sensitive ‘Naganofuji 2’ to show how sugar and amino acid metabolism, plus hormone signaling, underpin freeze tolerance during distinct dormancy phases, with galactose pathways dominating in endodormancy and lipid metabolism emerging in ecodormancy. Moving to mango (*Mangifera indica*), Kong et al. (2023) reported that the cold-tolerant cultivar ‘Jinhuang’ accumulated higher levels of flavonoids, terpenoids, lignans, coumarins, and alkaloids under cold conditions, alongside upregulation of ICE-CBF-COR and MAPK-calcium-H_2O_2 pathways, illustrating a coordinated metabolite-hormone-transcript network in tropical perennials. Altogether, these findings reinforce that metabolomic reprogramming—spanning sugars, phenolics, amino acids, lipids, and other pivotal metabolites—constitutes a critical layer by which rootstocks and scions adapt to cold stress, enhance graft compatibility, and optimize horticultural performance.

Despite the widespread use of grafting in apple production, a comprehensive understanding of how genetically and geographically distinct rootstocks influence the molecular and physiological responses of different scion cultivars under natural frost stress remains limited. Our study addresses this critical gap by investigating the transcriptional and metabolomic reprogramming, along with soluble sugar dynamics, in two commercially important apple scions—‘Fuji’ and ‘Gala’—grafted onto two contrasting rootstocks: ‘B9’and ‘M26’. These rootstocks, originating from Russia and England, respectively, represent diverse genetic backgrounds and climatic adaptations, making them ideal candidates for evaluating rootstock-mediated cold resilience. To date, no study has performed a tissue-specific, paired transcriptomic and metabolomic analysis across floral buds, scion leaves, and sucker leaves of these combinations in response to a naturally occurring late spring frost event. By identifying key metabolites and differentially expressed genes associated with lower bud mortality of the rootstock ‘B.9’, our research will provide novel insights into the mechanisms of frost tolerance in apple. These findings hold practical implications for breeding and orchard management strategies aimed at mitigating climate change–induced abiotic stress in Virginia and other temperate fruit-growing regions worldwide.

Objectives of this study:

Chapter 2

To perform untargeted transcriptomic analysis of distinct rootstock–scion combinations in response to a naturally occurring spring frost, aiming to identify differentially expressed genes and key regulatory pathways involved in cold stress tolerance.

Chapter 3

To evaluate how rootstock choice influences frost tolerance in apple trees by examining shifts in soluble sugar accumulation across multiple tissues, including scion leaves, sucker leaves, and floral buds.

Chapter 4

To carry out untargeted metabolomic profiling of apple rootstock–scion combinations to investigate the role of specific metabolites associated with cold resilience and spring frost damage mitigation.

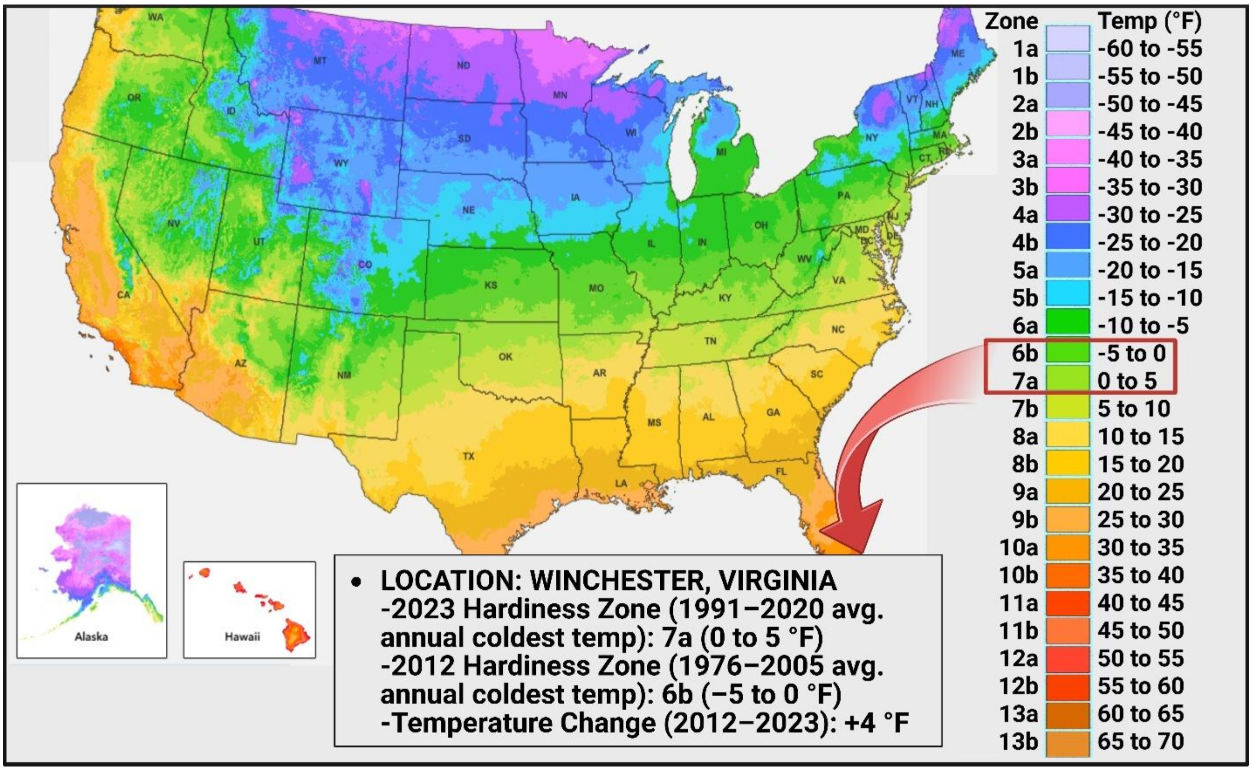

Figure 1: USDA Plant Hardiness Zone Map showing the shift in Winchester, Virginia from Zone 6b (-5 to 0 °F) to Zone 7a (0 to 5 °F) between 2012 and 2023. Source: U.S. Department of Agriculture (USDA). (Image From Saini et al., 2025 Extension article-submitted)

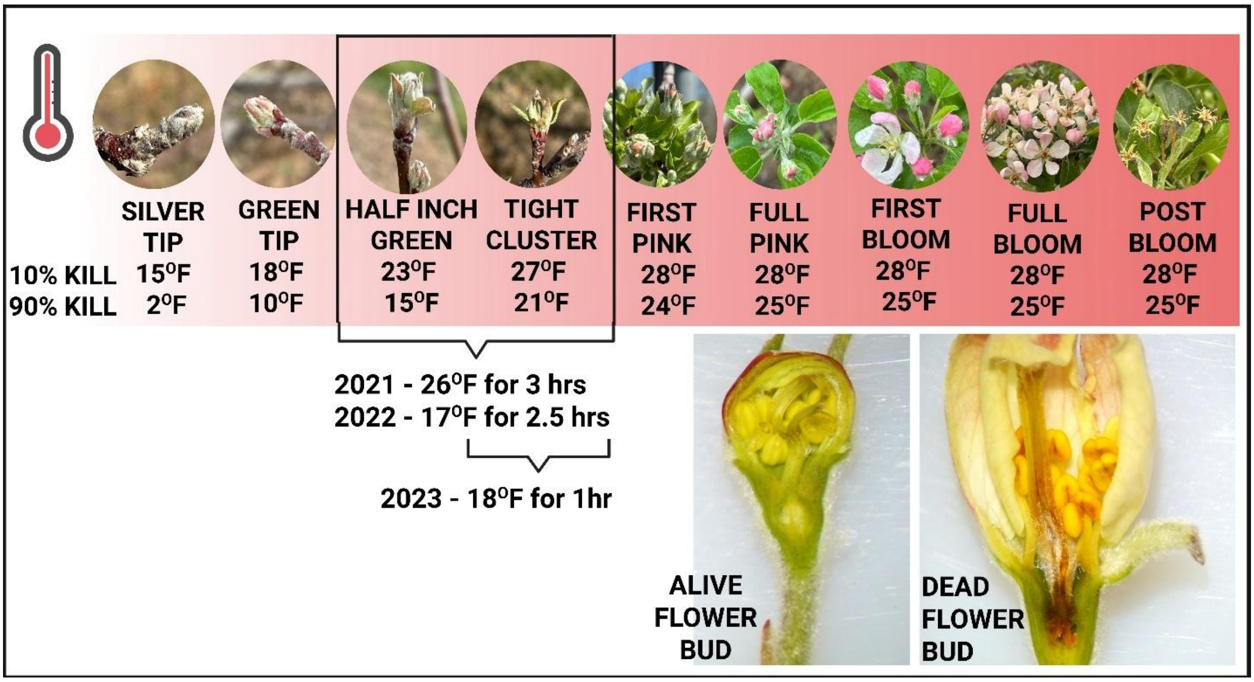

Figure 2: Critical spring temperatures for apple bud stages, with corresponding frost event conditions (temperature, duration, and stage) from 2021–2023 in our study. Cross-sections show live (left) and dead (right) flower buds. (Image From Saini et al., 2025 Extension article-submitted)

Output and Work in Progress

Peer-reviewed publications

Saini, A. K., Jahed, K. R., Neres, D. F., Wright, R. C., & Sherif, S. M. (2025). Investigating Frost Response, Rootstock-Dependent Cold Tolerance, and Floral Bud Mortality in Apple Cultivars through Transcriptomic Insights. *Plant Stress*, 100829. https://doi.org/10.1016/j.stress.2025.100829

Jahed, K. R., **Saini, A. K**., & Sherif, S. M. (2023). Coping with the cold: Unveiling cryoprotectants, molecular signaling pathways, and strategies for cold stress resilience. *Frontiers in Plant Science*, *14*. https://doi.org/10.3389/fpls.2023.1246093

Non-peer-reviewed extension publication

Saini, A. K., Jahed, K. R., & Sherif, S. M. (2025). Rootstock Effects on Flower Bud Mortality in 'Gala' and 'Fuji' Apples Under Natural Spring Frost Conditions (2021–2023). *Virginia Cooperative Extension*, Virginia Tech. https://www.pubs.ext.vt.edu/SPES/spes-713/spes-713.html

Manuscript in progress

Rootstock-Mediated Cold Resilience in Apple: Integrated Transcriptomic and Metabolomic Insights Under Natural Spring Frost

---

References

References

Ahsan, M. U., Hayward, A., Alam, M., Bandaralage, J. H., Topp, B., Beveridge, C. A., & Mitter, N. (2019). Scion control of miRNA abundance and tree maturity in grafted avocado. *BMC Plant Biology*, *19*(1), 382. https://doi.org/10.1186/s12870-019-1994-5

Albacete, A., Martínez-Andújar, C., Martínez-Pérez, A., Thompson, A. J., Dodd, I. C., & Pérez-Alfocea, F. (2015). Unravelling rootstock×scion interactions to improve food security. *Journal of Experimental Botany*, *66*(8), 2211–2226. https://doi.org/10.1093/jxb/erv027

Aloni, B., Cohen, R., Karni, L., Aktas, H., & Edelstein, M. (2010a). Hormonal signaling in rootstock–scion interactions. *Scientia Horticulturae*, *127*(2), 119–126. https://doi.org/10.1016/j.scienta.2010.09.003

Aoun, M. (2024). Unlocking heirloom diversity: A pathway to bridging global challenges in modern apple cultivation. *Frontiers in Horticulture*, *2*. https://doi.org/10.3389/fhort.2023.1268970

Augspurger, C. K. (2013). Reconstructing patterns of temperature, phenology, and frost damage over 124 years: Spring damage risk is increasing. *Ecology*, *94*(1), 41–50. https://doi.org/10.1890/12-0200.1

Baldassi, C., Berim, A., Roeder, S., Losciale, P., Serra, S., Gang, D. R., & Musacchi, S. (2023). Rootstock and Crop Load Effects on 'Honeycrisp' Photosynthetic Performance and Carbohydrate Accumulation. *Plants*, *12*(23), Article 23. https://doi.org/10.3390/plants12234035

Banerjee, A., & Roychoudhury, A. (2015). WRKY Proteins: Signaling and Regulation of Expression during Abiotic Stress Responses. *The Scientific World Journal*, *2015*(1), 807560. https://doi.org/10.1155/2015/807560

Baron, D., Esteves Amaro, A. C., Pina, A., & Ferreira, G. (2019a). An overview of grafting re-establishment in woody fruit species. *Scientia Horticulturae*, *243*, 84–91. https://doi.org/10.1016/j.scienta.2018.08.012

Benavides-Mendoza, A., González-García, Y., Pérez-Labrada, F., & González-Morales, S. (2024). Response to Abiotic Stresses in Horticultural Crops. *Horticulturae*, *10*(8), Article 8. https://doi.org/10.3390/horticulturae10080815

Brizzolara, S., Hertog, M., Tosetti, R., Nicolai, B., & Tonutti, P. (2018). Metabolic Responses to Low Temperature of Three Peach Fruit Cultivars Differently Sensitive to Cold Storage. *Frontiers in Plant Science*, *9*. https://doi.org/10.3389/fpls.2018.00706

Centinari, M., Smith, M. S., & Londo, J. P. (2016). Assessment of Freeze Injury of Grapevine Green Tissues in Response to Cultivars and a Cryoprotectant Product. *HortScience*, *51*(7), 856–860. https://doi.org/10.21273/HORTSCI.51.7.856

Chai, F., Liu, W., Xiang, Y., Meng, X., Sun, X., Cheng, C., Liu, G., Duan, L., Xin, H., & Li, S. (2019). Comparative metabolic profiling of Vitis amurensis and Vitis vinifera during cold acclimation. *Horticulture Research*, *6*(1), 8. https://doi.org/10.1038/s41438-018-0083-5

Charng, Y., Mitra, S., & Yu, S.-J. (2022). Maintenance of abiotic stress memory in plants: Lessons learned from heat acclimation. *The Plant Cell*, *35*(1), 187–200. https://doi.org/10.1093/plcell/koac313

Chitarra, W., Perrone, I., Avanzato, C. G., Minio, A., Boccacci, P., Santini, D., Gilardi, G., Siciliano, I., Gullino, M. L., Delledonne, M., Mannini, F., & Gambino, G. (2017). Grapevine Grafting: Scion Transcript Profiling and Defense-Related Metabolites Induced by Rootstocks. *Frontiers in Plant Science*, *8*. https://doi.org/10.3389/fpls.2017.00654

Climate change impacts | National Oceanic and Atmospheric Administration. (2024, January). https://www.noaa.gov/education/resource-collections/climate/climate-change-impacts

Cornille, A., Giraud, T., Smulders, M. J. M., Roldán-Ruiz, I., & Gladieux, P. (2014). The domestication and evolutionary ecology of apples. *Trends in Genetics*, *30*(2), 57–65. https://doi.org/10.1016/j.tig.2013.10.002

Corso, M., Vannozzi, A., Ziliotto, F., Zouine, M., Maza, E., Nicolato, T., Vitulo, N., Meggio, F., Valle, G., Bouzayen, M., Müller, M., Munné-Bosch, S., Lucchin, M., & Bonghi, C. (2016). Grapevine Rootstocks Differentially Affect the Rate of Ripening and Modulate Auxin-Related Genes in Cabernet Sauvignon Berries. *Frontiers in Plant Science*, *7*. https://doi.org/10.3389/fpls.2016.00069

Darbyshire, R., Webb, L., Goodwin, I., & Barlow, E. W. R. (2013). Evaluation of recent trends in Australian pome fruit spring phenology. *International Journal of Biometeorology*, *57*(3), 409–421. https://doi.org/10.1007/s00484-012-0567-1

Databases and Applications | USDA Foreign Agricultural Service. (n.d.). Retrieved March 30, 2025, from https://www.fas.usda.gov/data/databases-applications

Dong, C.-J., Li, L., Shang, Q.-M., Liu, X.-Y., & Zhang, Z.-G. (2014). Endogenous salicylic acid accumulation is required for chilling tolerance in cucumber (Cucumis sativus L.) seedlings. *Planta*, *240*(4), 687–700. https://doi.org/10.1007/s00425-014-2115-1

Duan, X., Zhang, W., Huang, J., Hao, L., Wang, S., Wang, A., Meng, D., Zhang, Q., Chen, Q., & Li, T. (2016). PbWoxT1 mRNA from pear (Pyrus betulaefolia) undergoes long-distance transport assisted by a polypyrimidine tract binding protein. *New Phytologist*, *210*(2), 511–524. https://doi.org/10.1111/nph.13793

Ellwood, E. R., Temple, S. A., Primack, R. B., Bradley, N. L., & Davis, C. C. (2013). RecordBreaking Early Flowering in the Eastern United States. PLoS ONE, 8(1), 1–9. https://doi.org/10.1371/journal.pone.0053788

Fadón, E., Herrero, M., & Rodrigo, J. (2015). Flower development in sweet cherry framed in the BBCH scale. *Scientia Horticulturae*, *192*, 141–147. https://doi.org/10.1016/j.scienta.2015.05.027

Feng, M., Augstein, F., Kareem, A., & Melnyk, C. W. (2024). Plant grafting: Molecular mechanisms and applications. *Molecular Plant*, *17*(1), 75–91. https://doi.org/10.1016/j.molp.2023.12.006

Ferreira, C. S. S., Soares, P. R., Guilherme, R., Vitali, G., Boulet, A., Harrison, M. T., Malamiri, H., Duarte, A. C., Kalantari, Z., & Ferreira, A. J. D. (2024). Sustainable Water Management in Horticulture: Problems, Premises, and Promises. *Horticulturae*, *10*(9), Article 9. https://doi.org/10.3390/horticulturae10090951

Forner-Giner, M. A., Rodriguez-Gamir, J., Martinez-Alcantara, B., Quiñones, A., Iglesias, D. J., Primo-Millo, E., & Forner, J. (2014). Performance of Navel orange trees grafted onto two new dwarfing rootstocks (Forner-Alcaide 517 and Forner-Alcaide 418). *Scientia Horticulturae*, *179*, 376–387. https://doi.org/10.1016/j.scienta.2014.07.032

Foster, T. M., McAtee, P. A., Waite, C. N., Boldingh, H. L., & McGhie, T. K. (2017). Apple dwarfing rootstocks exhibit an imbalance in carbohydrate allocation and reduced cell growth and metabolism. *Horticulture Research*, *4*(1), 1–13. https://doi.org/10.1038/hortres.2017.9

Francini, A., & Sebastiani, L. (2013). Phenolic Compounds in Apple (Malus x domestica Borkh.): Compounds Characterization and Stability during Postharvest and after Processing. *Antioxidants*, *2*(3), Article 3. https://doi.org/10.3390/antiox2030181

Fujisawa, M., & Kobayashi, K. (2010). Apple (Malus pumila var. domestica) phenology is advancing due to rising air temperature in northern Japan. Global Change Biology, 16(10), 2651–2660. https://doi.org/10.1111/j.1365-2486.2009.02126.x

Fruit: World production by type 2023. (n.d.). Statista. Retrieved March 30, 2025, from https://www.statista.com/statistics/264001/worldwide-production-of-fruit-by-variety/

Fu, X., Feng, Y.-Q., Zhang, X.-W., Zhang, Y.-Y., Bi, H.-G., & Ai, X.-Z. (2021). Salicylic Acid Is Involved in Rootstock–Scion Communication in Improving the Chilling Tolerance of Grafted Cucumber. *Frontiers in Plant Science*, *12*. https://doi.org/10.3389/fpls.2021.693344

Gallus, S., Talamini, R., Giacosa, A., Montella, M., Ramazzotti, V., Franceschi, S., Negri, E., & Vecchia, C. L. (2005). Does an apple a day keep the oncologist away? *Annals of Oncology*, *16*(11), 1841–1844. https://doi.org/10.1093/annonc/mdi361

Gautier, A. T., Chambaud, C., Brocard, L., Ollat, N., Gambetta, G. A., Delrot, S., & Cookson, S. J. (2019). Merging genotypes: Graft union formation and scion–rootstock interactions. *Journal of Experimental Botany*, *70*(3), 747–755. https://doi.org/10.1093/jxb/ery422

Gossé, F., Guyot, S., Roussi, S., Lobstein, A., Fischer, B., Seiler, N., & Raul, F. (2005). Chemopreventive properties of apple procyanidins on human colon cancer-derived metastatic SW620 cells and in a rat model of colon carcinogenesis. *Carcinogenesis*, *26*(7), 1291–1295. https://doi.org/10.1093/carcin/bgi074

Grab, S., & Craparo, A. (2011). Advance of apple and pear tree full bloom dates in response to climate change in the southwestern Cape, South Africa: 1973–2009. *Agricultural and Forest Meteorology*, *151*(3), 406–413. https://doi.org/10.1016/j.agrformet.2010.11.001

Gregory, P. J., Atkinson, C. J., Bengough, A. G., Else, M. A., Fernández-Fernández, F., Harrison, R. J., & Schmidt, S. (2013). Contributions of roots and rootstocks to sustainable, intensified crop production. *Journal of Experimental Botany*, *64*(5), 1209–1222. https://doi.org/10.1093/jxb/ers385

Gu, B., Zhang, B., Ding, L., Li, P., Shen, L., & Zhang, J. (2020). Physiological Change and Transcriptome Analysis of Chinese Wild Vitis amurensis and Vitis vinifera in Response to Cold Stress. *Plant Molecular Biology Reporter*, *38*(3), 478–490. https://doi.org/10.1007/s11105-020-01210-5

Haagenson, D. M., Cunningham, S. M., & Volenec, J. J. (2003). Root Physiology of Less Fall Dormant, Winter Hardy Alfalfa Selections. *Crop Science*, *43*(4), 1441–1447. https://doi.org/10.2135/cropsci2003.1441

Harris, Z. N., Pratt, J. E., Kovacs, L. G., Klein, L. L., Kwasniewski, M. T., Londo, J. P., Wu, A. S., & Miller, A. J. (2023). Grapevine scion gene expression is driven by rootstock and environment interaction. *BMC Plant Biology*, *23*(1), 211. https://doi.org/10.1186/s12870-023-04223-w

Hayat, F., Ma, C., Iqbal, S., Huang, X., Omondi, O. K., Ni, Z., Shi, T., Tariq, R., Khan, U., & Gao, Z. (2021). Rootstock-Mediated Transcriptional Changes Associated with Cold Tolerance in Prunus mume Leaves. *Horticulturae*, *7*(12), Article 12. https://doi.org/10.3390/horticulturae7120572

He, Z., Zhou, M., Feng, X., Di, Q., Meng, D., Yu, X., Yan, Y., Sun, M., & Li, Y. (2024). The Role of Brassinosteroids in Plant Cold Stress Response. *Life*, *14*(8), 1015. https://doi.org/10.3390/life14081015

Hernández-Elvira, M., & Sunnerhagen, P. (2022). Post-transcriptional regulation during stress. *FEMS Yeast Research*, *22*(1), foac025. https://doi.org/10.1093/femsyr/foac025

Hoffmann, H., & Rath, T. (2013). Future Bloom and Blossom Frost Risk for Malus domestica Considering Climate Model and Impact Model Uncertainties. PLoS ONE, 8(10). https://doi.org/10.1371/journal.pone.0075033

Huang, Y., Si, Y., & Dane, F. (2011). Impact of grafting on cold responsive gene expression in Satsuma mandarin (Citrus unshiu). *Euphytica*, *177*(1), 25–32. https://doi.org/10.1007/s10681-010-0243-7

Hudina, M., Orazem, P., Jakopic, J., & Stampar, F. (2014). The phenolic content and its involvement in the graft incompatibility process of various pear rootstocks (*Pyrus communis* L.). *Journal of Plant Physiology*, *171*(5), 76–84. https://doi.org/10.1016/j.jplph.2013.10.022

Iglesias, I., Giné-Bordonaba, J., Garanto, X., & Reig, G. (2019). Rootstock affects quality and phytochemical composition of 'Big Top' nectarine fruits grown under hot climatic conditions. *Scientia Horticulturae*, *256*, 108586. https://doi.org/10.1016/j.scienta.2019.108586

Ito, A., Sakamoto, D., & Moriguchi, T. (2012). Carbohydrate metabolism and its possible roles in endodormancy transition in Japanese pear. *Scientia Horticulturae*, *144*, 187–194. https://doi.org/10.1016/j.scienta.2012.07.009

Jahed, K. R., & Sherif, S. M. (2025). Whole-tree dormancy dynamics in peach: Carbohydrate reservoirs and crosstalk with hormones and fatty acids. *Plant Physiology and Biochemistry*, *228*, 110183. https://doi.org/10.1016/j.plaphy.2025.110183

Jaimez, R. E., Peña, G., Barragán, L., Chica, E., Arteaga, F., & Cedeño, G. (2023). The effect of water deficit on leaf stomatal conductance, water relations, chlorophyll fluorescence and growth of rootstock-scion combinations of cacao. *Scientia Horticulturae*, *321*, 112335. https://doi.org/10.1016/j.scienta.2023.112335

Jamshidi Goharrizi, K., Meru, G., Ghotbzadeh Kermani, S., Heidarinezhad, A., & Salehi, F. (2021). Short-term cold stress affects physiological and biochemical traits of pistachio rootstocks. *South African Journal of Botany*, *141*, 90–98. https://doi.org/10.1016/j.sajb.2021.04.029

Jia, Y., Wong, D. C., Sweetman, C., Bruning, J. B., & Ford, C. M. (2015). New insights into the evolutionary history of plant sorbitol dehydrogenase. *BMC Plant Biology*, *15*(1), 101. https://doi.org/10.1186/s12870-015-0478-5

Jing, Z., Liu, N., Zhang, Z., & Hou, X. (2024). Research Progress on Plant Responses to Stress Combinations in the Context of Climate Change. *Plants*, *13*(4), 469. https://doi.org/10.3390/plants13040469

Kalberer, S. R., Wisniewski, M., & Arora, R. (2006). Deacclimation and reacclimation of cold-hardy plants: Current understanding and emerging concepts. *Plant Science*, *171*(1), 3–16. https://doi.org/10.1016/j.plantsci.2006.02.013

Karabulut, B., & Çelik, H. (2022). Determination of Grafting Success and Carbohydrate Distributions of Foxy Grape (Vitis labrusca L.) Varieties Grafted on Different American Grape Rootstocks. *Horticulturae*, *8*(10), Article 10. https://doi.org/10.3390/horticulturae8100949

Kaur, A., Zhang, L., Maness, N. O., Ferguson, L., Graham, C. J., Sun, Y., Panta, S., Pokhrel, N., Yang, M., & Moss, J. Q. (2024). Dormant carbohydrate reserves enhance pecan tree spring freeze tolerance: Controlled environment observations. *Frontiers in Plant Science*, *15*. https://doi.org/10.3389/fpls.2024.1393305

Kaya, O. (2020). Defoliation alleviates cold-induced oxidative damage in dormant buds of grapevine by up-regulating soluble carbohydrates and decreasing ROS. Acta Physiologiae Plantarum, 42(7), 1–10. https://doi.org/10.1007/s11738-020-03093-1

Khan, M., Hu, J., Dahro, B., Ming, R., Zhang, Y., Wang, Y., Alhag, A., Li, C., & Liu, J.-H. (2021). ERF108 from Poncirus trifoliata (L.) Raf. Functions in cold tolerance by modulating raffinose synthesis through transcriptional regulation of PtrRafS. *The Plant Journal*, *108*(3), 705–724. https://doi.org/10.1111/tpj.15465

Khan, N. (2025). Decoding phytohormone signaling in plant stress physiology: Insights, challenges, and future directions. *Environmental and Experimental Botany*, *231*, 106099. https://doi.org/10.1016/j.envexpbot.2025.106099

Klumb, E. K., Braga, E. J. B., & Bianchi, V. J. (2020). Differential expression of genes involved in the response of *Prunus* spp. Rootstocks under soil flooding. *Scientia Horticulturae*, *261*, 109038. https://doi.org/10.1016/j.scienta.2019.109038

Kong, Y., Hou, X., Liu, Z., & Li, Y. (2024). Cold-stress induced metabolomic and transcriptomic changes in leaves of three mango varieties with different cold tolerance. *BMC Plant Biology*, *24*(1), 266. https://doi.org/10.1186/s12870-024-04983-z

Kumar, A. (2024). New Approaches of Root Stocks in Fruit Production: A Review. *Open Access Journal of Botanical Insights*, *2*(1), 1–43. https://doi.org/10.23880/oajbi-16000109

Kumar, V., Srivastava, A. K., & AbdElgawad, H. (2025). Transcriptional and Post-Transcriptional Regulation of Plant Growth, Development, and Stress Responses. *Journal of Plant Growth Regulation*. https://doi.org/10.1007/s00344-025-11681-z

Labarga, D., Mairata, A., Puelles, M., Martín, I., Albacete, A., García-Escudero, E., & Pou, A. (2023). The Rootstock Genotypes Determine Drought Tolerance by Regulating Aquaporin Expression at the Transcript Level and Phytohormone Balance. *Plants*, *12*(4), 718. https://doi.org/10.3390/plants12040718

Lamers, J., van der Meer, T., & Testerink, C. (2020). How Plants Sense and Respond to Stressful Environments1[OPEN]. *Plant Physiology*, *182*(4), 1624–1635. https://doi.org/10.1104/pp.19.01464

Lamichhane, J. R. (2021). Rising risks of late-spring frosts in a changing climate. Nature Climate Change, 11(7), 554–555. https://doi.org/10.1038/s41558-021-01090-x

Lee, J. I., Yu ,D. J., Lee ,J. H., Kim ,S. J., & and Lee, H. J. (2013). Comparison of mid-Winter cold-hardiness and soluble sugars contents in the shoots of 21 highbush blueberry (Vaccinium corymbosum) cultivars. *The Journal of Horticultural Science and Biotechnology*, *88*(6), 727–734. https://doi.org/10.1080/14620316.2013.11513031

Lee, Y., Hoang, N. V., Do, V. G., Foster, T. M., McGhie, T. K., Kim, S., Yang, S. J., Park, J.-H., Park, J., & Lee, J.-Y. (2023). Identification of genes associated with the regulation of cold tolerance and the RNA movement in the grafted apple. *Scientific Reports*, *13*(1), 11583. https://doi.org/10.1038/s41598-023-38571-2

Li, Y., Tian, Q., Wang, Z., Li, J., Liu, S., Chang, R., Chen, H., & Liu, G. (2023a). Integrated analysis of transcriptomics and metabolomics of peach under cold stress. *Frontiers in Plant Science*, *14*. https://doi.org/10.3389/fpls.2023.1153902

Li, W., Chen, S., Liu, Y., Wang, L., Jiang, J., Zhao, S., Fang, W., Chen, F., & Guan, Z. (2022). Long-distance transport RNAs between rootstocks and scions and graft hybridization. *Planta*, *255*(5), 96. https://doi.org/10.1007/s00425-022-03863-w

Li, X., Li, M., Zhou, B., Yang, Y., Wei, Q., & Zhang, J. (2019). Transcriptome analysis provides insights into the stress response crosstalk in apple (Malus × domestica) subjected to drought, cold and high salinity. *Scientific Reports*, *9*(1), 9071. https://doi.org/10.1038/s41598-019-45266-0

Liu, J., & Sherif, S. M. (2019). Hormonal Orchestration of Bud Dormancy Cycle in Deciduous Woody Perennials. Frontiers in Plant Science, 10(September), 1–21. https://doi.org/10.3389/fpls.2019.01136

Liu, X.-Y., Li, J., Liu, M.-M., Yao, Q., & Chen, J.-Z. (2017). Transcriptome Profiling to Understand the Effect of Citrus Rootstocks on the Growth of 'Shatangju' Mandarin. *PLOS ONE*, *12*(1), e0169897. https://doi.org/10.1371/journal.pone.0169897

Lordan, J., Fazio, G., Francescatto, P., & Robinson, T. (2017). Effects of apple (*Malus* × *domestica*) rootstocks on scion performance and hormone concentration. *Scientia Horticulturae*, *225*, 96–105. https://doi.org/10.1016/j.scienta.2017.06.050

Lordan, J., Zazurca, L., Maldonado, M., Torguet, L., Alegre, S., & Miarnau, X. (2019). Horticultural performance of 'Marinada' and 'Vairo' almond cultivars grown on a genetically diverse set of rootstocks. *Scientia Horticulturae*, *256*, 108558. https://doi.org/10.1016/j.scienta.2019.108558

Lu, K., Sun, J., Li, Q., Li, X., & Jin, S. (2021). Effect of Cold Stress on Growth, Physiological Characteristics, and Calvin-Cycle-Related Gene Expression of Grafted Watermelon Seedlings of Different Gourd Rootstocks. *Horticulturae*, *7*(10), Article 10. https://doi.org/10.3390/horticulturae7100391

Ma, Q., Huang, J.-G., Hänninen, H., & Berninger, F. (2019). Divergent trends in the risk of spring frost damage to trees in Europe with recent warming. *Global Change Biology*, *25*(1), 351–360. https://doi.org/10.1111/gcb.14479

Mahmoud, L. M., Killiny, N., & Dutt, M. (2024). Physiological and molecular responses of 'Hamlin' sweet orange trees expressing the VvmybA1 gene under cold stress conditions. *Planta*, *260*(3), 67. https://doi.org/10.1007/s00425-024-04496-x

Manzoor, M. A., Xu, Y., Lv, Z., Xu, J., Wang, Y., Sun, W., Liu, X., Wang, L., Wang, J., Liu, R., Whiting, M. D., Jiu, S., Zhang, C., Manzoor, M. A., Xu, Y., Lv, Z., Xu, J., Wang, Y., Sun, W., … Zhang, C. (2023). Fruit crop abiotic stress management: A comprehensive review of plant hormones mediated responses. *Fruit Research*, *3*(1). https://doi.org/10.48130/FruRes-2023-0030

Martínez-Ballesta, M. C., Alcaraz-López, C., Muries, B., Mota-Cadenas, C., & Carvajal, M. (2010). Physiological aspects of rootstock–scion interactions. *Scientia Horticulturae*, *127*(2), 112–118. https://doi.org/10.1016/j.scienta.2010.08.002

Mauro, R. P., Pérez-Alfocea, F., Cookson, S. J., Ollat, N., & Vitale, A. (2022). Editorial: Physiological and Molecular Aspects of Plant Rootstock-Scion Interactions. *Frontiers in Plant Science*, *13*, 852518. https://doi.org/10.3389/fpls.2022.852518

Mesa, K., Serra, S., Masia, A., Gagliardi, F., Bucci, D., & Musacchi, S. (2016). Seasonal trends of starch and soluble carbohydrates in fruits and leaves of 'Abbé Fétel' pear trees and their relationship to fruit quality parameters. *Scientia Horticulturae*, *211*, 60–69. https://doi.org/10.1016/j.scienta.2016.08.008

leeMierczak, K., & Garus-Pakowska, A. (2024). An Overview of Apple Varieties and the Importance of Apple Consumption in the Prevention of Non-Communicable Diseases—A Narrative Review. *Nutrients*, *16*(19), Article 19. https://doi.org/10.3390/nu16193307

Morandi, B., Manfrini, L., Lugli, S., Tugnoli, A., Boini, A., Perulli, G. D., Bresilla, K., Venturi, M., & Corelli Grappadelli, L. (2019). Sweet cherry water relations and fruit production efficiency are affected by rootstock vigor. *Journal of Plant Physiology*, *237*, 43–50. https://doi.org/10.1016/j.jplph.2019.04.007

Muthuramalingam, P., Shin, H., Adarshan, S., Jeyasri, R., Priya, A., Chen, J.-T., & Ramesh, M. (2022). Molecular Insights into Freezing Stress in Peach Based on Multi-Omics and Biotechnology: An Overview. *Plants*, *11*(6), 812. https://doi.org/10.3390/plants11060812

Ntatsi, G., Savvas, D., Papasotiropoulos, V., Katsileros, A., Zrenner, R. M., Hincha, D. K., Zuther, E., & Schwarz, D. (2017). Rootstock Sub-Optimal Temperature Tolerance Determines Transcriptomic Responses after Long-Term Root Cooling in Rootstocks and Scions of Grafted Tomato Plants. *Frontiers in Plant Science*, *8*. https://doi.org/10.3389/fpls.2017.00911

Opazo, I., Toro, G., Salvatierra, A., Pastenes, C., & Pimentel, P. (2020). Rootstocks modulate the physiology and growth responses to water deficit and long-term recovery in grafted stone fruit trees. *Agricultural Water Management*, *228*, 105897. https://doi.org/10.1016/j.agwat.2019.105897

Palonen, P., Buszard, D., & Donnelly, D. (2000). Changes in carbohydrates and freezing tolerance during cold acclimation of red raspberry cultivars grown in vitro and in vivo. *Physiologia Plantarum*, *110*(3), 393–401. https://doi.org/10.1111/j.1399-3054.2000.1100314.x

Pearce, R. S. (2001). Plant Freezing and Damage. *Annals of Botany*, *87*(4), 417–424. https://doi.org/10.1006/anbo.2000.1352

Perry, K. B. (1998). Basics of Frost and Freeze Protection for Horticultural Crops. *HortTechnology*, *8*(1), 10–15. https://doi.org/10.21273/HORTTECH.8.1.10

Pfleiderer, P., Menke, I., & Schleussner, C.-F. (2019). Increasing risks of apple tree frost damage under climate change. *Climatic Change*, *157*(3), 515–525. https://doi.org/10.1007/s10584-019-02570-y

Plavcová, L., Jupa, R., Mészáros, M., & Hoch, G. (2023). Whole-Tree Storage of Non-structural Carbohydrates in Apple and Pear Trees on Size-Controlling Rootstocks. *Journal of Plant Growth Regulation*, *42*(12), 7759–7769. https://doi.org/10.1007/s00344-023-11052-6

Primo-Capella, A., Forner-Giner, M. Á., Martínez-Cuenca, M.-R., & Terol, J. (2022). Comparative transcriptomic analyses of citrus cold-resistant vs. Sensitive rootstocks might suggest a relevant role of ABA signaling in triggering cold scion adaption. *BMC Plant Biology*, *22*, 209. https://doi.org/10.1186/s12870-022-03578-w

Primo-Capella, A., Martínez-Cuenca, M.-R., & Forner-Giner, M. Á. (2021). Cold Stress in Citrus: A Molecular, Physiological and Biochemical Perspective. *Horticulturae*, *7*(10), Article 10. https://doi.org/10.3390/horticulturae7100340

Prinsi, B., Simeoni, F., Galbiati, M., Meggio, F., Tonelli, C., Scienza, A., & Espen, L. (2021). Grapevine Rootstocks Differently Affect Physiological and Molecular Responses of the Scion under Water Deficit Condition. *Agronomy*, *11*(2), Article 2. https://doi.org/10.3390/agronomy11020289

Prodhomme, D., Valls Fonayet, J., Hévin, C., Franc, C., Hilbert, G., de Revel, G., Richard, T., Ollat, N., & Cookson, S. J. (2019). Metabolite profiling during graft union formation reveals the reprogramming of primary metabolism and the induction of stilbene synthesis at the graft interface in grapevine. *BMC Plant Biology*, *19*(1), 599. https://doi.org/10.1186/s12870-019-2055-9

Ramirez, V. E., & Poppenberger, B. (2020). Modes of Brassinosteroid Activity in Cold Stress Tolerance. *Frontiers in Plant Science*, *11*. https://doi.org/10.3389/fpls.2020.583666

Rasool, A., Mansoor, S., Bhat, K. M., Hassan, G. I., Baba, T. R., Alyemeni, M. N., Alsahli, A. A., El-Serehy, H. A., Paray, B. A., & Ahmad, P. (2020). Mechanisms Underlying Graft Union Formation and Rootstock Scion Interaction in Horticultural Plants. *Frontiers in Plant Science*, *11*. https://doi.org/10.3389/fpls.2020.590847

Razi, K., Suresh, P., Mahapatra, P. P., Al Murad, M., Venkat, A., Notaguchi, M., Bae, D. W., Prakash, M. A. S., & Muneer, S. (2024). Exploring the role of grafting in abiotic stress management: Contemporary insights and automation trends. *Plant Direct*, *8*(12), e70021. https://doi.org/10.1002/pld3.70021

Regier, N., Streb, S., Zeeman, S. C., & Frey, B. (2010). Seasonal changes in starch and sugar content of poplar (Populus deltoides × nigra cv. Dorskamp) and the impact of stem girdling on carbohydrate allocation to roots. *Tree Physiology*, *30*(8), 979–987. https://doi.org/10.1093/treephys/tpq047

Rodrigo, J. (2000). Spring frosts in deciduous fruit trees. Morphological damage and flower hardiness. In Scientia Horticulturae. https://doi.org/10.1016/S0304-4238(99)00150-8

Rosińska, W., Jurasz, J., Przestrzelska, K., Wartalska, K., & Kaźmierczak, B. (2024). Climate change's ripple effect on water supply systems and the water-energy nexus – A review. *Water Resources and Industry*, *32*, 100266. https://doi.org/10.1016/j.wri.2024.100266

Sageman-Furnas, K., & Strader, L. (2022). Connected phytohormone biosynthesis pathways at the core of growth-stress tradeoffs. *Molecular Plant*, *15*(7), 1087–1089. https://doi.org/10.1016/j.molp.2022.06.005

Salazar-Gutiérrez, M. R., Chaves, B., & Hoogenboom, G. (2016). Freezing tolerance of apple flower buds. Scientia Horticulturae, 198, 344–351. https://doi.org/10.1016/j.scienta.2015.12.003

Saini, A. K., Jahed, K. R., Neres, D. F., Wright, R. C., & Sherif, S. M. (2025). Investigating Frost Response, Rootstock-Dependent Cold Tolerance, and Floral Bud Mortality in Apple Cultivars through Transcriptomic Insights. *Plant Stress*, 100829. https://doi.org/10.1016/j.stress.2025.100829

Saini, A. K., Sherif, S. M., & Jahed, K. R. (n.d.). *Rootstock Effects on Flower Bud Mortality in 'Gala' and 'Fuji' Apples Under Natural Spring Frost Conditions (2021–2023)*. Retrieved July 25, 2025, from https://pubs.ext.vt.edu/content/pubs_ext_vt_edu/en/SPES/spes-713/spes-713.html

Saini, A. K., Singh, H., Jawandha, S. K., & Gill, K. S. (2020). Influence of *Prunus* rootstocks and spacing on performance of Japanese plum grown under sub–tropical conditions. *Scientia Horticulturae*, *268*, 109380. https://doi.org/10.1016/j.scienta.2020.109380

Samuolienė, G., Viškelienė, A., Sirtautas, R., & Kviklys, D. (2016). Relationships between apple tree rootstock, crop-load, plant nutritional status and yield. *Scientia Horticulturae*, *211*, 167–173. https://doi.org/10.1016/j.scienta.2016.08.027

Sapkota, S., Salem, M., Jahed, K. R., Artlip, T. S., & Sherif, S. M. (2023). From endodormancy to ecodormancy: The transcriptional landscape of apple floral buds. *Frontiers in Plant Science*, *14*. https://doi.org/10.3389/fpls.2023.1194244

Sendon, P. M., Seo, H. S., & Song, J. T. (2011). Salicylic Acid Signaling: Biosynthesis, Metabolism, and Crosstalk with Jasmonic Acid. *Journal of the Korean Society for Applied Biological Chemistry*, *54*(4), 501–506. https://doi.org/10.3839/jksabc.2011.077

Shahkoomahally, S., Chang, Y., Brecht, J. K., Chaparro, J. X., & Sarkhosh, A. (2021). Influence of rootstocks on fruit physical and chemical properties of peach cv. UFSun. *Food Science & Nutrition*, *9*(1), 401–413. https://doi.org/10.1002/fsn3.2005

Sharma, A., & Zheng, B. (2019). Molecular Responses during Plant Grafting and Its Regulation by Auxins, Cytokinins, and Gibberellins. *Biomolecules*, *9*(9), Article 9. https://doi.org/10.3390/biom9090397

Sherif, S. M. (2022). *Rootstock Effects on Tree Growth and Yield of 'Honeycrisp' Apple under Virginia State Climatic Conditions*. Virginia Cooperative Extension. https://pubs.ext.vt.edu/content/pubs_ext_vt_edu/en/SPES/spes-398/spes-398.html

Shi, Y., Ding, Y., & Yang, S. (2018). Molecular Regulation of CBF Signaling in Cold Acclimation. *Trends in Plant Science*, *23*(7), 623–637. https://doi.org/10.1016/j.tplants.2018.04.002

Shin, H., Min, K., & Arora, R. (2018). Exogenous salicylic acid improves freezing tolerance of spinach (*Spinacia oleracea* L.) leaves. *Cryobiology*, *81*, 192–200. https://doi.org/10.1016/j.cryobiol.2017.10.006

Snyder, R. L., Melo-Abreu, J. P. D., & Matulich, S. (2005). *Frost Protection: Fundamentals, Practice, And Economics (FAO Environment and Natural Resources)* (Pap/Cdr edition). Food & Agriculture Organization of the UN (FA).

Song, X., Wang, H., Wang, Y., Zeng, Q., & Zheng, X. (2024). Metabolomics combined with physiology and transcriptomics reveal how *Nicotiana tabacum* leaves respond to cold stress.

Plant Physiology and Biochemistry, *208*, 108464. https://doi.org/10.1016/j.plaphy.2024.108464

Sun, S., Fang, J., Lin, M., Hu, C., Qi, X., Chen, J., Zhong, Y., Muhammad, A., Li, Z., & Li, Y. (2021a). Comparative Metabolomic and Transcriptomic Studies Reveal Key Metabolism Pathways Contributing to Freezing Tolerance Under Cold Stress in Kiwifruit. *Frontiers in Plant Science*, *12*. https://doi.org/10.3389/fpls.2021.628969

Sun, S., Lin, M., Qi, X., Chen, J., Gu, H., Zhong, Y., Sun, L., Muhammad, A., Bai, D., Hu, C., & Fang, J. (2021b). Full-length transcriptome profiling reveals insight into the cold response of two kiwifruit genotypes (A. arguta) with contrasting freezing tolerances. *BMC Plant Biology*, *21*(1), 365. https://doi.org/10.1186/s12870-021-03152-w

Takahashi, F., Kuromori, T., Urano, K., Yamaguchi-Shinozaki, K., & Shinozaki, K. (2020). Drought Stress Responses and Resistance in Plants: From Cellular Responses to Long-Distance Intercellular Communication. *Frontiers in Plant Science*, *11*. https://doi.org/10.3389/fpls.2020.556972

Tan, Y., Yang, Y., Li, C., Liang, B., Li, M., & Ma, F. (2017). Overexpression of *MpCYS4*, a phytocystatin gene from *Malus prunifolia* (Willd.) Borkh., delays natural and stress-induced leaf senescence in apple. *Plant Physiology and Biochemistry*, *115*, 219–228. https://doi.org/10.1016/j.plaphy.2017.03.025

Tedesco, S., Erban, A., Gupta, S., Kopka, J., Fevereiro, P., Kragler, F., & Pina, A. (2021). The Impact of Metabolic Scion–Rootstock Interactions in Different Grapevine Tissues and Phloem Exudates. *Metabolites*, *11*(6), Article 6. https://doi.org/10.3390/metabo11060349

Toro, G., Pastenes, C., Salvatierra, A., & Pimientel, P. (2023). Trade-off between hydraulic sensitivity, root hydraulic conductivity and water use efficiency in grafted *Prunus* under water deficit. *Agricultural Water Management*, *282*, 108284. https://doi.org/10.1016/j.agwat.2023.108284

Tříska, J., Vrchotová, N., Balík, J., Soural, I., & Sotolář, R. (2017). Variability in the Content of Trans-Resveratrol, Trans-?-Viniferin and R2-Viniferin in Grape Cane of Seven Vitis vinifera L. Varieties during a Three-Year Study. *Molecules*, *22*(6), Article 6. https://doi.org/10.3390/molecules22060928

Tworkoski, T., & Fazio, G. (2016). Hormone and growth interactions of scions and size-controlling rootstocks of young apple trees. *Plant Growth Regulation*, *78*(1), 105–119. https://doi.org/10.1007/s10725-015-0078-2

Unterberger, C., Brunner, L., Nabernegg, S., Steininger, K. W., Steiner, A. K., Stabentheiner, E., Monschein, S., & Truhetz, H. (2018). Spring frost risk for regional apple production under a warmer climate. *PLOS ONE*, *13*(7), e0200201. https://doi.org/10.1371/journal.pone.0200201

Vargas, F., Romero, M., Clavé, J., Vergés, J., Santos, J., & Batlle, I. (2008). *'Vayro', 'Marinada', 'Constantí', and 'Tarraco' Almonds*. https://doi.org/10.21273/HORTSCI.43.2.535

Vittal, H., Sharma, N., Dubey, A. K., Shivran, M., Singh, S. K., Meena, M. C., Kumar, N., Sharma, N., Singh, N., Pandey, R., Bollinedi, H., Singh, B. P., & Sharma, R. M. (2023).

Rootstock-mediated carbohydrate metabolism, nutrient contents, and physiological modifications in regular and alternate mango (Mangifera indica L.) scion varieties. *PLOS ONE*, *18*(5), e0284910. https://doi.org/10.1371/journal.pone.0284910

Vitasse, Y., Schneider, L., Rixen, C., Christen, D., & Rebetez, M. (2018). Increase in the risk of exposure of forest and fruit trees to spring frosts at higher elevations in Switzerland over the last four decades. Agricultural and Forest Meteorology, 248(September 2017), 60–69. 24 https://doi.org/10.1016/j.agrformet.2017.09.005

Apple Fun Facts. (n.d.). Virginia Apples. Retrieved March 30, 2025, from https://www.virginiaapples.net/apple-facts

Volk, G. M., Chao, C. T., Norelli, J., Brown, S. K., Fazio, G., Peace, C., McFerson, J., Zhong, G.-Y., & Bretting, P. (2015). The vulnerability of US apple (Malus) genetic resources. *Genetic Resources and Crop Evolution*, *62*(5), 765–794. https://doi.org/10.1007/s10722-014-0194-2

Wang, H. B., Li, L. G., Cheng, L. L., Chen, X., Chang, Y. S., & He, P. (2019). Screening of transcription factors of apple cold-resistant dwarfing rootstock in response to cold stress. *Acta Horticulturae*, *1261*, 129–136. https://doi.org/10.17660/ActaHortic.2019.1261.21

Wang, H., Gong, M., Xin, H., Tang, L., Dai, D., Gao, Y., & Liu, C. (2018). Effects of chilling stress on the accumulation of soluble sugars and their key enzymes in Jatropha curcas seedlings. *Physiology and Molecular Biology of Plants*, *24*(5), 857–865. https://doi.org/10.1007/s12298-018-0568-6

Wang, K., Yin, X.-R., Zhang, B., Grierson, D., Xu, C.-J., & Chen, K.-S. (2017). Transcriptomic and metabolic analyses provide new insights into chilling injury in peach fruit. *Plant, Cell & Environment*, *40*(8), 1531–1551. https://doi.org/10.1111/pce.12951

Wang, Q., Liang, Z., Sun, M., Liu, J., JIn, W., & Liu, S. (2025). Transcriptome sequencing elucidates the adaptation mechanisms of Pyrus betulifolia to cold and drought conditions. *Plant Growth Regulation*. https://doi.org/10.1007/s10725-025-01285-8

Warschefsky, E. J., Klein, L. L., Frank, M. H., Chitwood, D. H., Londo, J. P., von Wettberg, E. J. B., & Miller, A. J. (2016). Rootstocks: Diversity, Domestication, and Impacts on Shoot Phenotypes. *Trends in Plant Science*, *21*(5), 418–437. https://doi.org/10.1016/j.tplants.2015.11.008

Wisniewski, M., Bassett, C., & Gusta, L. V. (2003). *An Overview of Cold Hardiness in Woody Plants: Seeing the Forest Through the Trees*. https://doi.org/10.21273/HORTSCI.38.5.952

Wolfe, D.W., DeGaetano, A. T., Peck, G. M., Carey, M., Ziska, L. H., Lea-Cox, J., Kemanian, A. R., Hoffmann, M. P., & Hollinger, D. Y. (2018). Unique challenges and opportunities for northeastern US crop production in a changing climate. Climatic Change, 146(1–2), 231–245. https://doi.org/10.1007/s10584-017-2109-7

Wong, B. L., Baggett, K. L., & Rye, A. H. (2009). Cold-season patterns of reserve and soluble carbohydrates in sugar maple and ice-damaged trees of two age classes following drought. *Botany*, *87*(3), 293–305. https://doi.org/10.1139/B08-123

Wu, J., Nadeem, M., Galagedara, L., Thomas, R., & Cheema, M. (2022). Recent insights into cell responses to cold stress in plants: Signaling, defence, and potential functions of phosphatidic acid. *Environmental and Experimental Botany*, *203*, 105068. https://doi.org/10.1016/j.envexpbot.2022.105068

Xu, G., Li, L., Zhou, J., He, M., Lyu, D., Zhao, D., & Qin, S. (2023a). Integrated transcriptomics and metabolomics analyses reveal key genes and essential metabolic pathways for the acquisition of cold tolerance during dormancy in apple. *Environmental and Experimental Botany*, *213*, 105413. https://doi.org/10.1016/j.envexpbot.2023.105413

Xu, G., Li, L., Zhou, J., Lyu, D., Zhao, D., & Qin, S. (2023b). Comparison of transcriptome and metabolome analysis revealed differences in cold resistant metabolic pathways in different apple cultivars under low temperature stress. *Horticultural Plant Journal*, *9*(2), 183–198. https://doi.org/10.1016/j.hpj.2022.09.002

Xu, H., & Ediger, D. (2021). Rootstocks with Different Vigor Influenced Scion–Water Relations and Stress Responses in AmbrosiaTM Apple Trees (Malus Domestica var. Ambrosia). *Plants*, *10*(4), 614. https://doi.org/10.3390/plants10040614

Xu, H., Huang, C., Jiang, X., Zhu, J., Gao, X., & Yu, C. (2022). Impact of Cold Stress on Leaf Structure, Photosynthesis, and Metabolites in Camellia weiningensis and C. oleifera Seedlings. *Horticulturae*, *8*(6), Article 6. https://doi.org/10.3390/horticulturae8060494

Yang, X., Chen, L.-S., & Cheng, L. (2021). Leaf Photosynthesis and Carbon Metabolism Adapt to Crop Load in 'Gala' Apple Trees. *Horticulturae*, *7*(3), Article 3. https://doi.org/10.3390/horticulturae7030047

Yeung, E., van Veen, H., Vashisht, D., Sobral Paiva, A. L., Hummel, M., Rankenberg, T., Steffens, B., Steffen-Heins, A., Sauter, M., de Vries, M., Schuurink, R. C., Bazin, J., Bailey-Serres, J., Voesenek, L. A. C. J., & Sasidharan, R. (2018). A stress recovery signaling network for enhanced flooding tolerance in Arabidopsis thaliana. *Proceedings of the National Academy of Sciences*, *115*(26), E6085–E6094. https://doi.org/10.1073/pnas.1803841115

Yu, D. J., Hwang, J. Y., Chung, S. W., Oh, H. D., Yun, S. K., & Lee, H. J. (2017). Changes in cold hardiness and carbohydrate content in peach (*Prunus persica*) trunk bark and wood tissues during cold acclimation and deacclimation. *Scientia Horticulturae*, *219*, 45–52. https://doi.org/10.1016/j.scienta.2017.02.038

Yu, D. J., Jun, S. H., Park, J., Kwon, J. H., & Lee, H. J. (2020). Transcriptome Analysis of Genes Involved in Cold Hardiness of Peach Tree (Prunus persica) Shoots during Cold Acclimation and Deacclimation. *Genes*, *11*(6), Article 6. https://doi.org/10.3390/genes11060611

Zhang, Y., Xu, J., Li, R., Ge, Y., Li, Y., & Li, R. (2023). Plants' Response to Abiotic Stress: Mechanisms and Strategies. *International Journal of Molecular Sciences*, *24*(13), 10915. https://doi.org/10.3390/ijms241310915

Zhao, D., Zhong, G., & Song, G. (2020). Transfer of endogenous small RNAs between branches of scions and rootstocks in grafted sweet cherry trees. *PLOS ONE*, *15*(7), e0236376. https://doi.org/10.1371/journal.pone.0236376

Zhou, Y., Tian, X., Yao, J., Zhang, Z., Wang, Y., Zhang, X., Li, W., Wu, T., Han, Z., Xu, X., & Qiu, C. (2020a). Morphological and photosynthetic responses differ among eight apple scion-rootstock combinations. *Scientia Horticulturae*, *261*, 108981. https://doi.org/10.1016/j.scienta.2019.108981

Zhou, H., He, Y., Zhu, Y., Li, M., Song, S., Bo, W., Li, Y., & Pang, X. (2020). Comparative transcriptome profiling reveals cold stress responsiveness in two contrasting Chinese jujube cultivars. *BMC Plant Biology*, *20*(1), 240. https://doi.org/10.1186/s12870-020-02450-z

Zhou, P., Li, X., Liu, X., Wen, X., Zhang, Y., & Zhang, D. (2021). Transcriptome profiling of Malus sieversii under freezing stress after being cold-acclimated. *BMC Genomics*, *22*(1), 681. https://doi.org/10.1186/s12864-021-07998-0

Zhou, Y., & Underhill, S. J. R. (2021). Differential transcription pathways associated with rootstock-induced dwarfing in breadfruit (Artocarpus altilis) scions. *BMC Plant Biology*, *21*(1), 261. https://doi.org/10.1186/s12870-021-03013-6

Zhu, Y., Yang, G., Yang, H., Zhao, F., Han, S., Chen, R., Zhang, C., Yang, X., Liu, M., Cheng, J., & Zhao, C. (2021). Estimation of apple flowering frost loss for fruit yield based on gridded meteorological and remote sensing data in luochuan, Shaanxi province, China. Remote Sensing, 13(9). https://doi.org/10.3390/rs13091630

Zombardo, A., Crosatti, C., Bagnaresi, P., Bassolino, L., Reshef, N., Puccioni, S., Faccioli, P., Tafuri, A., Delledonne, M., Fait, A., Storchi, P., Cattivelli, L., & Mica, E. (2020). Transcriptomic and biochemical investigations support the role of rootstock-scion interaction in grapevine berry quality. *BMC Genomics*, *21*(1), 468. https://doi.org/10.1186/s12864-020-06795-5

Chapter 2- Investigating Frost Response, Rootstock-Dependent Cold Tolerance, and Floral Bud Mortality in Apple Cultivars through Transcriptomic Insights

Amolpreet Kaur Saini[1], Khalil R. Jahed[1], Deisiany F. Neres[2], Robert C. Wright[2], Sherif M. Sherif[1]*

[1] *Alson H. Smith Jr. Agricultural Research and Extension Center, School of Plant and Environmental Sciences, Virginia Tech, Winchester, VA, 22602, United States*

[2]*Department of Biological Systems Engineering, Virginia Tech, Blacksburg, VA, 24061, United States*

Published in Plant Stress (Volume 16), June 2025, 100829

Available at https://doi.org/10.1016/j.stress.2025.100829

Attribution: Amolpreet Kaur Saini: Writing – original draft, Visualization, Software, Investigation, Formal analysis, Data curation. Khalil R. Jahed: Writing – review & editing, Software, Data curation. Deisiany F. Neres: Writing – review & editing, Software. Robert C. Wright: Writing – review & editing, Supervision, Funding acquisition. Sherif M. Sherif: Writing – review & editing, Validation, Supervision, Resources, Project administration, Methodology, Conceptualization.

Abstract

Late spring frosts threaten the productivity of deciduous fruit trees. In this study, we investigated frost tolerance in two apple (*Malus domestica* Borkh.) cultivars, 'Fuji' and 'Gala', grafted onto ten different rootstocks, over the springs of 2021–2023, to elucidate cold-responsive genes and regulatory mechanisms. Trees on the 'B.9' rootstock exhibited superior frost tolerance, with lower floral bud mortality compared to the susceptible 'M.26'. Using RNA-sequencing, we analyzed floral buds ('Gala'), scion leaves ('Gala'), and rootstock sucker leaves (B9, M26). Samples were collected 12 hours before and 6 hours after a natural frost event in April 2021. Transcriptome analysis revealed extensive transcriptional changes, with 4,549 genes upregulated and 5,469 downregulated. Weighted gene co-expression network analysis (WGCNA) identified three significant modules based on module eigengenes (ME 6, ME 7, and ME 9) associated with the frost response. The ME 6 and ME 7 modules comprised 1,210 and 1,011 genes, respectively, while the ME 9 module included 163 genes, of which 6 were differentially expressed post-frost. Applying a 90% module eigengene connectivity threshold, we identified key hub genes, including *MdAFP* (ABI five binding protein 3), *MdCBF4* (C-repeat-binding factor 4), *MdEXP8* (Expansin A8), *MdHSFC1* (Heat shock transcription factor C1), *MdHXXXD* (HXXXD/BAHD-type acyl-transferase family protein), *MdLRR-RK* (Leucine-rich repeat receptor-like protein kinase), *MdRPK2* (Receptor-like protein kinase 2), and *MdWBC11* (White-Brown Complex homolog/ABC transporter protein). These findings elucidate the genetic basis of frost resilience in apple rootstocks and pinpoint potential targets for genetic enhancement of frost tolerance.

Keywords

Spring frost-induced damage, Climate-Change, Climate-Resilient Apple Rootstock, Cold-Tolerant Rootstocks, Cold-Susceptible Rootstocks, Gene-Gene Interaction Networks, WGCNA; Hub genes

1 Introduction

Climate change is a confirmed phenomenon with widespread consequences on human activities and natural systems worldwide (IPCC, 2014). Projected global mean surface temperatures for 2081–2100 are expected to be 0.3–4.8°C higher than those in 1986–2005, varying by emission scenario (Ukey and Rai, 2021). Many wild and cultivated plant species may struggle to shift their geographical ranges quickly enough to adapt to these rapid changes, potentially leading to declines in production if they do not adapt to new stressors (De Rosa et al., 2021). Among the critical stress factors, late spring frosts pose a significant threat to cultivated fruit trees globally (Vitasse et al., 2019).

Natural frost events are significant environmental stresses that occur when air temperatures drop below 0°C, often accompanied by freezing dew points. These conditions pose a substantial threat to plant health. Frost damage occurs when ice forms on plant surfaces, leading to water stress and potential tissue damage. Freeze damage, which is typically more severe, results from the formation of ice crystals within plant cells (Perry, 1998; Pearce, 2001; Snyder et al., 2005). The susceptibility of plants to spring frost varies depending on species, developmental stage, and the critical temperature threshold (Centinari et al., 2016; Iowa State University Extension and Outreach, 2024). In apple trees, for example, floral buds exhibit varying levels of cold tolerance at different developmental stages. At the silver-tip stage, where the buds are just beginning to separate and appear silvery-gray, they can withstand temperatures as low as –17.6°C. However, as the buds progress to more advanced stages, such as the bloom and post-bloom stage, their cold tolerance significantly decreases; and at the bloom and post-bloom stage, 90% floral bud mortality can occur at temperatures as mild as –3°C (Michigan State University Extension, 2021; Jahed et al., 2023). These variations highlight the critical importance of timing and developmental stage in determining the vulnerability of apple buds to spring frost events.

Frost affects plant cells by causing a phase transition in cell membranes from a liquid crystalline to a gel-like solid state, resulting in energy deficits, ion leakage, and oxidative stress, which have been extensively reviewed (Jahed et al., 2023). These changes often lead to substantial economic losses due to tissue damage. For instance, notable economic impacts from spring frosts were recorded in the USA during 2007, 2010, and 2012 (Hufkens et al., 2012; Augspurger, 2013; Kistner et al., 2018) France in 1995 (Ningre and Colin, 2007) and in Switzerland, southern Germany, and northeastern France during 2011 and 2016 (Kreyling et al., 2012; Vitasse et al., 2019). Global warming exacerbates these risks by generally raising late winter and early spring temperatures, causing earlier flowering in apple trees (Fujisawa and Kobayashi, 2010). This shift in flowering times increases the likelihood of overlap with late spring frosts, heightening the risk of frost damage (Unterberger et al., 2018; Tominaga et al., 2022).

Perennial tree species in temperate climates are genetically programmed to withstand harsh winter conditions. However, these species often encounter challenges during unseasonably warm temperatures in early spring, which may trigger the deacclimation of ecodormant buds, leading to premature bud break. This early development phase increases their vulnerability to subsequent freezing temperatures, typically occurring several weeks later in April, and results in high levels of frost injury due to the flowers and early vegetative growths having little freezing tolerance (Wisniewski et al., 2016). Apple flowers are particularly susceptible, with even mild frosts causing a brown discoloration at the flower base, leading to significant potential yield losses (mentioned in Chapter 1-Introduction) Pfleiderer et al., 2019; Szalay et al., 2019; Chen et al., 2023).

Dormancy and cold hardiness in perennial, woody plants, while interconnected, are regulated by distinct mechanisms and developmental timing. The dormancy cycle progresses through various stages, influenced by internal factors such as paradormancy and endodormancy, and external cues like ecodormancy (Artlip et al., 2019). During paradormancy and endodormancy, growth cessation is driven by specific internal signals. Conversely, in ecodormancy, environmental factors such as temperature and daylight duration critically influence growth regulation. The transitions into and out of dormancy involve a complex interplay of genetic and epigenetic modifications that regulate gene expression (Tarancón et al., 2017).

Cold acclimation, critical for survival under freezing temperatures, entails a sophisticated network of biophysical and biochemical mechanisms. This process primarily relies on altering gene expression, including the upregulation or downregulation of key genes (Wisniewski et al., 2014). Research underscores the role of Cold-Responsive (COR) proteins, such as dehydrins, and transcription factors that regulate gene clusters known as a cold regulon. Notably, C-repeat Binding Factor/Dehydration-Responsive Element-Binding protein (CBF/DREB) transcription factors, part of the APETALA2/Ethylene-Responsive Factor (AP2/ERF) family, are pivotal in mediating the plant's response to cold and drought, binding to the promoter motif A/GCCGAC—often referred to as the C-repeat or Dehydration Response Element. These factors contribute to an estimated 12–20% of transcriptional changes induced by cold in species like Arabidopsis (Vogel et al., 2005; Mizoi et al., 2012). The presence of CBF genes across all examined higher angiosperm species, including woody perennials, demonstrates their broad importance (Artlip et al., 2016). Variations in the number of CBF genes among different species and the functional specificity of these genes, as observed in apples, underscore the potential value of RNA-Seq studies in elucidating the transcriptional regulation of these and other cold-responsive elements. Such studies are crucial for understanding how different plant genotypes respond to cold and freezing stresses.

In addition to the CBF genes, recent research has identified novel components in the cold resistance mechanisms of plants. For example, a study on apple by Xie et al. (2018) discovered that the transcription factors MdMYB88 and MdMYB124 regulate the expression of *CIRCADIAN CLOCK ASSOCIATED 1* (*MdCCA1*). This gene promotes the accumulation of anthocyanins, reduces hydrogen peroxide (H_2O_2) buildup, and enhances cold tolerance. Phytohormones also play a critical role in conferring cold tolerance by modulating cold-responsive pathways and promoting plant growth and development. Notably, ABA acts as a central regulator and crucial stress hormone, facilitating responses to low-temperature stress in various plant species (Sah et al., 2016; Bharath et al., 2021; Rai et al., 2024). Further, an increase in the expression of genes involved in the biosynthesis of sugars has been observed during the cold acclimation process (Satyakam et al., 2022). For instance, research on red-fleshed apple hybrids demonstrated that the sugar transporter known as Sugars Will Eventually be Exported Transporter 9b (MdSWEET9b), regulated by ABA through MdWRKY9, specifically mediates sucrose transport in yeast mutants and apple calli. This activity underscores its role in enhancing sugar accumulation in fruits (Zhang et al., 2023). The accumulation of soluble sugars during cold stress is also crucial as it stabilizes cellular components and the plasma membrane (Tarkowski and Van den Ende, 2015).

The response to cold stress is critical for many tree crops, particularly those that are routinely grafted onto rootstocks. Apple growers, for instance, can enhance cold adaptation by selecting rootstocks that are better suited to new climatic conditions (Moran et al., 2018; Wang et al., 2019; Hezema et al., 2021; Fazio and Robinson, 2022; Lee et al., 2023).

Rootstocks are known to impart beneficial traits to scion cultivars, such as increased growth vigor, disease or insect (e.g. Wooly apple aphid) resistance, and tolerance to abiotic stresses (Foster et al., 2017; Gautier et al., 2019; Rasool et al., 2020; Biasuz and Kalcsits, 2023; Harris et al., 2023). Previous research has demonstrated that grafting onto tolerant rootstocks can bolster the stress resilience of plants by mitigating photosynthesis inhibition, regulating osmotic substances, and boosting antioxidant defenses (Gautier et al., 2019). However, the molecular mechanisms that underline the interaction between stress-tolerant rootstocks and the scions grafted onto them, especially in their joint response to cold stress, are still not well understood and require further exploration.

With the rapid advancement of sequencing technologies, transcriptomics has become a crucial tool for investigating the molecular mechanisms that enable plants to cope with abiotic stresses (Wang et al., 2017; Bahrman et al., 2019; Chen et al., 2022). It provides a rapid, cost-effective means to identify new, functional, and regulatory genes associated with stress responses (Liaquat et al., 2022). In our study, we observed varied responses to natural frost events in the floral buds of 'Gala' and 'Fuji' apple trees grafted onto 10 different rootstocks over three consecutive years (2021-2023). We found that trees grafted onto 'B.9' exhibited consistently lower rates of floral bud mortality after spring frosts compared to those on 'M.26'. Utilizing RNA-Sequencing, we analyzed the transcriptional responses of 'Gala' apple scion grafted onto 'B.9' and 'M.26' rootstocks, before and after a spring frost event. We hypothesized that the cold-hardy rootstock B.9 would confer reduced bud mortality in 'Gala' by promoting a stronger expression of cold-responsive genes compared to the susceptible M.26. Accordingly, we aimed to identify differentially expressed genes and regulatory networks activated during natural frost events to uncover mechanisms underlying rootstock-mediated cold tolerance. Through this study, we hope to provide new insights into the cold stress signaling interactions between rootstock and scion. This research could serve as a valuable resource for future efforts to enhance cold tolerance in apple cultivars.

2 Material and methods

2.1 Plant Materials and Experimental Design

The experiment was conducted from 2021 to 2023 at the Alson H. Smith Jr. Agricultural Research and Extension Center (AREC) in Winchester, Virginia (VA), USA. Twelve-year-old 'Fuji' and 'Gala' apple trees grafted onto ten different rootstocks: 'B.9', 'M.26', 'G.935', 'G.11', 'G.16', 'G.30', 'G.41', 'M.111', 'M.7', and 'M.9' were studied. These trees were trained using the vertical axis system, spaced 1.22 meters within rows and 3.66 meters between rows. The trees were arranged in a Randomized Complete Block Design (RCBD) with four blocks; each block contained two trees per scion-rootstock combination. Annual maintenance included winter pruning and the scheduled application of pesticides and fertilizers, as per the guidelines in the Spray Bulletin for Commercial Tree Fruit Growers (https://vtechworks.lib.vt.edu/handle/10919/84225).

The rootstocks used in this study were developed in various locations: the Budagovsky series (e.g., 'B.9') originated in the Soviet Union (Hezema et al., 2021). The Malling series (e.g., 'M.7', 'M.9', 'M.26') and Malling Merton series (e.g., 'MM.111'), on the other hand, were developed in England; and the Geneva® series (e.g., 'G.11', 'G.16', 'G.30', 'G.41', and 'G.935') were developed through a joint venture between Cornell University and the United States Department of Agriculture (USDA) (Sherif, 2022).

Temperature data were captured every ten minutes using a logger (EasyLog, Lascar Electronics, USA), located within the blocks. The timing of the natural frost events was determined using forecasts from Weather Underground. Three distinct frost events were systematically documented and analyzed on the following dates: April 3, 2021; March 29, 2022; and March 20, 2023.

For floral bud mortality assessments, 30 floral buds were collected from each scion-rootstock combination six hours after the frost event. Each biological replicate consisted of floral buds sampled from three different trees, ensuring that our mortality data accurately represented variability within the experimental design. The king (central) flower from each cluster was separated from the four side blooms, and all flowers were bisected with a razor blade to visually inspect for typical symptoms of frost damage. Flowers were categorized as dead if their pistils had turned brown, and alive if their pistils remained green. An example is shown in Fig. 2G.

For transcriptional profiling, samples of floral buds (‘Gala’), scion leaves (‘Gala’), and rootstock sucker leaves (B9, M26) were collected from three trees per scion-rootstock combination ($n=3$) both 12 hours before and six hours after the frost event in 2021. To validate gene expression profiling, quantitative reverse transcription-polymerase chain reaction (qRT-PCR) analysis was conducted using samples from both 'Gala' and 'Fuji' cultivars. These samples were immediately frozen in liquid nitrogen and subsequently stored at –80°C for further molecular and biochemical analyses. A schematic diagram illustrating the experimental layout, sample collection, and data analysis is presented in Fig. 1.

2.2 Library Construction, Sequencing and Mapping

Total RNA from leaf and floral bud samples was extracted using a modified Cetyltrimethylammonium Bromide (CTAB) method originally described by Sherif et al. (2016). Tissue samples were cryogenically ground into a fine powder with a Geno/Grinder (SPEX SamplePrep, Metuchen, New Jersey, USA). The extracted RNA was then treated with DNase and purified using an EZ RNA Cleanup Kit (EZ Bioresearch LLC, Saint Louis, USA), according to the manufacturer's instructions.

Library preparation and RNA sequencing were conducted by Novogene Corporation Inc. (Novogene, Sacramento, California, USA), utilizing an Illumina NovaSeq platform. Each sample produced a total of 20 million Paired-End reads. Quality control was performed using FastQC (Andrews, 2010). Sequenced reads were then filtered with the fastp (Chen et al., 2018) platform to remove adapters, unknown bases, and low-quality sequences. The cleaned reads were aligned to the 'Golden Delicious' doubled-haploid apple reference transcriptome via Salmon inference (Patro et al., 2017).

Differentially expressed genes (DEGs) were identified using the DESeq2 package in R (Love et al., 2014). The criteria for significance were set at an absolute log2 fold change greater than 1 and an adjusted p-value of less than 0.05, using the Benjamini and Hochberg approach. The expression profiles of all DEGs were then clustered using the ComplexHeatmap package in R.

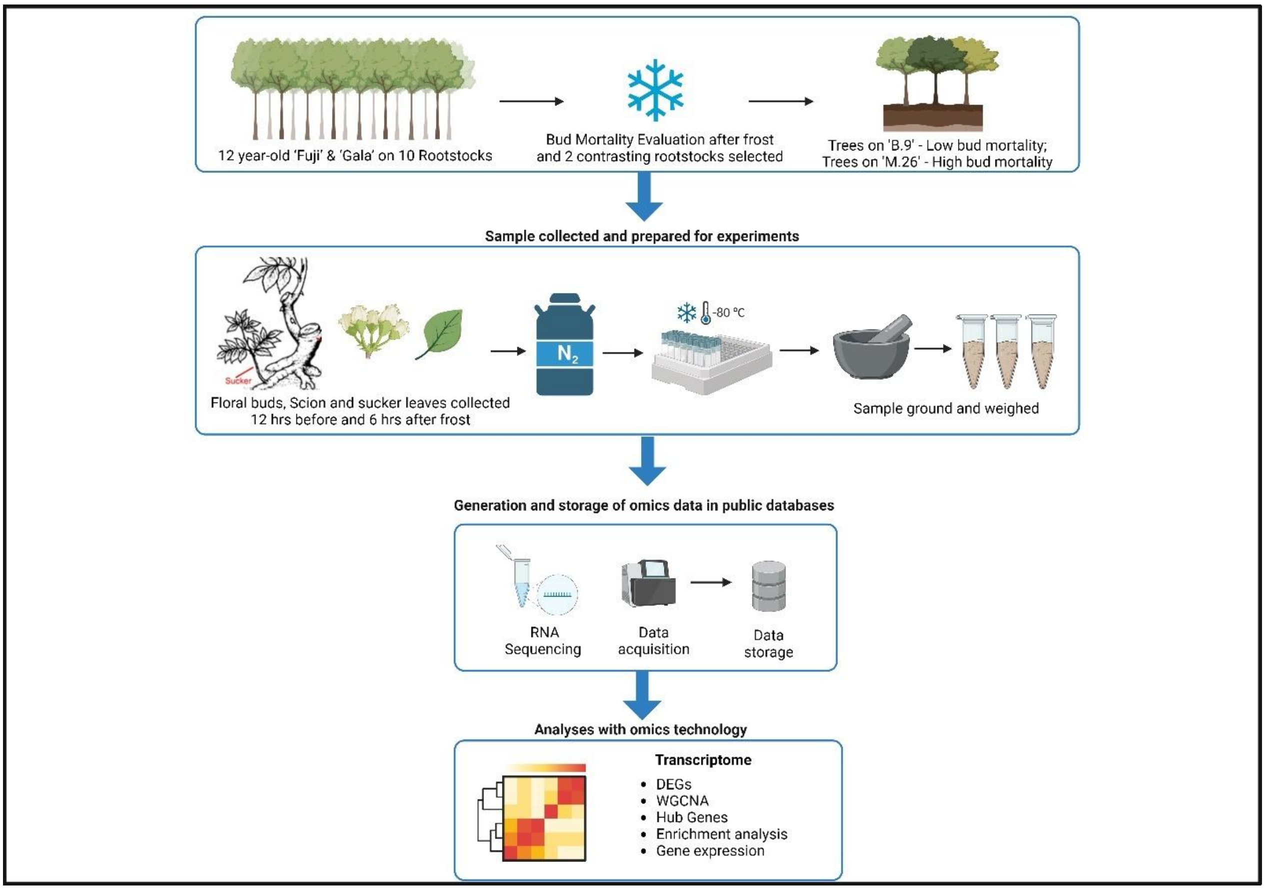

Figure 1: Schematic diagram of our experiment outline and sample collection.

2.3 Differential Co-expression and Identification of Key Modules

Modules of highly correlated genes were identified using the WGCNA with the WGCNA R package based on DESeq2 normalized gene expression data. Genes with more than 15 reads in over 75% of samples were selected, resulting in approximately 25,000 genes for the WGCNA analysis. Gene expression profiles were hierarchically clustered into modules using Pearson's correlation module eigengene. Genes within the same module shared similar expression patterns. The genes within each module were analyzed using the "heatmap" function in R. Modules showing significant correlations with frost events were selected for further analysis.

2.4 Identifying Hub Genes and Protein-Protein Interaction

In the co-expression network, each node represents a gene, and each edge represents an interaction between genes. Alterations in the expression of hub genes can significantly impact the network. Genes with high connectivity were prioritized as hub genes based on their module membership (kME). Genes with a kME ≥ 0.9 were identified as hub genes. These hub genes were analyzed for protein-protein interactions using Cytoscape (Maere et al., 2005).

2.5 Enrichment Analysis

Functional annotation and pathway enrichment analysis were conducted using the web-based tool Database for Annotation, Visualization and Integrated Discovery (DAVID), version 6.8

(Huang et al., 2009) (Fig. 5E, Table S1). This analysis focused on Gene Ontology (GO) terms and Kyoto Encyclopedia of Genes and Genomes (KEGG) pathway enrichment for a subset of 165 hub genes. The Arabidopsis homologs of these genes served as the input for the DAVID platform. The enrichment results were visualized using SRplot, generating bubble plots to effectively highlight significant GO terms and pathways (Tang et al., 2023).

2.6 Gene Expression Analysis by qRT-PCR

The DNase-treated RNA previously used for RNA-Seq was also employed for gene expression analyses. cDNA synthesis was conducted using the High-Capacity cDNA Reverse Transcription Kit (Applied Biosystems, Waltham, MA, USA) according to the manufacturer's instructions. The resulting complementary DNA (cDNA) was diluted 10-fold for subsequent qRT-PCR. We focused on the most significant hub genes, exhibiting $|Log2FoldChange| \geq 1$ and $padj < 0.05$, which were either highly upregulated or downregulated and were implicated in the pathways that were significantly enriched in the functional annotation analysis depicted in Figure 5E. Primers were designed using Primer3Plus software (Untergasser et al., 2007) to ensure specificity and efficiency, and their details are provided in Table S3. Primer specificity was confirmed through melting curve analysis, with each primer pair showing a distinct single peak, indicating their appropriateness for qRT-PCR. The qRT-PCR assays were performed on the CFX Connect Real-Time PCR Detection System (Bio-Rad Laboratories, Inc., Hercules, California, USA) using Fast EvaGreen® qPCR Master Mix (Biotium, Fremont, CA, USA). The standard cycling parameters were set as follows: initial denaturation at 90°C for 5 minutes, followed by 40 cycles of denaturation at 95°C for 20 seconds and annealing at 60°C for 20 seconds.

Gene expression levels were normalized to two reference genes, *MdActin* (Zhou et al., 2017) and *MdGAPDH* (Malladi and Hirst, 2010). The genes used were: *MdAFP3-1* (MD09G1067200), *MdAFP3-2* (MD16G1060400), *MdCBF4* (MD04G1067800), *MdHSFC1* (MD02G1046900), *MdARM* (Armadillo repeat superfamily protein) (MD06G1177100), *MdF-BOX* (MD03G1267000), *MdEXP_8* (MD07G1233100), *MdHXXXD* (MD16G1108700), *MdWBC11* (MD05G1042600), *MdLRR-RK* (MD06G1100200), *MdTRANSMEMBRANEPROTEIN* (MD13G1028100), and *MdRPK2* (MD13G1062000) (Fig. 6, 7). Detailed information about these genes is presented in Table S4, including full name, accession number, functional domain and relevant references.

Normalized expression was calculated relative to the control samples ('B.9' suckers before frost, separately for 'Gala' and 'Fuji') using the CFX Manager software (Bio-Rad). These results were analyzed using R version 4.2.2 to validate the RNA-Seq findings (Table S2).

2.7 Statistical Analyses

Statistical analyses of flower mortality rate and gene expression profiling data were performed using the R statistical computing software. Tukey's Honestly Significant Difference (HSD) test was utilized to compare the means of three biological replicates ($n = 3$) for gene expression, and 30 flowers ($n=30$) collected from three trees for bud mortality rate, with a statistical significance level of $P \leq 0.05$. For gene expression analysis, ANOVA analyses were performed, comparing the expression levels of a given gene between pre- and post-frost conditions for ‘B.9’ and ‘M.26’ as well as between ‘B.9’ and ‘M.26’ at a given condition. For bud mortality rate, percent bud mortality was compared among all the 10 rootstocks using student t-test.

3 Results

3.1 Frost Stress Conditions, Sample Collection and Bud Mortality Differences in Rootstocks

Frost damage was evaluated in floral buds of 'Gala' and 'Fuji' apple cultivars grafted onto ten distinct rootstocks across three consecutive growing seasons (2021–2023). In spring 2021, two discrete natural frost events occurred on April 3 and April 22, characterized by reduced air temperatures of –3.33°C (duration: 3 hours) and further dropping to –3.89°C (duration: 1 hour), and –6.1°C (duration: over 30 minutes), respectively (Fig. 2a). These events, usually associated with reduced dew point, induced observable tissue damage. Following the initial frost exposure, floral buds were collected from 'Gala' and 'Fuji' scions grafted onto the ten rootstocks for mortality assessment. At the time of collection, buds were at the half-inch green developmental stage, as defined by the Michigan State University phenological scale (Chapman and Catlin, 1976; Michigan State University Extension, 2021). Despite recorded temperatures not reaching the established 90 % bud mortality threshold for this developmental stage, significant inter-rootstock variation in bud mortality was observed. Specifically, 'Gala' and 'Fuji' scions grafted onto 'B.9' exhibited significantly lower bud mortality in both king (central) and side flowers, with 'Gala' side flowers showing negligible mortality, whereas 'M.26' grafted scions displayed among the highest mortality rates (Table 1). Importantly, the observed frost tolerance of 'B.9' was not due to any delay in flower development, as no visible differences in flower developmental stages on the two cultivars across different rootstocks were observed (Fig. S1; S2). These observations necessitated further investigation into the physiological mechanisms underlying the observed differential frost susceptibility. For subsequent molecular and physiological analyses, 'B.9' and 'M.26' rootstocks, demonstrating contrasting frost response (Fig. 2D), were selected. In anticipation of the second frost event on April 22, 2021, samples were collected from 'Gala' and 'Fuji' trees grafted onto 'B.9' and 'M.26' rootstocks. Samples included 'Gala' floral buds, 'Gala' scion leaves, and rootstock sucker leaves (B.9, M.26), collected at 12 h pre-frost and 6 h post-frost (minimum temperature: –6.1 °C, duration: over 30 min), a condition posing a severe risk of 90 % bud mortality for flower clusters in full bloom stage. Three trees per scion-rootstock combination were randomly selected, each serving as independent biological replicates. These samples were subsequently utilized for RNA-Seq and qRT-PCR analyses.

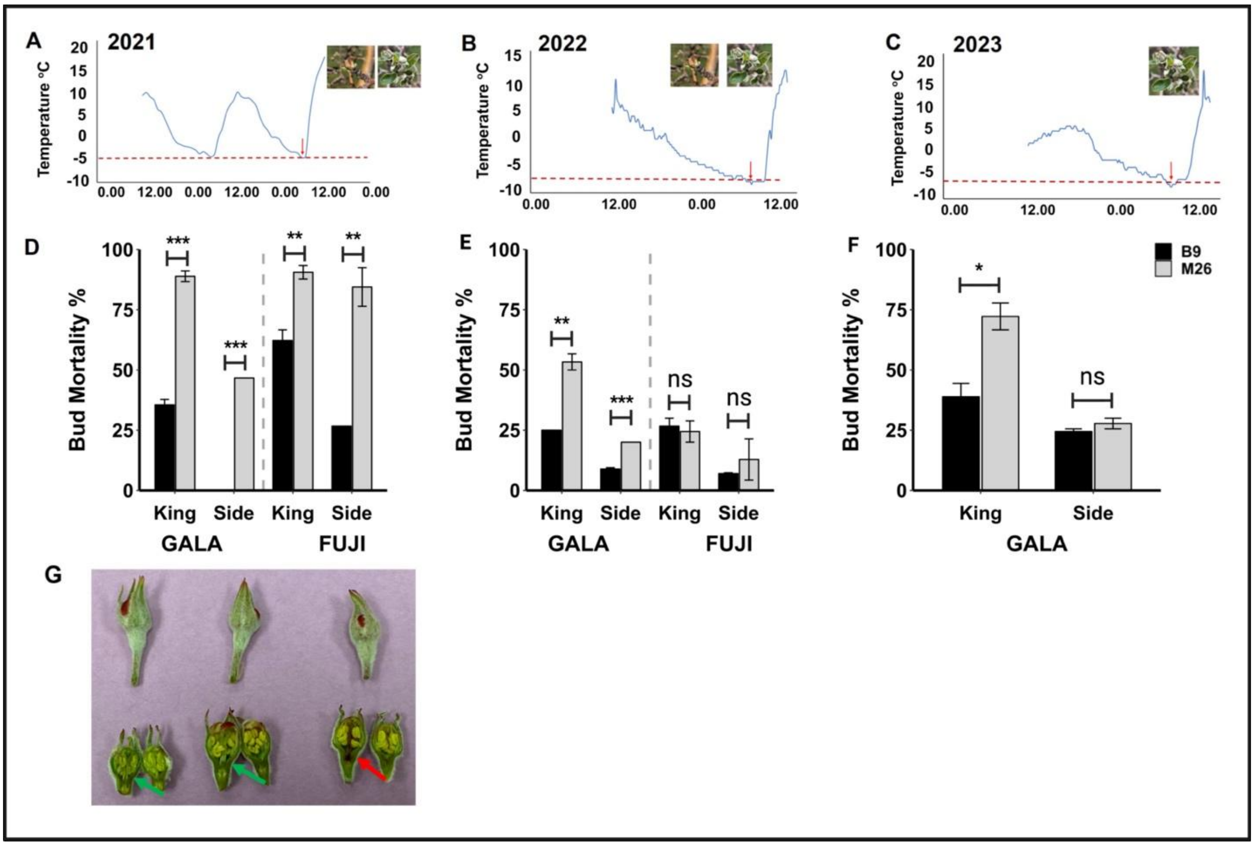

Figure 2: Percent bud mortality and corresponding weather data over three consecutive growing seasons. Recorded temperatures and durations causing damage were –6.1°C for 30 minutes in 2021 (**A)** –8.3°C for over 2.5 hours in 2022 (**B)** and –7.78°C for 1 hour and 20 minutes in 2023 (**C).** The red vertical dotted line refers to the critical temperature threshold at which 90% apple buds during their critical developmental stages were killed. Percentage of bud mortality of 'Gala' and 'Fuji' cultivars grafted onto 'B.9' and 'M.26'rootstocks after frost events in 2021 (**D)**, 2022 (**E**) and 2023 (**F**), respectively. Data represents the mean ± se (*n=30*) flowers. Asterisk ns,*,**,*** represent non-significant and significant differences from ANOVA analysis among rootstocks at $P = 0.05, 0.01, 0.001$, respectively, using Tukey's Honestly Significant Difference (HSD) test. **(G)** represents the longitudinal sections of apple flowers, assessing the potential frost damage. Green arrows denote surviving, while red arrows indicate dead flower's style and ovary.

Table 1: Bud mortality (%) of the apple cultivars 'Fuji' and 'Gala' grafted on ten different rootstocks after the late spring frost incidents of the year 2021, 2022 and 2023. Data represent the mean ± SE (n=3) flowers with rootstocks sharing different letters are significantly different at $p < 0.05$, according to two-way ANOVA and Tukey's Honestly Significant Difference (HSD) test.

		Bud mortality (%)																			
		King flower mortality (%)										Side flower mortality (%)									
Rootstock		B.9	M.26	G.935	G.11	G.16	G.30	G.41	M.7	M.9	M.111	B.9	M.26	G.935	G.11	G.16	G.30	G.41	M.7	M.9	M.111
	2021																				
Scion	Fuji	60 ± 3.84 b	98.88 ± 14.94 a	86.66 ± 3.84 ab	68.88 ± 5.87 ab	91.11 ± 5.87 ab	91.11 ± 5.87 ab	93.33 ± 3.84 ab	100 ± 3.84 a	96.66 ± 3.33 a	75.55 ± 9.68 ab	28.88 ± 2.22 c	88.88 ± 16.02 b	77.77 ± 2.22 ab	55.55 ± 2.22 abc	75.55 ± 5.87 ab	88.88 ± 5.87 b	71.11 ± 2.22 ab	55.55 ± 4.44 abc	51.11 ± 5.87 ac	78.88 ± 6.75 ab
Scion	Gala	35.55 ± 2.22 c	86.66 ± 3.84 ab	77.77 ± 2.22 ab	84.44 ± 2.22 ab	62.22 ± 4.44 ac	88.88 ± 5.87 ab	82.22 ± 2.22 ab	71.11 ± 5.87 ab	68.88 ± 4.44 ab	96.66 ± 13.47 b	0.0 ± 0.0 d	44.44 ± 2.22 c	42.22 ± 2.22 c	73.33 ± 0 a	64.44 ± 4.44 a	35.55 ± 2.22 bc	24.44 ± 2.22 b	35.55 ± 2.22 bc	60 ± 3.84 a	75 ± 5 a
	2022																				
Scion	Fuji	26.66 ± 3.33 a	20.74 ± 0.74 a	31.11 ± 1.11 a	25.26 ± 4.73 a	30 ± 0 a	76.66 ± 3.33 b	48.18 ± 4.29 c	30 ± 0 a	89.62 ± 0.37 b	22.85 ± 2.85 a	7.00 ± 0.34 a	13.52 ± 8.25 a	41.17 ± 29.43 a	7.26 ± 0.11 a	20.83 ± 9.61 a	71.42 ± 30.81 a	44.84 ± 27.62 a	15.87 ± 2.08 a	44.89 ± 4.91 a	6.95 ± 2.07 a
Scion	Gala	25 ± 0 d	53.33 ± 3.33 ac	31.11 ± 1.11 bd	43.61 ± 8.28 abc	43.33 ± 3.33 abc	36.66 ± 3.33 abd	20 ± 0 d	53.33 ± 3.33 ac	56.66 ± 3.33 c	60 ± 0 c	8.88 ± 0.55 a	20 ± 0 bc	20 ± 0 bc	9.44 ± 0.55 a	27.14 ± 2.85 b	18.88 ± 1.11 bc	19.39 ± 0.60 bc	20 ± 0 bc	46.66 ± 3.33 d	12.77 ± 3.64 ac
	2023																				
Scion	Gala	33.33 ± 0 a	77.77 ± 5.55 cd	66.66 ± 0 bc	50 ± 0 ab	44.44 ± 5.55 a	66.66 ± 0 bc	72.22 ± 5.55 cd	66.66 ± 0 bc	88.88 ± 5.55 d	77.77 ± 5.55 cd	23.33 ± 1.94 b	28.88 ± 1.11 b	26.66 ± 1.92 b	6.66 ± 0 a	10 ± 0 a	23.33 ± 1.92 b	3.33 ± 0 a	43.33 ± 1.92 d	58.88 ± 2.93 c	58.88 ± 2.93 c

Our evaluations of bud mortality over these three years consistently demonstrated superior frost tolerance in 'Gala' and 'Fuji' cultivars grafted onto 'B.9' compared to those grafted onto other ten rootstocks tested in this study, including ‘M.26’. However, despite the increased bud mortality rate in 'M26', due to the increased sampling variation, no statistically significant differences were observed in the 2022 dataset. For further molecular analyses of rootstock-scion combinations, we utilized 'Gala' grafted onto 'B.9' and 'M.26' as model systems. Given the strong annual bearing habit of 'Gala' and its consequent high economic value, these combinations were selected to investigate transcriptomic changes (RNA-Seq) in relatively tolerant and sensitive scion-rootstock interactions, respectively. The transcriptomic data generated from these 'Gala' apple studies were subsequently validated using qRT-PCR analyses on both 'Gala' and 'Fuji' trees grafted onto these two rootstocks.

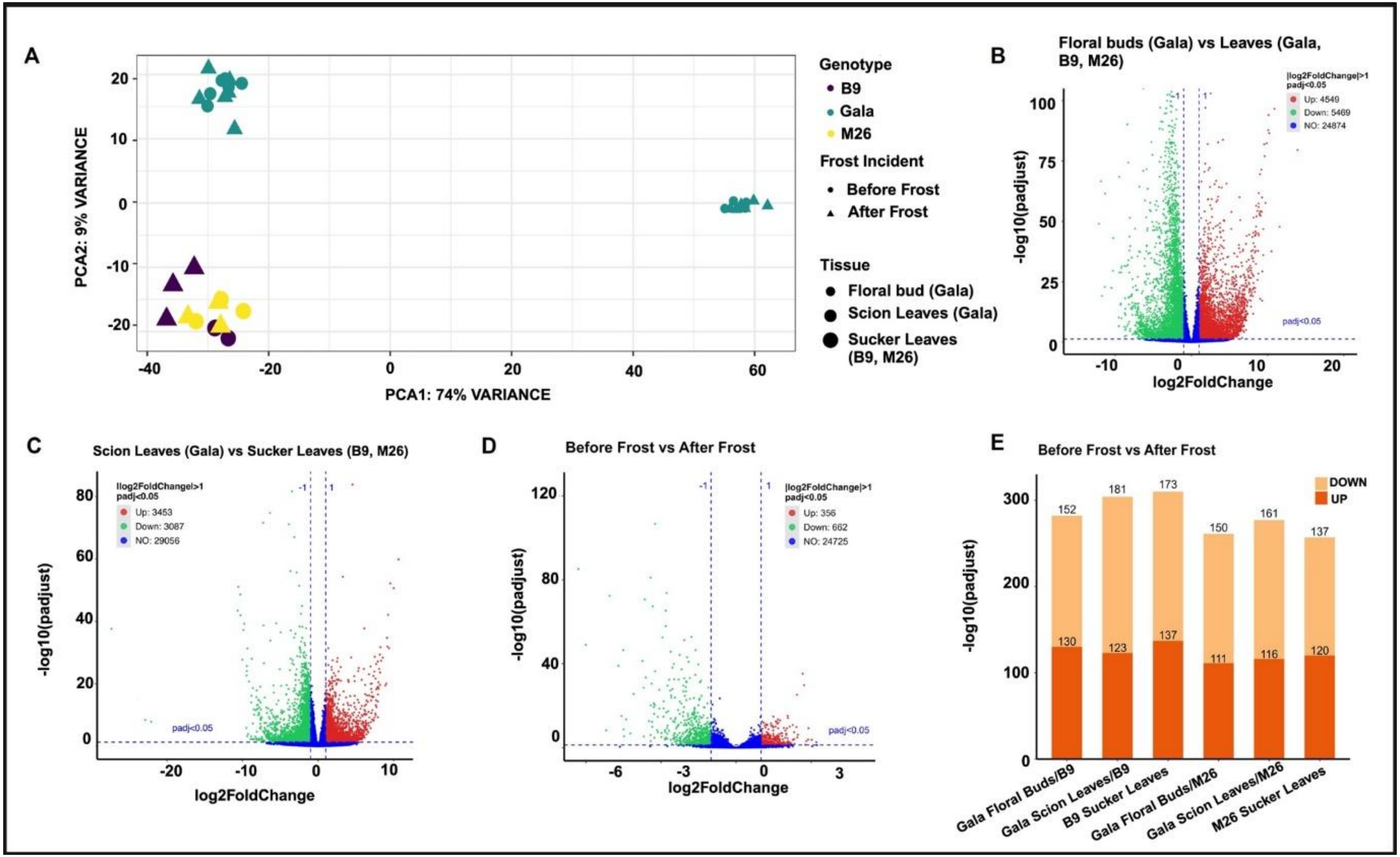
A
Genotype
B9
Gala
M26
Frost Incident
Before Frost
After Frost
Tissue
Floral bud (Gala)
Scion Leaves (Gala)
Sucker Leaves (B9, M26)
PCA2: 9% VARIANCE
PCA1: 74% VARIANCE
B
Floral buds (Gala) vs Leaves (Gala, B9, M26)
|log2FoldChange|>1
padj<0.05
Up: 4549
Down: 5469
NO: 24874
-log10(padjust)
log2FoldChange
C
Scion Leaves (Gala) vs Sucker Leaves (B9, M26)
|log2FoldChange|>1
padj<0.05
Up: 3453
Down: 3087
NO: 29056
D
Before Frost vs After Frost
|log2FoldChange|>1
padj<0.05
Up: 356
Down: 662
NO: 24725
E
Before Frost vs After Frost
DOWN
UP
Gala Floral Buds/B9
Gala Scion Leaves/B9
B9 Sucker Leaves
Gala Floral Buds/M26
Gala Scion Leaves/M26
M26 Sucker Leaves

Figure 3: Schematic overview of transcriptome analysis. (**A)** principal component analysis, containing rootstocks, tissue types and sampling time (before and after frost event). Differentially Expressed Genes (DEGs) are depicted from floral buds ('Gala') vs leaves (scion leaves from 'Gala' and sucker leaves from rootstocks 'B.9' and 'M.26') (**B**), scion leaves ('Gala') vs sucker leaves ('B.9' and 'M.26') (**C)**, and before frost vs after frost **(D)**. DEGs are considered significant having $\log_2$|(fold change)|> 1 and padj ≤0.05. (**E)** indicates number of DEGs expressed at each scion-rootstock compared between before and after frost event.

3.2 Transcriptome Sequencing and Identification of DEGs

We examined gene expression profiles in floral buds and scion leaves of 'Gala' trees, as well as leaves from 'B.9' and 'M.26' root-suckers, before and after exposure to the frost event in 2021. Utilizing the high-throughput capabilities of the Illumina paired-end sequencing platform, we generated more than 20 million paired-end reads per sample. Remarkably, the mapping efficiency to the apple reference genome surpassed 90%, ensuring robust data fidelity for subsequent analyses.

A principal component analysis (PCA) was employed to distill the multidimensional gene expression data, effectively segregating the samples along two principal axes. The first principal component (PC1) accounted for 74% of the total variance, delineating the gene expression differences between floral buds ('Gala') and leaf tissues (scion leaves from 'Gala' and sucker leaves from 'B.9' and 'M.26'). The second principal component (PC2), accounting for an additional 9% of the variance, provided clear demarcation between scion-derived tissues (floral buds and leaves from 'Gala') and rootstock sucker leaves ('B.9', 'M.26') (Fig. 3A).

DEGs were identified using a conservative significance cutoff of |Log2FoldChange| ≥1 and padj < 0.05. The comparative analysis revealed a substantial number of DEGs between floral buds and leaves, with 4,549 upregulated and 5,469 downregulated genes (Fig. 3B). Furthermore, comparisons of leaf tissue types uncovered 3,453 upregulated and 3,087 downregulated DEGs, underscoring the distinct transcriptional profiles between scion and sucker leaves (Fig. 3C). The comparison of conditions before versus after frost exposure revealed 356 upregulated and 662 downregulated DEGs, highlighting the transcriptomic impact of frost stress as evidenced by the greater number of DEGs (Fig. 3D). The DEG count plots for each experimental combination quantitatively illustrated the variability in gene expression changes, with a high degree of specificity observed for each unique combination (Fig. 3E). Using hierarchical clustering, the statistically significant DEGs were investigated to determine their expression patterns across all samples. Based on the expression levels of these DEGs, clustering of all samples revealed twelve separate groups corresponding to different sampling tissue types, genotypes, and frost conditions (Fig. 4A). Notably, the expression profiles in floral buds, both before and after frost, were significantly distinguishable from those in scion leaves and rootstock sucker leaves, also showing more pronounced clustering. The transcriptomic analysis, enriched with Venn diagrams, identified variations in the number of DEGs for each combination, as presented in Fig. 4B. The findings indicate high numbers of DEGs were unique to combinations between tissue types, but only a few DEGs were unique between before vs. after frost and between 'B.9' vs 'M.26' combinations.

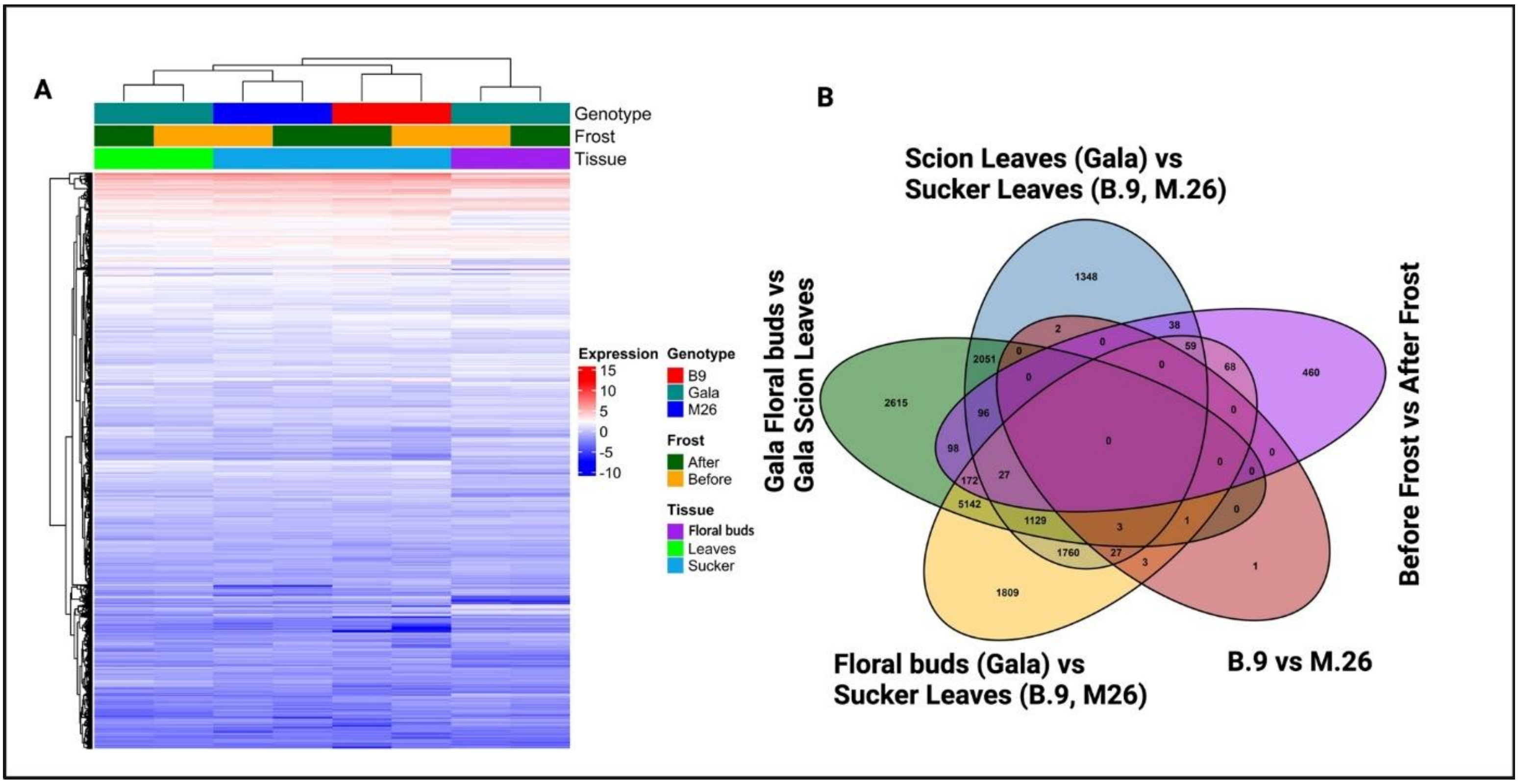

Figure 4: Hierarchical cluster analysis and Venn Diagrams for DEGs of genotypes, tissue types and frost incident. **A** Heatmap visualization of transcriptomic profiles. Rows correspond to individual transcripts, while columns represent different groups or samples. The color intensity reflects the gene expression levels (log2(NormalizedCounts+1)) among the different groups. The heatmap highlights the differentially expressed genes, identified based on their significant fold changes (|log2FoldChange| > 1) and adjusted p-values (p-adj< 0.05), with blue color indicating downregulation and red color representing upregulation. **B** Venn Diagram showing DEGS among different comparisons: floral buds (‘Gala’) vs scion leaves (‘Gala’); scion leaves (‘Gala’) vs sucker leaves (‘B.9’ and ‘M.26’); before vs after frost event, floral buds (‘Gala’) vs sucker leaves (‘B.9’ and ‘M.26’) and rootstock suckers ‘B.9’ vs ‘M.26’.

3.3 Identification of Hub Genes and Modules by Weighted Gene Co-expression Network Analysis

WGCNA was employed to identify significant modules, construct a gene co-expression network, and isolate hub genes. This method systematically groups genes exhibiting co-expression patterns correlated with specific traits or factors, facilitating a targeted analysis of genetic influences on observed biological phenomena. To gain a comprehensive understanding of the molecular mechanisms underlying cold tolerance in apples, genes were filtered with the criterion of ≥15 reads across at least 75% of the samples. The resultant 25,000 filtered genes from our RNAseq analysis were input into the WGCNA software R package (Langfelder and Horvath, 2008) to build a gene co-expression network. Pairwise correlation analyses of gene expression identified 18 merged co-expression modules, each marked with different colors. Three of these modules were significantly correlated with frost conditions (Fig. 5A). For instance, the ME 6 showed a significant negative correlation before frost (R = –0.69 and *P*-value ≤ 0.05) and a positive correlation after frost (R = 0.69 and P-value ≤ 0.05). The ME 7 was significantly negatively correlated with conditions before the frost (R = –0.98 and *P*-value ≤ 0.001) and positively correlated with conditions after the frost (R = 0.98 and *P*-value ≤ 0.001). The ME 9 was significantly positively correlated with conditions before frost (R = 0.61 and *P*-value ≤ 0.05) and negatively correlated after frost (R = –0.61 and P-value ≤ 0.05). Genes within each of these modules are clustered and co-expressed in response to the frost event. This indicates that modules exhibiting a positive correlation with the pre-frost condition contain genes that are upregulated before the frost event. Conversely, modules showing a positive correlation with the post-frost condition encompass genes that were downregulated before the frost and upregulated after frost events.

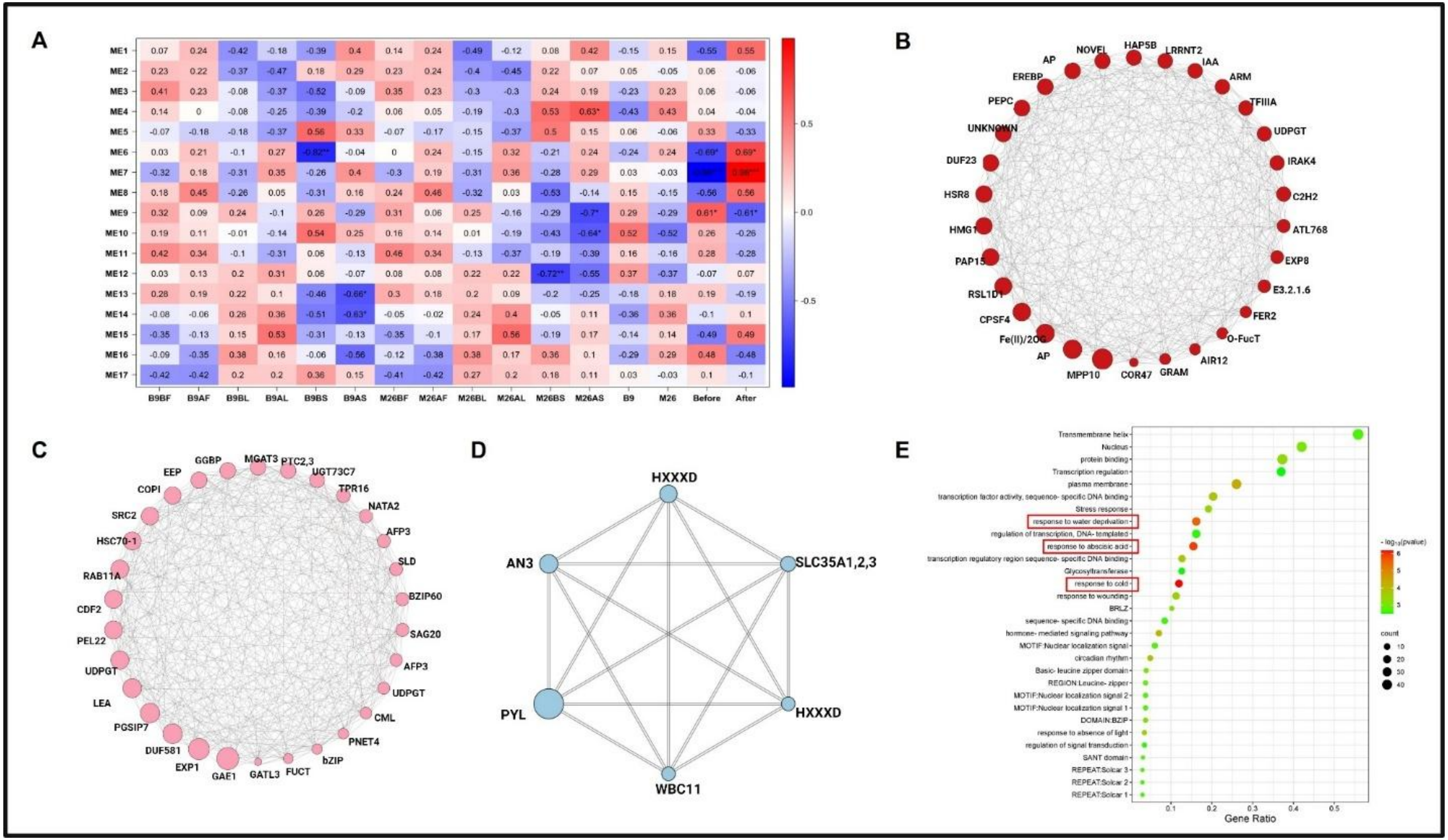

A
ME1 0.07 0.24 -0.42 -0.18 -0.39 0.4 0.14 0.24 -0.49 -0.12 0.08 0.42 -0.15 0.15 -0.55 0.55
ME2 0.23 0.22 -0.37 -0.47 0.18 0.29 0.23 0.24 -0.4 -0.45 0.22 0.07 0.05 -0.05 0.06 -0.06
ME3 0.41 0.23 -0.08 -0.37 -0.52 -0.09 0.35 0.23 -0.3 -0.3 0.24 0.19 -0.23 0.23 0.06 -0.06
ME4 0.14 0 -0.08 -0.25 -0.39 -0.2 0.06 0.05 -0.19 -0.3 0.53 0.63* -0.43 0.43 0.04 -0.04
ME5 -0.07 -0.18 -0.18 -0.37 0.56 0.33 -0.07 -0.17 -0.15 -0.37 0.5 0.15 0.06 -0.06 0.33 -0.33
ME6 0.03 0.21 -0.1 0.27 -0.82** -0.04 0 0.24 -0.15 0.32 -0.21 0.24 -0.24 0.24 -0.69* 0.69*
ME7 -0.32 0.18 -0.31 0.35 -0.26 0.4 -0.3 0.19 -0.31 0.36 -0.28 0.29 0.03 -0.03
ME8 0.18 0.45 -0.26 0.05 -0.31 0.16 0.24 0.46 -0.32 0.03 -0.53 -0.14 0.15 -0.15 -0.56 0.56
ME9 0.32 0.09 0.24 -0.1 0.26 -0.29 0.31 0.06 0.25 -0.16 -0.29 -0.7* 0.29 -0.29 0.61* -0.61*
ME10 0.19 0.11 -0.01 -0.14 0.54 0.25 0.16 0.14 0.01 -0.19 -0.43 -0.64* 0.52 -0.52 0.26 -0.26
ME11 0.42 0.34 -0.1 -0.31 0.06 -0.13 0.46 0.34 -0.13 -0.37 -0.19 -0.39 0.16 -0.16 0.28 -0.28
ME12 0.03 0.13 0.2 0.31 0.06 -0.07 0.08 0.08 0.22 0.22 -0.72** -0.55 0.37 -0.37 -0.07 0.07
ME13 0.28 0.19 0.22 0.1 -0.46 -0.66* 0.3 0.18 0.2 0.09 -0.2 -0.25 -0.18 0.18 0.19 -0.19
ME14 -0.08 -0.06 0.26 0.36 -0.51 -0.63* -0.05 -0.02 0.24 0.4 -0.05 0.11 -0.36 0.36 -0.1 0.1
ME15 -0.35 -0.13 0.15 0.53 -0.31 -0.13 -0.35 -0.1 0.17 0.56 -0.19 0.17 -0.14 0.14 -0.49 0.49
ME16 -0.09 -0.35 0.38 0.16 -0.06 -0.56 -0.12 -0.38 0.38 0.17 0.36 0.1 -0.29 0.29 0.48 -0.48
ME17 -0.42 -0.42 0.2 0.2 0.36 0.15 -0.41 -0.42 0.27 0.2 0.18 0.11 0.03 -0.03 0.1 -0.1
B9BF B9AF B9BL B9AL B9BS B9AS M26BF M26AF M26BL M26AL M26BS M26AS B9 M26 Before After
0.5
0.0
-0.5
B
NOVEL HAP5B LRRNT2 IAA ARM TFIIIA UDPGT IRAK4 C2H2 ATL768 EXP8 E3.2.1.6 FER2 O-FucT AIR12 GRAM COR47 MPP10 AP Fe(II)/2OG CPSF4 RSL1D1 PAP15 HMG1 HSR8 DUF23 UNKNOWN PEPC EREBP AP
C
MGAT3 PTC2,3 UGT73C7 TPR16 NATA2 AFP3 SLD BZIP60 SAG20 AFP3 UDPGT CML PNET4 bZIP FUCT GATL3 GAE1 EXP1 DUF581 PGSIP7 LEA UDPGT PEL22 CDF2 RAB11A HSC70-1 SRC2 COPI EEP GGBP
D
HXXXD
SLC35A1,2,3
HXXXD
WBC11
PYL
AN3
E
Transmembrane helix
Nucleus
protein binding
Transcription regulation
plasma membrane
transcription factor activity, sequence- specific DNA binding
Stress response
response to water deprivation
regulation of transcription, DNA- templated
response to abscisic acid
transcription regulatory region sequence- specific DNA binding
Glycosyltransferase
response to cold
response to wounding
BRLZ
sequence- specific DNA binding
hormone- mediated signaling pathway
MOTIF:Nuclear localization signal
circadian rhythm
Basic- leucine zipper domain
REGION:Leucine- zipper
MOTIF:Nuclear localization signal 2
MOTIF:Nuclear localization signal 1
DOMAIN:BZIP
response to absence of light
regulation of signal transduction
SANT domain
REPEAT:Solcar 3
REPEAT:Solcar 2
REPEAT:Solcar 1
0.1 0.2 0.3 0.4 0.5
Gene Ratio
count
10
20
30
40

Figure 5: Weighted Gene Co-expression Network Analysis (WGCNA) of floral buds (Gala), scion leaves (Gala) and sucker leaves of 'B.9' and 'M.26' rootstocks before and after frost events. (**A**) Module–sample relationships. Each row corresponds to a module eigengene, each column corresponds to a trait, and each cell consists of the corresponding correlation and asterisks if significant, where *,**,*** represent significant. The topmost significant hub genes from ME 6 (**B**) ME 7 (**C**) and ME 9 (**D**) modules are presented. **(E)** represents gene ontology (GO) enrichment analysis of Hub genes. BF: before frost floral buds, AF: after frost floral buds; BL: before frost leaves, AL: after frost leaves; BS: before frost sucker leaves, AS: after frost sucker leaves.

After selecting modules with significant correlation coefficients with the traits, we further filtered the gene lists with the DEGs identified between the 'before frost' and 'after frost' conditions. ME 6 and 7 comprised 1,210 and 1,011 genes, respectively, including 151 and 381 DEGs in each. These modules exhibited genes with mean eigenvalues showing lower expression before the frost that peaked after the event. In contrast, ME 9, containing just 163 genes, included 6 DEGs exhibiting a pattern contrary to the aforementioned modules after the frost.

To delve into the network's hub genes, we applied a 90% Module eigengene-based connectivity (kME) threshold, selecting genes with an increased degree of connectivity in the ME 6 (30 genes), ME 7 (129 genes), and ME 9 (6 genes). Notably, genes involved in abiotic stress processes were identified, including AFP3, genes related to cold acclimation, and lipid metabolism, namely, HXXXD and WBC11. These hub genes from the ME 6, 7 and 9 were used to construct a protein-protein interaction (PPI) network as depicted in Fig. 5B, C, and D, respectively. This network provides a visual and analytical representation of the interactions and potential regulatory pathways influenced by these genes, elucidating their collective role in the plant's response to cold stress and laying a foundational understanding for future studies targeting the improvement of cold tolerance in apple cultivars.

3.4 Functional Annotation of Hub genes

To ascertain the KEGG pathway-enriched genes and the potential GO classification, terms approximating biological process, molecular functions, and signaling pathways concerning KEGG pathways were used. DAVID facilitated the functional annotation and enrichment analysis, serving as a crucial tool for interpreting the biological significance of these genes. A threshold of adjusted p-value ≤ 0.05 was used to define significance of the GO terms. Our findings reveal a pronounced enrichment in GO terms associated with 'response to abscisic acid' (GO:0009737), 'response to cold' (GO:0009409), and 'response to water deprivation' (GO:0009414), as depicted in the bubble plot (Fig. 5E). The significance of these pathways was determined based on the –log10(p-value), with a higher value indicating greater statistical significance, underscoring the integral role of these pathways in the plant's adaptive responses to frost stress.

3.5 Gene expression analyses by qRT-PCR

In this study, we explored the differential expression of twelve key hub genes identified through qRT-PCR utilizing both 'Gala' and 'Fuji' cultivars. 'Fuji' tissue was employed to validate the expression profiling data of these genes obtained from 'Gala' tissue. These genes, selected for their significant regulatory changes with a |log2 fold change| ≥ 1, include *MdAFP3-1* (MD09G1067200), *MdAFP3-2* (MD16G1060400), *MdCBF4* (MD04G1067800), *MdHSFC1* (MD02G1046900), *MdARM* (Armadillo repeat superfamily protein) (MD06G1177100), *MdF-BOX* (MD03G1267000), *MdEXP_8* (MD07G1233100), *MdHXXXD* (MD16G1108700), *MdWBC11* (MD05G1042600), *MdLRR-RK* (MD06G1100200), *MdTRANSMEMBRANEPROTEIN* (MD13G1028100), and *MdRPK2* (MD13G1062000) (Fig. 6, 7). Detailed information about these genes is presented in Table S4, including full name, accession number, functional domain and relevant references.

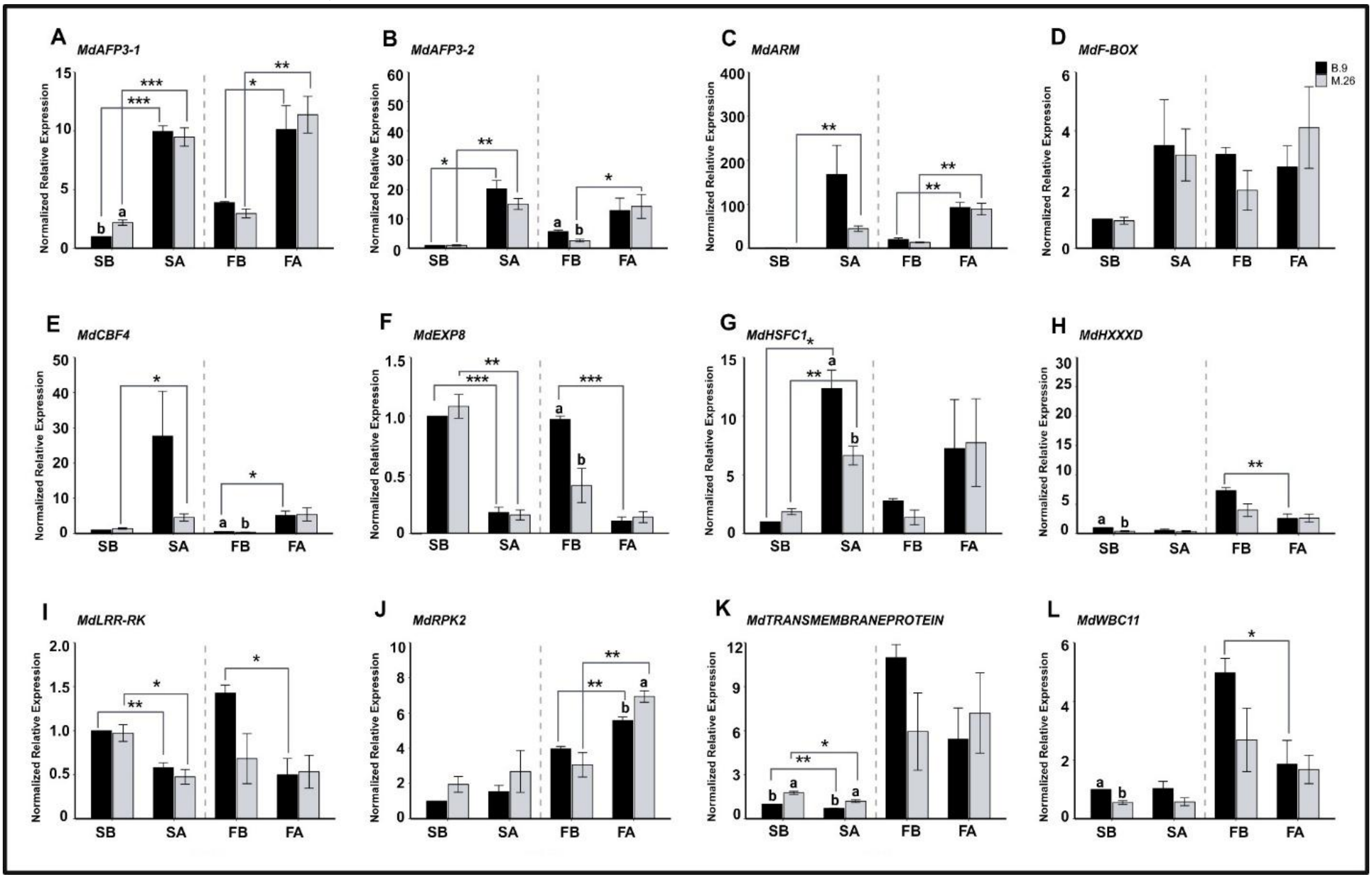

Figure 6: Expression profile of **A**, *MdAFP3-1* (MD09G1067200) **B**, *MdAFP3-2* (MD16G1060400) **C**, *MdARM* (MD06G1177100) D *MdF-BOX* (MD03G1267000) **E**, *MdCBF4* (MD04G1067800) **F**, *MdEXP_8* (MD07G1233100) **G**, *MdHSFC1* (MD02G1046900) **H**, *MdHXXXD* (MD16G1108700) **I**, *MdLRR-RK* (MD06G1100200) **J**, *MdRPK2* (MD13G1062000) **K**, *MdTRANSMEMBRANE PROTEIN* (MD13G1028100) and **L**, *MdWBC11* (MD05G1042600) genes in 'Gala' grafted on 'B.9' and 'M.26'. The expression of each gene was normalized to that of two reference genes (*MdActin* and *MdGAPDH*) and then calculated relative to the expression level in the control sample ('SB' for 'Gala'). Error bars represent the standard error of the means of three biological and two technical replicates. Asterisk *,**,*** represent significant differences from ANOVA analysis comparing the expression levels of a given gene between pre- and post-frost conditions for each rootstock at $P = 0.05, 0.01, 0.001$, respectively; and the alphabets

represent ANOVA analysis between ‘B.9’ and ‘M.26’ at a given condition, using Tukey's Honestly Significant Difference (HSD) test. The dashed vertical line separates sucker leaves samples from floral bud tissue. SB: Suckers Before Frost event, SA: Suckers After Frost incident; FB: Floral buds Before Frost event and FA: Floral Buds After Frost incident

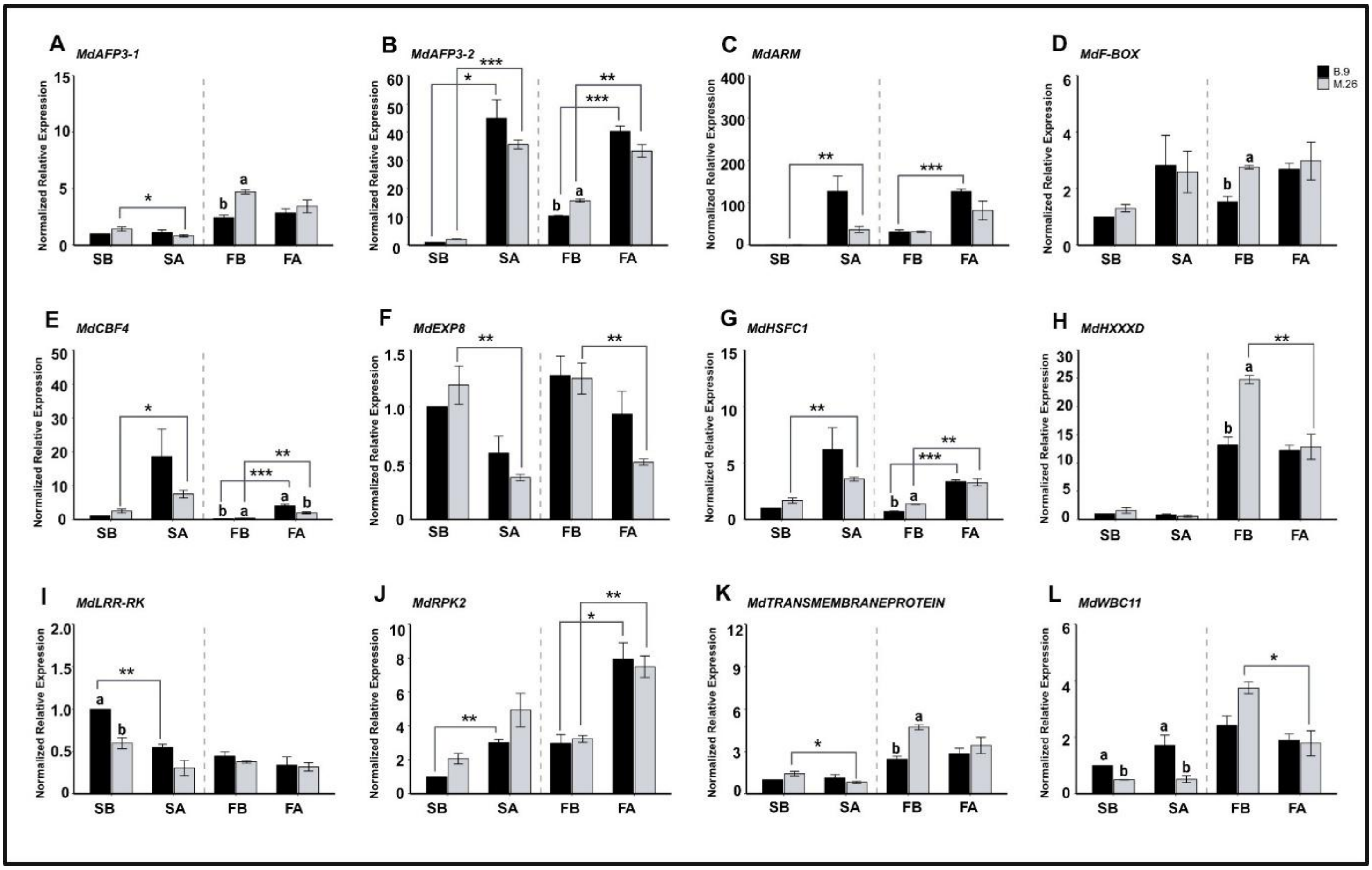

Figure 7: Expression profile of **A** *MdAFP3-1* (MD09G1067200) **B** *MdAFP3-2* (MD16G1060400) **C** *MdARM* (MD06G1177100) **D** *MdF-BOX* (MD03G1267000) **E** *MdCBF4* (MD04G1067800) **F** *MdEXP_8* (MD07G1233100) **G** *MdHSFC1* (MD02G1046900) **H** *MdHXXXD* (MD16G1108700) **I** *MdLRR-RK* (MD06G1100200) **J** *MdRPK2* (MD13G1062000**)** **K** *MdTRANSMEMBRANE PROTEIN* (MD13G1028100) and **L** *MdWBC11* (MD05G1042600) genes in ‘Fuji’ grafted on ‘B.9’ and ‘M.26’. The expression of each gene was normalized to that of two reference genes (*MdActin* and *MdGAPDH*) and then calculated relative to the expression level in the control sample (‘SB’ for ‘Fuji’). Error bars represent the standard error of the means of three biological and two technical replicates. Asterisk *,**,*** represent significant differences from ANOVA analysis comparing the expression levels of a given gene between pre- and post-frost conditions for each rootstock at $P = 0.05, 0.01, 0.001$, respectively; and the alphabets represent ANOVA analysis between ‘B.9’ and ‘M.26’ at a given condition, using Tukey's Honestly Significant Difference (HSD) test. The dashed vertical line separates sucker leaves samples from floral bud tissue. SB: Suckers Before Frost event, SA: Suckers After Frost incident; FB: Floral buds Before Frost event and FA: Floral Buds After Frost incident

Starting with *MdAFP3-1* (Fig. 6A; 7A), there was a significant increase in expression in 'Gala' suckers after frost on both rootstocks. Notably, 'M.26' exhibited higher basal expression compared to 'B.9'. Similarly, in floral buds, the expression increased after frost, with 'M.26' showing slightly higher levels than 'B.9'. In 'Fuji', suckers on 'M.26' exhibited higher expression than those on 'B.9' after frost, and floral buds on 'M.26' had a higher baseline expression as well.

For *MdAFP3-2* (Fig. 6B; 7B), expression was significantly upregulated in 'Gala' suckers after frost, particularly on 'M.26'. Floral buds also showed an increase in expression post-frost, with 'B.9' exhibiting higher baseline expression before frost. However, post-frost, only 'M.26' showed significant upregulation. In 'Fuji', suckers on 'M.26' demonstrated a significant increase in expression after frost, and there was a significant difference between 'B.9' and 'M.26', with 'M.26' having a higher increase than 'B.9'. The baseline expression was lower in floral buds on 'B.9', and post-frost expression significantly increased in both rootstocks.

Moving to *MdARM* (Fig. 6C; 7C), there was a substantial upregulation in 'Gala' suckers after frost on both rootstocks, though 'M.26' exhibited significant higher expression. 'B.9' also showed an increase, but it was not significant. In floral buds, both 'B.9' and 'M.26' displayed significant increases in expression after frost. In 'Fuji', suckers on 'M.26' showed significant upregulation post-frost, with 'B.9' also showing an increase, though it was not statistically significant. Floral buds on 'B.9' showed a significant increase in expression post-frost.

MdCBF4 (Fig. 6E; 7E) showed an increase in expression post-frost in 'Gala' suckers on 'B.9', although the increase was not significant, whereas 'M.26' exhibited a significant increase in expression. Baseline expression significantly less in 'M.26' floral buds before frost, and post-frost, there was a significant increase in expression on 'B.9' with no significant change observed on 'M.26'. In 'Fuji', there was a significant upregulation post-frost in suckers on 'M.26', with 'B.9' showing a more pronounced but not statistically significant increase. The baseline expression in floral buds on 'B.9' was significantly lower, but the increase post-frost was more significant compared to 'M.26'.

For *MdEXP8* (Fig. 6F; 7F), in 'Gala', there was a significant decrease in expression post-frost in suckers on both rootstocks, with a greater reduction observed on 'B.9'. Similarly, there was a significant decrease in expression in floral buds post-frost on both rootstocks, with 'B.9' showing a more notable reduction, although 'B.9' had a higher baseline expression before frost. In 'Fuji', there was also a significant reduction in expression post-frost in both suckers and floral buds on 'M.26'.

MdHSFC1 (Fig. 6G; 7G) exhibited a significant increase in expression in 'Gala' suckers post-frost on both rootstocks, with 'B.9' showing higher post-frost expression compared to 'M.26'. In 'Fuji', there was significant upregulation post-frost in suckers on 'M.26' compared to 'B.9', although 'B.9' showed a higher increase that was not statistically significant. In floral buds, there was a notable difference in expression regardless of frost, with 'M.26' showing significantly higher expression, though post-frost, 'B.9' exhibited a significantly more pronounced increase.

MdHXXXD (Fig. 6H; 7H) in 'Gala' showed significantly higher expression in suckers before frost on 'B.9' compared to 'M.26'. In case of floral buds, after frost, there was a significant reduction in expression on 'B.9'. In 'Fuji', floral buds on 'M.26' had significantly higher expression before frost compared to 'B.9', and after frost, there was a significantly higher decline in expression on 'M.26'.

In the case of *MdLRR-RK* (Fig. 6I; 7I), 'Gala' showed a significant decrease in expression post-frost in suckers on 'B.9' compared to 'M.26'. Floral bud expression also significantly decreased post-frost on 'B.9' compared to 'M.26'. In 'Fuji', the expression was higher in suckers on 'B.9' before frost, but there was also a significant decrease post-frost.

For *MdRPK2* (Fig. 6J; 7J), in 'Gala', there was a significant increase in expression post-frost in floral buds on both 'B.9' and 'M.26', with 'M.26' showing significantly higher expression than 'B.9'. In 'Fuji', there was a significant increase in expression post-frost in suckers on 'B.9', and in floral buds, there was a significant increase in expression on both rootstocks.

MdTRANSMEMBRANEPROTEIN (Fig. 6K; 7K) in 'Gala' showed higher expression in suckers on 'M.26' before and after frost, with a significant decrease in expression post-frost on both rootstocks. In 'Fuji', there was a significant decrease in expression in suckers on 'M.26' compared to 'B.9'; and in its floral buds the baseline expression on floral buds on ‘M.26’ was higher as compared to ‘B.9’.

Lastly, for *MdWBC11* (Fig. 6L; 7L), in 'Gala', floral bud expression post-frost significantly decreased on 'B.9' compared to 'M.26'. In 'Fuji', there was higher baseline expression in suckers on 'B.9' both before and after frost. In floral buds, there was a significant decrease in expression on 'M.26' post-frost.

It is noteworthy that the Pearson correlation coefficients between RNA-Seq and qRT-PCR data for the twelve genes associated with the ICE (Inducer of CBF expression)-CBF-COR pathway, ABA signaling, lipid metabolism, cell wall integrity, and protein kinase signaling were positive and significant ($P < 0.01$) for all genes except two (*MdHSFC1* and *MdRPK2*).

4 Discussion

Frost, a specific form of cold stress, is caused by the formation of ice crystals within or on plant tissues under freezing conditions, which may be induced by advective cold air masses or radiative cooling under clear skies (Leske and Biddulph, 2022). This phenomenon represents a significant agricultural threat by causing extensive damage to crops (Jahed et al., 2023). Apple trees, for example, have developed sophisticated strategies to withstand such conditions (He et al., 2018; Liu et al., 2019). Our study moves beyond traditional methods that utilize plant cuttings in controlled settings, which fail to capture the full spectrum of adaptive responses. Instead, we examined 12-year-old mature apple trees that have encountered natural frost events, offering unique insights into the inherent adaptive mechanisms these trees use in real-world conditions and illustrating the complex interaction of genetic and environmental factors affecting frost tolerance.

Our analysis covered two apple cultivars, 'Fuji' and 'Gala', grafted onto ten different rootstocks over three years and exposed to three natural frost events expected to cause significant damage (Table 1). Results consistently showed that floral buds on scions grafted to ‘B.9’ rootstocks exhibited low mortality rates after frost events compared to those on other rootstocks. Numerous studies have documented the influence of rootstocks on the phenology of floral bud development in peaches, noting variations in bloom dates (Young and Houser, 1980; Durner and Goffreda, 1992; Beckman et al., 1992), while such effects were not observed in apples (Racskó et al., 2004; Tworkoski and Miller, 2007). Our findings from the 2021 and 2022 growing seasons also indicate minimal differences in the developmental stages of floral buds across various rootstocks, as illustrated in Fig. S1 and S2. Highlighting the stage of floral bud development is crucial because it directly impacts how the buds respond to different critical temperatures. For instance, apple floral buds at the silver-tip stage, marked by a slight separation and a shimmery gray appearance, can withstand temperatures down to –17.6˚C, whereas in the post-bloom stage, there is a risk of 90% floral bud mortality at temperatures around –3˚C (Jahed et al., 2023).

Our transcriptomic analysis employed RNA-Seq to explore how these different tissues respond to frost stress. The PC1, which captured 74% of the variance, revealed significant differences in gene expression between the floral buds and leaf tissues, indicative of their unique adaptations to frost. The PC2 contributed an additional 9% to the variance, distinguishing further between scion-derived tissues and sucker leaves (Fig. 3A). This highlights the variability in genetic responses based on tissue origin, reflecting the complex genetic dynamics at play. A study by Kumari et al. (2015) supports this complexity, demonstrating distinct biosynthetic and stress response pathways in scion versus rootstock. These pathways involve various secondary metabolites and stress response genes, each uniquely activated depending on the tissue's genetic background and environmental interactions.

Building on these insights, we noted that numerous DEGs were specific to particular tissue types, though fewer were uniquely expressed when comparing pre- and post-frost conditions or between the ‘B.9’ and ‘M.26’ rootstocks. To deepen our understanding of the molecular regulation of frost tolerance in apple trees, we employed WGCNA analysis (Fig. 5A). This analysis helped us identify significant modules and hub genes that correlate strongly with frost exposure (Fig. 5B, C, D). Further analysis of these hub genes revealed a pronounced enrichment in GO terms related to response to abscisic acid, cold, and water deprivation (Fig. 5E, Table S1). Among the hub genes, key genes involved in cold acclimation—such as *MdCBF4* and *MdHSFC1* were further examined by qRT-PCR. Our results indicate significant variations in the expression of these genes across different tissues in cultivars grafted onto the 'B.9' rootstock (Fig. 6, 7). This suggests a genetic predisposition in these cultivars to activate cold-responsive pathways prior to frost events (Zhao et al., 2016; Liu and Sherif, 2019).

The ICE-CBF-COR pathway plays a crucial role in defense against cold stress, involving key components such as ICE, CBF transcription factors, and COR proteins (Hwarari et al., 2022). CBF4 is particularly notable for its unique kinetic response, displaying a slower but more sustained induction compared to other CBFs, which is essential for cold acclimation in plants including kiwi, garden strawberry, and grapevines (Siddiqua and Nassuth, 2011; Takuhara et al., 2011; Koehler et al., 2012; Tillett et al., 2012; Cai et al., 2019). It regulates genes critical for membrane fluidity, osmotic adjustment, and the production of cryoprotective proteins and soluble sugars, all of which enhance freezing tolerance (Shi et al., 2022; Jahed et al., 2023). Additionally, the overexpression of CBFs, especially CBF4, markedly increases cold tolerance by elevating levels of antioxidant enzymes like catalase (CAT), ascorbate peroxidase (APX), peroxidase (POD), and superoxide dismutase (SOD). These enzymes are crucial in reducing oxidative stress markers such as electrolyte leakage, malondialdehyde, hydrogen peroxide, and superoxide anion, thereby protecting plant cells from damage (Sun et al., 2019; Hu et al., 2020; Ritonga et al., 2021). Our analysis indicates that *MdCBF4* is upregulated in 'B.9' grafted cultivars (Fig. 6E; 7E), probably playing a key role in maintaining reactive oxygen species (ROS) at levels conducive to plant health.

Our study also highlights the role of heat shock factors (HSFs), particularly *MdHSFC1*, in managing cold stress through a regulatory pathway distinct from CBFs. HSFs regulate heat shock proteins (HSPs), initiating a multi-chaperone network essential for plant survival under various stress conditions. The interaction between HSFs and the ROS signaling pathway, particularly through respiratory burst oxidase homologues (RBOHs) proteins, illustrates a complex network that governs the production of antioxidant enzymes (Park et al., 2018; ul Haq et al., 2019; Abdullah et al., 2022; Sohrabi et al., 2022).

There is mounting evidence that plant hormones, particularly ABA signaling, are central to the response to low-temperature stress. Notably, the overexpression of *CBF4* not only enhances freezing tolerance but also suggests potential interactions between ABA-dependent and ABA-independent pathways (Haake et al., 2002; Guttikonda et al., 2014; Vonapartis et al., 2022). Our enrichment analysis supports this, revealing a significant response to ABA that underscores its pivotal role in the molecular mechanisms underpinning frost tolerance (Fig. 5E, Table S1).

Our findings highlight the important roles of ABI5 Binding Proteins, specifically *MdAFP3*-1 (MD09G1067200), in modulating cold stress responses in apple varieties. We observed a significant increase in *MdAFP3-1* and *MdAFP3-2* expression following cold exposure, which aligns with ABA's role in stress perception and response (Fig. 6A, B; 7A, B). Interestingly, the increased AFP expression suggests a feedback inhibition mechanism, portraying AFPs as negative regulators in the ABA signaling pathway, a finding supported by their identification in yeast two-hybrid screens using ABI5 as bait (Lopez-Molina et al., 2003; Lynch et al., 2017). This feedback mechanism, which prevents overaccumulation of ABA and mitigates excessive stress responses, is vital for maintaining cellular homeostasis and fine-tuning the plant's response to cold stress while supporting growth and development.

Furthermore, the observed increase in *MdAFP3* expression in tissue types of cultivars on the susceptible 'M.26' rootstock suggests a higher basal expression of this negative regulator. This pattern indicates that inherently lower ABA production in susceptible cultivars may be a fundamental factor in their vulnerability to frost, revealing a limitation in ABA-mediated stress responses that compromises their ability to effectively initiate cold acclimation processes. In contrast, cultivars on the 'B.9' rootstock show higher endogenous ABA levels under osmotic stress conditions (Hezema et al., 2021), correlating with a lower expression of *MdAFP3* in 'B.9' suckers and suggesting an enhanced ability to tolerate frost through an ABA-dependent pathway (Fig. 6A, B; 7A, B). Importantly, this interpretation is supported by Lordan et al. (2017), who demonstrated that the 'B.9' rootstock conferred significantly higher ABA concentrations to the scion xylem sap compared to other rootstocks when using the cultivar 'Honeycrisp'. Their findings further reinforce our observations that rootstock-modulated hormonal dynamics, particularly ABA levels, play a critical role in the scion's ability to cope with abiotic stress. Interestingly, the 'B.9' rootstock is also known for its distinctive red pigmentation in its leaves, a trait derived from its parentage involving red-leaved selections (Sampson and Cameron, 1965; Zwintzscher, 1973; Cummins and Aldwinckle 1983). Historical breeding records suggest that this pigmentation is controlled by dominant genes, with some studies indicating a link between red wood coloration and anthocyanin accumulation (Usova, 1973; Cummins and Aldwinckle 1983). Anthocyanins are well-established antioxidants that can mitigate oxidative stress induced by cold temperatures (Zhang et al., 2019), suggesting that the red pigmentation observed in 'B.9' may confer an added protective advantage under cold stress. This genetic predisposition for higher anthocyanin content could have further contributed to the improved frost stress tolerance observed in scions grafted on 'B.9', complementing its enhanced ABA-mediated responses.

Armadillo (ARM) repeat proteins, first identified in Drosophila's Wingless/Wnt pathway, are evolutionarily conserved and play significant roles in the biology of various plant species including *Physcomitrella patens*, *Arabidopsis thaliana*, and *Oryza sativa* (Nüsslein-Volhard and Wieschaus, 1980; Mudgil et al., 2004; Sharma et al., 2014). These proteins are involved in ubiquitination processes mediated by U-box E3 ubiquitin ligases, targeting proteins for degradation, which is crucial in plant stress responses (Sharma et al., 2014). Our research shows approximately 150-fold increase in expression of Armadillo-related proteins (*MdARM*; MD06G1177100) under frost stress, indicating the activation of ubiquitination pathways essential for both biotic and abiotic stress adaptation (Fig. 6C; 7C). ARM/U-box proteins also participate in transcriptional regulation by forming complexes with key components like Arabidopsis arm repeat protein (ARIA) with a broad complex, tramtrak, and bric-a-brac/poxvirus and zinc finger (BTB/POZ) domain and ABSCISIC ACID RESPONSE ELEMENT-BINDING FACTOR2 (ABF2), a crucial transcription factor in ABA signaling.

The role of genes involved in lipid metabolism and membrane fluidity, which are critical for a cultivar's ability to withstand cold stress has also been investigated in the present study (Uemura and Steponkus, 1999; Sapkota et al., 2023). The lipid composition and membrane fluidity are vital for maintaining cellular integrity and function under freezing temperatures, as they significantly influence the plant's stress response due to changes in membrane permeability and fluidity (Jahed et al., 2023). We investigate the expression dynamics of the *MdWBC11* gene (MD05G1042600), also known as ABCG11, an ATP Binding Cassette (ABC) transporter, across different tissues and grafting conditions within apple varieties, focusing on the cold stress response (Fig. 6L; 7L). Notably, 'Fuji' apples on 'B.9' rootstock show higher *MdWBC11* expression in sucker tissues compared to those on 'M.26', highlighting its role in enhancing membrane fluidity and stress tolerance (Fig. 7L). In general, the expression of *WBC11* is more pronounced in floral buds than in suckers, indicating tissue-specific patterns and confirming its significant role in the aerial parts of plants. This aligns with findings on its homologs *ZxABCG11* and *AtABCG11*, which are primarily expressed in above-ground organs (Bird et al., 2007; Hwang et al., 2016; Liu et al., 2021). These transporters are crucial in plant stress adaptation, transporting essential lipids for cuticle development—a protective layer composed of wax and cutin that shields against environmental threats (Luo et al., 2007; Seo and Koshiba, 2011; Dhara and Raichaudhuri, 2021). Moreover, ABA-induced upregulation of WBC11 underscores its importance in cuticle reinforcement to reduce non-stomatal water loss, enhancing plant tolerance against environmental stress (Luo et al., 2007). These findings highlight the critical role of ABCG transporters in abiotic stress response and emphasize ABA's central role in this process, suggesting that modulation of *MdWBC11* expression by ABA's regulatory mechanisms is key to plant cold stress adaptation.

The role of HXXXD/BAHD-type acyl-transferase family proteins, key in synthesizing extracellular lipids for the protective cuticular wax layer against environmental stresses, is underlined by their varying expression among apple cultivars and rootstocks. These proteins play a critical role in cold stress adaptation, though their specific roles in cold response remain to be fully elucidated (Molina and Kosma, 2015). Notably, the expression of *MdHXXXD* (MD16G1108700) is significantly lower in 'Gala' than in 'Fuji', suggesting varietal differences in cold stress mechanisms (Fig. 6H; 7H). Additionally, 'Gala' grafted onto the 'B.9' rootstock shows higher *MdHXXXD* expression before frost compared to those on 'M.26', indicating rootstock-dependent responses (Fig. 6H). HXXXD acyltransferases are also crucial for synthesizing and modifying a range of metabolites, enhancing plant resistance to various stresses, including UV radiation and cold. For example, the rice acyltransferase (*OsAt10*) has demonstrated enhanced cold tolerance across species by boosting antioxidative activities and polyamine levels, making it a valuable resource for breeding (de Oliveira et al., 2015; Tohge et al., 2016; Tang and Thompson, 2022; Xu et al., 2023). Interestingly, 'Fuji' grafted onto the susceptible 'M.26' rootstock exhibited increased *MdHXXXD* expression in floral buds (Fig. 7H) compared to 'Gala', highlighting not only varietal differences but also tissue-specific responses to frost. These findings align with previous research indicating varied responses of HXXXD-type acyl-transferase proteins under cold conditions and their importance in apple cultivation under varying crop loads (Hao et al., 2018; Milyaev et al., 2021; Onyemaobi et al., 2022).

Our analysis revealed that expansin A8 (*MdExp_8*; MD07G1233100) expression was significantly higher in the floral buds of both cultivars grafted on the cold-tolerant 'B.9' rootstock compared to those on 'M.26' (Fig. 6F; 7F). This finding suggests a link between expansin gene expression and biophysical adaptations in plant biomembranes across different rootstocks. Expansins are critical in the plant's response to environmental stresses, aiding in cell wall flexibility which is essential during acclimation to cold and sub-zero temperatures (Choi et al., 2006; Marowa et al., 2016; Chen et al., 2019). Despite increases in *MdExp_8* expression under cold conditions in 'B.9', there was a notable decline in expression post-frost across all tissues and genotypes. This reduction may be attributed to the plant shifting to energy conservation modes under stress, decreasing energy-intensive expansin production to allocate resources to essential survival processes. Moreover, there's a greater need for cell wall stabilization through the accumulation of rigid components, reducing the demand for expansin-mediated cell wall loosening. Research has shown that short-term exposure (12 to 48 hours) of *Arabidopsis thaliana* to 4°C suppresses genes involved in cell expansion (Hannah et al., 2005; Tenhaken, 2015), while prolonged exposure activates genes related to matrix polysaccharides and cell wall remodeling enzymes, which can vary the rigidity of the cell wall depending on the tissue involved (Tenhaken, 2015; Panter et al., 2020). This nuanced response underscores the role of protein kinases as central components in the plant's adaptation to abiotic stresses (Chaffai et al., 2024).

Our study also identified elevated expression levels of protein kinases such as receptor-like protein kinase 2 (*MdRPK2*; MD13G1062000), also known as TOAD2, and an unnamed transmembrane protein (*MdTRANSMEMBRANE PROTEIN*; MD13G1028100), presumed to be part of the Plasma membrane intrinsic protein (PIP) family, in response to frost in tissues of 'Gala' and 'Fuji' on the cold-susceptible 'M.26' rootstock (Fig. 6J, K; 7J, K). This expression pattern indicates a genetically programmed response to cold stress, consistent across various frost incidents.

MdRPK2, known for its role in embryonic and radial pattern formation, appears to be crucial for the plant's cold stress response, potentially shifting resource allocation from defense to support growth and development under stress (Nodine et al., 2007). This is particularly pronounced in cold-sensitive cultivars, highlighting their reliance on RPK2-mediated pathways for growth during cold stress. Additionally, the presumed role of PIPs is supported by the increased expression of a transmembrane protein after frost (Fig. 6K; 7K), aligning with known functions of PIPs in cold adaptation. For instance, *RcPIP1;3* and *RcPIP2;2* are known to increase in response to cold in various species, enhancing water transport and cellular hydration, while the downregulation of *RcPIP2;1* is linked to stomatal closure mechanisms to prevent dehydration (Zou et al., 2016; Zhou et al., 2022). Further comparisons with transgenic tobacco studies, where aquaporin overexpression (a member of the PIP family) resulted in decreased drought resistance due to faster wilting, suggest that heightened PIP levels following frost may similarly affect cold tolerance (Aharon et al., 2003; Nouri and Komatsu, 2013). Thus, in cold-sensitive varieties, an increase in PIP expression could theoretically enhance growth and transpiration under optimal conditions but might exacerbate cold susceptibility by altering water management and inducing osmotic stress.

Our research also highlights the significant role of Brassinosteroid Insensitive 1 (BRI1), a member of the Leucine-Rich Repeat Receptor-Like Kinase (LRR-RLK) family, in the perception and signaling of brassinosteroids (BRs), which are crucial for plant growth, development, and stress adaptation (Nolan et al., 2017; Soltabayeva et al., 2022). We observed that the basal expression of BRI1 (*MdLRR-RLK*; MD06G1100200) was elevated prior to the frost incident but decreased under all conditions following the frost, indicating a dynamic regulation of BR signaling in response to cold stress (Fig. 6I; 7I). This change underscores the complex interactions within and between different hormonal pathways, emphasizing BRI1's role in the integrated network of plant hormone signaling. Specifically, BRI1 facilitates crosstalk with the ABA pathway through interactions with components like ABI1 (ABA INSENSITIVE 1), a phosphatase crucial for ABA-induced responses such as stomatal closure. This interaction highlights the intricate relationship between BR and ABA pathways in plant stress responses. Additionally, BRI1's engagement with other hormonal pathways, including those involving auxins and jasmonic acid (JA), demonstrates the multifaceted role of LRR-RLKs in phytohormone signaling. These kinases interact with various signaling partners such as ABSCISIC ACID-INSENSITIVE2 (ABI2), FERONIA (FER), and OsRPK1, regulating a broad range of plant responses to environmental stimuli, impacting root architecture, auxin distribution, and stress responses (Bulgakov and Avramenko, 2020).

5 Conclusion

In conclusion, our research provides crucial insights into frost tolerance mechanisms in apple trees, with a particular focus on specific genes, gene expression dynamics, and the interplay between environmental and genetic factors. To our knowledge, this study is the first to investigate the transcriptomic response of a fruit tree species to natural frost events, representing a significant advancement in agricultural genomics. We have identified critical pathways and genetic mechanisms that enhance resilience to frost, highlighting the complex interactions among molecular, physiological, and biochemical processes. Our findings confirm the essential role of the 'B.9' rootstock in boosting frost tolerance through the upregulation of pivotal genes such as *MdCBF4* and *MdHSFC1*, which activate cold-responsive pathways, thereby enhancing the adaptability of apple trees to freezing temperatures. Furthermore, our study reveals the crucial role of interactions between heat shock factors and the ROS signaling pathway in managing stress responses, complemented by the integration of ABA signaling components such as ABI5 Binding Proteins. Additionally, we have demonstrated the importance of lipid metabolism and membrane fluidity, with genes like *MdWBC11* and *MdHXXXD* showing tissue- and rootstock-dependent expression that is vital for maintaining cellular integrity under stress conditions. These findings suggest that different apple cultivars and rootstocks may employ unique strategies to cope with cold stress. This knowledge could be instrumental in breeding programs aimed at enhancing frost resilience in apple varieties. Looking forward, we encourage further research to delve into the intricate networks of stress responses at a deeper molecular level and to evaluate the practical applications of these discoveries in improving frost management practices in apple cultivation.

CRediT authorship contribution statement

Amolpreet Kaur Saini: Writing – Original Draft, Visualization, Formal analysis, Software, Investigation, Data Curation. **Khalil Jahed:** Writing - Review & Editing, Software, Data Curation. **Deisiany F. Neres:** Software. **Clay Wright:** Writing - Review & Editing, Funding acquisition, Supervision. **Sherif M. Sherif:** Conceptualization, Methodology, Validation, Resources, Writing - Review & Editing, Supervision, Project administration.

Funding

This project was partially funded by the United States Department of Agriculture National Institute of Food and Agriculture grant 2022-67013-36293.

Acknowledgments

We would like to express our gratitude to Drs. Jiayang Liu and Md. Tabibul Islam for their invaluable assistance with sample collection, preservation, and preparation. We also thank Mr. Kenneth Savia for his valuable contribution in orchard management and Dr. Diana McHenry for her assistance with lab management. Additionally, we acknowledge the Statistical Application and Innovation Group (SAIG) at Virginia Tech for their indispensable assistance with statistical consulting.

Declaration of competing interest

The authors declare that the research was conducted in the absence of any commercial or financial relationships that could be construed as a potential conflict of interest.

Data Availability

The RNAseq datasets generated and analyzed during the current study have been deposited in the NCBI Sequence Read Archive (SRA). The Submission ID is SUB14526028, and the BioProject ID is PRJNA1122567.

Supplementary Data

https://github.com/Amolpreet1/Supplementary/blob/acb22a60edc6e16b013c3d8d6fb91b8df203ca76/Supplementary%20Link.docx

References

Abdullah, S.N.A., Azzeme, A.M., Yousefi, K., 2022. Fine-Tuning Cold Stress Response Through Regulated Cellular Abundance and Mechanistic Actions of Transcription Factors. Front. Plant Sci. 13. https://doi.org/10.3389/fpls.2022.850216

Aharon, R., Shahak, Y., Wininger, S., Bendov, R., Kapulnik, Y., Galili, G., 2003. Overexpression of a Plasma Membrane Aquaporin in Transgenic Tobacco Improves Plant Vigor under Favorable Growth Conditions but Not under Drought or Salt Stress. Plant Cell 15, 439–447. https://doi.org/10.1105/tpc.009225

Andrews, S., 2010. Fastqc. a quality control tool for high throughput sequence data.

AR5 Climate Change 2013: The Physical Science Basis — IPCC, n.d. URL https://www.ipcc.ch/report/ar5/wg1/ (accessed 2.4.25).

Artlip, T., McDermaid, A., Ma, Q., Wisniewski, M., 2019. Differential gene expression in non-transgenic and transgenic "M.26" apple overexpressing a peach CBF gene during the transition from eco-dormancy to bud break. Hortic Res 6, 1–16. https://doi.org/10.1038/s41438-019-0168-9

Artlip, T.S., Wisniewski, M.E., Arora, R., Norelli, J.L., 2016. An apple rootstock overexpressing a peach CBF gene alters growth and flowering in the scion but does not impact cold hardiness or dormancy. Hortic Res 3, 1–9. https://doi.org/10.1038/hortres.2016.6

Augspurger, C.K., 2013. Reconstructing patterns of temperature, phenology, and frost damage over 124 years: Spring damage risk is increasing. Ecology 94, 41–50. https://doi.org/10.1890/12-0200.1

Bahrman, N., Hascoët, E., Jaminon, O., Dépta, F., Hû, J.-F., Bouchez, O., Lejeune-Hénaut, I., Delbreil, B., Legrand, S., 2019. Identification of Genes Differentially Expressed in Response to Cold in Pisum sativum Using RNA Sequencing Analyses. Plants 8, 288. https://doi.org/10.3390/plants8080288

Beckman, T.G., Okie, W.R., Meyers, S.C., 1992. Rootstock Affect Bloom Date and Fruit Maturation of `Redhaven' Peach. https://doi.org/10.21273/JASHS.117.3.377

Bharath, P., Gahir, S., Raghavendra, A.S., 2021. Abscisic Acid-Induced Stomatal Closure: An Important Component of Plant Defense Against Abiotic and Biotic Stress. Front. Plant Sci. 12. https://doi.org/10.3389/fpls.2021.615114

Biasuz, E.C., Kalcsits, L., 2023. Rootstock effects on leaf function and isotope composition in apple occurred on both scion grafted and ungrafted rootstocks under hydroponic conditions. Front. Plant Sci. 14. https://doi.org/10.3389/fpls.2023.1274195

Bird, D., Beisson, F., Brigham, A., Shin, J., Greer, S., Jetter, R., Kunst, L., Wu, X., Yephremov, A., Samuels, L., 2007. Characterization of Arabidopsis ABCG11/WBC11, an ATP binding cassette (ABC) transporter that is required for cuticular lipid secretion. The Plant Journal 52, 485–498. https://doi.org/10.1111/j.1365-313X.2007.03252.x

Bulgakov, V.P., Avramenko, T.V., 2020. Linking Brassinosteroid and ABA Signaling in the Context of Stress Acclimation. International Journal of Molecular Sciences 21, 5108. https://doi.org/10.3390/ijms21145108

Cai, X., Magwanga, R.O., Xu, Y., Zhou, Z., Wang, X., Hou, Y., Wang, Y., Zhang, Y., Liu, F., Wang, K., 2019. Comparative transcriptome, physiological and biochemical analyses reveal response mechanism mediated by CBF4 and ICE2 in enhancing cold stress tolerance in Gossypium thurberi. AoB PLANTS 11, plz045. https://doi.org/10.1093/aobpla/plz045

Centinari, M., Smith, M.S., Londo, J.P., 2016. Assessment of Freeze Injury of Grapevine Green Tissues in Response to Cultivars and a Cryoprotectant Product. https://doi.org/10.21273/HORTSCI.51.7.856

Chaffai, R., Ganesan, M., Cherif, A., 2024. Gene Expression Regulation in Plant Abiotic Stress Response, in: Chaffai, R., Ganesan, M., Cherif, A. (Eds.), Plant Adaptation to Abiotic Stress: From Signaling Pathways and Microbiomes to Molecular Mechanisms. Springer Nature, Singapore, pp. 275–302. https://doi.org/10.1007/978-981-97-0672-3_12

Chapman, P. J., & Catlin, G. A. (n.d.). *Growth Stages in Fruit Trees—From Dormant to Fruit Set*.

Chen, D., Mubeen, B., Hasnain, A., Rizwan, M., Adrees, M., Naqvi, S.A.H., Iqbal, S., Kamran, M., El-Sabrout, A.M., Elansary, H.O., Mahmoud, E.A., Alaklabi, A., Sathish, M., Din, G.M.U., 2022. Role of Promising Secondary Metabolites to Confer Resistance Against Environmental Stresses in Crop Plants: Current Scenario and Future Perspectives. Front. Plant Sci. 13. https://doi.org/10.3389/fpls.2022.881032

Chen, R., Wang, J., Li, Y., Song, Y., Huang, M., Feng, P., Qu, Z., Liu, L., 2023. Quantifying the impact of frost damage during flowering on apple yield in Shaanxi province, China. European Journal of Agronomy 142, 126642. https://doi.org/10.1016/j.eja.2022.126642

Chen, S., Zhou, Y., Chen, Y., Gu, J., 2018. fastp: an ultra-fast all-in-one FASTQ preprocessor. Bioinformatics 34, i884–i890. https://doi.org/10.1093/bioinformatics/bty560

Chen, Y., Zhang, B., Li, C., Lei, C., Kong, C., Yang, Y., Gong, M., 2019. A comprehensive expression analysis of the expansin gene family in potato (Solanum tuberosum) discloses stress-responsive expansin-like B genes for drought and heat tolerances. PLOS ONE 14, e0219837. https://doi.org/10.1371/journal.pone.0219837

Choi, D., Cho, H.-T., Lee, Y., 2006. Expansins: expanding importance in plant growth and development. Physiologia Plantarum 126, 511–518. https://doi.org/10.1111/j.1399-3054.2006.00612.x

Cummins, J.N., Aldwinckle, H.S., 1983. Breeding Apple Rootstocks, in: Janick, J. (Ed.), Plant Breeding Reviews: Volume 1. Springer US, Boston, MA, pp. 294–394. https://doi.org/10.1007/978-1-4684-8896-8_10

de Oliveira, D.M., Finger-Teixeira, A., Rodrigues Mota, T., Salvador, V.H., Moreira-Vilar, F.C., Correa Molinari, H.B., Craig Mitchell, R.A., Marchiosi, R., Ferrarese-Filho, O., Dantas dos Santos, W., 2015. Ferulic acid: a key component in grass lignocellulose recalcitrance to hydrolysis. Plant Biotechnology Journal 13, 1224–1232. https://doi.org/10.1111/pbi.12292

De Rosa, V., Vizzotto, G., Falchi, R., 2021. Cold Hardiness Dynamics and Spring Phenology: Climate-Driven Changes and New Molecular Insights Into Grapevine Adaptive Potential. Front. Plant Sci. 12. https://doi.org/10.3389/fpls.2021.644528

Dhara, A., Raichaudhuri, A., 2021. ABCG transporter proteins with beneficial activity on plants. Phytochemistry 184, 112663. https://doi.org/10.1016/j.phytochem.2021.112663

Durner, E.F., Goffreda, J.C., 1992. Rootstock-induced Differences in Flower Bud Phenology in Peach. https://doi.org/10.21273/JASHS.117.5.690

Fazio, G., Robinson, T.L., 2022. Apple rootstocks can modulate the chilling requirements of grafted scions. Acta Hortic. 723–728. https://doi.org/10.17660/ActaHortic.2022.1346.91

Foster, T.M., McAtee, P.A., Waite, C.N., Boldingh, H.L., McGhie, T.K., 2017. Apple dwarfing rootstocks exhibit an imbalance in carbohydrate allocation and reduced cell growth and metabolism. Hortic Res 4, 1–13. https://doi.org/10.1038/hortres.2017.9

Fujisawa, M., Kobayashi, K., 2010. Apple (Malus pumila var. domestica) phenology is advancing due to rising air temperature in northern Japan. Global Change Biology 16, 2651–2660. https://doi.org/10.1111/j.1365-2486.2009.02126.x

Gautier, A.T., Chambaud, C., Brocard, L., Ollat, N., Gambetta, G.A., Delrot, S., Cookson, S.J., 2019. Merging genotypes: graft union formation and scion–rootstock interactions. Journal of Experimental Botany 70, 747–755. https://doi.org/10.1093/jxb/ery422

Genome-Wide Identification and Expression Profiles of C-Repeat Binding Factor Transcription Factors in Betula platyphylla under Abiotic Stress [WWW Document], n.d. URL https://www.mdpi.com/1422-0067/24/13/10573 (accessed 2.5.25).

Guttikonda, S.K., Valliyodan, B., Neelakandan, A.K., Tran, L.-S.P., Kumar, R., Quach, T.N., Voothuluru, P., Gutierrez-Gonzalez, J.J., Aldrich, D.L., Pallardy, S.G., Sharp, R.E., Ho, T.-H.D., Nguyen, H.T., 2014. Overexpression of AtDREB1D transcription factor improves drought tolerance in soybean. Mol Biol Rep 41, 7995–8008. https://doi.org/10.1007/s11033-014-3695-3

Haake, V., Cook, D., Riechmann, J., Pineda, O., Thomashow, M.F., Zhang, J.Z., 2002. Transcription Factor CBF4 Is a Regulator of Drought Adaptation in Arabidopsis. Plant Physiology 130, 639–648. https://doi.org/10.1104/pp.006478

Hannah, M.A., Heyer, A.G., Hincha, D.K., 2005. A Global Survey of Gene Regulation during Cold Acclimation in Arabidopsis thaliana. PLOS Genetics 1, e26. https://doi.org/10.1371/journal.pgen.0010026

Hao, X., Wang, B., Wang, L., Zeng, J., Yang, Y., Wang, X., 2018. Comprehensive transcriptome analysis reveals common and specific genes and pathways involved in cold acclimation and cold stress in tea plant leaves. Scientia Horticulturae 240, 354–368. https://doi.org/10.1016/j.scienta.2018.06.008

Harris, Z.N., Pratt, J.E., Kovacs, L.G., Klein, L.L., Kwasniewski, M.T., Londo, J.P., Wu, A.S., Miller, A.J., 2023. Grapevine scion gene expression is driven by rootstock and environment interaction. BMC Plant Biology 23, 211. https://doi.org/10.1186/s12870-023-04223-w

He, M., He, C.-Q., Ding, N.-Z., 2018. Abiotic Stresses: General Defenses of Land Plants and Chances for Engineering Multistress Tolerance. Front. Plant Sci. 9. https://doi.org/10.3389/fpls.2018.01771

Hezema, Y.S., Shukla, M.R., Ayyanath, M.M., Sherif, S.M., Saxena, P.K., 2021. Physiological and Molecular Responses of Six Apple Rootstocks to Osmotic Stress. International Journal of Molecular Sciences 22, 8263. https://doi.org/10.3390/ijms22158263

Hu, Z., Huang, X., Amombo, E., Liu, A., Fan, J., Bi, A., Ji, K., Xin, H., Chen, L., Fu, J., 2020. The ethylene responsive factor CdERF1 from bermudagrass (*Cynodon dactylon*) positively regulates cold tolerance. Plant Science 294, 110432. https://doi.org/10.1016/j.plantsci.2020.110432

Huang, D.W., Sherman, B.T., Lempicki, R.A., 2009. Systematic and integrative analysis of large gene lists using DAVID bioinformatics resources. Nat Protoc 4, 44–57. https://doi.org/10.1038/nprot.2008.211

Hufkens, K., Friedl, M.A., Keenan, T.F., Sonnentag, O., Bailey, A., O'Keefe, J., Richardson, A.D., 2012. Ecological impacts of a widespread frost event following early spring leaf-out. Global Change Biology 18, 2365–2377. https://doi.org/10.1111/j.1365-2486.2012.02712.x

Hwang, J.-U., Song, W.-Y., Hong, D., Ko, D., Yamaoka, Y., Jang, S., Yim, S., Lee, E., Khare, D., Kim, K., Palmgren, M., Yoon, H.S., Martinoia, E., Lee, Y., 2016. Plant ABC Transporters Enable Many Unique Aspects of a Terrestrial Plant's Lifestyle. Molecular Plant 9, 338–355. https://doi.org/10.1016/j.molp.2016.02.003

Hwarari, D., Guan, Y., Ahmad, B., Movahedi, A., Min, T., Hao, Z., Lu, Y., Chen, J., Yang, L., 2022. ICE-CBF-COR Signaling Cascade and Its Regulation in Plants Responding to Cold Stress. International Journal of Molecular Sciences 23, 1549. https://doi.org/10.3390/ijms23031549

Iowa State University Extension and Outreach (2024). Spray Schedule for Home Apple Trees. Iowa State University Extension and Outreach. Available at: https://hortnews.extension.iastate.edu/spray-schedule-home-apple-trees

Jahed, K.R., Saini, A.K., Sherif, S.M., 2023. Coping with the cold: unveiling cryoprotectants, molecular signaling pathways, and strategies for cold stress resilience. Front. Plant Sci. 14. https://doi.org/10.3389/fpls.2023.1246093

Kistner, E., Kellner, O., Andresen, J., Todey, D., Morton, L.W., 2018. Vulnerability of specialty crops to short-term climatic variability and adaptation strategies in the Midwestern USA. Climatic Change 146, 145–158. https://doi.org/10.1007/s10584-017-2066-1

Koehler, G., Wilson, R.C., Goodpaster, J.V., Sønsteby, A., Lai, X., Witzmann, F.A., You, J.-S., Rohloff, J., Randall, S.K., Alsheikh, M., 2012. Proteomic Study of Low-Temperature Responses in Strawberry Cultivars (*Fragaria* × *ananassa*) That Differ in Cold Tolerance. Plant Physiology 159, 1787–1805. https://doi.org/10.1104/pp.112.198267

Kreyling, J., Thiel, D., Simmnacher, K., Willner, E., Jentsch, A., Beierkuhnlein, C., 2012. Geographic origin and past climatic experience influence the response to late spring frost in four common grass species in central Europe. Ecography 35, 268–275. https://doi.org/10.1111/j.1600-0587.2011.07173.x

Kumari, A., Kumar, J., Kumar, A., Chaudhury, A., Singh, S.P., 2015. Grafting Triggers Differential Responses between Scion and Rootstock. PLoS One 10, e0124438. https://doi.org/10.1371/journal.pone.0124438

Langfelder, P., Horvath, S., 2008. WGCNA: an R package for weighted correlation network analysis. BMC Bioinformatics 9, 559. https://doi.org/10.1186/1471-2105-9-559

Lee, Y., Hoang, N.V., Do, V.G., Foster, T.M., McGhie, T.K., Kim, S., Yang, S.J., Park, J.H., Park, J., Lee, J.Y., 2023. Identification of genes associated with the regulation of cold tolerance and the RNA movement in the grafted apple. Scientific Reports 13, 11583. https://doi.org/10.1038/s41598-023-38571-2

Leske, B.A., Biddulph, T.B., 2022. Estimating Effects of Radiation Frost on Wheat Using a Field-Based Frost Control Treatment to Stop Freezing Damage. Genes 13, 578. https://doi.org/10.3390/genes13040578

Liaquat, F., Munis, M.F.H., Arif, S., Manzoor, M.A., Haroon, U., Shah, I.H., Ashraf, M., Kim, H.S., Che, S., Qunlu, L., 2022. Reprisal of Schima superba to Mn stress and exploration of its defense mechanism through transcriptomic analysis. Front Plant Sci 13, 1022686. https://doi.org/10.3389/fpls.2022.1022686

Liu, J., Sherif, S.M., 2019. Combating Spring Frost With Ethylene. Front. Plant Sci. 10. https://doi.org/10.3389/fpls.2019.01408

Liu, L., Xu, H., Zhang, W., Xing, J., Zhu, M., Zhang, Y., Wang, Y., 2023. Genome-Wide Analysis of the BAHD Family in Welsh Onion and CER2-LIKEs Involved in Wax Metabolism. Genes 14, 1286. https://doi.org/10.3390/genes14061286

Liu, L.-B., Bai, W.-P., Li, H.-J., Tian, Y., Yuan, H.-J., Garant, T.M., Liu, H.-S., Zhang, J., Bao, A.-K., Rowland, O., Wang, S.-M., 2021. ZxABCG11 from the xerophyte *Zygophyllum xanthoxylum* enhances drought tolerance in *Arabidopsis thaliana* through modulating cuticular wax accumulation. Environmental and Experimental Botany 190, 104570. https://doi.org/10.1016/j.envexpbot.2021.104570

Liu, Y., Dang, P., Liu, L., He, C., 2019. Cold acclimation by the CBF–COR pathway in a changing climate: Lessons from Arabidopsis thaliana. Plant Cell Rep 38, 511–519. https://doi.org/10.1007/s00299-019-02376-3

Lopez-Molina, L., Mongrand, S., Kinoshita, N., Chua, N.-H., 2003. AFP is a novel negative regulator of ABA signaling that promotes ABI5 protein degradation. Genes Dev 17, 410–418. https://doi.org/10.1101/gad.1055803

Lordan, J., Fazio, G., Francescatto, P., Robinson, T., 2017. Effects of apple (*Malus × domestica*) rootstocks on scion performance and hormone concentration. Scientia Horticulturae 225, 96–105. https://doi.org/10.1016/j.scienta.2017.06.050

Love, M.I., Huber, W., Anders, S., 2014. Moderated estimation of fold change and dispersion for RNA-seq data with DESeq2. Genome Biology 15, 550. https://doi.org/10.1186/s13059-014-0550-8

Luo, B., Xue, X.-Y., Hu, W.-L., Wang, L.-J., Chen, X.-Y., 2007. An ABC Transporter Gene of Arabidopsis thaliana, AtWBC11, is Involved in Cuticle Development and Prevention of Organ Fusion. Plant and Cell Physiology 48, 1790–1802. https://doi.org/10.1093/pcp/pcm152

Lynch, T.J., Erickson, B.J., Miller, D.R., Finkelstein, R.R., 2017. ABI5-binding proteins (AFPs) alter transcription of ABA-induced genes via a variety of interactions with chromatin modifiers. Plant Mol Biol 93, 403–418. https://doi.org/10.1007/s11103-016-0569-1

Ma, Q., Hu, Z., Mao, Z., Mei, Y., Feng, S., Shi, K., 2022. The novel leucine-rich repeat receptor-like kinase MRK1 regulates resistance to multiple stresses in tomato. Horticulture Research 9, uhab088. https://doi.org/10.1093/hr/uhab088

Maere, S., Heymans, K., Kuiper, M., 2005. BiNGO: a Cytoscape plugin to assess overrepresentation of Gene Ontology categories in Biological Networks. Bioinformatics 21, 3448–3449. https://doi.org/10.1093/bioinformatics/bti551

Malladi, A., Hirst, P.M., 2010. Increase in fruit size of a spontaneous mutant of 'Gala' apple (Malus×domestica Borkh.) is facilitated by altered cell production and enhanced cell size. Journal of Experimental Botany 61, 3003–3013. https://doi.org/10.1093/jxb/erq134

Marowa, P., Ding, A., Kong, Y., 2016. Expansins: roles in plant growth and potential applications in crop improvement. Plant Cell Rep 35, 949–965. https://doi.org/10.1007/s00299-016-1948-4

Michigan State University Extension, 2021. *Picture table of critical spring temperatures for tree fruit bud development stages*. [online] Michigan State University Extension. Available at: https://www.canr.msu.edu/resources/picture-table-critical-spring-temperatures-for-tree-fruit-bud-development-stages.

Milyaev, A., Kofler, J., Klaiber, I., Czemmel, S., Pfannstiel, J., Flachowsky, H., Stefanelli, D., Hanke, M.-V., Wünsche, J.-N., 2021. Toward Systematic Understanding of Flower Bud Induction in Apple: A Multi-Omics Approach. Front. Plant Sci. 12. https://doi.org/10.3389/fpls.2021.604810

Mizoi, J., Shinozaki, K., Yamaguchi-Shinozaki, K., 2012. AP2/ERF family transcription factors in plant abiotic stress responses. Biochimica et Biophysica Acta (BBA) - Gene Regulatory Mechanisms, Plant gene regulation in response to abiotic stress 1819, 86–96. https://doi.org/10.1016/j.bbagrm.2011.08.004

Molina, I., Kosma, D., 2015. Role of HXXXD-motif/BAHD acyltransferases in the biosynthesis of extracellular lipids. Plant Cell Rep 34, 587–601. https://doi.org/10.1007/s00299-014-1721-5

Moran, R.E., Peterson, B.J., Fazio, G., Cline, J., 2018. Genotypic Variation in Apple Rootstock Low Temperature Tolerance During Spring and Fall. https://doi.org/10.21273/JASHS04470-18

Mudgil, Y., Shiu, S.-H., Stone, S.L., Salt, J.N., Goring, D.R., 2004. A Large Complement of the Predicted Arabidopsis ARM Repeat Proteins Are Members of the U-Box E3 Ubiquitin Ligase Family. Plant Physiol 134, 59–66. https://doi.org/10.1104/pp.103.029553

Ningre, F., Colin, F., 2007. Frost damage on the terminal shoot as a risk factor of fork incidence on common beech (Fagus sylvatica L.). Ann. For. Sci. 64, 79–86. https://doi.org/10.1051/forest:2006091

Nodine, M.D., Yadegari, R., Tax, F.E., 2007. RPK1 and TOAD2 Are Two Receptor-like Kinases Redundantly Required for Arabidopsis Embryonic Pattern Formation. Developmental Cell 12, 943–956. https://doi.org/10.1016/j.devcel.2007.04.003

Nolan, T., Chen, J., Yin, Y., 2017. Cross-talk of Brassinosteroid signaling in controlling growth and stress responses. Biochemical Journal 474, 2641–2661. https://doi.org/10.1042/BCJ20160633

Nouri, M.-Z., Komatsu, S., 2013. Subcellular protein overexpression to develop abiotic stress tolerant plants. Front. Plant Sci. 4. https://doi.org/10.3389/fpls.2013.00002

Nüsslein-Volhard, C., Wieschaus, E., 1980. Mutations affecting segment number and polarity in Drosophila. Nature 287, 795–801. https://doi.org/10.1038/287795a0

Onyemaobi, O., Sangma, H., Garg, G., Wallace, X., Kleven, S., Dolferus, R., 2022. Transcriptome profiling of the chilling response in wheat spikes: I, acclimation response to long-term chilling treatment. Current Plant Biology 31, 100255. https://doi.org/10.1016/j.cpb.2022.100255

Panter, P.E., Panter, J.R., Knight, H., 2020. Impact of Cell-wall Structure and Composition on Plant Freezing Tolerance, in: Annual Plant Reviews Online. John Wiley & Sons, Ltd, pp. 607–642. https://doi.org/10.1002/9781119312994.apr0746

Park, J., Lim, C.J., Shen, M., Park, H.J., Cha, J.-Y., Iniesto, E., Rubio, V., Mengiste, T., Zhu, J.-K., Bressan, R.A., Lee, S.Y., Lee, B., Jin, J.B., Pardo, J.M., Kim, W.-Y., Yun, D.-J., 2018. Epigenetic switch from repressive to permissive chromatin in response to cold stress. Proceedings of the National Academy of Sciences 115, E5400–E5409. https://doi.org/10.1073/pnas.1721241115

Patro, R., Duggal, G., Love, M.I., Irizarry, R.A., Kingsford, C., 2017. Salmon provides fast and bias-aware quantification of transcript expression. Nat Methods 14, 417–419. https://doi.org/10.1038/nmeth.4197

Pearce, R.S., 2001. Plant Freezing and Damage. Annals of Botany 87, 417–424. https://doi.org/10.1006/anbo.2000.1352

Perry, K.B., 1998. Basics of Frost and Freeze Protection for Horticultural Crops. horttech 8, 10–15. https://doi.org/10.21273/HORTTECH.8.1.10

Pfleiderer, P., Menke, I., Schleussner, C.-F., 2019. Increasing risks of apple tree frost damage under climate change. Climatic Change 157, 515–525. https://doi.org/10.1007/s10584-019-02570-y

Picture Table of Critical Spring Temperatures for Tree Fruit Bud Development Stages [WWW Document], n.d. . Fruit & Nuts. URL https://www.canr.msu.edu/resources/picture-table-critical-spring-temperatures-for-tree-fruit-bud-development-stages (accessed 2.4.25).

Racskó, J., Nyéki, J., Szabó, Z., Soltész, M., Farkas, E., 2004. Effect of Rootstocks on Blooming Capacity and Productivity of AppleCultivars, in: Acta Agraria Debreceniensis. pp. 14–20. https://doi.org/10.34101/actaagrar/15/3351

Rai, G.K., Khanday, D.M., Choudhary, S.M., Kumar, P., Kumari, S., Martínez-Andújar, C., Martínez-Melgarejo, P.A., Rai, P.K., Pérez-Alfocea, F., 2024. Unlocking nature's stress buster: Abscisic acid's crucial role in defending plants against abiotic stress. Plant Stress 11, 100359. https://doi.org/10.1016/j.stress.2024.100359

Rasool, A., Mansoor, S., Bhat, K.M., Hassan, G.I., Baba, T.R., Alyemeni, M.N., Alsahli, A.A., El-Serehy, H.A., Paray, B.A., Ahmad, P., 2020. Mechanisms Underlying Graft Union Formation and Rootstock Scion Interaction in Horticultural Plants. Front. Plant Sci. 11. https://doi.org/10.3389/fpls.2020.590847

Ritonga, F.N., Ngatia, J.N., Wang, Y., Khoso, M.A., Farooq, U., Chen, S., 2021. AP2/ERF, an important cold stress-related transcription factor family in plants: A review. Physiol Mol Biol Plants 27, 1953–1968. https://doi.org/10.1007/s12298-021-01061-8

Sah, S.K., Reddy, K.R., Li, J., 2016. Abscisic Acid and Abiotic Stress Tolerance in Crop Plants. Front. Plant Sci. 7. https://doi.org/10.3389/fpls.2016.00571

Sampson, D.R. and Cameron, D.F., 1965. Inheritance of bronze foliage, extra petals and pendulous habit in ornamental crabapples. *Proceedings of the American Society for Horticultural Science*, 86, pp.717–722.

Sapkota, S., Salem, M., Jahed, K.R., Artlip, T.S., Sherif, S.M., 2023. From endodormancy to ecodormancy: the transcriptional landscape of apple floral buds. Front. Plant Sci. 14. https://doi.org/10.3389/fpls.2023.1194244

Satyakam, Zinta, G., Singh, R.K., Kumar, R., 2022. Cold adaptation strategies in plants—An emerging role of epigenetics and antifreeze proteins to engineer cold resilient plants. Front. Genet. 13. https://doi.org/10.3389/fgene.2022.909007

Seo, M., Koshiba, T., 2011. Transport of ABA from the site of biosynthesis to the site of action. J Plant Res 124, 501–507. https://doi.org/10.1007/s10265-011-0411-4

Sharma, M., Pandey, A., Pandey, G.K., 2014. β-catenin in plants and animals: common players but different pathways. Front. Plant Sci. 5. https://doi.org/10.3389/fpls.2014.00143

Sherif, S.M., 2022. Rootstock Effects on Tree Growth and Yield of 'Honeycrisp' Apple under Virginia State Climatic Conditions [WWW Document]. Virginia Cooperative Extension. URL https://pubs.ext.vt.edu/content/pubs_ext_vt_edu/en/SPES/spes-398/spes-398.html (accessed 2.4.25).

Sherif, S.M., Shukla, M.R., Murch, S.J., Bernier, L., Saxena, P.K., 2016. Simultaneous induction of jasmonic acid and disease-responsive genes signifies tolerance of American elm to Dutch elm disease. Sci Rep 6, 21934. https://doi.org/10.1038/srep21934

Shi, W., Riemann, M., Rieger, S.-M., Nick, P., 2022. Cold-Induced Nuclear Import of CBF4 Regulates Freezing Tolerance. International Journal of Molecular Sciences 23, 11417. https://doi.org/10.3390/ijms231911417

Siddiqua, M., Nassuth, A., 2011. Vitis CBF1 and Vitis CBF4 differ in their effect on Arabidopsis abiotic stress tolerance, development and gene expression. Plant, Cell & Environment 34, 1345–1359. https://doi.org/10.1111/j.1365-3040.2011.02334.x

Snyder, R.L., Melo-Abreu, J.P.D., Matulich, S., 2005. Frost Protection: Fundamentals, Practice, And Economics (FAO Environment and Natural Resources), Pap/Cdr edition. ed. Food & Agriculture Organization of the UN (FA.

Sohrabi, S.S., Ismaili, A., Nazarian-Firouzabadi, F., Fallahi, H., Hosseini, S.Z., 2022. Identification of key genes and molecular mechanisms associated with temperature stress in lentil. Gene 807, 145952. https://doi.org/10.1016/j.gene.2021.145952

Soltabayeva, A., Dauletova, N., Serik, S., Sandybek, M., Omondi, J.O., Kurmanbayeva, A., Srivastava, S., 2022. Receptor-like Kinases (LRR-RLKs) in Response of Plants to Biotic and Abiotic Stresses. Plants 11, 2660. https://doi.org/10.3390/plants11192660

Song, J., Shang, L., Chen, S., Lu, Y., Zhang, Y., Ouyang, B., Ye, Z., Zhang, J., 2021. Interactions between ShPP2-1, an F-box family gene, and ACR11A regulate cold tolerance of tomato. Hortic Res 8, 148. https://doi.org/10.1038/s41438-021-00582-3

Spray Schedule for Home Apple Trees [WWW Document], n.d. . Yard and Garden. URL https://yardandgarden.extension.iastate.edu/how-to/spray-schedule-home-apple-trees (accessed 2.4.25).

Su, C., Chen, K., Ding, Q., Mou, Y., Yang, R., Zhao, M., Ma, B., Xu, Z., Ma, Y., Pan, Y., Chen, M., Xi, Y., 2018. Proteomic Analysis of the Function of a Novel Cold-Regulated Multispanning Transmembrane Protein COR413-PM1 in Arabidopsis. International Journal of Molecular Sciences 19, 2572. https://doi.org/10.3390/ijms19092572

Sun, X., Zhu, Z., Zhang, L., Fang, L., Zhang, J., Wang, Q., Li, S., Liang, Z., Xin, H., 2019. Overexpression of ethylene response factors *VaERF080* and *VaERF087* from *Vitis amurensis* enhances cold tolerance in Arabidopsis. Scientia Horticulturae 243, 320–326. https://doi.org/10.1016/j.scienta.2018.08.055

Szalay, L., György, Z., Tóth, M., 2019. Frost hardiness of apple (*Malus X domestica*) flowers in different phenological phases. Scientia Horticulturae 253, 309–315. https://doi.org/10.1016/j.scienta.2019.04.055

Takuhara, Y., Kobayashi, M., Suzuki, S., 2011. Low-temperature-induced transcription factors in grapevine enhance cold tolerance in transgenic *Arabidopsis* plants. Journal of Plant Physiology 168, 967–975. https://doi.org/10.1016/j.jplph.2010.11.008

Tang, D., Chen, M., Huang, X., Zhang, Guicheng, Zeng, L., Zhang, Guangsen, Wu, S., Wang, Y., 2023. SRplot: A free online platform for data visualization and graphing. PLOS ONE 18, e0294236. https://doi.org/10.1371/journal.pone.0294236

Tang, W., Thompson, W.A., 2022. Role of the Rice BAHD Acyltransferase Gene OsAt10 in Plant Cold Stress Tolerance. Plant Mol Biol Rep 40, 482–499. https://doi.org/10.1007/s11105-021-01328-0

Tarancón, C., González-Grandío, E., Oliveros, J.C., Nicolas, M., Cubas, P., 2017. A Conserved Carbon Starvation Response Underlies Bud Dormancy in Woody and Herbaceous Species. Front. Plant Sci. 8. https://doi.org/10.3389/fpls.2017.00788

Tarkowski, Ł.P., Van den Ende, W., 2015. Cold tolerance triggered by soluble sugars: a multifaceted countermeasure. Front. Plant Sci. 6. https://doi.org/10.3389/fpls.2015.00203

Tenhaken, R., 2015. Cell wall remodeling under abiotic stress. Front. Plant Sci. 5. https://doi.org/10.3389/fpls.2014.00771

Tillett, R.L., Wheatley, M.D., Tattersall, E.A.R., Schlauch, K.A., Cramer, G.R., Cushman, J.C., 2012. The Vitis vinifera C-repeat binding protein 4 (VvCBF4) transcriptional factor enhances freezing tolerance in wine grape. Plant Biotechnology Journal 10, 105–124. https://doi.org/10.1111/j.1467-7652.2011.00648.x

Tohge, T., Wendenburg, R., Ishihara, H., Nakabayashi, R., Watanabe, M., Sulpice, R., Hoefgen, R., Takayama, H., Saito, K., Stitt, M., Fernie, A.R., 2016. Characterization of a recently evolved flavonol-phenylacyltransferase gene provides signatures of natural light selection in Brassicaceae. Nat Commun 7, 12399. https://doi.org/10.1038/ncomms12399

Tominaga, A., Ito, A., Sugiura, T., Yamane, H., 2022. How Is Global Warming Affecting Fruit Tree Blooming? “Flowering (Dormancy) Disorder” in Japanese Pear (Pyrus pyrifolia) as a Case Study. Front. Plant Sci. 12. https://doi.org/10.3389/fpls.2021.787638

Tworkoski, T., Miller, S., 2007. Rootstock effect on growth of apple scions with different growth habits. Scientia Horticulturae 111, 335–343. https://doi.org/10.1016/j.scienta.2006.10.034

Uemura, M., Steponkus, P.L., 1999. Cold Acclimation in Plants: Relationship Between the Lipid Composition and the Cryostability of the Plasma Membrane. J Plant Res 112, 245–254. https://doi.org/10.1007/PL00013882

Ukey, R., Rai, A.C., 2021. Impact of global warming on heating and cooling degree days in major Indian cities. Energy and Buildings 244, 111050. https://doi.org/10.1016/j.enbuild.2021.111050

ul Haq, S., Khan, A., Ali, M., Khattak, A.M., Gai, W.-X., Zhang, H.-X., Wei, A.-M., Gong, Z.-H., 2019. Heat Shock Proteins: Dynamic Biomolecules to Counter Plant Biotic and Abiotic Stresses. International Journal of Molecular Sciences 20, 5321. https://doi.org/10.3390/ijms20215321

Unterberger, C., Brunner, L., Nabernegg, S., Steininger, K.W., Steiner, A.K., Stabentheiner, E., Monschein, S., Truhetz, H., 2018. Spring frost risk for regional apple production under a warmer climate. PLOS ONE 13, e0200201. https://doi.org/10.1371/journal.pone.0200201

Untergasser, A., Nijveen, H., Rao, X., Bisseling, T., Geurts, R., Leunissen, J.A.M., 2007. Primer3Plus, an enhanced web interface to Primer3. Nucleic Acids Research 35, W71–W74. https://doi.org/10.1093/nar/gkm306

Usova, G.S., 1973. The genetic nature of red-leaved and green-leaved apple clones (in Russian). *Nauchnye Trudy Voronezh*, 55, pp.90–93. [Plant Breeding Abstracts, 46, p.2729].

Vitasse, Y., Bottero, A., Cailleret, M., Bigler, C., Fonti, P., Gessler, A., Lévesque, M., Rohner, B., Weber, P., Rigling, A., Wohlgemuth, T., 2019. Contrasting resistance and resilience to extreme drought and late spring frost in five major European tree species. Global Change Biology 25, 3781–3792. https://doi.org/10.1111/gcb.14803

Vogel, J.T., Zarka, D.G., Van Buskirk, H.A., Fowler, S.G., Thomashow, M.F., 2005. Roles of the CBF2 and ZAT12 transcription factors in configuring the low temperature transcriptome of Arabidopsis. The Plant Journal 41, 195–211. https://doi.org/10.1111/j.1365-313X.2004.02288.x

Vonapartis, E., Mohamed, D., Li, J., Pan, W., Wu, J., Gazzarrini, S., 2022. CBF4/DREB1D represses to attenuate ABA, osmotic and drought stress responses in Arabidopsis. The Plant Journal 110, 961–977. https://doi.org/10.1111/tpj.15713

Wang, D.-Z., Jin, Y.-N., Ding, X.-H., Wang, W.-J., Zhai, S.-S., Bai, L.-P., Guo, Z.-F., 2017. Gene regulation and signal transduction in the ICE–CBF–COR signaling pathway during cold stress in plants. Biochemistry Moscow 82, 1103–1117. https://doi.org/10.1134/S0006297917100030

Wang, Y., Li, W., Xu, X., Qiu, C., Wu, T., Wei, Q., Ma, F., Han, Z., 2019. Progress of Apple Rootstock Breeding and Its Use. Horticultural Plant Journal 5, 183–191. https://doi.org/10.1016/j.hpj.2019.06.001

Wisniewski, M., Artlip, T., Norelli, J., 2016. Dealing with Frost Damage and Climate Change in Tree Fruit Crops.

Wisniewski, M., Gusta, L., Neuner, G., 2014. Adaptive mechanisms of freeze avoidance in plants: A brief update. Environmental and Experimental Botany 99, 133–140. https://doi.org/10.1016/j.envexpbot.2013.11.011

Xie, Y., Chen, P., Yan, Y., Bao, C., Li, X., Wang, L., Shen, X., Li, H., Liu, X., Niu, C., Zhu, C., Fang, N., Shao, Y., Zhao, T., Yu, J., Zhu, J., Xu, L., van Nocker, S., Ma, F., Guan, Q., 2018. An atypical R2R3 MYB transcription factor increases cold hardiness by CBF-dependent and CBF-independent pathways in apple. New Phytologist 218, 201–218. https://doi.org/10.1111/nph.14952

Xu, D., Wang, Z., Zhuang, W., Wang, T., Xie, Y., 2023. Family characteristics, phylogenetic reconstruction, and potential applications of the plant BAHD acyltransferase family. Front. Plant Sci. 14. https://doi.org/10.3389/fpls.2023.1218914

Young, E., Houser, J., 1980. Influence of Siberian C Rootstock on Peach Bloom Delay, Water Potential, and Pollen Meiosis1. J. Amer. Soc. Hort. Sci. 105, 242–245. https://doi.org/10.21273/JASHS.105.2.242

Zhang, Q., Zhai, J., Shao, L., Lin, W., Peng, C., 2019. Accumulation of Anthocyanins: An Adaptation Strategy of Mikania micrantha to Low Temperature in Winter. Front. Plant Sci. 10. https://doi.org/10.3389/fpls.2019.01049

Zhang, S., Wang, H., Wang, T., Zhang, J., Liu, W., Fang, H., Zhang, Z., Peng, F., Chen, X., Wang, N., 2023. Abscisic acid and regulation of the sugar transporter gene MdSWEET9b promote apple sugar accumulation. Plant Physiol 192, 2081–2101. https://doi.org/10.1093/plphys/kiad119

Zhao, C., Zhang, Z., Xie, S., Si, T., Li, Y., Zhu, J.-K., 2016. Mutational Evidence for the Critical Role of CBF Transcription Factors in Cold Acclimation in Arabidopsis. Plant Physiology 171, 2744–2759. https://doi.org/10.1104/pp.16.00533

Zhou, Y., Wang, B., Yuan, F., 2022a. The Role of Transmembrane Proteins in Plant Growth, Development, and Stress Responses. International Journal of Molecular Sciences 23, 13627. https://doi.org/10.3390/ijms232113627

Zhou, Y., Wang, B., Yuan, F., 2022b. The Role of Transmembrane Proteins in Plant Growth, Development, and Stress Responses. International Journal of Molecular Sciences 23, 13627. https://doi.org/10.3390/ijms232113627

Zhou, Z., Cong, P., Tian, Y., Zhu, Y., 2017. Using RNA-seq data to select reference genes for normalizing gene expression in apple roots. PLoS ONE 12, e0185288. https://doi.org/10.1371/journal.pone.0185288

Zou, Z., Yang, L., Gong, J., Mo, Y., Wang, J., Cao, J., An, F., Xie, G., 2016. Genome-Wide Identification of Jatropha curcas Aquaporin Genes and the Comparative Analysis Provides Insights into the Gene Family Expansion and Evolution in Hevea brasiliensis. Front. Plant Sci. 7. https://doi.org/10.3389/fpls.2016.00395

Zwintzscher, M., 1973. *Malus pumsila var. niedzwetzkyana and its role in apple breeding*. In: Symposium on Apple Breeding, Canterbury. pp.154–159.

Chapter 3: Role of Carbohydrates in Apple (*Malus* × *Domestica* Borkh) Phenology and Frost Tolerance

Abstract

Apple (*Malus* × *domestica* Borkh.) production is increasingly threatened by climate change, with spring frosts causing significant yield losses by damaging floral buds during critical phenological stages and developmental windows. This study hypothesizes that changes in carbohydrate metabolism, particularly soluble sugar and starch dynamics, could drive the progressive decline in frost tolerance of apple buds as they develop. Using floral buds from 'Fuji' and 'Gala' apple trees grafted onto two rootstocks ('B.9' and 'M.26'), we analyzed carbohydrate profiles and gene expression across developmental stages, spanning from silver tip (2505 GDH) to full bloom (10,410 GDH). Buds were cryogenically processed immediately after collection to preserve integrity, enabling comprehensive biochemical, and molecular analyses. Carbohydrate profiles and gene expression varied significantly along the GDH gradient. Early stages (silver tip to green tip) exhibited moderate starch levels and gradual increase in soluble sugars, such as sucrose, glucose, and sorbitol. Major transition occurred during tight cluster stage which marked a critical shift, characterized by significant sugar depletion and reduced expression of genes regulating sugar hydrolysis. This depletion coincided with heightened frost vulnerability and morphological demands, increasing susceptibility to damage at temperatures as mild as –2°C. Partial sugar recovery was observed around full pink bud stage. These findings demonstrate the intricate relationship between carbohydrate dynamics and frost tolerance in apple floral buds. By elucidating how sugar allocation and gene regulation coincide with frost susceptibility, this study clarifies the crucial role of carbohydrate metabolism in apple bud phenology and frost tolerance. However, despite the later-stage increase in soluble sugars, frost tolerance continued to decline, suggesting that sugar accumulation alone was insufficient to maintain low critical temperature thresholds for bud survival.

Keywords

Non-structural carbohydrates, Apple bud phenology, Source-sink relationship, Spring frost-induced damage, Climate-Change, Rootstocks, *Malus* x *domestica* Borkh.

1 Introduction

Apple (*Malus* x *domestica* Borkh.) production is a cornerstone of agriculture in temperate regions, but it faces mounting challenges from extreme weather events exacerbated by climate change (Ahmadi et al., 2019; Chen et al., 2025). Rising temperatures, altered precipitation patterns, and increasing unpredictability in seasonal transitions have disrupted the phenological calendar of apple trees, including their progression from dormancy through budbreak to bloom (Fadón et al., 2020). Plant phenology, which serves as a critical indicator of plant responses to climate change (Menzel et al., 2020), plays a pivotal role in carbon uptake, tree growth, and ecosystem feedbacks, such as canopy structure and carbon and water fluxes (Richardson et al., 2013; Luo et al., 2024). For perennial fruit trees, these phenological shifts often lead to a misalignment between developmental stages and environmental conditions, heightening the risk of frost damage and yield losses (Chen et al., 2023). This recognition has spurred extensive research into the drivers of phenology, particularly the influence of meteorological factors like temperature and precipitation (Piao et al., 2019; Zohner et al., 2023).

However, while environmental cues are crucial, internal physiological processes, including the mobilization of carbon and nutrients, remain less explored. These processes integrate source and sink activities with phenological timing, balancing carbon remobilization and growth (Deslauriers et al., 2019; Zohner et al., 2023; Luo et al., 2024). For perennial fruit trees like apple, these dynamics become particularly critical during spring transitions, where frost events can severely impact floral buds, reducing yield potential (Hubmann et al., 2023). Understanding how phenology integrates external cues with internal physiological processes is key to improving predictions of developmental stages and mitigating spring frost-related damage.

Natural frost events are a significant environmental stressor, occurring when air temperatures drop below 0°C and often coincide with freezing dew points (Jahed et al., 2023). Frost damage typically arises from surface ice formation, which leads to cellular dehydration and tissue damage, while more severe freeze damage results from intracellular ice crystal formation, often causing irreversible injury (Stegner et al., 2022). The susceptibility of plants to frost varies based on species, developmental stage, and critical temperature thresholds (Centinari et al., 2016). In apple trees, for instance, floral buds at the silver-tip stage, where the buds are just beginning to separate and appear silvery-gray, can withstand temperatures as low as -17.6°C. However, as the buds progress to more advanced stages, such as the bloom and post-bloom stages, their frost tolerance declines significantly, with critical damage observed at temperatures as mild as -2°C. At these later stages, frost events can result in up to 90% floral bud mortality (Jahed et al., 2023). These stage-dependent variations in critical temperature thresholds underscore the complex interplay between phenological development and frost susceptibility, necessitating a deeper understanding of the physiological processes that influence these vulnerabilities.

Carbohydrates play a central role in plant responses to abiotic stress, including frost stress (Kwon et al., 2022). In apple trees, carbohydrates synthesized in photosynthetically active leaves during the growing season are transported as non-structural carbohydrates (NSCs), including starch and soluble sugars, to roots, stems, and other organs for storage (Breen et al., 2020). These reserves are later remobilized during early spring to support metabolic functions, provide energy for bud development, and enhance osmoprotection (Tixier et al., 2019). Soluble sugars, such as glucose, fructose, sucrose, and sorbitol, are particularly critical as they lower osmotic potential, stabilize cellular membranes, and prevent ice formation under freezing conditions (Afzal et al., 2021). Sorbitol, the primary sugar-alcohol in apple and pear, serves as a major product of photosynthesis and is metabolized into other sugars, underscoring the dynamic interconversion of carbohydrate forms (Breen et al., 2020). These carbohydrate pools form a vital buffer against environmental stress, enabling plants to maintain cellular integrity and metabolic readiness (Blumstein et al., 2023) during cold stress.

The mobilization and utilization of stored carbohydrates during frost-prone periods depend on a coordinated network of sugar transporters and metabolic pathways. Key genes, such as Sugars Will Eventually be Exported Transporters (SWEETs), Sugar Transporter 14 (STPs), Delta tonoplast Integral Protein (TONO), and Early Responsive to Dehydration Proteins (ERD), regulate the transport and allocation of sugars from storage tissues to developing buds (Borghi & Fernie, 2017; Zhu et al., 2021). Additionally, enzymes like Beta-Amylase (AMY), Plant invertase/pectin methylesterase inhibitor superfamily protein (INV), Sucrose Synthase 4 (SUS4), Starch Synthase 2 (SS2), and Starch Branching Enzyme 2.2 (SSE) mediate the breakdown of starch into soluble sugars, ensuring an adequate supply of energy and osmoprotectants (Mirajkar et al., 2016; Thalmann & Santelia, 2017; Dong & Beckles, 2019;

Saddhe et al., 2021).These processes are essential for maintaining bud viability during frost events, particularly as phenological stages progress and carbohydrate demands increase (Vitra et al., 2017). Carbohydrate partitioning, or the allocation of sugars between source tissues (e.g., leaves) and sink tissues (e.g., buds, roots, stems), further influences the availability of sugars for abiotic stress resilience (MacNeill et al., 2017; Kong et al., 2019; Abdelrahman et al., 2020). During periods of low photosynthetic activity, such as winter dormancy, stored carbohydrates act as the primary energy source for metabolic activities and bud development. Roots and stems, which store significant proportions of assimilated starch during autumn, play a pivotal role in sustaining early spring growth through the remobilization of these reserves highlighting the importance of coordinated resource allocation during developmental stages (Fermaniuk et al., 2021).

Despite significant advances in understanding carbohydrate dynamics, critical gaps remain in linking these processes to frost tolerance across phenological stages. For instance, the extent to which changes in soluble sugar profiles influence critical temperature thresholds during frost events has not been fully elucidated. Furthermore, the role of rootstock-scion combinations in modulating carbohydrate storage and remobilization—potentially influencing varietal differences in frost resilience—remains poorly understood. Addressing these gaps is essential for developing targeted orchard management strategies and breeding programs aimed at enhancing frost tolerance in apple trees.

The current study aimed to explore the role of carbohydrates in apple phenology and frost tolerance, focusing on whether changes in sugar content can explain differences in critical temperature thresholds across developmental stages. Using 'Fuji' and 'Gala' apple varieties grafted on 'B.9' and 'M.26' rootstocks, we collected floral buds across key phenological stages, from silver tip (~2,505 GDH) to full bloom (~10,410 GDH), to examine the dynamics of soluble sugars (glucose, fructose, sucrose, sorbitol) and starch content. By analysing key sugar-related genes, including *MdSWT* (SWEET/ Nodulin MtN3 family protein), *MdSTP* (Sugar Transporter 14), *MdTONO* (Delta tonoplast Integral Protein), *MdERD* (Dehydration-induced Protein), *MdSUS4* (Sucrose Synthase 4), *MdSS2* (Starch Synthase 2), *MdSSE* (Starch Branching Enzyme 2.2), *MdAMY* (Beta-Amylase), and *MdINV* (Plant invertase/pectin methylesterase inhibitor superfamily protein), we seek to elucidate the molecular mechanisms underlying carbohydrate allocation and frost resilience. This approach provides a more precise framework for understanding the interplay between carbohydrate metabolism and frost susceptibility in apple buds. These insights will contribute to the development of resilient orchard management practices to mitigate the impacts of climate change on apple production.

2 Materials and Methods

2.1 Plant Materials and Experimental Layout

This experiment was conducted in 2024 at the Alson H. Smith Jr. Agricultural Research and Extension Center (AREC) in Winchester, VA, USA, using twelve-year-old mature apple trees (*Malus × domestica* Borkh.) of two cultivars, 'Fuji' and 'Gala', grafted onto two different rootstocks, 'B.9' and 'M.26'. Growing Degree Hours were calculated using a base temperature of 4.4 °C (40 °F), a standard threshold for apple bud development. Bud samples were collected on ten distinct sampling dates corresponding to key developmental stages, spanning from silver tip to full bloom: February 15 (2,505 GDH; silver tip), February 22 (2,612 GDH; silver tip), February 29 (3,130 GDH; silver tip), March 7 (3,773 GDH; green tip), March 14 (4,583 GDH, green tip), March 21 (5,672 GDH; half-inch green), March 28

(5,986 GDH; tight cluster), April 4 (6,797 GDH; tight cluster), April 11 (8,157 GDH; full pink bud), and April 18 (10,410 GDH, full bloom). These dates were chosen to capture the progressive transition of floral buds through key phenological phases **(Figure 1)**.

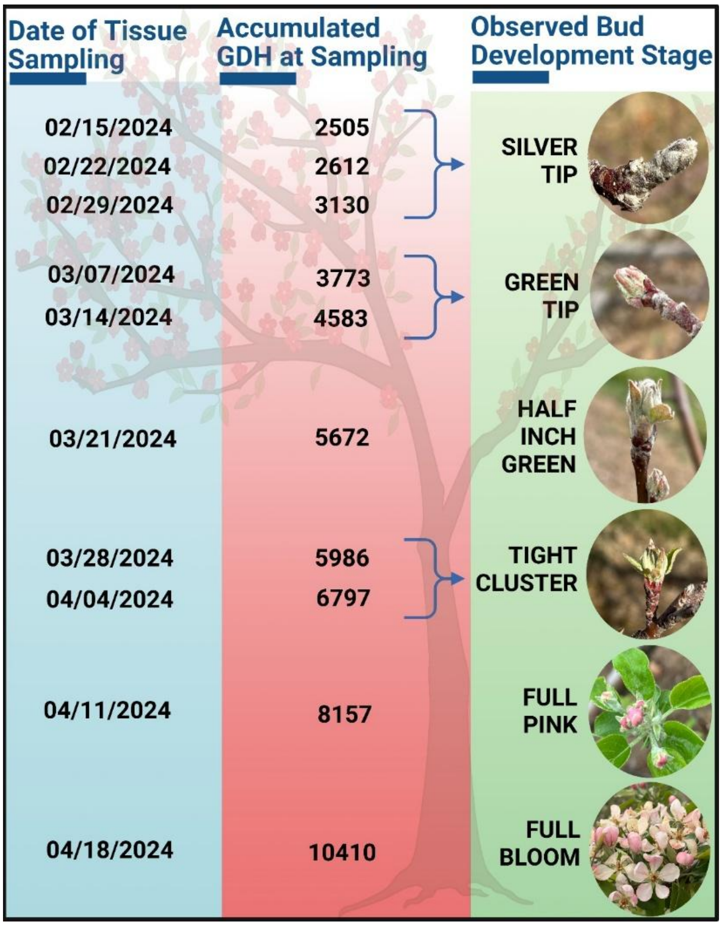

Figure 1: Timeline of floral bud development stages in apple during the 2024 spring season. Sampling dates, corresponding accumulated growing degree hours (GDH), and observed bud phenological stages are shown. Developmental progression was recorded from silver tip through full bloom

For each rootstock-cultivar combination, three biological replicates were collected to ensure statistical robustness. Each biological replicate consisted of floral buds sampled from three different trees with buds pooled into a single 15 mL tube per replicate, ensuring that our data accurately represented variability within the experimental design. Buds were immediately frozen in liquid nitrogen upon collection to preserve their integrity for biochemical, and molecular analyses. All bud samples were then cryogenically ground into a fine powder using a Geno/Grinder (SPEX SamplePrep, Metuchen, NJ, USA) to ensure uniformity and enable subsequent soluble sugar and starch analysis.

2.2 Estimation of chilling and heat accumulation

Chilling hours (CH) and Growing degree hours (GDH) were calculated as described in our previous studies (Liu et al., 2021). Briefly, we first calculated the hourly temperatures (T) by averaging the field temperatures from a data logger (EasyLog, Lascar, Erie, PA, the United States), which were kept enclosed in the field and recorded temperatures at 10 min intervals. Starting on October 15, one chilling hour was registered when the hourly temperature fell within 0–7.2 °C (Das et al., 2024). To calculate GDH, hourly temperatures lower than 4.5 °C were ignored (T<4.5 ⟹ GDH = 0); temperatures between 4.5–25 °C registered as the temperature value minus 4.5 (4.5≤T≤ 25 ⟹ GDH = T-4.5); and hourly temperatures higher than 25 °C registered as 20.5 (T>25 ⟹ GDH = 20.5) (Richardson et al., 1975).

2.3 Soluble Sugar and Starch Analyses

Soluble sugars were extracted from 0.2 g of homogenized floral bud tissue using 1 mL of 80% ethanol, according to the method previously described by Islam et al. (2021). Prior to extraction, the fresh and dry weights of the tissue were determined to account for moisture content. Approximately 500 mg of fresh tissue was weighed into 2 mL tubes and oven-dried at 50°C for 24 hours. The weights of the samples were monitored every 6 hours until a consistent dry weight was achieved, indicating complete removal of moisture. The moisture content was then calculated by subtracting the dry weight from the fresh weight, providing precise tissue weight measurements for the analysis. Glucose, sucrose, and fructose concentrations were quantified with the Megazyme Sucrose/D-Fructose/D-Glucose Assay Kit (Megazyme, Bray, Ireland) following the manufacturer's instructions. Total soluble sugar content was calculated as the sum of glucose, fructose, and sucrose concentrations. For starch quantification, the dried pellet obtained after soluble sugar extraction was resuspended in 500 µL deionized water and heated at 80°C for 20 minutes to gelatinize the starch. The supernatant pH was adjusted to 5.1 using 400 µL of 200 mM acetate buffer. Starch digestion was performed by adding 100 µL of a reaction mixture containing 0.2 U amyloglucosidase and 40 U α-amylase, followed by a 24-hour incubation at 37°C. The mixture was centrifuged at 14,000 rpm for 5 minutes, and glucose concentration in the supernatant was measured using the Megazyme Sucrose/D-Fructose/D-Glucose Assay Kit. Starch concentration was calculated as 0.9 x glucose concentration.

2.4 Reverse Transcription Quantitative PCR

Total RNA was reverse-transcribed into complementary DNA (cDNA) using the High-Capacity cDNA Reverse Transcription Kit (Applied Biosystems, Waltham, MA, USA), following the manufacturer's instructions. Gene-specific primers were designed using Primer3Plus software (Untergasser et al., 2012) and are listed in Table S1 for genes *MdSWT*, *MdSTP*, *MdTONO*, *MdERD*, *MdSUS4*, *MdSS2*, *MdSSE*, *MdAMY*, and *MdINV*. Primer specificity was confirmed via melting curve analysis at the conclusion of each RT-qPCR reaction. Quantitative RT-PCR analyses were performed on a CFX Connect Real-Time PCR Detection System (Bio-Rad Laboratories, Inc., Hercules, CA, USA), using standard cycling mode and reaction parameters as outlined in Sapkota et al. (2023). Expression was normalized using two reference genes, *MdActin* and *MdGAP*, and calculated relative to the expression level observed in the February 15, silver tip (2,505 GDH) bud sample from both 'Gala' and 'Fuji'. Statistical analysis was conducted using analysis of variance (ANOVA) to compare gene expression across different sampling points, with a significance threshold of $P \leq 0.05$ for a given tissue type using R programming language for statistical computing and graphics (version 4.4.2).

2.5 Statistical Analyses

Statistical analyses of the sugar and starch content data were conducted using R software for statistical computing. Tukey's HSD test was employed to compare the means of separate replicates ($n=3$) with a statistical significance threshold of $P \leq 0.05$. Analysis of variance (ANOVA) was performed among different tissue types collected at ten sampling points, corresponding to key phenological stages, sampling dates and GDH, as described in sub-heading 2.1.

3 Results

3.1 Starch Analysis

3.1.1 ‘Gala’

Starch concentrations in floral buds of the ‘Gala’ cultivar varied across developmental stages and between the rootstocks ‘B.9’ and ‘M.26’, with some stages showing significant differences **(Figure 2A).**

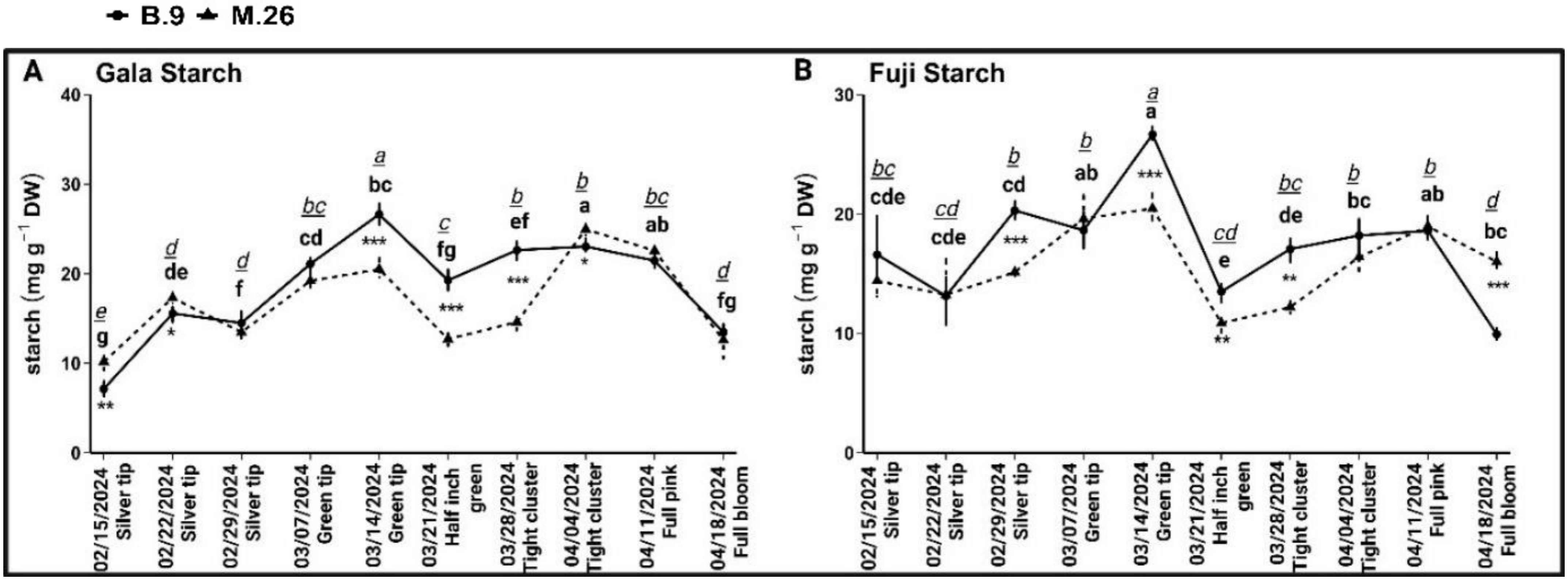
B.9
M.26
A
Gala Starch
starch (mg g^{-1} DW)
02/15/2024 Silver tip
02/22/2024 Silver tip
02/29/2024 Silver tip
03/07/2024 Green tip
03/14/2024 Green tip
03/21/2024 Half inch green
03/28/2024 Tight cluster
04/04/2024 Tight cluster
04/11/2024 Full pink
04/18/2024 Full bloom
B
Fuji Starch
starch (mg g^{-1} DW)
02/15/2024 Silver tip
02/22/2024 Silver tip
02/29/2024 Silver tip
03/07/2024 Green tip
03/14/2024 Green tip
03/21/2024 Half inch green
03/28/2024 Tight cluster
04/04/2024 Tight cluster
04/11/2024 Full pink
04/18/2024 Full bloom

Figure 2: Starch content in floral buds of (A) 'Gala' and (B) 'Fuji' cultivars grafted onto rootstocks 'B.9' and 'M.26' (full and dashed graph lines, respectively) during different phenological stages, spanning from white tip to full bloom, measured at ten distinct sampling points. Samples were collected on ten dates: 02/15 (Silver tip), 02/22 (Silver tip), 02/29 (Silver tip), 03/07 (Green tip), 03/14 (Green tip), 03/21 (Half inch green), 03/28 (Tight cluster), 04/04 (Tight cluster), 04/11 (Full pink bud), and 04/18 (Full bloom). The italicized underlined letters indicate significant differences within the 'B.9' rootstock across time based on one-way ANOVA, while the bold letters indicate significance for the 'M.26' rootstock across time. Asterisks represent Tukey's test results comparing 'B.9' and 'M.26' at each sampling point. Error bars indicate the mean±SE ($n=3$). Significance levels are denoted as $*P \leq 0.05$, $**P \leq 0.01$, and $***P \leq 0.001$, using Tukey's Honestly Significant Difference (HSD) test.

At silver tip on 15 February 2024, starch levels in 'Gala'/ 'M.26' were significantly higher than in 'Gala'/ 'B.9'. The week after that, at silver tip on 22 February 2024, 'Gala'/ 'M.26' again exhibited higher starch concentrations than 'Gala'/ 'B.9'. However, on 14 March 2024 (green tip), 'Gala'/ 'B.9' exhibited significantly higher starch levels compared to 'Gala'/ 'M.26'. On 21 March (half inch green) and 28 March 2024 (tight cluster), 'Gala'/ 'M.26' showed significantly lower starch concentrations than 'Gala'/ 'B.9'. By 4 April 2024 (tight cluster), starch levels in 'Gala'/ 'B.9' were again lower than those in 'Gala'/ 'M.26'. Within 'Gala'/ 'B.9', starch levels gradually increased from early developmental stages, reaching their highest accumulation on 14 March 2024 (green tip) which was significantly higher than earlier stages. After this peak, starch levels declined significantly by 21 March 2024 (half inch green), followed by a slight increase on 28 March 2024 (tight cluster). However, starch concentrations then progressively decreased through later developmental stages, with significantly lower levels recorded on 18 April 2024 (full bloom) compared to peak accumulation. Within 'Gala'/ 'M.26', starch concentrations followed a similar trajectory, however, the peak starch levels in 'Gala'/ 'M.26' were lower than in 'Gala'/ 'B.9'. After this stage, starch concentrations in 'Gala'/ 'M.26' declined significantly by 28 March 2024 (tight cluster), showed a slight increase on 4 April 2024 (tight cluster), and then continued to decline by 18 April 2024 (full bloom).

3.1.2 'Fuji'

Starch concentrations in floral buds of the 'Fuji' cultivar exhibited distinct patterns across developmental stages and between rootstocks 'B.9' and 'M.26' **(Figure 2B)**. During silver tip (15-22 February), there were no significant differences between 'Fuji'/'B.9' and 'Fuji'/ 'M.26'. However, by 29 February 2024 (silver tip), 'Fuji'/ 'B.9' exhibited significantly higher starch levels than 'Fuji'/ 'M.26'. On 14 March 2024 (green tip), starch levels in 'Fuji'/ 'B.9' peaked and were significantly higher than in 'Fuji'/ 'M.26'. This trend continued 28 March 2024 (tight cluster) where 'Fuji'/ 'B.9' maintained significantly higher starch levels than 'Fuji'/ 'M.26'. By full bloom, 'Fuji'/ 'M.26' exhibited significantly higher starch concentrations compared to 'Fuji'/ 'B.9'. Within 'Fuji'/ 'B.9', starch concentrations peaked on 14 March 2024 (green tip), significantly higher than all earlier stages. The lowest starch levels in 'Fuji'/ 'B.9' were recorded 18 April (full bloom), significantly lower than earlier developmental stages except 22 February (Silver tip). In 'Fuji'/ 'M.26', starch concentrations also peaked on 14 March 2024 (green tip), significantly exceeding earlier developmental stages, but further analysis revealed a non-significant increase in starch levels at later points.

3.2 Non-structural Carbohydrate analysis in floral buds

3.2.1 ‘Gala’

3.2.1(a) Glucose

Glucose concentrations displayed some significant differences between rootstocks at specific developmental stages **(Figure 3A)**. On 15 February 2024 (silver tip), glucose levels in ‘Gala’/ ‘B.9’ were significantly higher than in ‘Gala’/ ‘M.26’. Similarly, on 14 March 2024 (green tip), ‘Gala’/ ‘B.9’ exhibited significantly higher glucose levels than ‘Gala’/ ‘M.26’. However, during 28 March 2024 (tight cluster), ‘Gala’/ ‘M.26’ showed significantly lower glucose concentrations compared to ‘Gala’/ ‘B.9’. Within ‘B.9’, glucose levels gradually increased from 15 February 2024 (silver tip) until peaking on 21 March 2024 (half inch green), after which they declined slightly on 4 April 2024 (tight cluster). However, levels increased again on 11 April 2024 (full pink bud) and 18 April 2024 (full bloom), where the highest accumulation was observed. In ‘Gala’/ ‘M.26’, glucose followed a similar increasing trend until 21 March 2024 (half inch green), but unlike ‘Gala’/ ‘B.9’, glucose levels in ‘Gala’/ ‘M.26’ exhibited a more pronounced decline on 28 March 2024 (tight cluster) and continued decreasing until 4 April 2024 (tight cluster). After this, glucose concentrations in ‘Gala’/ ‘M.26’ increased from 11 April 2024 (full pink bud) onward, peaking at full bloom.

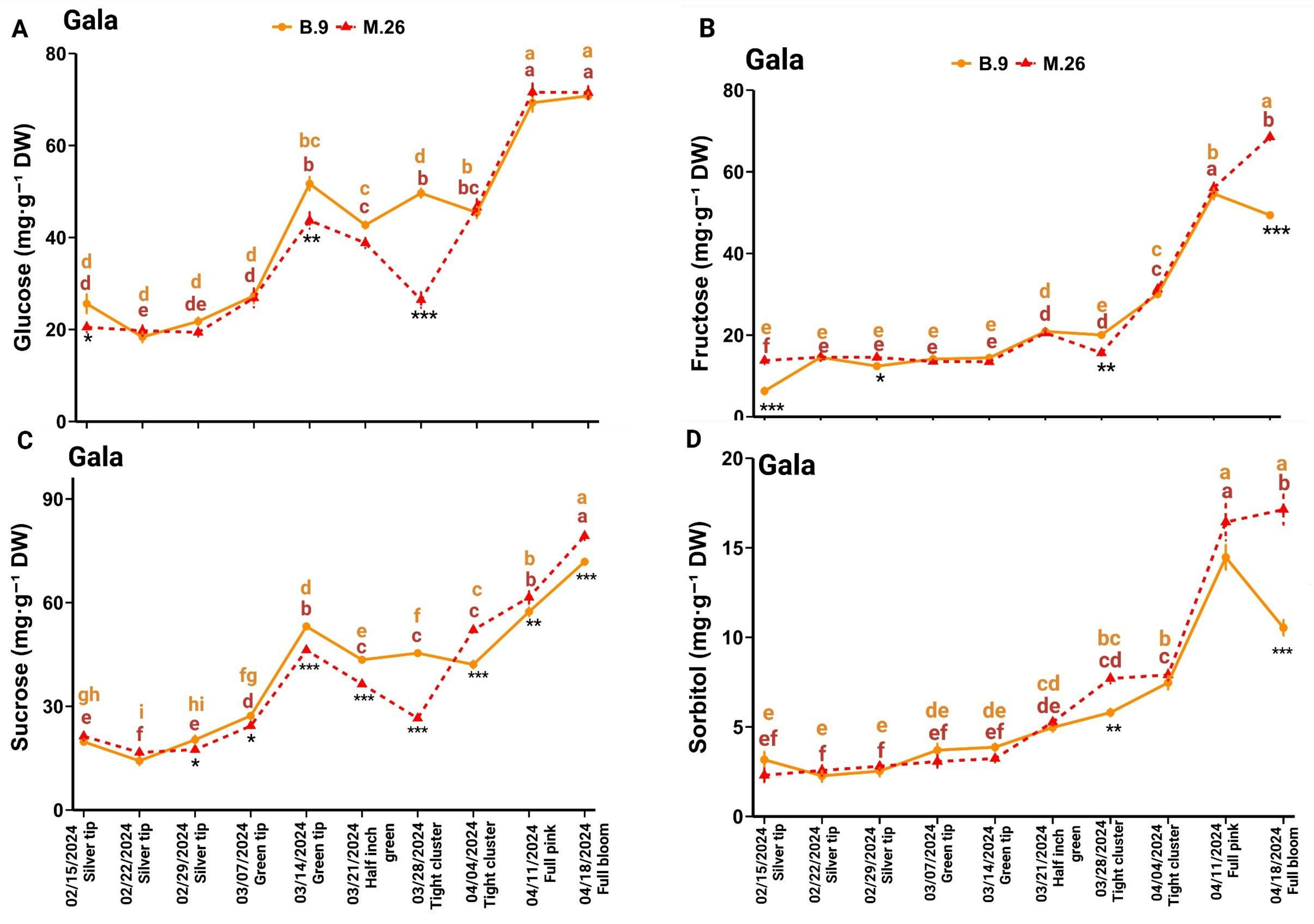

A
B
C
D
Gala
B.9
M.26
Glucose (mg·g⁻¹ DW)
Fructose (mg·g⁻¹ DW)
Sucrose (mg·g⁻¹ DW)
Sorbitol (mg·g⁻¹ DW)
02/15/2024 Silver tip
02/22/2024 Silver tip
02/29/2024 Silver tip
03/07/2024 Green tip
03/14/2024 Green tip
03/21/2024 Half inch green
03/28/2024 Tight cluster
04/04/2024 Tight cluster
04/11/2024 Full pink
04/18/2024 Full bloom

Figure 3: Soluble sugars (A) Glucose, (B) Fructose, (C) Sucrose, and (D) Sorbitol in floral buds of the 'Gala' cultivar grafted onto rootstocks 'B.9' (Full graph line) and 'M.26' (Dashed graph line) during different phenological stages, spanning from white tip to full bloom, measured at ten distinct sampling points. Samples were collected on ten dates: 02/15 (Silver tip), 02/22 (Silver tip), 02/29 (Silver tip), 03/07 (Green tip), 03/14 (Green tip), 03/21 (Half inch green), 03/28 (Tight cluster), 04/04 (Tight cluster), 04/11 (Full pink bud), and 04/18 (Full bloom). The italicized underlined letters indicate significant differences within the 'B.9' rootstock across time based on one-way ANOVA, while the bold letters indicate significance for the 'M.26' rootstock across time. Asterisks represent Tukey's test results comparing 'B.9' and 'M.26' at each sampling point. Error bars indicate the mean±SE (n=3). Significance levels are denoted as $*P \leq 0.05$, $**P \leq 0.01$, and $***P \leq 0.001$, using Tukey's Honestly Significant Difference (HSD) test.

3.2.1(b) Fructose

Fructose concentrations exhibited a few significant differences across developmental stages and between rootstocks **(Figure 3B)**. On 15 February 2024 (silver tip), fructose levels in 'Gala'/ 'M.26' were significantly higher than in 'Gala'/ 'B.9'. On 28 March 2024 (tight cluster), 'Gala'/ 'M.26' exhibited significantly lower fructose levels than 'Gala'/ 'B.9'. However, at full bloom, fructose levels in 'Gala'/ 'B.9' were significantly lower than in 'Gala'/ 'M.26'. Within 'Gala'/ 'B.9', fructose levels exhibited minimal fluctuations, with only a gradual increase from 15 February 2024 (silver tip) to 21 March 2024 (half inch green). A decrease followed on 28 March 2024 (tight cluster), but levels rebounded and increased again until peaking on 11 April 2024 (full pink bud). However, fructose levels declined significantly at full bloom. In 'Gala'/ 'M.26', fructose followed a similar trend, but the decline on 28 March 2024 (tight cluster) was more pronounced compared to 'Gala'/ 'B.9'. Following this dip, fructose levels recovered, peaking on 11 April 2024 (full pink bud) and full bloom.

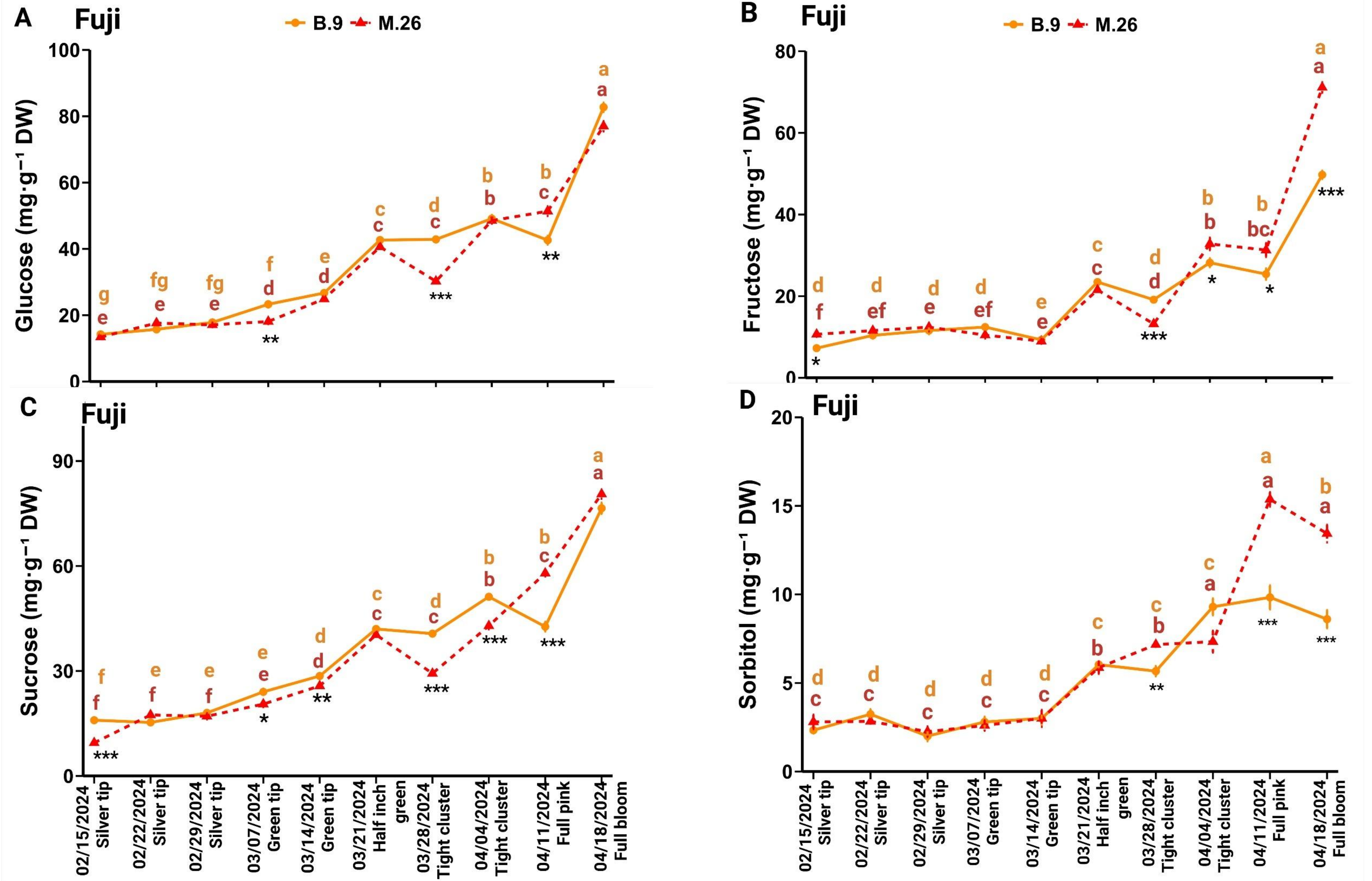
A
B
C
D
Fuji
B.9
M.26
Glucose (mg·g⁻¹ DW)
Fructose (mg·g⁻¹ DW)
Sucrose (mg·g⁻¹ DW)
Sorbitol (mg·g⁻¹ DW)
02/15/2024 Silver tip
02/22/2024 Silver tip
02/29/2024 Silver tip
03/07/2024 Green tip
03/14/2024 Green tip
03/21/2024 Half inch green
03/28/2024 Tight cluster
04/04/2024 Tight cluster
04/11/2024 Full pink
04/18/2024 Full bloom

Figure 4: Soluble sugars (A) Glucose, (B) Fructose, (C) Sucrose, and (D) Sorbitol in floral buds of the 'Fuji' cultivar grafted onto rootstocks 'B.9' (Full graph line) and 'M.26' (Dashed graph line) during different phenological stages, spanning from white tip to full bloom, measured at ten distinct sampling points. Samples were collected on ten dates: 02/15 (Silver tip), 02/22 (Silver tip), 02/29 (Silver tip), 03/07 (Green tip), 03/14 (Green tip), 03/21 (Half inch green), 03/28 (Tight cluster), 04/04 (Tight cluster), 04/11 (Full pink bud), and 04/18 (Full bloom). The italicized underlined letters indicate significant differences within the 'B.9' rootstock across time based on one-way ANOVA, while the bold letters indicate significance for the 'M.26' rootstock across time. Asterisks represent Tukey's test results comparing 'B.9' and 'M.26' at each sampling point. Error bars indicate the mean±SE (*n=3*). Significance levels are denoted as $*P \leq 0.05$, $**P \leq 0.01$, and $***P \leq 0.001$, using Tukey's Honestly Significant Difference (HSD) test.

3.2.1(c) Sucrose

On 29 February 2024 (silver tip) and 7 March 2024 (green tip), 'Gala'/ 'B.9' exhibited few significantly higher sucrose levels compared to 'Gala'/ 'M.26' **(Figure 3C)**. On 14 March 2024 (green tip), 'Gala'/ 'B.9' maintained significantly higher sucrose levels. However, during 21 March 2024 (half inch green) and 28 March 2024 (tight cluster), 'Gala'/ 'M.26' exhibited significantly lower sucrose concentrations. By full bloom, 'Gala'/ 'B.9' showed significantly lower sucrose levels compared to 'Gala'/ 'M.26'. Within 'Gala'/ 'B.9', sucrose levels increased steadily from 15 February 2024 (silver tip) until reaching a peak on 14 March 2024 (green tip), after which they declined on 21 March 2024 (half-inch green). Sucrose levels then increased again on 11 April 2024 (full pink bud) and 18 April 2024 (full bloom). In 'Gala'/ 'M.26', sucrose followed a similar increasing trend until 21 March 2024 (half inch green), but its decline on 28 March 2024 (tight cluster) was significantly greater than in 'Gala'/ 'B.9'. However, 'Gala'/ 'M.26' displayed a strong recovery from 4 April 2024 onward, surpassing 'Gala'/ 'B.9' and remaining higher than 'Gala'/ 'B.9' through full bloom.

3.2.1(d) Sorbitol

On 28 March 2024 (tight cluster), 'Gala'/ 'B.9' had significantly lower sorbitol concentrations compared to 'Gala'/ 'M.26'. Within 'Gala'/ 'B.9', sorbitol levels increased gradually across developmental stages. However, on 28 March 2024 (tight cluster), 'Gala'/ 'M.26' exhibited a significantly greater increase in sorbitol compared to 'B.9'. After this peak in 'M.26', both rootstocks followed a similar pattern, with sorbitol declining toward the last stage in 'Gala'/ 'B.9' **(Figure 3D)**.

3.2.2 'Fuji'

3.2.2(a) Glucose

Glucose concentrations in floral buds of the 'Fuji' cultivar displayed some significant differences across developmental stages and between rootstocks **(Figure 4A)**. On 28 March 2024 (tight cluster), 'Fuji'/ 'M.26' exhibited significantly lower glucose concentrations compared to 'Fuji'/ 'B.9'. At full pink bud, glucose levels in 'Fuji'/ 'M.26' was significantly higher than in 'Fuji'/ 'B.9'. Within 'Fuji'/ 'B.9', glucose levels peaked at full bloom, significantly higher than earlier stages. For ‘Fuji’/ ‘M.26’, glucose concentrations also peaked at full bloom, exceeding all earlier sampling points.

3.2.2(b) Fructose

Fructose concentrations in floral buds of the ‘Fuji’ cultivar displayed a few significant differences across developmental stages and between rootstocks **(Figure 4B)**. On 15 February 2024 (silver tip), fructose levels in ‘Fuji’/ ‘M.26’ were significantly higher than in ‘Fuji’/ ‘B.9’. On 18 April 2024 (full bloom), fructose levels in ‘Fuji’/ ‘M.26’ was significantly higher than in ‘Fuji’/ ‘B.9’. Within ‘Fuji’/ ‘B.9’, fructose levels peaked on 18 April 2024 (full bloom). Fructose levels in ‘Fuji’/ ‘M.26’ showed a continuous increase, also peaking at full bloom.

3.2.2(c) Sucrose

Sucrose concentrations in floral buds of the ‘Fuji’ cultivar exhibited few significant differences across developmental stages and between rootstocks **(Figure 4C)**. On 15 February 2024 (silver tip), sucrose levels in ‘Fuji’/ ‘B.9’ were significantly higher than in ‘Fuji’/ ‘M.26’. On 14 March 2024 (green tip), sucrose levels in ‘Fuji’/ ‘B.9’ remained significantly higher. However, on 28 March 2024 (tight cluster) and 4 April 2024 (tight cluster) ‘Fuji’/ ‘M.26’ exhibited significantly lower sucrose concentrations compared to ‘Fuji’/ ‘B.9’. Within ‘Fuji’/ ‘B.9’, sucrose levels peaked at full bloom. In ‘Fuji’/ ‘M.26’, sucrose levels also peaked at full bloom, showing a steady increase across all developmental stages.

3.2.2(d) Sorbitol

On 15 February 2024 (silver tip) until 21 March 2024 (Half inch green), sorbitol levels were comparable between ‘Fuji’/ ‘B.9’ and ‘Fuji’/ ‘M.26’, with no significant differences observed. On 28 March 2024 (tight cluster), ‘Fuji’/ ‘M.26’ exhibited significantly higher sorbitol concentrations compared to ‘B.9’. Within ‘Fuji’/ ‘B.9’, sorbitol concentrations peaked at full pink bud. For ‘Fuji’/ ‘M.26’, sorbitol concentrations followed a similar trend, peaking at full pink bud **(Figure 4D)**.

3.3 Expression Profiling of Carbohydrate Metabolism Genes

The expression patterns of key carbohydrate metabolism genes in floral buds of the ‘Gala’ cultivar exhibited significant differences between the rootstocks ‘B.9’ and ‘M.26’ across developmental stages (Figure 4). *MdSS2* (Starch Synthase 2, **Figure 5A**) expression in ‘Gala’/ ‘M.26’ was significantly higher than in ‘Gala’/ ‘B.9’ at 22 and 29 February 2024 (silver tip). *MdSSE* (Starch Branching Enzyme 2.2, **Figure 5B**) also showed rootstock-dependent trends, with ‘‘Gala’/M.26’ displaying significantly higher expression on 15 February 2024 (silver tip), while ‘Gala’/ ‘B.9’ peaked later 28 March 2024 (tight cluster). In contrast, *MdAMY* (Beta-Amylase, **Figure 5C**) exhibited its highest expression in ‘Gala’/ ‘M.26’ on 15 February 2024 (silver tip), while ‘Gala’/ ‘B.9’ peaked later on 22 February 2024 with expression levels in both rootstocks subsequently declining. *MdSUS4* (Sucrose Synthase 4, **Figure 5D**) followed a distinct pattern, where ‘Gala’/ ‘M.26’ had significantly higher expression on 15 February 2024 (silver tip), but by full bloom, ‘Gala’/ ‘B.9’ exhibited the highest expression, increasing steadily from earlier stages. *MdINV* (Plant Invertase, **Figure 5E**) was significantly upregulated in ‘Gala’/ ‘B.9’ on 4 April 2024 (tight cluster) and 11 April 2024 (full pink bud), whereas both rootstocks showed an initial peak on 22 February

2024 (silver tip) before declining. *MdSTP* (Sugar Transporter Protein 14, **Figure 5F**) exhibited higher expression in 'Gala'/ 'M.26' across all phenological stages, with significant differences on 15 February 2024 (silver tip), 22 February 2024 (silver tip), and 29 February 2024 (silver tip), suggesting a rootstock-dependent advantage in sugar transport. Similarly, *MdSWT* (SWEET/Nodulin MtN3 Family Protein, **Figure 5G**) displayed rootstock-specific regulation, with 'Gala'/ 'B.9' showing significantly higher expression 14 March 2024 (green tip), while 'Gala'/ 'M.26' peaked on 4 April 2024 (tight cluster). *MdERD* (Dehydration-Induced Protein 15, **Figure 5H**) expression was highest in 'Gala'/ 'M.26' on 15 February 2024 (silver tip). Finally, *MdTONO* (Delta Tonoplast Integral Protein, **Figure 5I**) showed early-stage peaks in 'Gala'/ 'M.26' on 7 March 2024 (green tip), whereas 'Gala'/ 'B.9' exhibited higher expression during 28 March 2024 (tight cluster) and 4 April 2024 (tight cluster), with 'Gala'/ 'M.26' peaking again at full bloom.

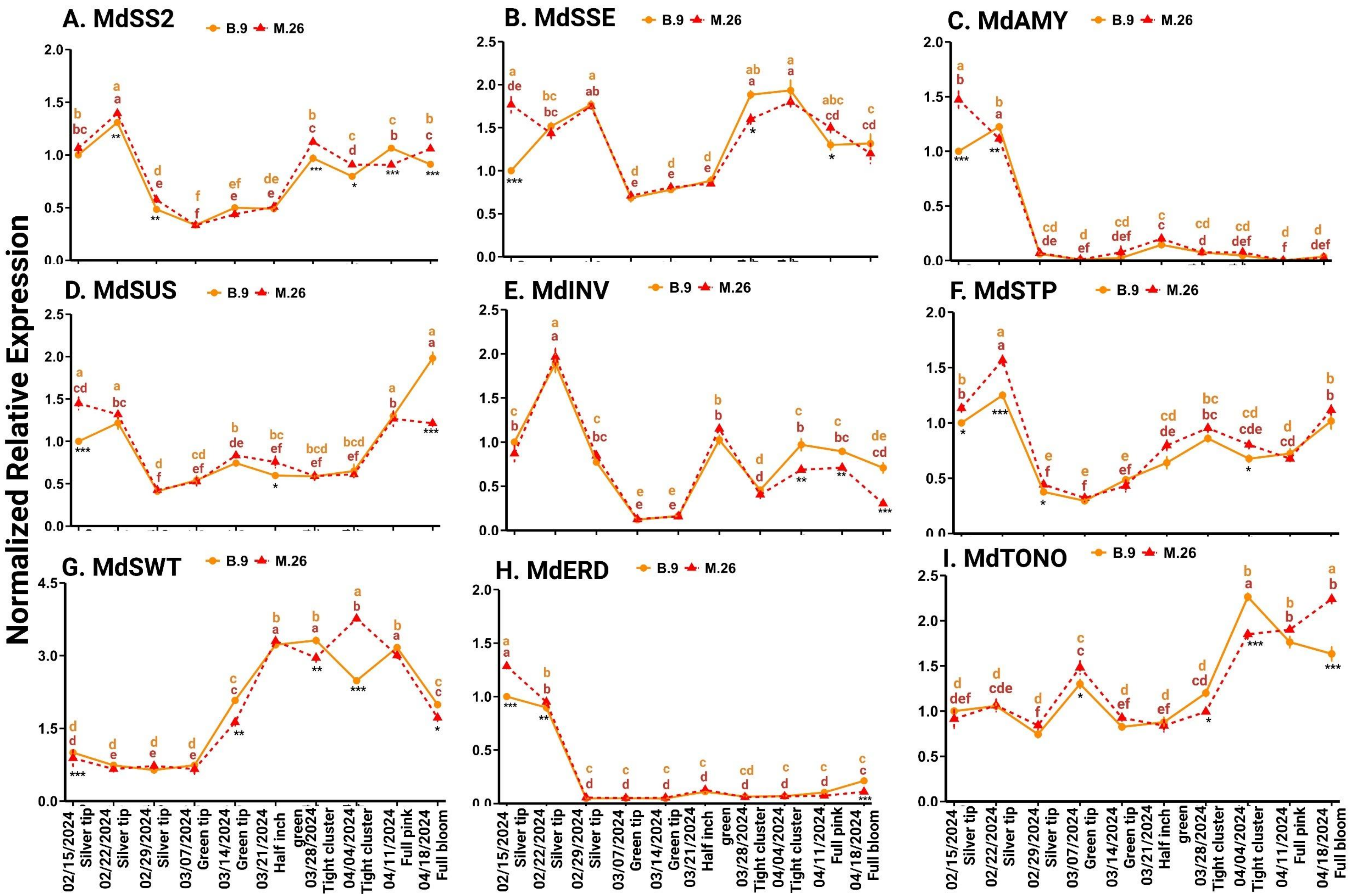

Normalized Relative Expression
A. MdSS2
B. MdSSE
C. MdAMY
D. MdSUS
E. MdINV
F. MdSTP
G. MdSWT
H. MdERD
I. MdTONO
B.9
M.26
02/15/2024 Silver tip
02/22/2024 Silver tip
02/29/2024 Silver tip
03/07/2024 Green tip
03/14/2024 Green tip
03/21/2024 Half inch green
03/28/2024 Tight cluster
04/04/2024 Tight cluster
04/11/2024 Full pink
04/18/2024 Full bloom

Figure 5: Expression profiles of genes (A) *MdSS2* (B) *MdSSE* (C) *MdAMY* (D) *MdSUS* (E) *MdINV* (F) *MdSTP* (G) *MdSWT* (H) *MdERD* (I) *MTONO* in floral buds of the 'Gala' cultivar grafted onto rootstocks 'B.9' (Full graph line) and 'M.26' (Dashed graph line) during different phenological stages, spanning from white tip to full bloom, measured at ten distinct sampling points. Samples were collected on ten dates: 02/15 (Silver tip), 02/22 (Silver tip), 02/29 (Silver tip), 03/07 (Green tip), 03/14 (Green tip), 03/21 (Half inch green), 03/28 (Tight cluster), 04/04 (Tight cluster), 04/11 (Full pink bud), and 04/18 (Full bloom). The italicized underlined letters indicate significant differences within the 'B.9' rootstock across time based on one-way ANOVA, while the bold letters indicate significance for the 'M.26' rootstock across time. The expression of each gene was normalized to that of two reference genes (*MdActin* and *MdGAPDH*) and then calculated relative to the expression level in the control sample ('B.9' at 2505 GDH; 15 February 2024). Error bars indicate the standard error of the mean of three biological and two technical replicates. Significance levels are denoted as $*P \leq 0.05$, $**P \leq 0.01$, and $***P \leq 0.001$, using Tukey's Honestly Significant Difference (HSD) test.

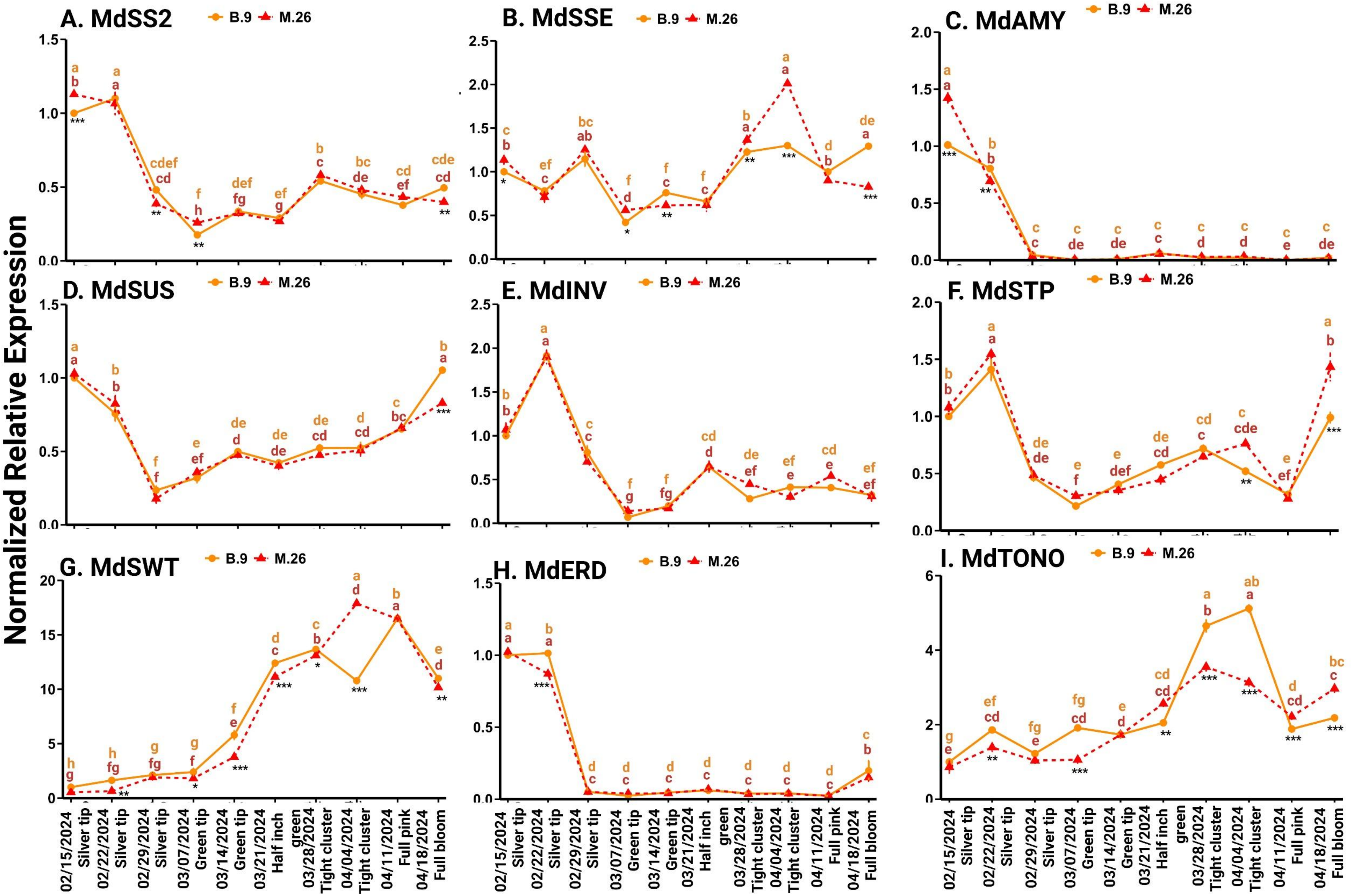

Normalized Relative Expression
A. MdSS2
B. MdSSE
C. MdAMY
D. MdSUS
E. MdINV
F. MdSTP
G. MdSWT
H. MdERD
I. MdTONO
B.9
M.26
0.0
0.5
1.0
1.5
2.0
2.5
0
2
4
6
5
10
15
20
02/15/2024 Silver tip
02/22/2024 Silver tip
02/29/2024 Silver tip
03/07/2024 Green tip
03/14/2024 Green tip
03/21/2024 Half inch green
03/28/2024 Tight cluster
04/04/2024 Tight cluster
04/11/2024 Full pink
04/18/2024 Full bloom

Figure 6: Expression profiles of genes (A) *MdSS2* (B) *MdSSE* (C) *MdAMY* (D) *MdSUS* (E) *MdINV* (F) *MdSTP* (G) *MdSWT* (H) *MdERD* (I) *MTONO* in floral buds of the 'Fuji' cultivar grafted onto rootstocks 'B.9' (Full graph line) and 'M.26' (Dashed graph line) during different phenological stages, spanning from white tip to full bloom, measured at ten distinct sampling points. Samples were collected on ten dates: 02/15 (Silver tip), 02/22 (Silver tip), 02/29 (Silver tip), 03/07 (Green tip), 03/14 (Green tip), 03/21 (Half inch green), 03/28 (Tight cluster), 04/04 (Tight cluster), 04/11 (Full pink bud), and 04/18 (Full bloom). The italicized underlined letters indicate significant differences within the 'B.9' rootstock across time based on one-way ANOVA, while the bold letters indicate significance for the 'M.26' rootstock across time. Asterisks represent Tukey's test results comparing 'B.9' and 'M.26' at each sampling point. The expression of each gene was normalized to that of two reference genes (*MdActin* and *MdGAPDH*) and then calculated relative to the expression level in the control sample ('B.9' at 2505 GDH; 15 February 2024). Error bars indicate the standard error of the mean of three biological and two technical replicates Significance levels are denoted as $*P \leq 0.05$, $**P \leq 0.01$, and $***P \leq 0.001$, using Tukey's Honestly Significant Difference (HSD) test.

The expression of *MdSS2* (Starch Synthase 2, **Figure 6A**) in 'Fuji' exhibited significant rootstock-specific variations across developmental stages. 'Fuji'/ 'M.26' showed significantly higher expression than 'Fuji'/ 'B.9' on 15 February 2024 (silver tip), but this trend reversed on 29 February 2024 (silver tip), where 'Fuji'/ 'B.9' demonstrated higher expression. Similarly, *MdSSE* (Starch Branching Enzyme 2.2, **Figure 6B**) was consistently higher in 'Fuji'/ 'M.26' during early stages, including 15 February 2024 (silver tip) and 7 March 2024 (green tip) but 'Fuji'/ 'B.9' exhibited higher expression on 14 March 2024 (green tip)**.** 'Fuji'/ 'M.26' regained dominance on 28 March 2024 (tight cluster) and peaked on 4 April 2024 (tight cluster), though 'Fuji'/ 'B.9' had the highest expression on 18 April 2024 (full bloom). *MdAMY* (Beta-Amylase, **Figure 6C**) followed a similar pattern, with significantly higher expression in 'Fuji'/ 'M.26' on 15 February 2024 (silver tip), while 'Fuji'/ 'B.9' exhibited the highest expression on 22 February 2024 (silver tip) followed by a sharp and consistent decline through later phenological stages. *MdSTP* (Sugar Transporter 14, **Figure 6F**) expression was consistently higher in 'Fuji'/ 'M.26' at several stages, with significant differences on 4 April 2024 (tight cluster) and 18 April 2024 (full bloom). Both rootstocks peaked on 22 February 2024 (silver tip) before declining sharply. *MdSWT* (SWEET/Nodulin MtN3 Family Protein, **Figure 6G**) displayed rootstock-dependent variations, with 'Fuji'/ 'B.9' showing significantly higher expression on 22 February 2024 (silver tip), 7 March 2024 (green tip), and 14 March 2024 (green tip). Both rootstocks followed a trend of peaking on 28 March 2024 (tight cluster) and 'Fuji'/ 'M.26' showed higher trend on 4 April 2024. *MdER*D (Dehydration-Induced Protein 15, **Figure 6H**) expression was highest on 22 February 2024 (silver tip) for 'Fuji'/ 'B.9'. Expression declined sharply after this stage, remaining low through intermediate phases before a slight increase at full bloom. Finally, *MdTONO* (Delta Tonoplast Integral Protein, **Figure 6I**) exhibited significant rootstock-specific differences, with 'Fuji'/ 'M.26' exhibited higher expression on 21 March 2024 (half inch green) and full bloom. On 28 March 2024 (tight cluster)**,** and 4 April 2024 'Fuji'/ 'B.9' had highest expression, underscoring the dynamic regulation of *MdTONO* expression.

4 Discussion

In perennial fruit trees like apple (*Malus* × *domestica* Borkh.), the transition from dormancy to floral bud development is a pivotal phase that directly determines crop yield and quality. Over decades of research, critical spring temperatures for survival have been identified for each bud stage—from silver tip to full bloom—revealing that frost tolerance progressively declines as phenology advances (Jahed et al., 2023). For instance, at tight cluster stage, temperatures of about –6°C for more than thirty minutes can cause extensive bud mortality (up to 90%), posing a grave threat to production (Michigan State University Extension, 2021). Despite widespread awareness of these damaging thresholds, the mechanistic basis behind shifting frost sensitivity remains poorly understood. This study investigated whether changes in carbohydrate metabolism, particularly soluble sugars and starch, contribute to the progressive decline in frost tolerance. By monitoring sugar content and key genes involved in carbohydrate metabolism across critical developmental windows, we aimed to elucidate how apple buds regulate their carbohydrate pools and whether these shifts align with known frost vulnerability periods.

4.1 Early Spring Sugar Mobilization and Bud Development from start of silver tip to beginning of green tip stage (2,505–3,773 GDH; 15 February–7 March)

In deciduous trees, reserve carbohydrates—largely starch and stored sugars in roots, stems, and bark—are remobilized as buds exit dormancy (Fermaniuk et al., 2021). Throughout late winter, these reserves function as source pools, while developing floral buds become strong sink organs drawing on available sugars and nutrients to initiate growth (Furze et al., 2019). Initial sampling between 15 February 2024 (silver tip) and 7 March 2024 (starting of green tip) revealed moderate starch levels alongside rising concentrations of glucose, fructose, sucrose and sorbitol collectively indicating a notable increase in bud sink strength. This trend aligns with patterns reported in apple (Sapkota et al., 2021), sweet cherry (Fadón et al., 2018), and petunia (Bauerfeind et al., 2015), where "source leaves" accumulate sugars, while the "sink apex" depletes starch as growth progresses. Such prioritization of carbon toward developing buds is crucial when morphological demands and ambient temperatures fluctuate.

Gene expression analyses highlighted a coordinated shift toward soluble sugar mobilization rather than robust starch biosynthesis during these early stages. Gene expression of starch synthase 2 (*MdSS2*) exhibited a sharp decline by February 29, indicating reduced starch synthesis in favor of soluble sugar availability. Concurrently, gene expression of starch branching enzyme (*MdSSE)* briefly rose on February 29 (silver tip), potentially indicating an early reorganization of starch granules that could facilitate subsequent carbohydrate mobilization. In contrast, expression of the gene amylase (*MdAMY)* and dehydration-induced protein (*MdERD*) involved in starch breakdown (Das and Kayastha 2019) and vacuolar sugar efflux (Yamada et al., 2010), respectively, decreased significantly after 22 February 2024 (silver tip), suggesting minimal active starch breakdown and limited vacuolar sugar export during this phase. Additionally, reduced expression of sucrose synthase 4 (*MdSUS4)* and invertase (*MdINV*) resulted in little increase in glucose and fructose, reflecting limited downstream sugars demand (Koch 2004). The gradual accumulation of soluble sugars in early spring, particularly in 'Gala'/'B.9' and 'Fuji'/'B.9', could have provided essential osmoprotection and energy supply to safeguard buds against temperature dips.

4.2 Mid-March Sugar Peak and the Role of Key Organelles from green tip to half inch green stage (4,583–5,672 GDH; 14–21 March)

Within developing bud cells, plastids (amyloplasts or chloroplasts, depending on developmental stage and light exposure) coordinate carbohydrate flow with the cytosol (Zhu et al., 2021). Early during dormancy release, starch reserves often accumulate within plastids, available for mobilization in response to cold signals (Sheikh et al., 2022) or increased sink demands (Martinoia, 2018). On 14 March 2024 (green tip), a notable peak in soluble sugars—particularly sucrose and glucose—was observed, aligning with a dynamic rise in starch concentration that peaked on 14 March 2024 (green tip), followed by a subsequent decline. This indicates active mobilization of starch reserves to support metabolic demands and rapid morphological expansion of developing floral buds. Alternatively, increased sugar levels could reflect temporary storage of phloem-delivered carbohydrates in the vacuole or cytosol (Liesche and Schulz 2013).

Gene expression analyses further clarified the starch dynamics at this critical stage. Expression of starch synthase 2 (*MdSS2)*, an enzyme crucial for plant starch biosynthesis, exhibited a modest recovery following an initial drop in expression, coinciding with increased expression of gene for enzyme involved in the synthesis of amylopectin, *MdSSE*, by early March. This suggests dynamic starch metabolism, balancing reserve replenishment and hydrolysis to maintain consistent energy supplies during periods of demand (Thalmann & Santelia, 2017). Concurrently, moderate expression of sucrose synthase gene *MdSUS* and plant invertase enzyme gene *MdINV* supported controlled sucrose cleavage into hexoses and glucose, fueling respiration and biosynthetic pathways essential for bud expansion (Ruan et al., 2010). Additionally, sugar transporter protein genes such as *MdSTP*, initially downregulated, began recovering during this period, reflecting adjustments in intracellular sugar availability and transport to sink cells. Rootstock-specific differences became pronounced during this critical phase. In 'Fuji' on 'B.9', genes involved in sugar transport and vacuolar mobilization, notably *MdTONO*, coding an aquaporin membrane protein which facilitates transport across cell membranes, exhibited steadier expression or quicker recoveries, suggesting a coordinated sugar flux that maintained stable cytosolic sugar availability. 'Gala' and 'Fuji' on 'B.9' displayed stronger but transient peaks in expression of sugar transporter gene *MdSWT*. These fluctuations suggest an "overshoot and decline" pattern, which could mean that by timing these expression peaks with periods of intense bud demand, 'B.9' ultimately maintains a higher net sugar availability than 'M.26'. The vacuole, highlighted through the expression patterns of *MdTONO*, emerged as an essential regulator of sugar homeostasis and osmotic equilibrium (Jiang et al., 2021). *MdTONO* expression peaked around 7 March 2024 in 'Fuji' on 'B.9', suggesting active sugar mobilization from vacuoles into the cytosol, likely to maintain osmotic balance and support growth under conditions of high metabolic activity. However, 'M.26''s intermittent spikes in *MdTONO* in 'Gala' and other sugar transporter gene activities indicate less efficient coordination of vacuolar sugar flux, potentially resulting in periods of depleted cytosolic sugar levels, while 'B.9''s steadier expression profiles likely stabilized cytosolic sugar pools. These findings reinforce the principle that effective frost tolerance relies on maintaining stable intracellular sugar pools. Abrupt or imbalanced sugar transport—such as excessive *MdSWT* activity or insufficient tonoplast sugar import—could possibly reduce cytosolic sugar concentrations (Klemens et al., 2014).

4.3 A Critical Transition from end of half inch green stage to tight cluster (5,672–6,797 GDH; 21 March–4 April)

Our data from 5,672–6,797 GDH (tight cluster stage) revealed a reduction in soluble sugars—particularly glucose, fructose, and sucrose—across most samples from 'Gala' and 'Fuji' on 'M.26'. However, in the 'Gala' cultivar on rootstock 'B.9', a decrease in soluble sugars was noted but it was notably less pronounced than in 'M.26' —coinciding with intense morphological demands such as the rapid expansion of floral structures like petals, stamens, pistils (Klein et al., 2016; Luo et al., 2024). This reduction aligns with previous findings showing that increased sink demands during critical developmental periods can exceed sugar reimport or supply, thus transiently diminishing cytosolic sugar reserves and exacerbating frost sensitivity (Weiszmann et al., 2018; Vu et al., 2020). During this stage, *MdSS2* and *MdSSE* exhibited increased expression tight cluster, signifying active starch synthesis likely intended to replenish reserves. However, the low rise in starch suggests that newly synthesized starch was rapidly mobilized to meet immediate metabolic needs rather than stored long-term.

Rootstock-specific differences were pronounced during this critical phase. In 'Gala' and 'Fuji' on 'B.9', the coordinated surge in *MdSWT* expression on 28 March 2024 (tight cluster), coupled with partial *MdSTP* expression, suggested a balanced sugar flux maintaining adequate cytosolic sugar levels despite high metabolic demands (Borghi & Fernie, 2017) followed by significant drops in *MdINV* expression. Such oscillatory dynamics likely compromised the steady influx of hexoses into cells, worsening sugar shortages at critical times and increasing vulnerability to frost. Vacuolar dynamics further underscored these differences. *MdTONO* expression in 'B.9' peaked during tight cluster stage from 28 March to 4 April, which could be reflecting active vacuolar sugar mobilization into the cytosol to maintain osmotic balance and sugar availability. 'M.26' showed intermittent peaks in *MdTONO* expression, but these were often poorly synchronized with other sugar transport processes, potentially leading to inefficient cytosolic sugar maintenance. Meanwhile, consistently low expression of *MdERD* gene for dehydration stress protective protein 15, suggested limited vacuolar glucose mobilization overall, reinforcing the challenge of maintaining cytosolic sugars during this high-demand stage. Additionally, a marked reduction in *MdINV* expression on 28 March 2024 (tight cluster) impaired sucrose hydrolysis into glucose and fructose, further exacerbating sugar deficits. This sucrose decline could have impaired the critical pathway by which sugars are unloaded from the phloem to the apoplast, subsequently entering sink cells or being cleaved for metabolic use —a concept supported by findings of Stein & Granot (2019).

4.4 Pink-Bud Cluster Recovery and Shifting Sink Dynamics till full bloom (6,797–10,410 GDH; 4–18 April)

Following the tight cluster stage, a partial resurgence in sugar levels became evident in 'Gala' from end of tight cluster onwards (4 April 2024), driven largely by newly unfolded leaves initiating photosynthesis. This phase could have marked a significant redistribution of carbohydrate resources, transitioning opening buds from dominant sinks to entities sharing resources with emerging, photosynthetically active leaves. Such redistribution aligns closely with the broader concept of a "sink hierarchy," wherein newly autotrophic tissues alleviate buds' dependence on imported carbohydrates, allowing for a more balanced carbohydrate supply (Borghi & Fernie, 2017). All floral organs, except for sepals, depend upon sugar import in a measure that correlates with their growth and stage of development and are sustained mainly by postphloem sucrose delivery and only to a minor extent by carbohydrates produced via floral carbon fixation (Aschan and Pfanz, 2003). Regarding metabolism, petals are mixotrophic: young green petals can perform photosynthesis, but they progressively lose the ability to fix carbon as they mature and ultimately become fully heterotrophic (Thomas, 2003; Muhlemann et al., 2012). This metabolic shift, documented in species like *Nicotiana tabacum* and *Antirrhinum majus*, redirects carbohydrate allocation toward secondary metabolism and pigment accumulation, crucial for floral maturation and expansion (Tsanakas et al., 2014). In apples, the observed sugar recovery during bloom stages likely reflects this redistribution of resources to sustain floral growth and newly photosynthetically active leaves.

Soluble sugar profiles demonstrated a nuanced pattern: glucose levels, for instance, generally increased until 14 March 2024 (green tip), subsequently decreased, and then recovered notably by 11 April 2024 (full pink bud) and peaked at full bloom in both rootstocks. However, rootstock-specific patterns emerged clearly during this period. 'M.26' exhibited higher soluble sugar concentrations at full pink bud and full bloom. In parallel, elevated *MdTONO* expression in 'M.26' at full bloom may suggest a delayed or less synchronized remobilization of vacuolar sugars, while *MdSUS* was more upregulated in 'B.9'—in both 'Gala' and 'Fuji'—potentially aiding a more effective sugar supply at earlier stages. Although these patterns could indicate a rootstock-specific strategy in carbohydrate management, the timing and coordination of sugar accumulation and gene expression may be more critical than total sugar levels alone. Consequently, while 'M.26' maintained higher sugar concentrations towards the end of the developmental window. Other factors not captured in this study may contribute to developmental sensitivity at these stages, highlighting the need for a broader physiological context when interpreting sugar dynamics alone.

5 Conclusion

This study demonstrates the crucial role of carbohydrate metabolism in determining frost tolerance across different floral bud developmental stages in apple (*Malus × domestica* Borkh.) cultivars 'Fuji' and 'Gala' grafted onto two rootstocks 'B.9' and 'M.26'. Early phenological stages (2,505–3,773 GDH; silver tip to start of green tip) showed moderate starch reserves alongside steadily rising soluble sugars (glucose, fructose, sucrose, sorbitol), reflecting coordinated expression of key carbohydrate metabolism genes *MdSS2* (Starch Synthase 2), *MdSSE* (Starch Branching Enzyme 2.2), *MdSUS4* (Sucrose Synthase 4), *MdSWT*. During the end of half inch green stage (21 March; 5,672 GDH) to the end of tight cluster (4 April; 6,797 GDH), significant depletion of glucose and sucrose could coincide with increased susceptibility to late spring frost conditions. Rootstock differences were particularly evident during this critical transition, with floral buds of 'Gala' and 'Fuji' on 'B.9' consistently maintaining balanced carbohydrate pools through coordinated expression of *MdSWT*, *MdSTP* (Sugar Transporter 14), and *MdTONO* (Delta tonoplast Integral Protein) genes, while 'M.26' exhibited marked fluctuations that potentially compromised sugar availability. Post–tight cluster i.e. at pink bud (4–18 April; 8,157–10,410 GDH), a partial recovery in soluble sugars, supported by newly photosynthetic leaves, further underscored rootstock-specific dynamics. However, despite this recovery, soluble sugar accumulation did not correspond with improved physiological conditions, suggesting that sugar levels alone are not sufficient to explain the progressive changes in bud status. This underscores the importance of rootstock-mediated regulation of carbohydrate metabolism as a developmental determinant during key transitions in floral bud maturation.

Supplementary Data

https://github.com/Amolpreet1/Supplementary/blob/acb22a60edc6e16b013c3d8d6fb91b8df203ca76/Supplementary%20Link.docx

References

Abdelrahman, M., Burritt, D. J., Gupta, A., Tsujimoto, H., & Tran, L.-S. P. (2020). Heat stress effects on source–sink relationships and metabolome dynamics in wheat. *Journal of Experimental Botany*, *71*(2), 543–554. https://doi.org/10.1093/jxb/erz296

Afzal, S., Chaudhary, N., & Singh, N. K. (2021). Role of Soluble Sugars in Metabolism and Sensing Under Abiotic Stress. In T. Aftab & K. R. Hakeem (Eds.), *Plant Growth Regulators* (pp. 305–334). Springer International Publishing. https://doi.org/10.1007/978-3-030-61153-8_14

Ahmadi, H., Ghalhari, G. F., & Baaghideh, M. (2019). Impacts of climate change on apple tree cultivation areas in Iran. *Climatic Change*, *153*(1–2), 91–103. https://doi.org/10.1007/s10584-018-2316-x

Aschan, G., & Pfanz, H. (2003). Non-foliar photosynthesis – a strategy of additional carbon acquisition. *Flora - Morphology, Distribution, Functional Ecology of Plants*, *198*(2), 81–97. https://doi.org/10.1078/0367-2530-00080

Bauerfeind, M. A., Winkelmann, T., Franken, P., & Druege, U. (2015). Transcriptome, carbohydrate, and phytohormone analysis of Petunia hybrida reveals a complex disturbance of plant functional integrity under mild chilling stress. *Frontiers in Plant Science*, *6*. https://doi.org/10.3389/fpls.2015.00583

Blumstein, M., Gersony, J., Martínez-Vilalta, J., & Sala, A. (2023). Global variation in nonstructural carbohydrate stores in response to climate. *Global Change Biology*, *29*(7), 1854–1869. https://doi.org/10.1111/gcb.16573

Borghi, M., & Fernie, A. R. (2017). Floral Metabolism of Sugars and Amino Acids: Implications for Pollinators' Preferences and Seed and Fruit Set. *Plant Physiology*, *175*(4), 1510–1524. https://doi.org/10.1104/pp.17.01164

Breen, K., Tustin, S., Palmer, J., Boldingh, H., & Close, D. (2020). Revisiting the role of carbohydrate reserves in fruit set and early-season growth of apple. *Scientia Horticulturae*, *261*, 109034. https://doi.org/10.1016/j.scienta.2019.109034

Büttner, M. (2010). The *Arabidopsis* sugar transporter (AtSTP) family: An update. *Plant Biology*, *12*(s1), 35–41. https://doi.org/10.1111/j.1438-8677.2010.00383.x

Centinari, M., Smith, M. S., & Londo, J. P. (2016). Assessment of Freeze Injury of Grapevine Green Tissues in Response to Cultivars and a Cryoprotectant Product. *HortScience*, *51*(7), 856–860. https://doi.org/10.21273/HORTSCI.51.7.856

Chang, C. Y., Bräutigam, K., Hüner, N. P. A., & Ensminger, I. (2021). Champions of winter survival: Cold acclimation and molecular regulation of cold hardiness in evergreen conifers. *New Phytologist*, *229*(2), 675–691. https://doi.org/10.1111/nph.16904

Chen, R., Wang, J., Li, Y., Song, Y., Huang, M., Feng, P., Qu, Z., & Liu, L. (2023). Quantifying the impact of frost damage during flowering on apple yield in Shaanxi province, China. *European Journal of Agronomy*, *142*, 126642. https://doi.org/10.1016/j.eja.2022.126642

Chen, R., Wang, J., Wang, B., Li, Y., Bai, R., Huang, M., Qu, Z., & Liu, L. (2025). Flowering delay in apple could alleviate frost-induced yield loss under climate change in China. *Agricultural and Forest Meteorology*, *360*, 110313. https://doi.org/10.1016/j.agrformet.2024.110313

Das, R., & Kayastha, A. M. (2019). β-Amylase: General Properties, Mechanism and Panorama of Applications by Immobilization on Nano-Structures. In Q. Husain & M. F. Ullah (Eds.), *Biocatalysis: Enzymatic Basics and Applications* (pp. 17–38). Springer International Publishing. https://doi.org/10.1007/978-3-030-25023-2_2

Deslauriers, A., Fournier, M.-P., Cartenì, F., & Mackay, J. (2019). Phenological shifts in conifer species stressed by spruce budworm defoliation. *Tree Physiology*, *39*(4), 590–605. https://doi.org/10.1093/treephys/tpy135

Dong, S., & Beckles, D. M. (2019). Dynamic changes in the starch-sugar interconversion within plant source and sink tissues promote a better abiotic stress response. *Journal of Plant Physiology*, *234–235*, 80–93. https://doi.org/10.1016/j.jplph.2019.01.007

Fadón, E., Fernandez, E., Behn, H., & Luedeling, E. (2020). A Conceptual Framework for Winter Dormancy in Deciduous Trees. *Agronomy*, *10*(2), 241. https://doi.org/10.3390/agronomy10020241

Fadón, E., Herrero, M., & Rodrigo, J. (2018). Dormant Flower Buds Actively Accumulate Starch over Winter in Sweet Cherry. *Frontiers in Plant Science*, *9*, 171. https://doi.org/10.3389/fpls.2018.00171

Fermaniuk, C., Fleurial, K. G., Wiley, E., & Landhäusser, S. M. (2021). Large seasonal fluctuations in whole-tree carbohydrate reserves: Is storage more dynamic in boreal ecosystems? *Annals of Botany*, *128*(7), 943–957. https://doi.org/10.1093/aob/mcab099

Furze, M. E., Huggett, B. A., Aubrecht, D. M., Stolz, C. D., Carbone, M. S., & Richardson, A. D. (2019). Whole-tree nonstructural carbohydrate storage and seasonal dynamics in five temperate species. *New Phytologist*, *221*(3), 1466–1477. https://doi.org/10.1111/nph.15462

Hubmann, A. M., Roth, A., & Monschein, S. (2023). Breaking Buds—Stop and Go? Acid Invertase Activities in Apple Leaf Buds during Dormancy Release until Bud Break. *Agronomy*, *13*(10), 2659. https://doi.org/10.3390/agronomy13102659

Islam, M. T., Liu, J., & Sherif, S. M. (2021). Ethephon-Mediated Bloom Delay in Peach Is Associated With Alterations in Reactive Oxygen Species, Antioxidants, and Carbohydrate Metabolism During Dormancy. *Frontiers in Plant Science*, *12*. https://doi.org/10.3389/fpls.2021.765357

Jahed, K. R., Saini, A. K., & Sherif, S. M. (2023). Coping with the cold: Unveiling cryoprotectants, molecular signaling pathways, and strategies for cold stress resilience. *Frontiers in Plant Science*, *14*, 1246093. https://doi.org/10.3389/fpls.2023.1246093

Jiang, Y.-T., Yang, L.-H., Ferjani, A., & Lin, W.-H. (2021). Multiple functions of the vacuole in plant growth and fruit quality. *Molecular Horticulture*, *1*(1), 4. https://doi.org/10.1186/s43897-021-00008-7

Klein, T., Vitasse, Y., & Hoch, G. (2016). Coordination between growth, phenology and carbon storage in three coexisting deciduous tree species in a temperate forest. *Tree Physiology*, *36*(7), 847–855. https://doi.org/10.1093/treephys/tpw030

Klemens, P. A. W., Patzke, K., Trentmann, O., Poschet, G., Büttner, M., Schulz, A., Marten, I., Hedrich, R., & Neuhaus, H. E. (2014). Overexpression of a proton-coupled vacuolar glucose exporter impairs freezing tolerance and seed germination. *New Phytologist*, *202*(1), 188–197. https://doi.org/10.1111/nph.12642

Koch, K. (2004). Sucrose metabolism: Regulatory mechanisms and pivotal roles in sugar sensing and plant development. *Current Opinion in Plant Biology*, *7*(3), 235–246. https://doi.org/10.1016/j.pbi.2004.03.014

Kong, W., An, B., Zhang, Y., Yang, J., Li, S., Sun, T., & Li, Y. (2019). Sugar Transporter Proteins (STPs) in Gramineae Crops: Comparative Analysis, Phylogeny, Evolution, and Expression Profiling. *Cells*, *8*(6), 560. https://doi.org/10.3390/cells8060560

Kwon, J. H., Nam, E. Y., Yun, S. K., Kim, S. J., Yu, D. J., & Lee, H. J. (2022). Comparative carbohydrate metabolism in the shoots of a cold-hardy and a cold-sensitive peach (Prunus persica) cultivar during cold acclimation and deacclimation. *Horticulture, Environment, and Biotechnology*, *63*(1), 39–53. https://doi.org/10.1007/s13580-021-00382-7

Liesche, J., & Schulz, A. (2013). Symplasmic Transport in Phloem Loading and Unloading. In K. Sokołowska & P. Sowiński (Eds.), *Symplasmic Transport in Vascular Plants* (pp. 133–163). Springer. https://doi.org/10.1007/978-1-4614-7765-5_5

Luo, Y., Zohner, C., Crowther, T. W., Feng, J., Hoch, G., Li, P., Richardson, A. D., Vitasse, Y., & Gessler, A. (2024). Internal physiological drivers of leaf development in trees: Understanding the relationship between non-structural carbohydrates and leaf phenology. *Functional Ecology*, 1365-2435.14694. https://doi.org/10.1111/1365-2435.14694

MacNeill, G. J., Mehrpouyan, S., Minow, M. A. A., Patterson, J. A., Tetlow, I. J., & Emes, M. J. (2017). Starch as a source, starch as a sink: The bifunctional role of starch in carbon allocation. *Journal of Experimental Botany*, *68*(16), 4433–4453. https://doi.org/10.1093/jxb/erx291

Martinoia, E. (2018). Vacuolar Transporters – Companions on a Longtime Journey. *Plant Physiology*, *176*(2), 1384–1407. https://doi.org/10.1104/pp.17.01481

Menzel, A., Yuan, Y., Matiu, M., Sparks, T., Scheifinger, H., Gehrig, R., & Estrella, N. (2020). Climate change fingerprints in recent European plant phenology. *Global Change Biology*, *26*(4), 2599–2612. https://doi.org/10.1111/gcb.15000

Mirajkar, S. J., Suprasanna, P., & Vaidya, E. R. (2016). Spatial distribution and dynamics of sucrose metabolising enzymes in radiation induced mutants of sugarcane. *Plant Physiology and Biochemistry*, *100*, 85–93. https://doi.org/10.1016/j.plaphy.2015.12.018

Muhlemann, J. K., Maeda, H., Chang, C.-Y., San Miguel, P., Baxter, I., Cooper, B., Perera, M. A., Nikolau, B. J., Vitek, O., Morgan, J. A., & Dudareva, N. (2012). Developmental Changes in the Metabolic Network of Snapdragon Flowers. *PLoS ONE*, *7*(7), e40381. https://doi.org/10.1371/journal.pone.0040381

Piao, S., Liu, Q., Chen, A., Janssens, I. A., Fu, Y., Dai, J., Liu, L., Lian, X., Shen, M., & Zhu, X. (2019). Plant phenology and global climate change: Current progresses and challenges. *Global Change Biology*, *25*(6), 1922–1940. https://doi.org/10.1111/gcb.14619

Picture Table of Critical Spring Temperatures for Tree Fruit Bud Development Stages [WWW Document], n.d. . Fruit & Nuts. URL https://www.canr.msu.edu/resources/picture-table-critical-spring-temperatures-for-tree-fruit-bud-development-stages (accessed 3.12.25, Michigan University Extension)

Richardson, A. D., Keenan, T. F., Migliavacca, M., Ryu, Y., Sonnentag, O., & Toomey, M. (2013). Climate change, phenology, and phenological control of vegetation feedbacks to the climate system. *Agricultural and Forest Meteorology*, *169*, 156–173. https://doi.org/10.1016/j.agrformet.2012.09.012

Ruan, Y.-L., Jin, Y., Yang, Y.-J., Li, G.-J., & Boyer, J. S. (2010). Sugar Input, Metabolism, and Signaling Mediated by Invertase: Roles in Development, Yield Potential, and Response to Drought and Heat. *Molecular Plant*, *3*(6), 942–955. https://doi.org/10.1093/mp/ssq044

Saddhe, A. A., Manuka, R., & Penna, S. (2021). Plant sugars: Homeostasis and transport under abiotic stress in plants. *Physiologia Plantarum*, *171*(4), 739–755. https://doi.org/10.1111/ppl.13283

Sapkota, S., Liu, J., Islam, M. T., & Sherif, S. M. (2021). Changes in Reactive Oxygen Species, Antioxidants and Carbohydrate Metabolism in Relation to Dormancy Transition and Bud Break in Apple (Malus × domestica Borkh) Cultivars. *Antioxidants*, *10*(10), 1549. https://doi.org/10.3390/antiox10101549

Simard, S., Giovannelli, A., Treydte, K., Traversi, M. L., King, G. M., Frank, D., & Fonti, P. (2013). Intra-annual dynamics of non-structural carbohydrates in the cambium of mature conifer trees reflects radial growth demands. *Tree Physiology*, *33*(9), 913–923. https://doi.org/10.1093/treephys/tpt075

Stegner, M., Flörl, A., Lindner, J., Plangger, S., Schaefernolte, T., Strasser, A., Thoma, V., Walde, J., & Neuner, G. (2022). Freeze dehydration vs. supercooling of mesophyll cells: Impact of cell wall, cellular and tissue traits on the extent of water displacement. *Physiologia Plantarum*, *174*(6), e13793. https://doi.org/10.1111/ppl.13793

Stein, O., & Granot, D. (2019). An Overview of Sucrose Synthases in Plants. *Frontiers in Plant Science*, *10*, 95. https://doi.org/10.3389/fpls.2019.00095

Sheikh, F. R., Jose-Santhi, J., Kalia, D., Singh, K., & Singh, R. K. (2022). Sugars as the regulators of dormancy and sprouting in geophytes. *Industrial Crops and Products*, *189*, 115817. https://doi.org/10.1016/j.indcrop.2022.115817

Thalmann, M., & Santelia, D. (2017). Starch as a determinant of plant fitness under abiotic stress. *New Phytologist*, *214*(3), 943–951. https://doi.org/10.1111/nph.14491

Thomas, H. (2003). Defining senescence and death. *Journal of Experimental Botany*, *54*(385), 1127–1132. https://doi.org/10.1093/jxb/erg133

Tixier, A., Gambetta, G. A., Godfrey, J., Orozco, J., & Zwieniecki, M. A. (2019). Non-structural Carbohydrates in Dormant Woody Perennials; The Tale of Winter Survival and Spring Arrival. *Frontiers in Forests and Global Change*, *2*, 18. https://doi.org/10.3389/ffgc.2019.00018

Trugman, A. T., & Anderegg, L. D. L. (2025). Source vs sink limitations on tree growth: From physiological mechanisms to evolutionary constraints and terrestrial carbon cycle implications. *New Phytologist*, *245*(3), 966–981. https://doi.org/10.1111/nph.20294

Tsanakas, G. F., Manioudaki, M. E., Economou, A. S., & Kalaitzis, P. (2014). De novo transcriptome analysis of petal senescence in Gardenia jasminoides Ellis. *BMC Genomics*, *15*(1), 554. https://doi.org/10.1186/1471-2164-15-554

Untergasser, A., Cutcutache, I., Koressaar, T., Ye, J., Faircloth, B. C., Remm, M., & Rozen, S. G. (2012). Primer3—New capabilities and interfaces. *Nucleic Acids Research*, *40*(15), e115. https://doi.org/10.1093/nar/gks596

Vargas-Madriz, Á. F., Kuri-García, A., Luzardo-Ocampo, I., Vargas-Madriz, H., Pérez-Ramírez, I. F., Anaya-Loyola, M. A., Ferriz-Martínez, R. A., Roldán-Padrón, O., Hernández-Sandoval, L., Guzmán-Maldonado, S. H., & Chávez-Servín, J. L. (2023). Impact of Drying

Process on the Phenolic Profile and Antioxidant Capacity of Raw and Boiled Leaves and Inflorescences of Chenopodium berlandieri ssp. Berlandieri. *Molecules*, *28*(20), 7235. https://doi.org/10.3390/molecules28207235

Vitra, A., Lenz, A., & Vitasse, Y. (2017). Frost hardening and dehardening potential in temperate trees from winter to budburst. *New Phytologist*, *216*(1), 113–123. https://doi.org/10.1111/nph.14698

Vu, D. P., Martins Rodrigues, C., Jung, B., Meissner, G., Klemens, P. A. W., Holtgräwe, D., Fürtauer, L., Nägele, T., Nieberl, P., Pommerrenig, B., & Neuhaus, H. E. (2020). Vacuolar sucrose homeostasis is critical for plant development, seed properties, and night-time survival in Arabidopsis. *Journal of Experimental Botany*, *71*(16), 4930–4943. https://doi.org/10.1093/jxb/eraa205

Weiszmann, J., Fürtauer, L., Weckwerth, W., & Nägele, T. (2018). Vacuolar sucrose cleavage prevents limitation of cytosolic carbohydrate metabolism and stabilizes photosynthesis under abiotic stress. *The FEBS Journal*, *285*(21), 4082–4098. https://doi.org/10.1111/febs.14656

Yamada, K., Osakabe, Y., Mizoi, J., Nakashima, K., 'Fuji'ta, Y., Shinozaki, K., & Yamaguchi-Shinozaki, K. (2010). Functional Analysis of an Arabidopsis thaliana Abiotic Stress-inducible Facilitated Diffusion Transporter for Monosaccharides. *Journal of Biological Chemistry*, *285*(2), 1138–1146. https://doi.org/10.1074/jbc.M109.054288

Zhu, L., Li, B., Wu, L., Li, H., Wang, Z., Wei, X., Ma, B., Zhang, Y., Ma, F., Ruan, Y.-L., & Li, M. (2021). MdERDL6-mediated glucose efflux to the cytosol promotes sugar accumulation in the vacuole through up-regulating TSTs in apple and tomato. *Proceedings of the National Academy of Sciences*, *118*(1), e2022788118. https://doi.org/10.1073/pnas.2022788118

Zohner, C. M., Mirzagholi, L., Renner, S. S., Mo, L., Rebindaine, D., Bucher, R., Palouš, D., Vitasse, Y., Fu, Y. H., Stocker, B. D., & Crowther, T. W. (2023). Effect of climate warming on the timing of autumn leaf senescence reverses after the summer solstice. *Science*, *381*(6653), eadf5098. https://doi.org/10.1126/science.adf5098

Liu, J., Islam, M.T., Sapkota, S., Ravindran, P., Kumar, P.P., Artlip, T.S., Sherif, S.M., 2021. Ethylene-Mediated Modulation of Bud Phenology, Cold Hardiness, and Hormone Biosynthesis in Peach (Prunus persica). Plants 10, 1266. https://doi.org/10.3390/plants10071266

Rani Das, P., Islam, M.T., Liu, J., Liu, Z., Dardick, C., Sherif, S.M., 2024. Temporal changes in the proanthocyanidins to anthocyanins ratio during dormancy associate with bloom time variations in peach. Current Plant Biology 40, 100393. https://doi.org/10.1016/j.cpb.2024.100393

Richardson, A.D., Keenan, T.F., Migliavacca, M., Ryu, Y., Sonnentag, O., Toomey, M., 2013. Climate change, phenology, and phenological control of vegetation feedbacks to the climate system. Agricultural and Forest Meteorology 169, 156–173. https://doi.org/10.1016/j.agrformet.2012.09.012

Chapter 4: Natural Frost Triggers Distinct Rootstock and Tissue-Dependent Metabolomic Responses in Apple

Abstract

Understanding rootstock-mediated frost tolerance mechanisms in apple is critical for improving resilience under increasingly erratic spring temperature regimes. In this study, we employed untargeted metabolomics to characterize tissue-specific and rootstock-dependent metabolic shifts in response to a natural frost event. 'Gala' scions grafted onto the cold-tolerant rootstock B.9—identified as tolerant based on consistently low floral bud mortality across three years—and onto the frost-susceptible rootstock M.26—associated with significantly higher bud mortality—were used as a model system. Samples were collected from floral buds, scion leaves, and sucker leaves 12 hours before and 6 hours after a frost event at the tight cluster stage. Metabolites were extracted and analyzed using ultra-high-performance liquid chromatography–mass spectrometry (UHPLC-MS), followed by statistical analyses including principal component analysis (PCA), volcano plots, t-tests, and metabolite set enrichment analysis (MSEA). The results revealed striking rootstock- and tissue-specific reprogramming of metabolite profiles in response to frost. In 'Gala' grafted on B.9, the floral buds had post-frost upregulation of cold signaling metabolites LysoPA and colnelenic acid, was also accompanied by significant enrichment in ascorbate and aldarate metabolism, highlighting robust antioxidant responses. Notably, the B.9 sucker leaves also exhibited enhanced accumulation of arginine-derived polyamines, NAD(P)(H)-related redox metabolites, maltose and melibiose, possibly pointing to systemic cold signaling from rootstock to scion. Conversely, the susceptible M.26 rootstock showed fragmented responses. M.26 floral buds exhibited disjointed phospholipid turnover and reduced antioxidant capacity, with diminished accumulation of key osmolytes. Scion leaves of M.26 displayed strong glutathione pathway enrichment post-frost, but in a pattern that suggests stress-induced redox imbalance rather than adaptive signaling, given its high bud mortality. The sucker leaves of M.26 also showed minimal enrichment of polyamine, sugar, or redox pathways, indicating insufficient metabolic plasticity. Altogether, this study demonstrates that shifts in metabolome landscape and rootstock genotype significantly shape tissue-specific frost responses in apple. These insights provide a biochemical basis for selecting resilient rootstocks and offer targets for metabolic engineering of cold tolerance in perennial fruit crops.

Introduction

Recent shifts in global climate patterns have markedly increased the severity of late spring frosts, imposing substantial and recurrent constraints on temperate fruit production (Song et al., 2024). Sudden temperature declines disrupt plant membranes, nucleic acids, and proteins, and slow key metabolic processes such as lipid and fatty acid synthesis (Nievola et al. 2017). Apple (*Malus domestica* Borkh.), a major deciduous fruit cultivated worldwide, is especially susceptible: floral tissues, expanding leaves, and developing fruitlets suffer irreversible injury when temperatures fall below their developmental thresholds (Szalay et al., 2019; Ritonga & Chen 2020; Jahed et al., 2023). Chilling disturbs membrane lipid order, impairs ion transport, and slows enzymatic reactions, whereas freezing promotes extra- and intra-cellular ice formation, raises solute concentrations, degrades proteins, and compromises plasma membrane integrity, often culminating in extensive cell death (Liang et al., 2017;

Gong et al., 2020; Bai et al., 2022; Zhao et al., 2021). Temperate deciduous trees normally acquire cold tolerance through cold acclimation characterized by membrane desaturation, compatible solute accumulation, and activation of antioxidant defenses (Jahed et al., 2023; Saini et al., 2025). Membrane desaturation is a process where the fatty acid composition of cellular membranes changes by increasing the proportion of unsaturated fatty acids during cold acclimation. Warmer temperatures in recent decades delay acclimation, shorten chilling fulfilment, or trigger midwinter deacclimation, thereby exposing dehardened buds to subsequent freezes and increasing frost injury across fruit regions (Unterberger et al. 2018). Consequently, enhancing both chilling tolerance and freezing tolerance through cultivar improvement and rootstock selection has become essential for maintaining apple productivity under increasingly variable climatic regimes (Sun et al. 2019; Sun et al. 2021).

Cold perception and acclimation are coordinated through a multitier network in which the ICE–CBF–COR pathway forms the central hub (Xu et al., 2023a). Inducer of CBF Expression 1 and 2, ICE1 and ICE2, basic helix loop helix transcription factors, bind MYC elements in the C-Repeat Binding Factor 3 (*CBF3*) promoter, while CBF1 and CBF2 are induced in parallel, together activating countless cold responsive (COR) targets that stabilize membranes, adjust osmotic potential, and detoxify reactive oxygen species (Wang et al., 2017; Hwarari et al., 2022). The cascade is reinforced by positive regulators Calmodulin-binding transcription activators, CAMTA1/2/3, and brassinosteroid responsive BZR1 (Brassinazole Resistant 1)/BES1 (BRI1-EMS-Suppressor 1) transcription foctors, but constrained by repressors such as Myeloblastosis 15 transcription factor, MYB15, phytochrome interacting factors (PIFs), and Ethylene Insensitive 3 transcription factor (EIN3), balancing energy costs against protection (Shi et al., 2018; Liu et al., 2019; Gu et al., 2021; OwusuAdjei et al., 2023). Functional conservation is highlighted by heterologous expression of peach *PpCBF1* (*Prunus persica* C-Repeat Binding Factor 1), which increases apple bark freezing tolerance by > 3 °C (Wisniewski et al., 2015; Li et al., 2023). Additional CBF independent routes further refine cold responses (Qian et al., 2024). In apple, *M. domestica* MYB transcription factors, MdMYB88 and MdMYB124, upregulate *Malus domestica* Cold Shock Protein 3, *MdCSP3*, and *M. domestica* CIRCADIAN CLOCK ASSOCIATED 1 gene, *MdCCA1*, augment anthocyanin accumulation, and lower H_2O_2 levels, collectively improving survival at freezing temperatures (Xie et al., 2018). *M. domestica* B-Box Zinc Finger Protein 37, MdBBX37 interacts with MdICE1 to increase *MdCBF1/4* transcription and promote jasmonic acid (JA)–mediated freezing tolerance, while BZR1 connects brassinosteroid signaling to downstream COR genes such as *WRKY6, SOC1, JMT,* and *SAG21*, i.e. genes coding for WRKY transcription factor 6, SUPPRESSOR OF OVEREXPRESSION OF CONSTANS 1, enzyme Jasmonic Acid Carboxyl Methyltransferase and Senescence-Associated Gene 21, respectively (Li et al., 2017; An et al., 2021). Phytohormones act as crucial modulators beyond ABA and JA: auxin, ethylene, and gibberellins have each been shown to intersect with CBF dependent and – independent pathways (Waadt et al., 2022; Castro-Camba et al., 2022).

Metabolomic reprogramming translates transcriptional signals into the small molecule profile that ultimately determines physiological performance under cold (Xing et al., 2025). Untargeted metabolomics using GC–MS, LC–MS, and NMR can now detect hundreds of metabolites at very low concentrations—from picomolar to millimolar levels (Wen et al., 2015; Takahashi et al., 2011; Barding et al., 2012). These metabolic profiles offer a functional snapshot of cellular activity that complements what we learn from transcriptomic data (Demarque et al., 2020). Cold acclimated tissues typically accumulate raffinose family oligosaccharides, soluble sugars, proline, γ-aminobutyric acid, polyamines, and tricarboxylic acid intermediates that jointly stabilize membranes, regulate osmotic potential, and buffer reactive oxygen species (Rohde et al., 2004; Hannah et al., 2006; Crosatti et al., 2013; Fürtauer et al., 2019; Krasensky and Jonak 2012).

Consistently high levels of certain metabolites often indicate built-in stress tolerance: *Haberlea rhodopensis* maintains raffinose and galactinol year round and withstands –20 °C (Benina et al., 2013), *Vitis amurensis*, for example, builds up galactinol, raffinose, proline, putrescine, and ascorbate during cold stress, along with turning on key genes like Galactinol and Raffinose Synthases, *GolS*, and *RafS*, that help make these protective compounds (Chai et al., 2019). Comparative metabolomics further shows that the peach cultivar 'Donghe No. 1' enriches saccharides, phenolic acids, and flavones via galactose and flavonoid pathways (Li et al., 2023), whereas chilling tolerant 'Red Haven' fruit accumulate sorbitol, maltitol, myoinositol, sucrose, putrescine, and urea, reducing flesh browning (Brizzolara et al., 2020). In trifoliate orange, *Poncirus trifoliata* Ethylene-Responsive Factor 108, PtrERF108, upregulates raffinose synthase, and its transfer to lemon improves freezing tolerance; silencing the gene abolishes raffinose accumulation unless raffinose is supplied exogenously (Khan et al., 2021). Freezing resilient kiwifruit genotypes induce chalcone isomerase and anthocyanin acyltransferase while accumulating lysophospholipids and free fatty acids for membrane repair (Sun et al., 2021). Similar protective signatures—trehalose, glutathione, and ascorbate—rise sharply in cold adapted *Phyllostachys edulis* (Wang et al., 2022) and recur in olive, mulberry, rubber, poplar, and bamboo (Guerra et al., 2015; Cheng et al., 2018; Adolf et al., 2021; Yang et al., 2019). Controlled studies corroborate these field observations: exposure of barley seedlings to cold for 24 h yielded 770 differentially abundant metabolites, with flavonoids, organic acids, and amino acids representing 45 % of the profile (Yang et al., 2020); cold treated tobacco leaves showed ~200 metabolic shifts dominated by primary metabolites linked to tolerance (Jin et al., 2017). Secondary compounds such as flavonoids, phenylpropanoids, anthocyanins, lignans, and steroids also accumulate and contribute osmotic buffering or antioxidant capacity (Brunetti et al., 2013; Song et al., 2024). Multi-omics integration has become indispensable for assigning these metabolites to regulatory circuits: combined metabolome–transcriptome analyses reveal concordant induction of galactose, phenylpropanoid, and flavonoid pathways in cold tolerant peach branches (Li et al., 2023), coordinated phosphate dependent shifts in alfalfa (Wang et al., 2023), and enrichment of hormone, carbohydrate, and amino acid metabolism in cold tolerant *Cucurbita maxima* and *Capsicum annuum* (Li et al., 2021; Zhang et al., 2022). Apple and other woody species exhibit comparable patterns: cold resistant cultivars accumulate quercetin, kaempferol, galactinol, raffinose, and amino acid derivatives, while integrating flavonoid gene expression and enhanced antioxidant activity (Xu et al., 2023; Yazdanpanah et al., 2021).

Grafting introduces an additional layer of complexity because rootstocks can reshape scion gene expression and metabolite allocation (Harris et al., 2023; Huang et al., 2023). In grapevine, drought tolerant rootstocks reposition transpiration QTLs (Marguerit et al., 2012) and remodel scion transcriptomes under contrasting soils (Marè et al., 2013). Water stress studies reveal enhanced stilbene accumulation and reduced ABA catabolism in scion leaves on specific stocks (Chitarra et al., 2021). At the graft interface, heterografted vines elevate branched chain amino acids, neutral invertase, phenylalanine ammonia-lyase, and stilbene biosynthesis (Prodhomme et al., 2019). Graft incompatibility in *Prunus* relates to vacuolar leakage of catechins and proanthocyanidins that disrupt lignification (Gainza et al., 2015); pear combinations with high arbutin, procyanidin B1, and chlorogenic acid show similar patterns (Hudina et al., 2014). In apple, 'Gala' on Geneva 202 rootstock accumulates chlorogenic acid, eriodictyol, and phloretin glycosides and activates lignin and flavonoid pathway genes relative to M.9 (Lee et al., 2023). Cold tolerant apple 'Hanfu' upregulates galactinol, raffinose, and stachyose synthase transcripts and increases raffinose, stachyose, spermidine, and ascorbate after –5 °C, whereas the sensitive 'Naganofuji 2' shows a muted response (Xu et al., 2022; 2023a).

Recent advances in omics approaches, particularly metabolomics, have provided deeper insights into the molecular basis of plant cold tolerance. These approaches connect gene expression patterns with downstream metabolic changes, revealing the coordinated regulation of pathways involved in stress adaptation. For example, Xu et al. (2023b) demonstrated that low-temperature treatment in *Argyranthemum frutescens* led to the enrichment of differentially expressed genes (DEGs) in flavonoid biosynthesis, phenylpropanoid metabolism, circadian rhythm, and phenylalanine pathways, alongside the accumulation of key sugars such as sucrose, trehalose, and maltose. Similarly, cold-tolerant pepper lines showed the upregulation of carbohydrate metabolism, tricarboxylic acid cycle (TCA), and flavonoid biosynthesis pathways, along with increased levels of compatible solutes (Gao et al., 2022). Despite these advances, no study has performed untargeted metabolomics across multiple tissues of grafted apple plants during a naturally occurring frost or compared rootstocks from diverse genetic backgrounds under identical field conditions. To fill this gap, we investigated 'Gala' scions grafted onto two contrasting stocks— 'Budagovsky 9' (B.9) and 'Malling 26' (M.26)—during a late spring frost in Winchester, Virginia. Floral buds, fully expanded scion leaves, and rootstock sucker leaves were collected both before and after the natural frost event and analyzed using untargeted LC–MS metabolomics. We hypothesize that the metabolomic response to natural frost is rootstock-dependent and tissue-specific, with the cold-tolerant rootstock B.9 exhibiting a more coordinated and adaptive metabolic reprogramming across scion floral buds, scion leaves, and rootstock (sucker) leaves compared to the frost-susceptible 'Malling 26' (M.26). By comparing metabolite profiles across these different tissues, our study offers new insights into how genetically distinct apple rootstocks influence scion metabolism under cold stress. These findings help identify potential metabolic markers and targets that can support breeding and orchard strategies aimed at improving frost resilience.

2 Material and methods

2.1 Plant Materials and Experimental Design

The foundational experiment for the present study, which examined rootstock-mediated cold responses in 'Gala' apple through untargeted transcriptomic analysis, has been previously described in detail (Saini et al., 2025). This study utilized the same orchard and biological samples to investigate tissue-specific metabolic reprogramming under cold stress. In anticipation of a naturally occurring frost event on April 22, 2021, samples were collected from 'Gala' trees grafted onto 'B.9' and 'M.26' rootstocks. Tissue types included 'Gala' floral buds, ‘Gala’ scion leaves, and rootstock sucker leaves (B.9, M.26), sampled at 12 hours pre-frost and 6 hours post-frost. During the event, temperatures dropped to –6.1 °C for over 30 minutes—conditions associated with approximately 90% floral bud mortality at full bloom. Three trees per scion–rootstock combination were randomly selected, with each tree serving as a biological replicate. All samples were immediately frozen in liquid nitrogen and stored at –80 °C for subsequent metabolomic analysis.

2.2 Untargeted Metabolomics

For untargeted metabolomics analysis, approximately 50 mg of each sample—apple floral buds, scion leaves, and rootstock sucker leaves—was extracted with 800 µL of 80% methanol following the method described by Das et al. (2024). Metabolite separation was performed using an Ultimate 3000 LC system coupled with a Q Exactive mass spectrometer (Thermo Fisher Scientific), operated in both positive and negative electrospray ionization (ESI+ and ESI–) modes. The mobile phase consisted of solvent A (0.05% formic acid in water) and solvent B (acetonitrile), delivered through a gradient elution program optimized for each ionization mode. MS/MS spectra of the most significant metabolites were acquired and annotated by comparison with reference spectra in the Human Metabolome Database (www.hmdb.ca). Data processing included retention time correction, peak alignment, and feature detection. All metabolite features were normalized using median normalization and $\log_2$ transformation. Quality control samples were used to correct for batch effects and assess analytical reproducibility, with >88% of features demonstrating a relative standard deviation (RSD) below 30%.

2.3 Statistical Analysis

Statistical analyses were conducted using MetaboAnalyst 5.0 and custom R-based pipelines. Principal Component Analysis (PCA) was used to evaluate treatment clustering and biological variation. Differentially accumulated metabolites were identified through two-sample unpaired *t*-tests ($p < 0.05$), fold-change analysis ($\log_2$FC threshold $\geq \pm 1$), and variable importance in projection (VIP > 1.5). Visualization outputs included volcano plots, PCA score plots with 95% confidence ellipses, and *t*-test significance plots annotated by m/z-retention time pairs. Pathway-level insights were derived using Metabolite Set Enrichment Analysis (MSEA), based on KEGG-defined metabolic pathways. Bar plots displayed enrichment ratios and *p*-values to highlight significant shifts in key biosynthetic and catabolic processes, such as glutathione metabolism, starch and sucrose metabolism, and arginine biosynthesis.

2 Results

2.1 Frost Exposure, Sampling Conditions, and Experimental Context

The environmental conditions, frost severity, and biological sampling design used for untargeted metabolomics in this study have been described in detail in Chapter 2 (Section 3.1, Transcriptomic Results). Briefly, a naturally occurring spring frost event on April 22, 2021, resulted in air temperatures dropping to –6.1 °C for over 30 minutes—conditions known to induce up to 90% floral bud mortality in apples at full bloom. Samples were collected from ‘Gala’ trees grafted onto two contrasting rootstocks, ‘B.9’ (cold-tolerant) and ‘M.26’ (cold-susceptible), which showed marked differences in floral bud survival following the frost (see Fig. 2D, Chapter 2). Tissues sampled for metabolomic analysis included ‘Gala’ floral buds, ‘Gala’ scion leaves, and rootstock sucker leaves from both B.9 and M.26. Collections were made at two time points: 12 hours before frost (BF) and 6 hours after frost (AF). Each sample represented one of three biological replicates per tissue–treatment–rootstock combination.

2.2 Comprehensive Metabolomic Profiling Reveals Rootstock- and Tissue-Specific Responses to Natural Frost in Apple

Untargeted metabolomic profiling was conducted on ‘Gala’ floral buds, scion leaves, and rootstock sucker leaves sampled before and after a naturally occurring frost event from trees grafted onto the cold-tolerant ‘B.9’ and susceptible ‘M.26’ rootstocks. Principal Component Analysis (PCA) of all tissue types showed clear separation along the first principal component (PC1), which explained 54% of the total variance (**Figure 1**).

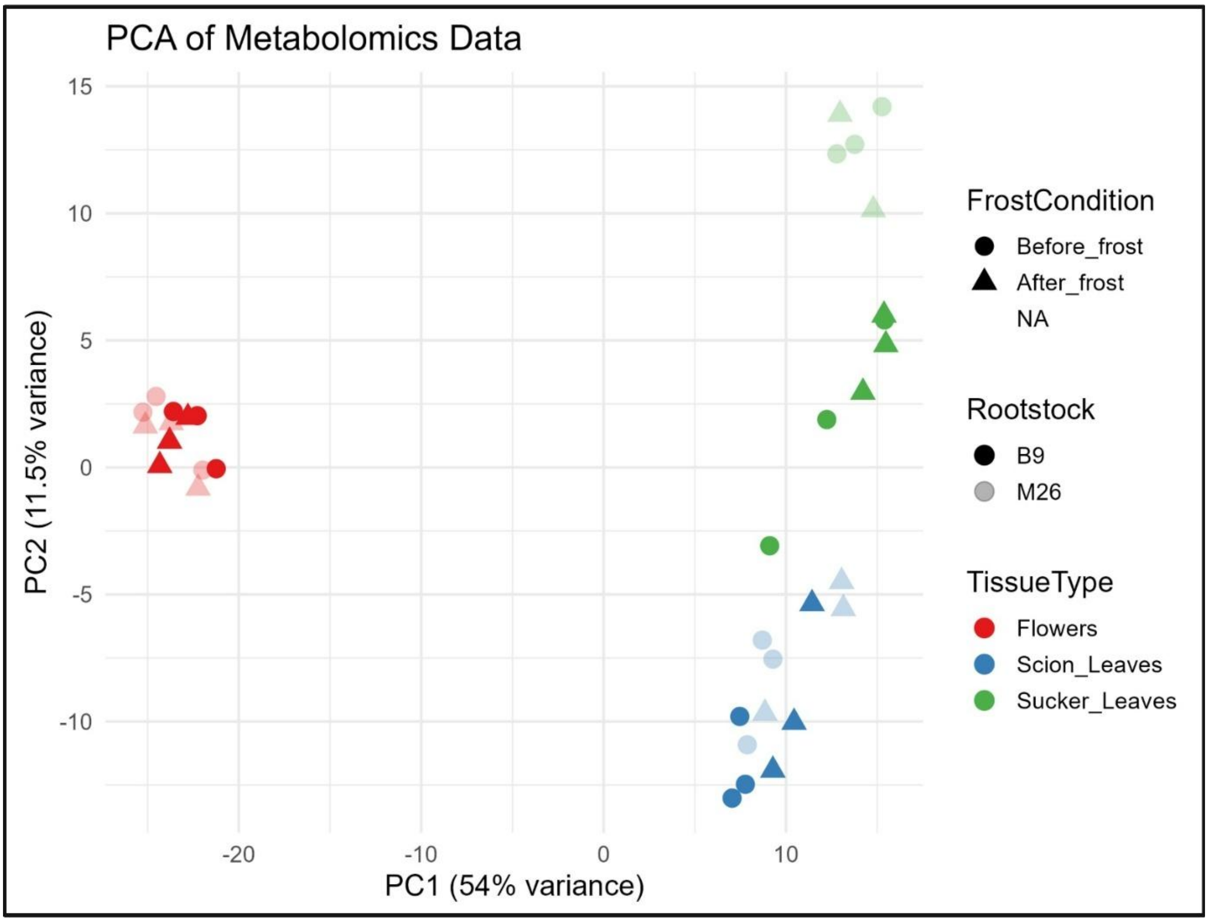

Figure 1. Principal Component Analysis (PCA) of untargeted metabolomic profiles in apple tissues across frost conditions and rootstocks.

Floral bud samples clustered on the negative end of PC1, while scion leaf and sucker leaf samples grouped on the positive side, indicating strong metabolite-level differences between these three tissue types. In contrast, the second principal component (PC2), which accounted for 11.5% of the variance, captured only minor variation and did not clearly separate samples by frost condition or rootstock. These results confirm that tissue type was the primary driver of metabolomic variation in the dataset. Based on this, further analyses were conducted separately for each tissue to identify frost-induced and rootstock-dependent metabolite shifts in floral buds, scion leaves, and sucker leaves.

2.2.1 Metabolomic Reprogramming in Floral Buds, Scion Leaves, and Sucker Leaves of Cold-Tolerant Rootstock B.9 Following Natural Frost Exposure

Following the general PCA analysis, metabolomic profiling of floral buds from the cold-tolerant rootstock B.9 revealed clear frost-induced shifts in metabolic composition (**Figure 2**).

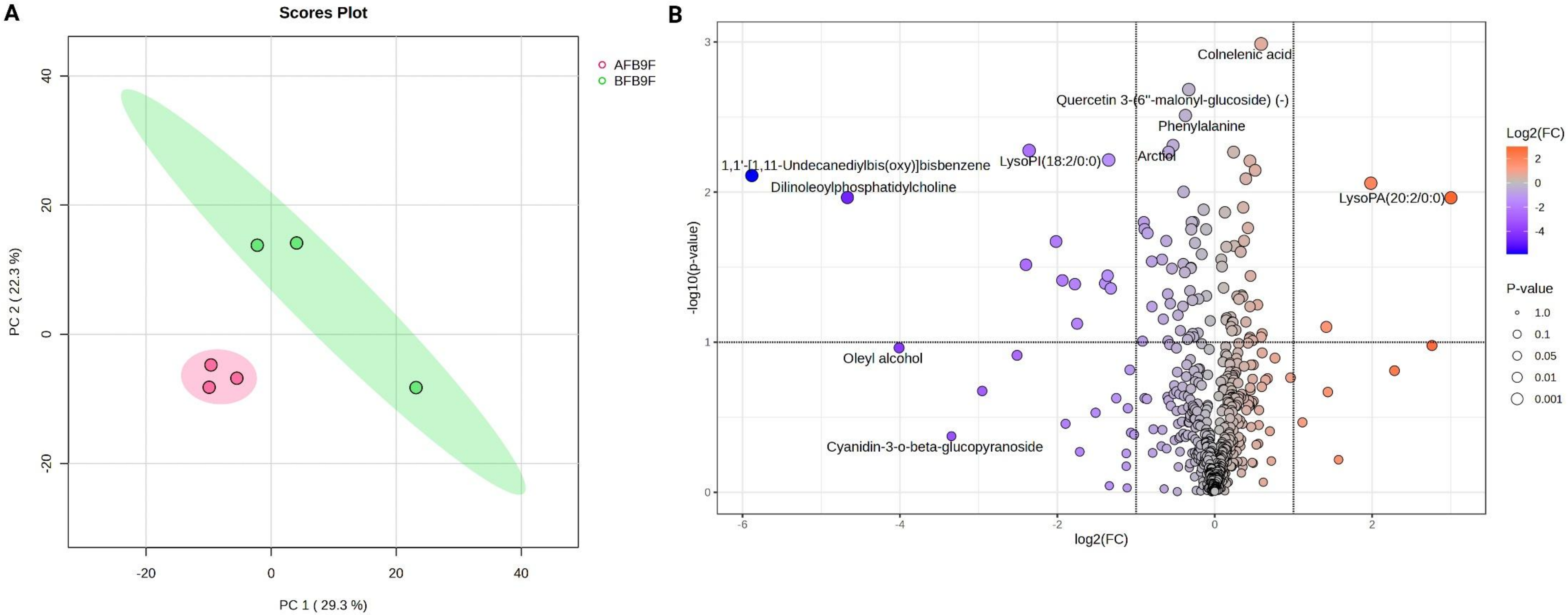
A
Scores Plot
AFB9F
BFB9F
PC 1 (29.3 %)
PC 2 (22.3 %)
B
Colnelenic acid
Quercetin 3-(6"-malonyl-glucoside) (-)
Phenylalanine
Arctiol
LysoPI(18:2/0:0)
1,1'-[1,11-Undecanediylbis(oxy)]bisbenzene
Dilinoleoylphosphatidylcholine
LysoPA(20:2/0:0)
Oleyl alcohol
Cyanidin-3-o-beta-glucopyranoside
log2(FC)
-log10(p-value)
Log2(FC)
P-value

C

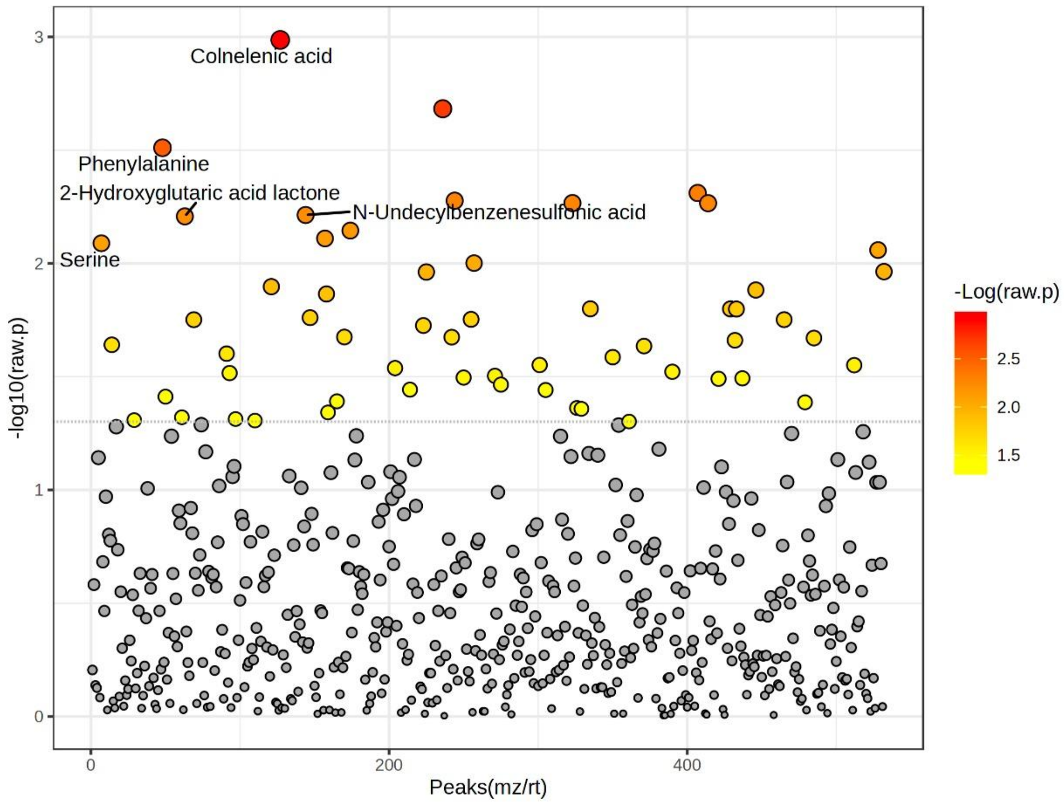
Colnelenic acid
Phenylalanine
2-Hydroxyglutaric acid lactone
N-Undecylbenzenesulfonic acid
Serine
-log10(raw.p)
Peaks(mz/rt)
-Log(raw.p)
2.5
2.0
1.5
0
200
400
1
2
3

D

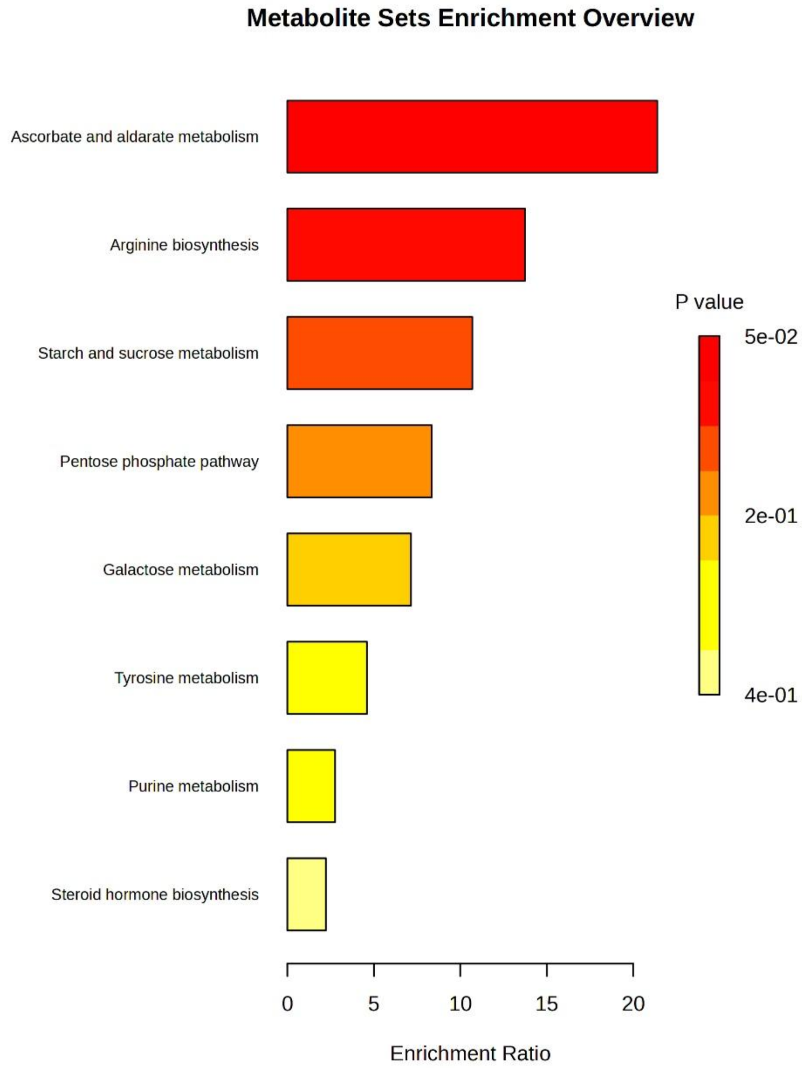
Metabolite Sets Enrichment Overview
Ascorbate and aldarate metabolism
Arginine biosynthesis
Starch and sucrose metabolism
Pentose phosphate pathway
Galactose metabolism
Tyrosine metabolism
Purine metabolism
Steroid hormone biosynthesis
P value
5e-02
2e-01
4e-01
0
5
10
15
20
Enrichment Ratio

Figure 2. Post-frost metabolomic shifts in 'Gala' floral buds grafted on cold-tolerant rootstock B.9. (A) Principal Component Analysis (PCA) score plot demonstrating clear separation between before-frost (BF_B9F; green ellipse) and after-frost (AF_B9F; pink ellipse) metabolite profiles in floral buds. **(B)** Volcano plot of differentially accumulated metabolites between AF and BF treatments. The x-axis represents $\log_2$ fold change (FC) and the y-axis denotes $-\log_{10}(p\text{-value})$. Significantly upregulated and downregulated metabolites ($FC \geq \pm1$, $p < 0.05$) are highlighted in red and purple, respectively, with point size indicating *p*-value significance. **(C)** Two-sample unpaired *t*-test results for floral bud metabolites, plotted by $-\log_{10}(p\text{-value})$ against detected m/z-retention time pairs. The dashed horizontal line indicates the significance threshold ($p = 0.05$). **(D)** Metabolite Set Enrichment Analysis (MSEA) reveals pathway-level enrichment following frost exposure. Bar lengths indicate enrichment ratios, and color intensity reflects pathway-level *p*-values.

Principal Component Analysis (PCA) showed distinct clustering between before-frost (BF_B9F) and after-frost (AF_B9F) floral bud samples along PC1 (29.3%) and PC2 (22.3%), with no overlap between the 95% confidence intervals of the two groups, confirming robust biological reproducibility and strong treatment-specific metabolic separation (**Figure 2A**). The volcano plot (**Figure 2B**) identified multiple significantly altered metabolites in floral buds ($|\log_2 FC| \geq 1$, $p < 0.05$), with key upregulated compounds including LysoPA(20:2(0:0)), Colnelenic acid, and Phenylalanine, while metabolites such as Cyanidin-3-O-beta-glucopyranoside, Dilinoleoyl-phosphatidylcholine, and 1,1′-[1,11-Undecanediyl-bis(oxy)]bisbenzene were markedly downregulated. Several of these metabolites exhibited fold changes exceeding ±2 and *p*-values below 0.01, as indicated by point size and color. Consistently, *t*-test results (**Figure 2C**) further highlighted the significant differential accumulation of Colnelenic acid, Phenylalanine, and 2-hydroxyglutaric acid lactone, all of which crossed the statistical threshold ($-\log_{10}(p) > 1.3$). Metabolite Set Enrichment Analysis (**Figure 2D**) indicated that frost-triggered metabolomic remodeling in B.9 floral buds prominently involved the ascorbate and aldarate metabolism, arginine biosynthesis, and starch and sucrose metabolism pathways, each with high enrichment ratios (ranging from ~10–18) and relatively low *p*-values (top pathways < 0.05). These shifts suggest a coordinated activation of antioxidant defenses, amino acid metabolism, and carbohydrate adjustment, underlying the robust frost resilience observed in B.9 floral tissues.

Scion leaves of 'Gala' grafted on the cold-tolerant rootstock B.9 exhibited distinct metabolic responses following natural frost exposure. Principal Component Analysis (**Figure 3A**) showed a clear separation between before-frost (BF_B9SL) and after-frost (AF_B9SL) samples along PC1 (39.6% variance), with non-overlapping 95% confidence ellipses confirming strong treatment-specific clustering and biological reproducibility.

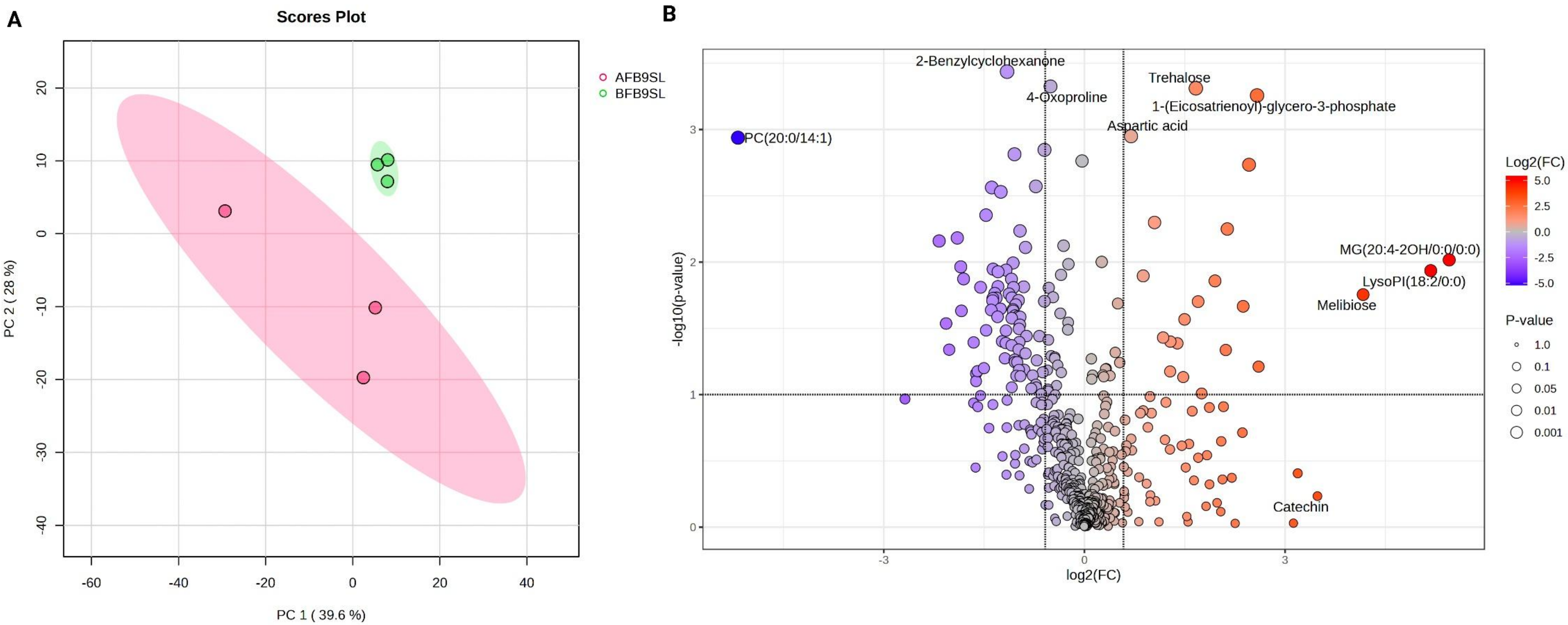
A
Scores Plot
AFB9SL
BFB9SL
PC 1 (39.6 %)
PC 2 (28 %)
B
2-Benzylcyclohexanone
4-Oxoproline
Trehalose
1-(Eicosatrienoyl)-glycero-3-phosphate
Aspartic acid
PC(20:0/14:1)
MG(20:4-2OH/0:0/0:0)
LysoPI(18:2/0:0)
Melibiose
Catechin
log2(FC)
-log10(p-value)
Log2(FC)
P-value

C

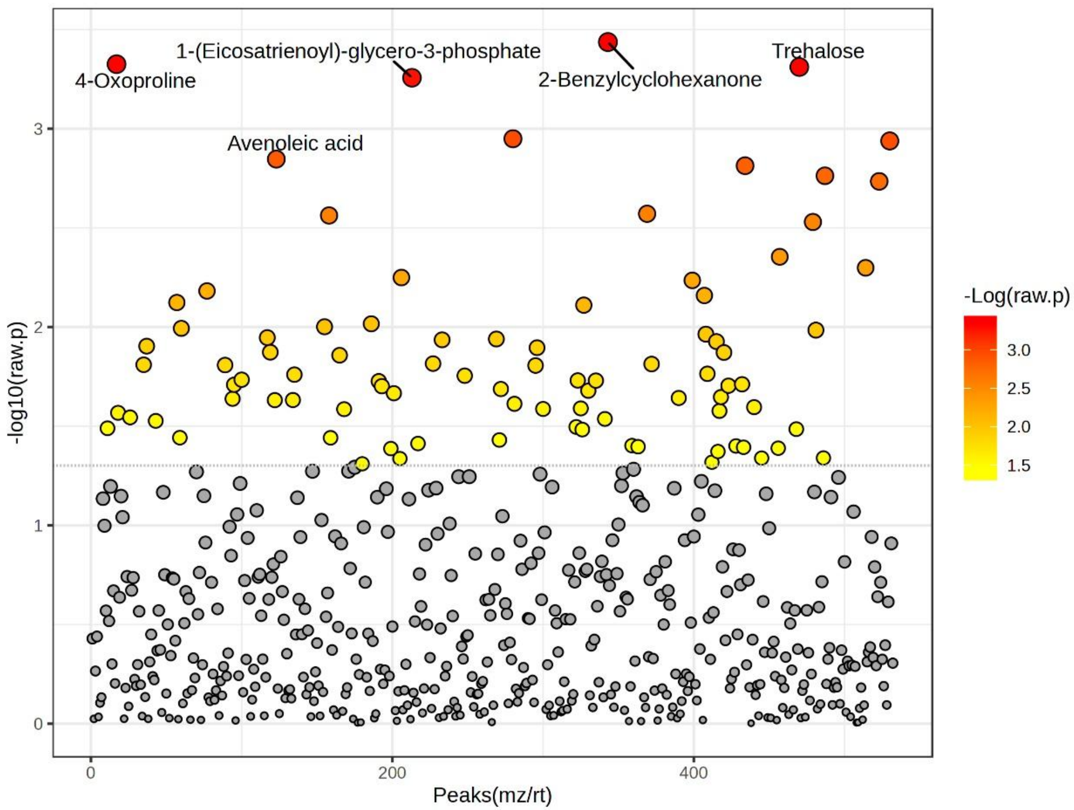

4-Oxoproline
1-(Eicosatrienoyl)-glycero-3-phosphate
2-Benzylcyclohexanone
Trehalose
Avenoleic acid
-log10(raw.p)
Peaks(mz/rt)
-Log(raw.p)
3.0
2.5
2.0
1.5

D

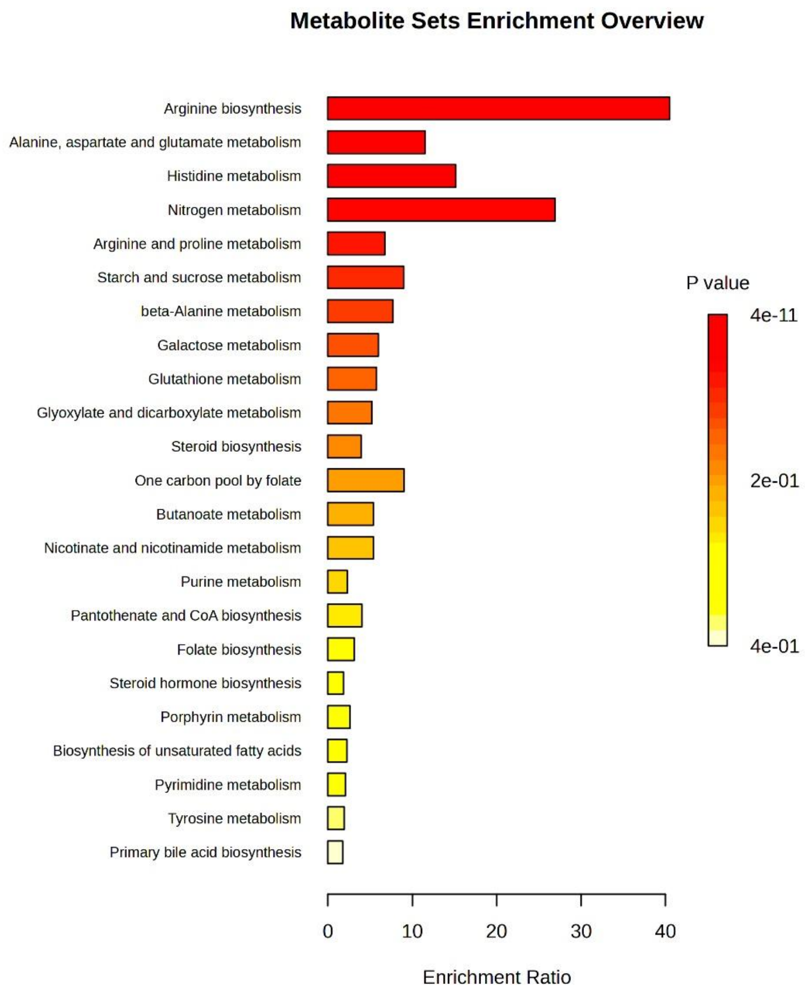

Metabolite Sets Enrichment Overview
Arginine biosynthesis
Alanine, aspartate and glutamate metabolism
Histidine metabolism
Nitrogen metabolism
Arginine and proline metabolism
Starch and sucrose metabolism
beta-Alanine metabolism
Galactose metabolism
Glutathione metabolism
Glyoxylate and dicarboxylate metabolism
Steroid biosynthesis
One carbon pool by folate
Butanoate metabolism
Nicotinate and nicotinamide metabolism
Purine metabolism
Pantothenate and CoA biosynthesis
Folate biosynthesis
Steroid hormone biosynthesis
Porphyrin metabolism
Biosynthesis of unsaturated fatty acids
Pyrimidine metabolism
Tyrosine metabolism
Primary bile acid biosynthesis
Enrichment Ratio
P value
4e-11
2e-01
4e-01

Figure 3. Post-frost metabolomic shifts in 'Gala' scion leaves grafted on cold-tolerant rootstock B.9. (A) Principal Component Analysis (PCA) score plot showing clear separation between before-frost (BF_B9SL; green ellipse) and after-frost (AF_B9SL; pink ellipse) metabolite profiles in scion leaves. **(B)** Volcano plot of differentially accumulated metabolites between AF and BF treatments. The x-axis denotes $\log_2$ fold change (FC), and the y-axis shows $-\log_{10}$(p-value). Red and purple points highlight significantly upregulated and downregulated metabolites, respectively (FC $\geq \pm 1$, $p < 0.05$), with point size proportional to significance. **(C)** Two-sample unpaired t-test results for scion leaf metabolites, plotted by $-\log_{10}$(p-value) against detected m/z-retention time pairs. The dashed horizontal line marks the significance cutoff ($p = 0.05$). **(D)** Metabolite Set Enrichment Analysis (MSEA) of significantly altered compounds reveals pathway-level trends. Bar lengths reflect enrichment ratios, and color intensity corresponds to statistical significance (p-values).

Volcano plot analysis (**Figure 3B**) revealed significant post-frost accumulation of several metabolites, including trehalose, melibiose, 4-oxoproline, and 1-(eicosatrienoyl)-glycero-3-phosphate, while lipid-related compounds such as PC(20:0/14:1) were downregulated. These patterns were reinforced by two-sample *t*-test results (**Figure 3C**), which highlighted highly significant *p*-values ($-\log_{10} > 2.5$) for key frost-responsive compounds such as trehalose, 2-benzylcyclohexanone, and aspartic acid. Metabolite Set Enrichment Analysis (**Figure 3D**) further revealed strong enrichment of pathways associated with cold resilience, including arginine biosynthesis, alanine/aspartate/glutamate metabolism, starch and sucrose metabolism, nitrogen metabolism, and galactose metabolism, indicating a coordinated osmotic and redox regulatory response in 'Gala' scion leaves under frost stress on B.9 rootstock.

B.9 rootstock-derived sucker leaves with 'Gala' grafted on it showed a distinct but partially overlapping metabolic response to frost, as illustrated by the Principal Component Analysis (**Figure 4A**), where before-frost (BF_B9RL) and after-frost (AF_B9RL) samples clustered separately along PC1 (40.6%) with modest overlap along PC2.

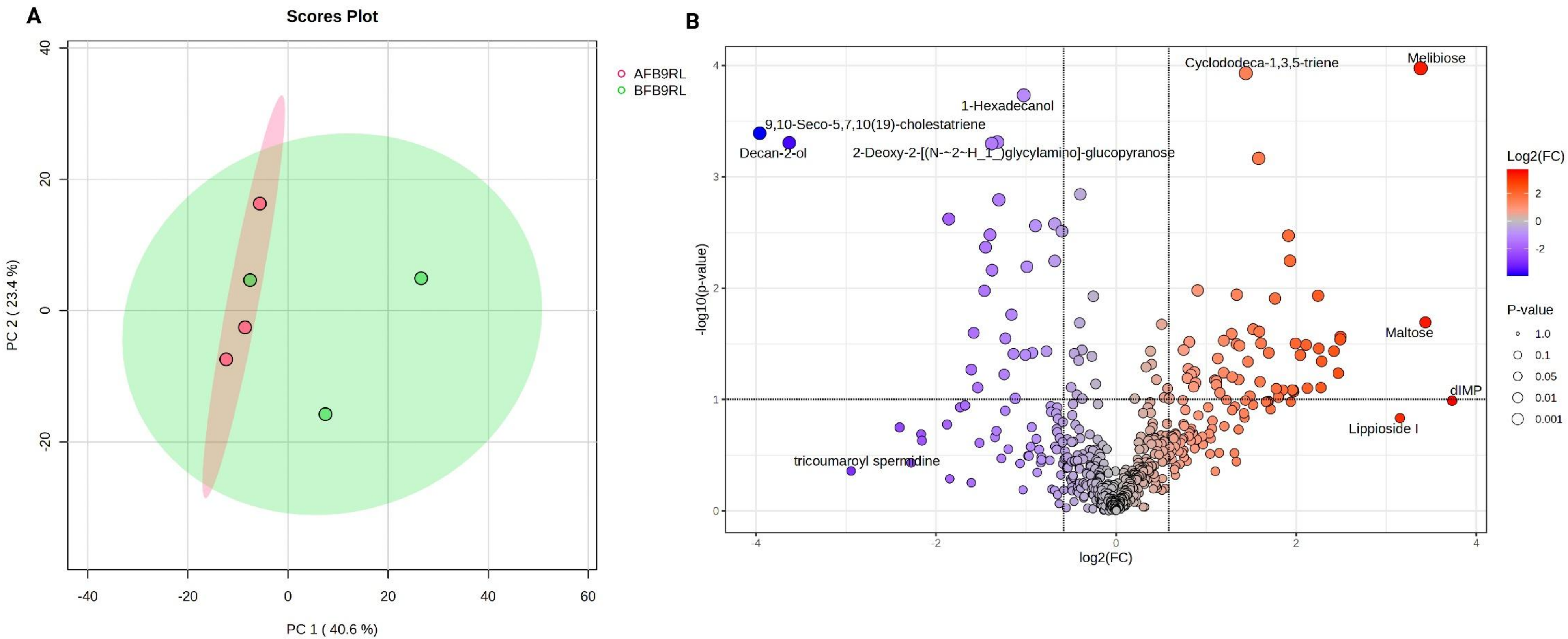

A
Scores Plot
AFB9RL
BFB9RL
PC 1 (40.6 %)
PC 2 (23.4 %)
B
Melibiose
Cyclododeca-1,3,5-triene
1-Hexadecanol
9,10-Seco-5,7,10(19)-cholestatriene
Decan-2-ol
2-Deoxy-2-[(N-~2~-H_1_)glycylamino]-glucopyranose
Maltose
dIMP
Lippioside I
tricoumaroyl spermidine
Log2(FC)
P-value
log2(FC)
-log10(p-value)

C

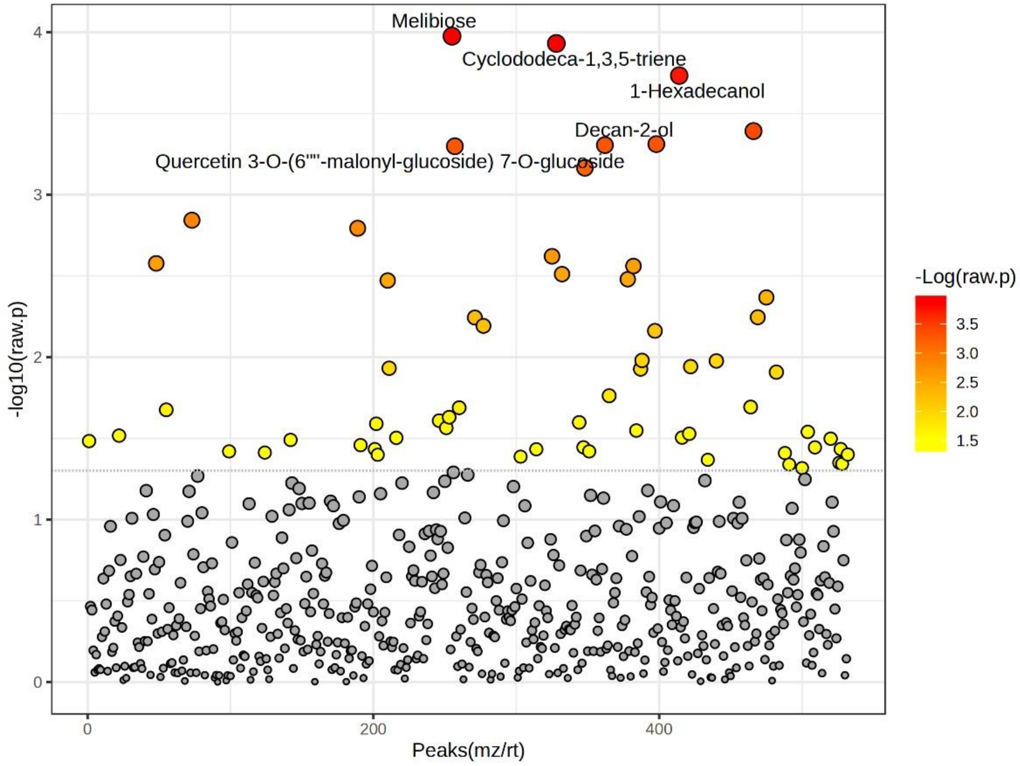

Melibiose
Cyclododeca-1,3,5-triene
1-Hexadecanol
Decan-2-ol
Quercetin 3-O-(6""-malonyl-glucoside) 7-O-glucoside
-log10(raw.p)
Peaks(mz/rt)
-Log(raw.p)

D

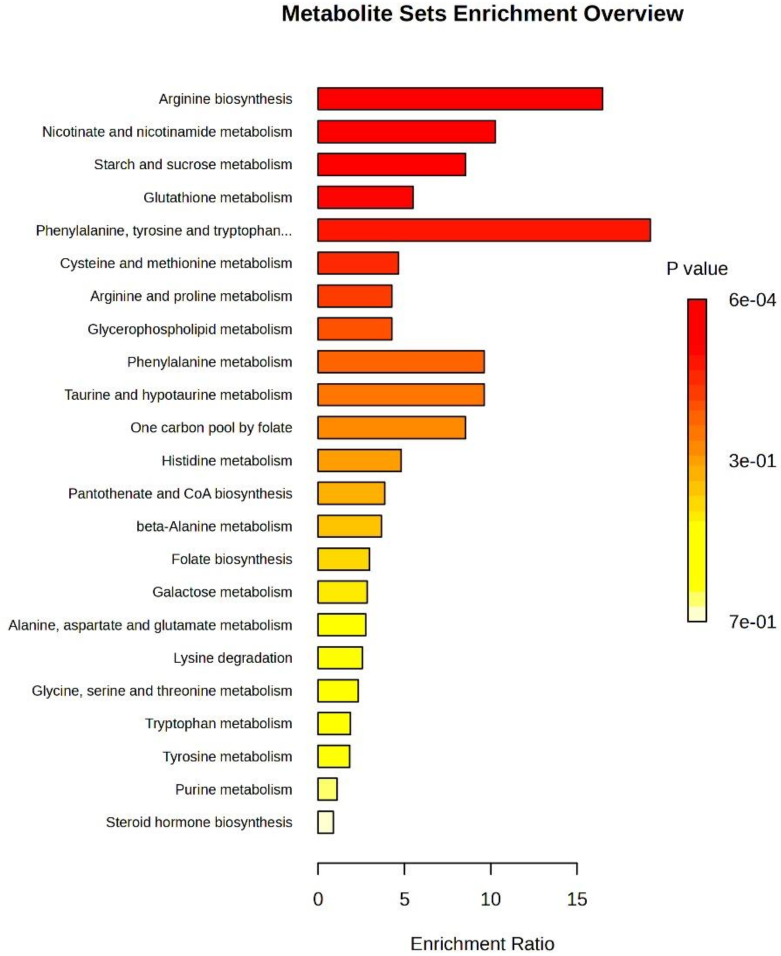

Metabolite Sets Enrichment Overview
Arginine biosynthesis
Nicotinate and nicotinamide metabolism
Starch and sucrose metabolism
Glutathione metabolism
Phenylalanine, tyrosine and tryptophan...
Cysteine and methionine metabolism
Arginine and proline metabolism
Glycerophospholipid metabolism
Phenylalanine metabolism
Taurine and hypotaurine metabolism
One carbon pool by folate
Histidine metabolism
Pantothenate and CoA biosynthesis
beta-Alanine metabolism
Folate biosynthesis
Galactose metabolism
Alanine, aspartate and glutamate metabolism
Lysine degradation
Glycine, serine and threonine metabolism
Tryptophan metabolism
Tyrosine metabolism
Purine metabolism
Steroid hormone biosynthesis
P value
Enrichment Ratio

Figure 4. Post-frost metabolomic shifts in B.9 rootstock sucker leaves. (A) Principal Component Analysis (PCA) score plot showing separation between before-frost (BF_B9RL; green ellipse) and after-frost (AF_B9RL; pink ellipse) metabolite profiles in sucker leaves. **(B)** Volcano plot of differentially accumulated metabolites between AF and BF treatments. The x-axis represents $\log_2$ fold change (FC), and the y-axis indicates $-\log_{10}$(p-value). Significantly upregulated and downregulated metabolites ($FC \geq \pm1$, $p < 0.05$) are highlighted in red and purple, respectively. **(C)** Two-sample unpaired t-test results for sucker leaf metabolites, plotted by $-\log_{10}$(*p*-value) against detected m/z-retention time pairs. The dashed horizontal line marks the statistical significance threshold ($p = 0.05$). **(D)** Metabolite Set Enrichment Analysis (MSEA) reveals enrichment of multiple frost-responsive pathways. Bar lengths indicate enrichment ratios, and bar color reflects the p-value.

The volcano plot (**Figure 4B**) revealed significant upregulation of key sugars such as melibiose and maltose, along with defense- and lipid-related metabolites like cyclododeca-1,3,5-triene and lipopidoside I, while several sterols and alcohols including decan-2-ol were suppressed. These changes were corroborated by the two-sample *t*-test (**Figure 4C**), where melibiose, decan-2-ol, and quercetin 3-O-(6″″-malonyl-glucoside) 7-O-glucoside showed highly significant *p*-values ($-\log_{10} > 2.5$). Pathway enrichment analysis (**Figure 4D**) confirmed strong induction of cold-responsive metabolic networks including arginine biosynthesis, nicotinate and nicotinamide metabolism, starch and sucrose metabolism, and glutathione-related redox pathways. Together, these results highlight the multifaceted metabolic reprogramming occurring in B.9 rootstock tissue under natural frost conditions.

2.2.1 Metabolomic Reprogramming in Floral Buds, Scion Leaves, and Sucker Leaves of Cold-Susceptible Rootstock M.26 Following Natural Frost Exposure

Floral buds from 'Gala' grafted on the cold-susceptible rootstock M.26 exhibited moderate yet discernible metabolomic shifts in response to frost, as shown by the Principal Component Analysis (**Figure 5A**).

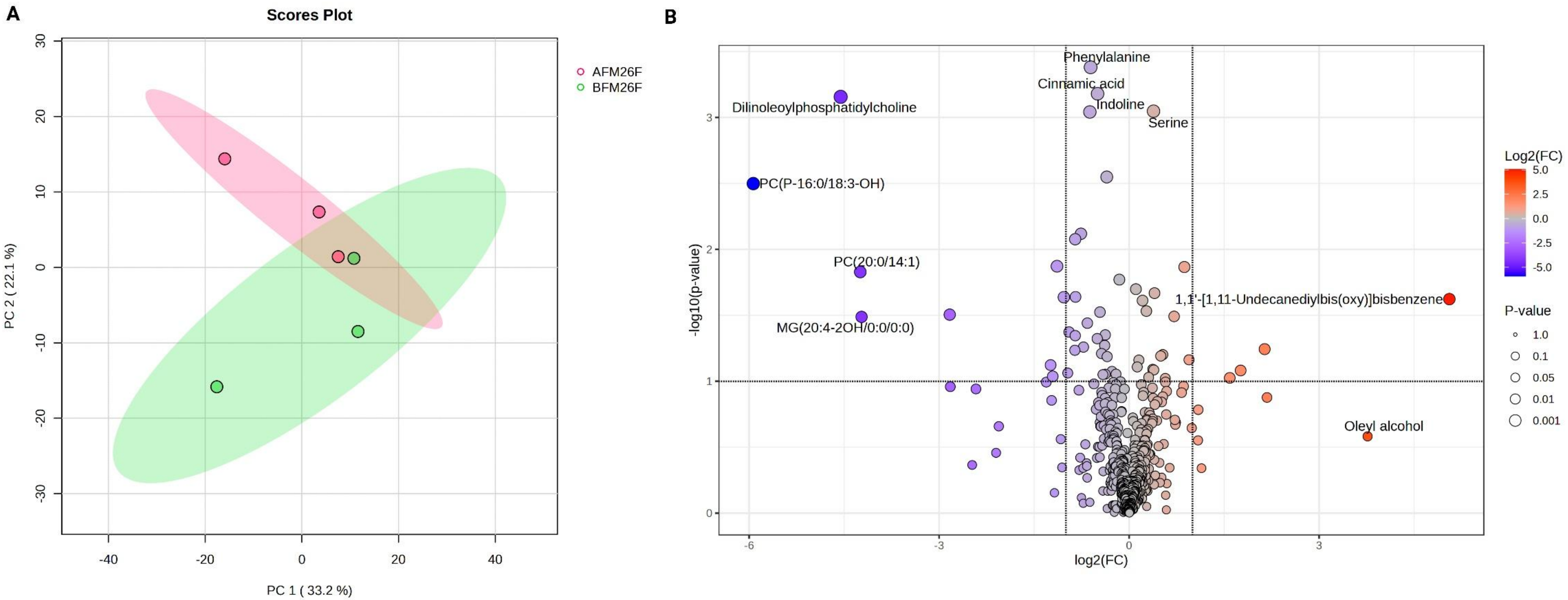
A
Scores Plot
AFM26F
BFM26F
PC 1 (33.2 %)
PC 2 (22.1 %)
B
Phenylalanine
Cinnamic acid
Indoline
Serine
Dilinoleoylphosphatidylcholine
PC(P-16:0/18:3-OH)
PC(20:0/14:1)
MG(20:4-2OH/0:0/0:0)
1,1'-[1,11-Undecanediylbis(oxy)]bisbenzene
Oleyl alcohol
log2(FC)
-log10(p-value)
Log2(FC)
P-value

C

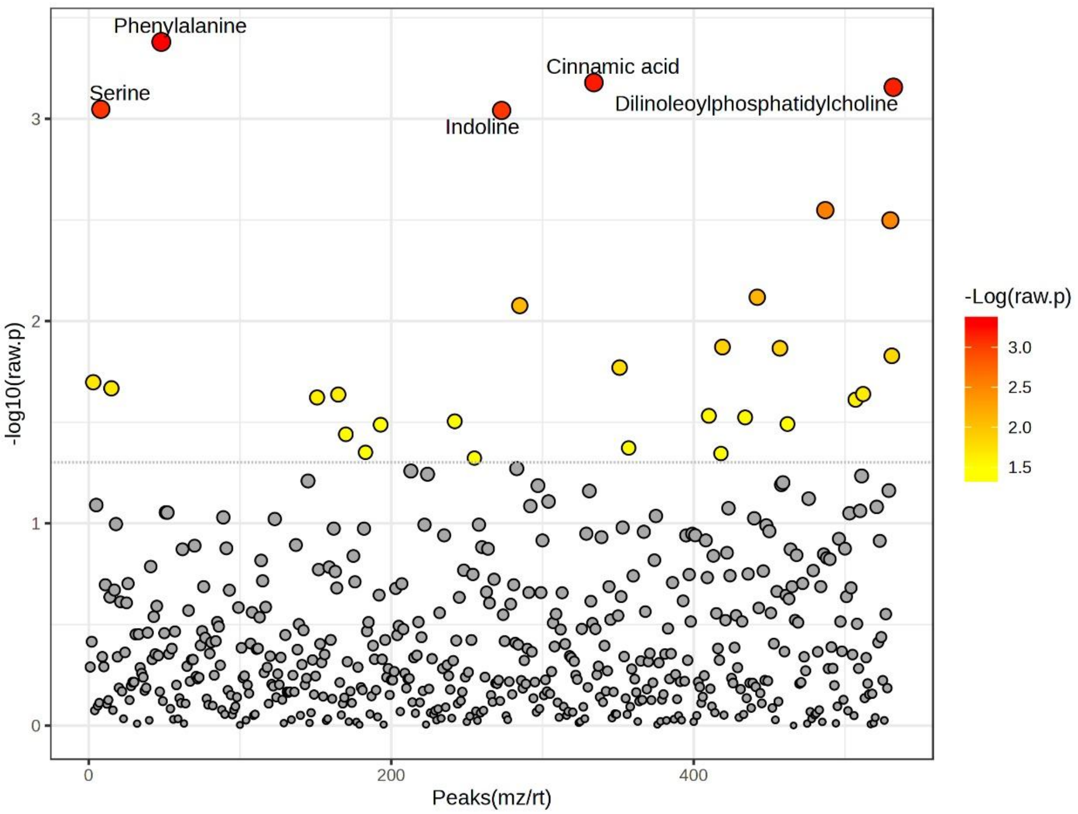

Phenylalanine
Serine
Cinnamic acid
Indoline
Dilinoleoylphosphatidylcholine
-log10(raw.p)
0
1
2
3
0
200
400
Peaks(mz/rt)
-Log(raw.p)
3.0
2.5
2.0
1.5

D

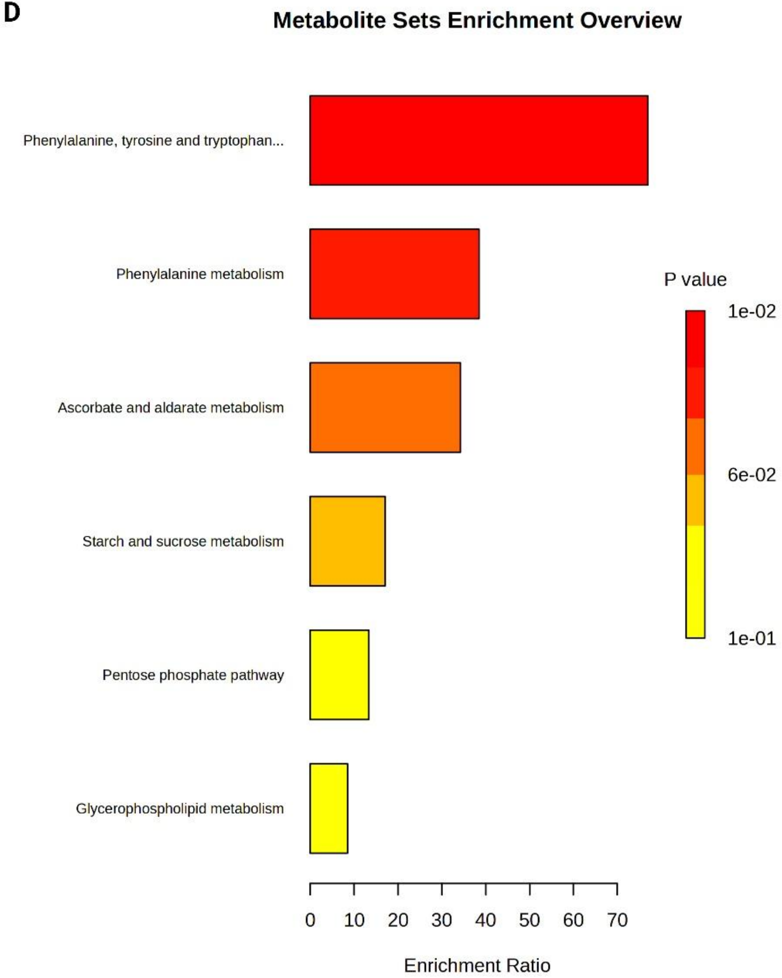

Metabolite Sets Enrichment Overview
Phenylalanine, tyrosine and tryptophan...
Phenylalanine metabolism
Ascorbate and aldarate metabolism
Starch and sucrose metabolism
Pentose phosphate pathway
Glycerophospholipid metabolism
0
10
20
30
40
50
60
70
Enrichment Ratio
P value
1e-02
6e-02
1e-01

Figure 5. Post-frost metabolomic shifts in 'Gala' floral buds grafted on cold-susceptible rootstock M.26. (A) Principal Component Analysis (PCA) score plot showing partial separation between before-frost (BF_M26F; green ellipse) and after-frost (AF_M26F; pink ellipse) metabolite profiles in floral buds. **(B)** Volcano plot of differentially accumulated metabolites between AF and BF treatments. The x-axis denotes $\log_2$ fold change (FC), and the y-axis shows $-\log_{10}(p\text{-value})$. Significantly upregulated and downregulated metabolites ($FC \geq \pm1$, $p < 0.05$) are shown in red and purple, respectively. **(C)** Two-sample unpaired t-test results for floral bud metabolites, plotted by $-\log_{10}(p\text{-value})$ against m/z-retention time pairs. The dashed horizontal line represents the $p = 0.05$ significance threshold. **(D)** Metabolite Set Enrichment Analysis (MSEA). Bar lengths indicate enrichment ratios, and color gradients reflect pathway-level *p*-values.

Although before-frost (BF_M26F) and after-frost (AF_M26F) groups demonstrated partial overlap, they also showed clear directional clustering, suggesting biologically meaningful divergence in metabolite composition. The volcano plot (**Figure 5B**) revealed several significantly altered metabolites ($FC \geq \pm1$, $p < 0.05$), including the upregulation of oleyl alcohol and 1,1′-[1,11-Undecanediyl-bis(oxy)]bisbenzene, alongside the downregulation of key membrane lipids such as dilinoleoylphosphatidylcholine. Statistical confirmation from the two-sample *t*-test (**Figure 5C**) highlighted frost-induced changes in phenylpropanoid-related compounds—phenylalanine, cinnamic acid, and serine—implicating active biosynthetic and stress-associated processes. The corresponding pathway-level analysis (**Figure 5D**) showed enrichment of phenylalanine, tyrosine and tryptophan biosynthesis, phenylalanine metabolism, and ascorbate-related antioxidant pathways, indicating frost-induced activation of aromatic amino acid metabolism and redox signaling in this susceptible tissue.

Leaves of 'Gala' scion grafted on cold-susceptible M.26 rootstock showed pronounced metabolomic divergence following frost exposure, as confirmed by the PCA (**Figure 6A**), where before-frost (BF_M26SL) and after-frost (AF_M26SL) samples were clearly separated with non-overlapping 95% confidence ellipses, indicating strong biological reproducibility and treatment-specific separation.

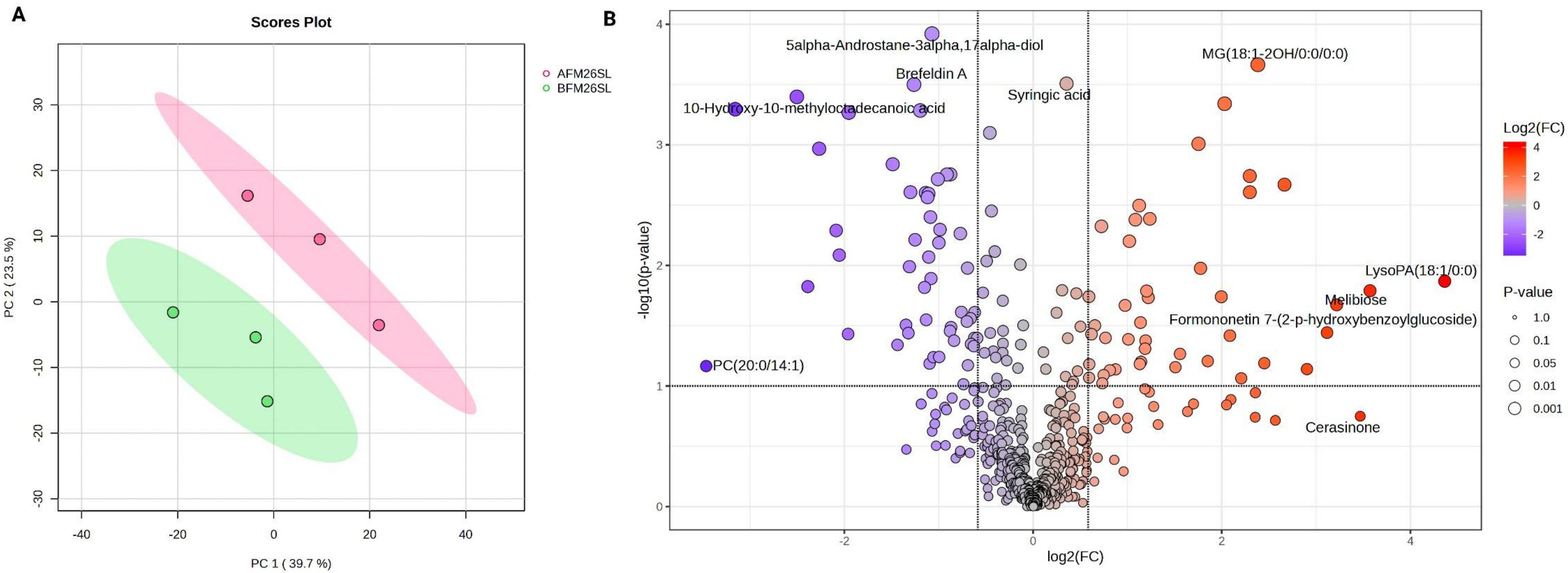

A
Scores Plot
AFM26SL
BFM26SL
PC 1 (39.7 %)
PC 2 (23.5 %)
B
5alpha-Androstane-3alpha,17alpha-diol
Brefeldin A
Syringic acid
10-Hydroxy-10-methyloctadecanoic acid
MG(18:1-2OH/0:0/0:0)
LysoPA(18:1/0:0)
Melibiose
Formononetin 7-(2-p-hydroxybenzoylglucoside)
PC(20:0/14:1)
Cerasinone
log2(FC)
-log10(p-value)
Log2(FC)
P-value

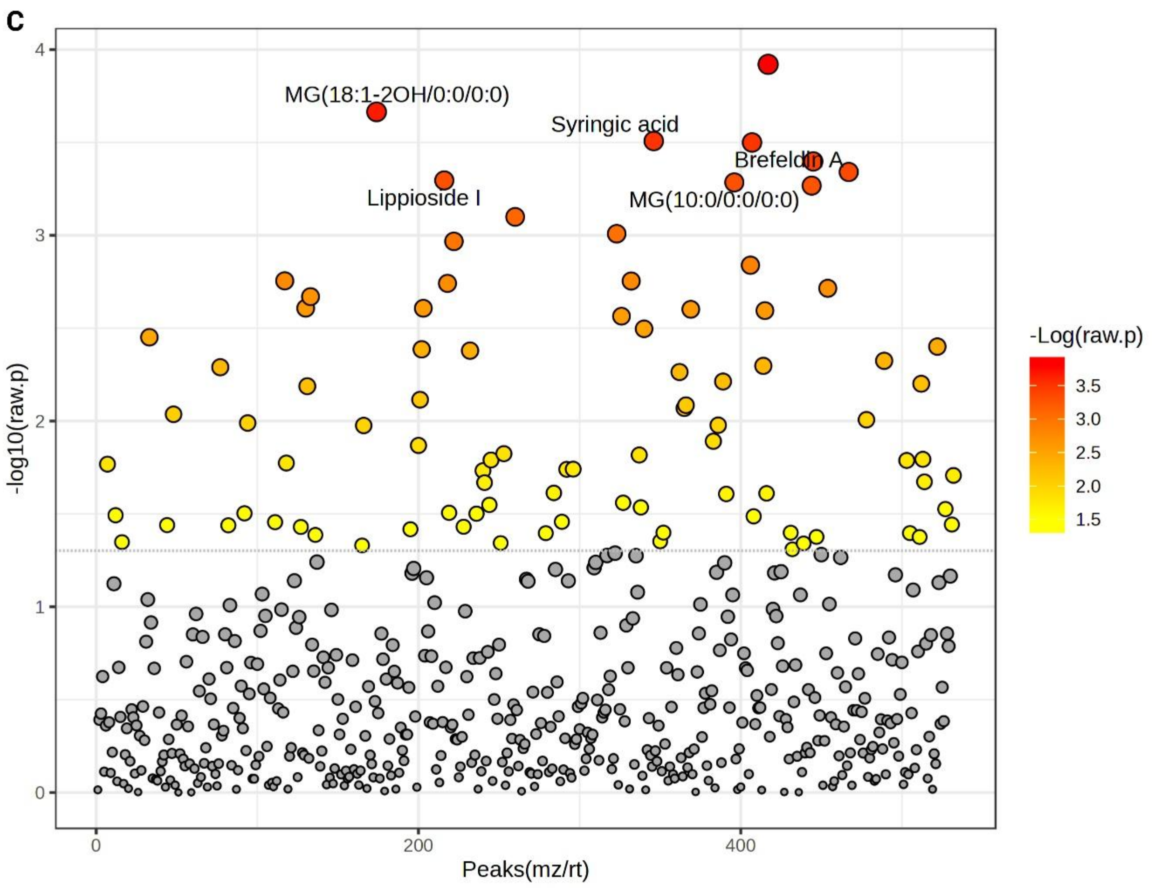
C
MG(18:1-2OH/0:0/0:0)
Syringic acid
Brefeldin A
Lippioside I
MG(10:0/0:0/0:0)
-log10(raw.p)
Peaks(mz/rt)
-Log(raw.p)
3.5
3.0
2.5
2.0
1.5

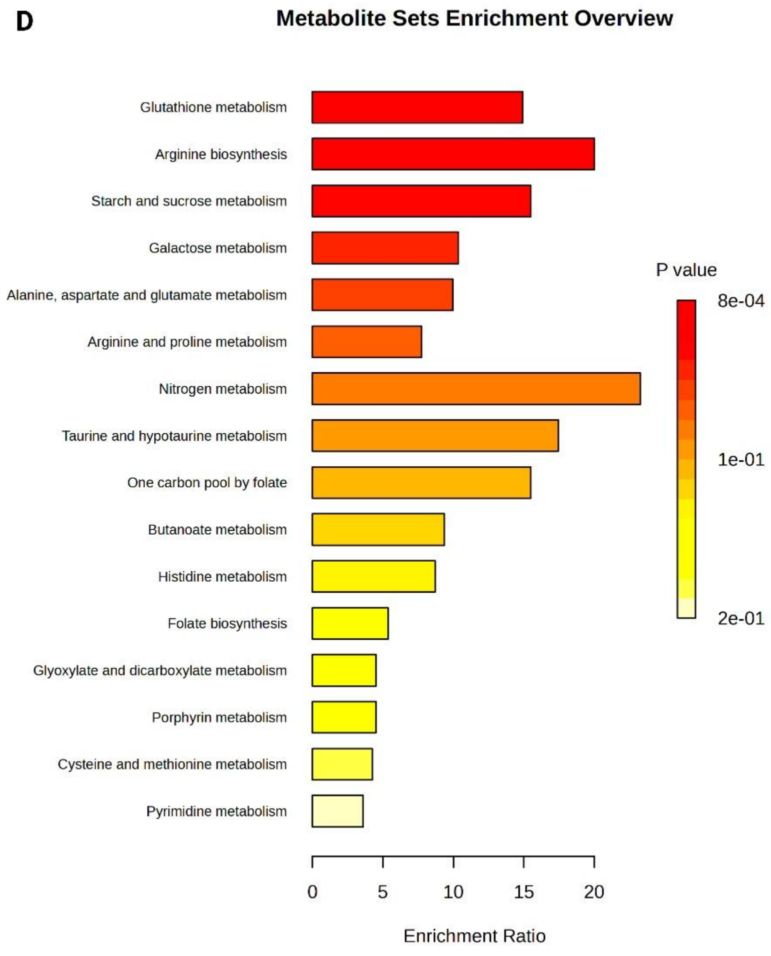
D
Metabolite Sets Enrichment Overview
Glutathione metabolism
Arginine biosynthesis
Starch and sucrose metabolism
Galactose metabolism
Alanine, aspartate and glutamate metabolism
Arginine and proline metabolism
Nitrogen metabolism
Taurine and hypotaurine metabolism
One carbon pool by folate
Butanoate metabolism
Histidine metabolism
Folate biosynthesis
Glyoxylate and dicarboxylate metabolism
Porphyrin metabolism
Cysteine and methionine metabolism
Pyrimidine metabolism
Enrichment Ratio
P value
8e-04
1e-01
2e-01

Figure 6. Post-frost metabolomic shifts in 'Gala' scion leaves grafted on cold-susceptible rootstock M.26. (A) Principal Component Analysis (PCA) score plot showing distinct separation between before-frost (BF_M26SL; green ellipse) and after-frost (AF_M26SL; pink ellipse) metabolite profiles in scion leaves. **(B)** Volcano plot of differentially accumulated metabolites between AF and BF treatments. The x-axis shows $\log_2$ fold change (FC), while the y-axis represents $-\log_{10}(p\text{-value})$. Metabolites significantly upregulated or downregulated (FC $\geq \pm 1$, $p < 0.05$) are shown in red and purple, respectively. **(C)** Two-sample unpaired *t*-test results for scion leaf metabolites, plotted by $-\log_{10}$(p-value) against detected m/z-retention time pairs. The dashed horizontal line marks the p = 0.05 significance cutoff. **(D)** Metabolite Set Enrichment Analysis (MSEA) identifies pathway-level enrichment in response to frost stress. Bar lengths indicate enrichment ratios, and bar color corresponds to statistical significance.

The volcano plot (**Figure 6B**) revealed significant upregulation and downregulation of multiple metabolites (FC $\geq \pm 1$, $p < 0.05$), with key compounds including syringic acid, MG(18:1-2OH/0:0/0:0), lipopisside I, and the isoflavonoid formononetin 7-(2-p-hydroxybenzoylglucoside). The *t*-test plot (**Figure 6C**) further reinforced these trends, highlighting syringic acid, brefeldin A, MG(10:0/0:0/0:0), and lipopisside I as statistically significant metabolites showing frost-induced shifts. Pathway-level analysis via MSEA (**Figure 6D**) showed strong enrichment in frost-relevant pathways such as glutathione metabolism, arginine biosynthesis, starch and sucrose metabolism, and galactose metabolism, collectively indicating a redox-sensitive and sugar-associated response signature under frost stress in this susceptible rootstock context.

In M.26 rootstock sucker leaves, metabolomic profiles revealed partial separation between before-frost (BF_M26RL) and after-frost (AF_M26RL) samples, as shown in the PCA (**Figure 7A**), where the ellipses overlapped slightly but displayed directional clustering, indicating moderate treatment-associated differentiation.

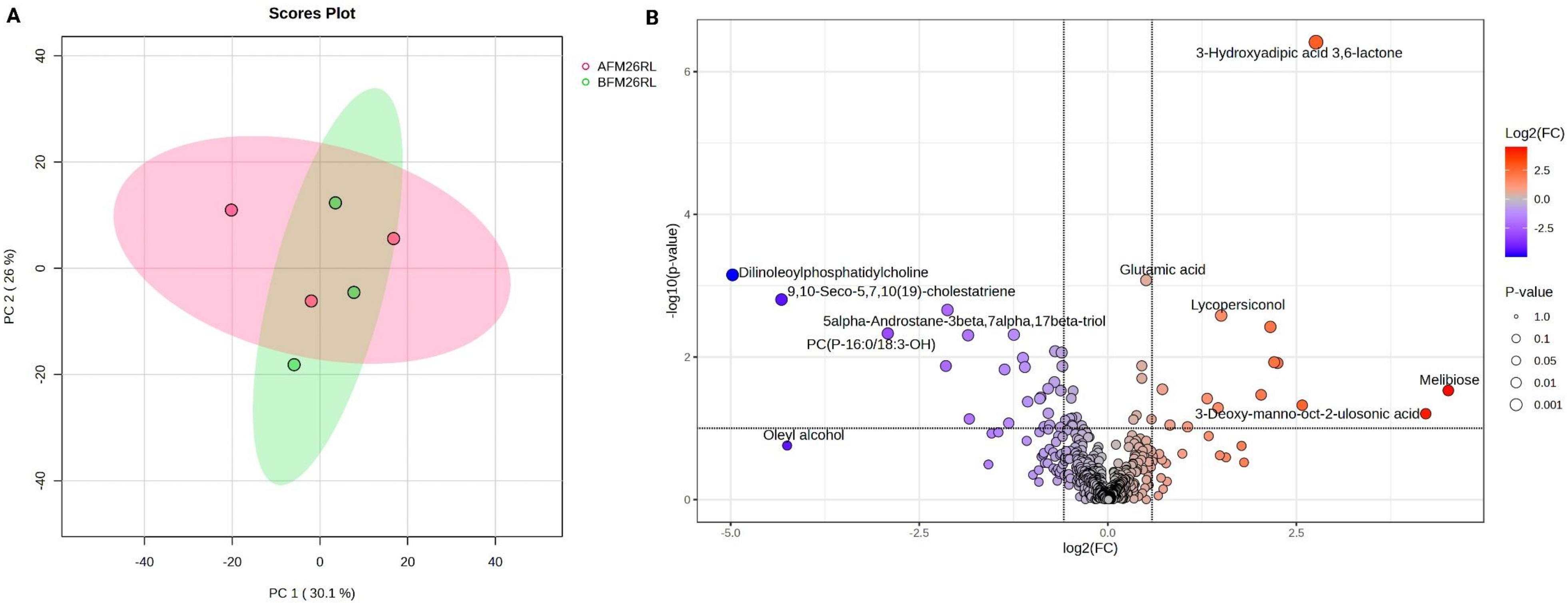
A
Scores Plot
AFM26RL
BFM26RL
PC 1 (30.1 %)
PC 2 (26 %)
-40
-20
0
20
40
B
3-Hydroxyadipic acid 3,6-lactone
Dilinoleoylphosphatidylcholine
9,10-Seco-5,7,10(19)-cholestatriene
5alpha-Androstane-3beta,7alpha,17beta-triol
PC(P-16:0/18:3-OH)
Glutamic acid
Lycopersiconol
Melibiose
3-Deoxy-manno-oct-2-ulosonic acid
Oleyl alcohol
-log10(p-value)
log2(FC)
-5.0
-2.5
0.0
2.5
Log2(FC)
P-value
1.0
0.1
0.05
0.01
0.001

C

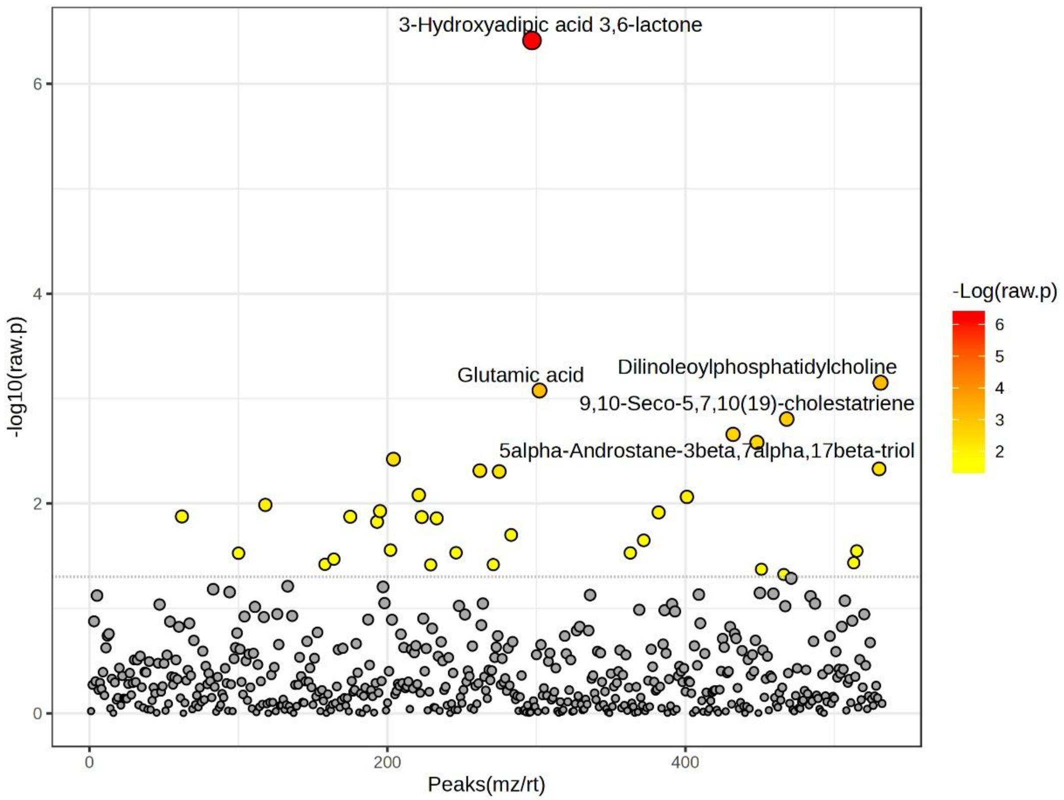
3-Hydroxyadipic acid 3,6-lactone
Glutamic acid
Dilinoleoylphosphatidylcholine
9,10-Seco-5,7,10(19)-cholestatriene
5alpha-Androstane-3beta,7alpha,17beta-triol
-log10(raw.p)
Peaks(mz/rt)
-Log(raw.p)
0
2
4
6
200
400

D

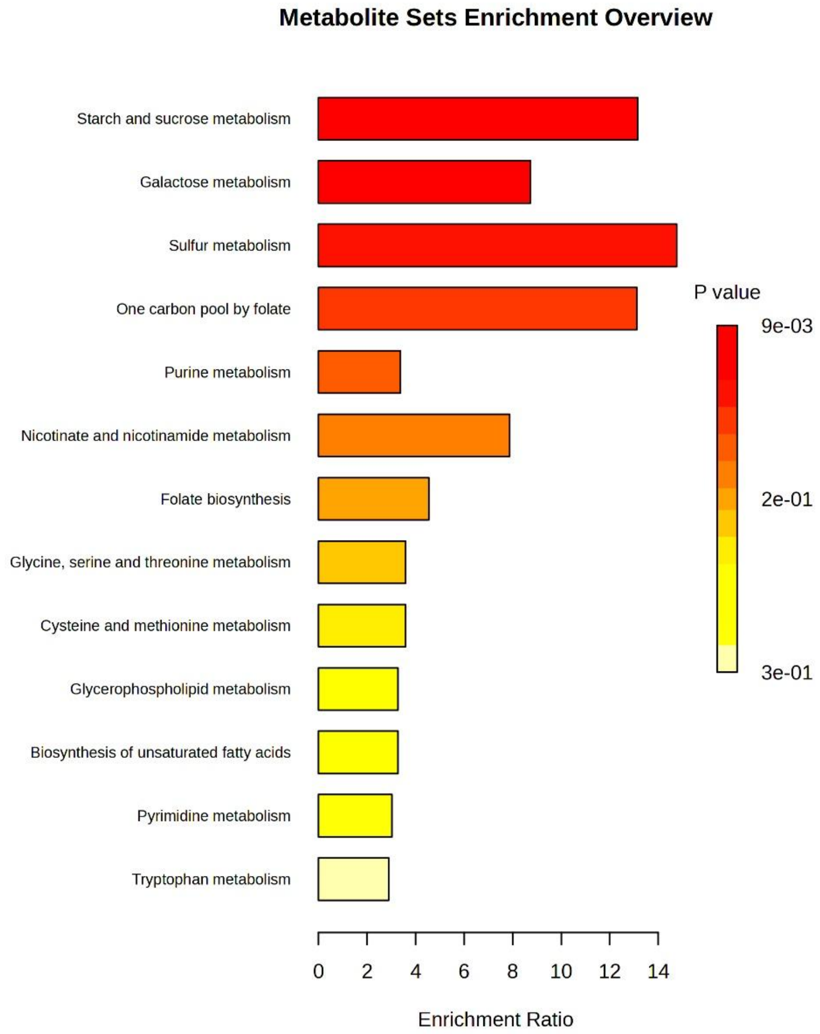
Metabolite Sets Enrichment Overview
Starch and sucrose metabolism
Galactose metabolism
Sulfur metabolism
One carbon pool by folate
Purine metabolism
Nicotinate and nicotinamide metabolism
Folate biosynthesis
Glycine, serine and threonine metabolism
Cysteine and methionine metabolism
Glycerophospholipid metabolism
Biosynthesis of unsaturated fatty acids
Pyrimidine metabolism
Tryptophan metabolism
P value
9e-03
2e-01
3e-01
0 2 4 6 8 10 12 14
Enrichment Ratio

Figure 7. Post-frost metabolomic shifts in M.26 rootstock sucker leaves. (A) Principal Component Analysis (PCA) score plot showing partial separation between before-frost (BF_M26RL; green ellipse) and after-frost (AF_M26RL; pink ellipse) metabolite profiles in sucker leaves. **(B)** Volcano plot of differentially accumulated metabolites between AF and BF treatments. The x-axis represents $\log_2$ fold change (FC) and the y-axis shows $-\log_{10}(p\text{-value})$. Significantly upregulated and downregulated metabolites ($FC \geq \pm 1$, $p < 0.05$) are colored red and purple, respectively. **(C)** Two-sample unpaired t-test results for sucker leaf metabolites, plotted by $-\log_{10}(p\text{-value})$ against detected m/z-retention time pairs. The dashed horizontal line marks the significance threshold ($p = 0.05$). (**D**) Metabolite Set Enrichment Analysis (MSEA) highlights pathway-level responses to frost. Bar lengths represent enrichment ratios, and color intensity indicates statistical significance (p-values).

The volcano plot (**Figure 7B**) displayed both significantly upregulated and downregulated metabolites ($FC \geq \pm 1$, $p < 0.05$), with annotated compounds such as 3-hydroxyadipic acid 3,6-lactone, melibiose, glutamic acid, and dilinoleoyl-phosphatidylcholine contributing to the frost-induced shifts. This finding was reinforced by the *t*-test results (**Figure 7C**), where 3-hydroxyadipic acid 3,6-lactone emerged as the most statistically significant compound, along with modest alterations in glutamic acid and sterol-related metabolites. Pathway enrichment analysis (**Figure 7D**) further supported these trends, revealing moderate enrichment in starch and sucrose metabolism, galactose metabolism, sulfur metabolism, and one-carbon metabolism, collectively pointing to frost-driven perturbations in sugar handling, redox balance, and membrane-associated metabolism in the frost-sensitive M.26 sucker tissue.

3 Discussion

Frost, a major form of cold stress, occurs when freezing temperatures lead to ice formation within plant tissues, often triggered by radiative cooling on clear nights or the arrival of cold air masses. This environmental condition poses a serious threat to apple production, particularly during the sensitive floral stages (Jahed et al., 2023). While many studies rely on controlled environments or excised plant parts, such approaches may not reflect the full physiological response under natural frost conditions. In contrast, our metabolomic study was conducted on mature, field-grown 'Gala' apple trees exposed to real frost events, allowing us to observe authentic, tissue-specific metabolic changes associated with frost tolerance and susceptibility. We examined within-rootstock responses across tissues to identify tissue-specific metabolic adjustments associated with frost stress.

We show that metabolic profiles were clearly separated in floral buds, scion leaves, and sucker leaves, and subsequent analyses revealed distinct shifts in key metabolites and pathways following frost in each tissue. These findings provide insight into how individual tissues activate different biochemical strategies depending on their physiological roles and rootstock background, laying the foundation for identifying robust metabolic markers linked to cold stress adaptation in apple.

3.1 Comprehensive Tissue-Level Metabolomics of Gala on B.9 Under Frost Stress

3.1.1 Sugar Metabolism, Osmoprotection, and Redox Regulation

Following frost, B.9 sucker leaves showed strong enrichment in the starch/sucrose metabolism pathway, with marked post-frost maltose accumulation. Maltose, a disaccharide from starch breakdown, functions as a compatible solute for membrane and protein stabilization. Soluble sugars generally serve dual roles as vital osmoprotectants and energy reserves in cold responses (Thalmann & Santelia, 2017; Dong & Beckles, 2019). This is supported by evidence like cold-induced β-amylases (e.g., *Arabidopsis* BMY7/8) increasing maltose and enhancing stress tolerance (Kaplan & Guy, 2004; Peng et al., 2014; Zhu et al., 2024), and Beta-Amylase 3 (BAM3) overexpression improving freezing tolerance in other species (Monroe et al., 2014; Zhao et al., 2019; Sun et al., 2021). Our data suggest B.9 initiates a proactive starch degradation program for local protection and energy. Disaccharides (maltose, trehalose, sucrose) also protect membranes via hydrogen bonding and altered lipid dynamics (Roy et al., 2016). Beyond structural and energetic roles, sugars are integral to redox homeostasis.

The ascorbate and aldarate metabolism pathway, which synthesizes ascorbate (ASC) from glucose-derived precursors via the Smirnoff–Wheeler pathway (Akram et al., 2017), was strongly enriched in B.9 floral buds after frost. This upregulation points to enhanced ROS scavenging and redox buffering capacity, as ASC detoxifies ROS and is crucial for maintaining cellular redox ratios (Talla et al., 2011; Ivanov, 2014; Lin et al., 2016). Aldarate metabolism further complements ASC by metabolizing cell wall-derived hexuronic acids, which can feed into sugar pools for osmoprotection (Wu et al., 2023). Co-enrichment of starch/sucrose and pentose phosphate pathways further suggests an integrated strategy for redox and sugar resource mobilization. Sugars also directly support ROS detoxification, as shown by increased antioxidant enzyme activity in sugar-rich tomato lines under cold (Liu et al., 2020), and modulate transcription through sugar-responsive pathways, such as CdWRKY2-mediated induction of CdSPS1 in bermudagrass (Huang et al., 2022; Zhao et al., 2020).

Post-frost melibiose accumulation was observed in both B.9 and M.26 suckers, but its induction was markedly higher in B.9. This reinforces the role of this RFO (raffinose family oligosaccharide)-derived sugar in the tolerant rootstock's enhanced osmoprotective response. Melibiose, an RFO hydrolytic product, functions in osmoprotection and signaling (Lingner et al., 2011; Liu et al., 2024), similarly to *Vitis amurensis* cold acclimation (Chai et al., 2019). RFOs are transported via polymer-trapping (Turgeon & Gowan, 1990; Zhang & Turgeon, 2018; Ma et al., 2019) and hydrolyzed to smaller sugars including melibiose (Vinson et al., 2020; Zhang et al., 2021). While trehalose and melibiose were not enriched in B.9 buds, their significant elevation in B.9 scion leaves indicates tissue-specific roles in osmoprotection and systemic redox regulation, complementing the ASC-centered antioxidant responses in reproductive buds. This overall sugar enrichment reflects stress-buffering and dynamic source–sink sugar redistribution—a B.9 strategy enhancing rootstock/scion frost resilience.

3.1.2 Differential Accumulation of Phenylalanine Following Frost Exposure

Following frost, phenylalanine levels increased in 'Gala' floral buds on B.9, indicating early metabolic priming. As the direct substrate for phenylalanine ammonia-lyase (PAL), this increase suggests activation of the phenylpropanoid pathway, a well-established stress response also seen in grape and eggplant (Liu et al., 2021, 2025; Barzegar et al., 2021). Downstream enzymes—CHS, CHI, and F3H (Chalcone Synthase, Chalcone Isomerase, Flavanone 3-Hydroxylase) —redirect flux toward flavonol synthase (FLS), culminating in the production of flavonols and anthocyanins that enhance stress resilience (Li et al., 2025).

These compounds scavenge ROS (e.g., singlet oxygen, hydroxyl radicals), absorb UV-B radiation during exposure (Schulz et al., 2021), and stabilize membranes by integrating into phospholipid headgroups (Chaudhuri et al., 2007; Xu et al., 2022).

Anthocyanin accumulation, as shown in PAP1 (Production of Anthocyanin Pigment 1) activation-tagged lines and Ruby1-expressing citrus, is linked to improved freezing tolerance via reduced chlorophyll degradation and better Photosystem II function (Schulz et al., 2016; Liu et al., 2020; Wang et al., 2024). In apple, regulators like MdMYB23 (*M. domestica* MYB transcription factor 23) and MdMYBPA1 (*M. domestica* MYB transcription factor PA1 /Proanthocyanidin/) contribute similarly (An et al., 2018). This response is metabolically supported by frost-induced increases in osmoprotective sugars (melibiose, maltose) in B.9 sucker leaves, which may be translocated to buds to offset the high carbon demand of flavonoid biosynthesis. Concurrently, the accumulation of colnelenic acid in buds suggests 9-LOX–DES (9-Lipoxygenase–Divinyl Ether Synthase)-driven oxylipin signaling (Becker et al., 2007), while hormone-mediated regulation is evidenced by ABA-inducible ABA-Insensitive 5 (ABI5) activating flavonoid genes under stress (Li et al., 2025). Together, this PAL-initiated pathway integrates sugar mobilization, lipid signaling, and hormone-responsive transcriptional control, forming a multi-layered metabolic defense network in B.9 under frost.

3.1.3. Lipid-Derived Signaling & Membrane Remodeling

B.9 tissues exhibit dynamic membrane lipid remodeling and signaling in response to frost. Oxylipins like colneleic and colnelenic acids, synthesized by divinyl ether synthase (DES) from 9-hydroperoxides (Grechkin, 2002), act as early lipid stress signals. Colnelenic acid significantly increased in B.9 floral buds after frost, likely reflecting membrane phase shifts (Vellosillo et al., 2007). These 9-LOX oxylipins, including ketols, are increasingly recognized in abiotic stress (e.g., salinity, light, temperature; Berg-Falloure & Kolomiets, 2023).

Frost also induces divergent lysophospholipid changes in B.9 floral buds: LysoPA(20:2/0:0) increased, while LysoPI(18:2/0:0) decreased, signaling membrane stress. These Phospholipase A (PLA)-generated lipids (Effendi et al., 2014; Hou et al., 2016) can initiate extracellular cascades. Elevated LysoPA is rapidly synthesized under abiotic stress (Scherer et al., 2002; Welti et al., 2002; Wi et al., 2014) and may drive Ca^{2+} influx via plasma membrane channels (Vaultier et al., 2006), activating Phosphatidic Acid (PA) production (Welti et al., 2002; Li et al., 2004). Lysophospholipids likely modulate Ca^{2+} dynamics by interacting with H^+-ATPases or calcium transporters (Scherer, 2002; Wielandt et al., 2015). Cold-induced PA and lyso-PLs stimulate Ca^{2+} influx and activate ICE–CBF transcription (Zhang et al., 2013), suggesting LysoPA enhances cold signaling via calcium-mediated ICE1–CBF cascades. LysoPI's decline implies its conversion to inositol phosphates (Meijer & Munnik, 2003) mobilizing internal calcium (Lemtiri-Chlieh et al., 2003) and linking to jasmonate signaling via IP_6 (Tan et al., 2007; Sheard et al., 2010). This reciprocal regulation signifies a finely tuned calcium- and hormone-mediated frost response.

Similar systemic remodeling occurred in B.9 scion leaves: LysoPI was upregulated, PC(20:0) downregulated, and (Eicosatrienoyl)-glycerophosphate enriched, indicating active membrane-derived signal generation and fluidity adjustments. Further reflecting dynamic lipid mobilization, dilinoleoyl-phosphatidylcholine (PC 18:2/18:2) showed sharp pre-frost accumulation and post-frost depletion in B.9 floral buds. This structural glycerophospholipid supports membrane architecture and stress signaling. Phosphatidylcholines (PCs) are key Phospholipase D (PLD) substrates, yielding phosphatidic acid (PA)—a signaling lipid accumulating under cold/drought (Wang, 2004; Testerink & Munnik, 2005, 2011). They also provide polyunsaturated fatty acids (e.g., linoleic acid) liberated by phospholipases and oxidized by LOXs to generate oxylipins (Smith & Lands, 1972; Yamamoto, 1992; Maccarrone et al., 1994). While Lipoxygenases (LOXs) prefer free fatty acids, they can oxidize esterified linoleoyl groups in solubilized PCs (e.g., to 13-hydroperoxy-9,11-octadecadienoic acid (HPODE; Huang et al., 2006), indicating membrane-bound PCs serve as stress-responsive oxylipin precursors during membrane disassembly. Thus, dilinoleoyl-PC reduction suggests lipid peroxidation, PLD activity, or diversion into LOX-mediated signaling, contributing to membrane fluidity and lipid-derived signal generation. Beyond signaling, B.9 displays active membrane structural stabilization. Post-frost accumulation of 9,10-seco-5,7,10(19)-cholestatatriene in B.9 suckers indicates sterol remodeling, a strategy for preserving membrane fluidity and integrity under freezing (Rogowska & Szakiel, 2020). Plant sterols modulate bilayer rigidity via lipid rafts for ion transport/signaling, counteracting freezing-induced stiffening and influencing ABA–membrane interactions (Takahashi et al., 2016; Stillwell et al., 1990). Conversely, post-frost downregulation of 1-hexadecanol and decan-2-ol in B.9 suckers likely reflects their active incorporation into protective wax structures via cuticular wax biosynthesis (Bernard et al., 2012; Lee & Suh, 2013). This suggests active utilization for structural reinforcement during freeze–thaw recovery (Dahlin et al., 2019; Lee & Suh, 2022).

3.1.4 Nitrogen-Associated Stress Metabolism

One of the most prominent metabolic shifts in B.9 sucker tissues after frost was the strong enrichment of the arginine biosynthesis pathway, indicating a nitrogen-directed reprogramming that supports stress adaptation. Arginine, a high nitrogen-to-carbon amino acid, serves as a precursor to polyamines such as putrescine (Put) and spermidine (Spd), which stabilize membranes, maintain redox balance, and regulate stress-responsive genes (Winter et al., 2015; Yoshikawa et al., 2007; Cheng et al., 2023). This metabolic rerouting is consistent with the concurrent increase in maltose and melibiose—osmoprotectants that further reinforce B.9's stress resilience. Under abiotic stress, arginine flux is often redirected via the arginine decarboxylase (ADC) pathway to produce polyamines (Kou et al., 2018). These small, positively charged molecules interact with negatively charged nucleic acids and phospholipids, potentially reinforcing plasma membrane integrity in frost-sensitive tissues (Zhang et al., 2025).

Beyond structural roles, polyamines modulate reactive oxygen species (ROS) by directly scavenging radicals and enhancing activities of antioxidant enzymes like Catalase, Superoxide Dismutase, and Ascorbate Peroxidase i.e. CAT, SOD, and APX (Gao et al., 2020). Their controlled degradation via polyamine oxidases (PAOs) also generates H_2O_2 as a signaling molecule to trigger downstream defense cascades (Liu et al., 2007; Zhang et al., 2009). Crucially, polyamines can activate the ICE–CBF–COR transcriptional cascade central to cold acclimation (Cook et al., 2004; Nakashima and Shinozaki, 2006), and their biosynthesis is modulated by ABA (Kolesnikov et al., 2024). Given that B.9 exhibits elevated basal ABA levels and heightened ABA sensitivity (Saini et al., 2025), it is plausible that an ABA–polyamine interaction amplifies its frost resilience. A parallel enrichment of arginine biosynthesis was observed in B.9 scion leaves, with significant upregulation of nitrogenous metabolites like aspartic acid and 4-oxoproline. Together, these findings indicate that B.9 rootstock initiates a coordinated nitrogen-based defense program across both rootstock and scion tissues to mitigate frost-induced injury.

3.1.5 Redox Homeostasis

In B.9 sucker tissues, Nicotinate and Nicotinamide metabolism was among the most significantly enriched pathways following frost, highlighting its central role in redox buffering, ROS detoxification, and metabolic coordination during stress. Pyridine nucleotides—NAD(H) and NADP(H)—act as key redox carriers in glycolysis, the Tricarboxylic Acid i.e. TCA cycle, mitochondrial respiration, and biosynthetic pathways (Lu et al., 2023). Cold-induced redox homeostasis depends on NAD^+/$NADP^+$ turnover through both *de novo* biosynthesis (from L-aspartate) and the salvage of nicotinamide (Smith et al., 2021). Similar flux shifts were seen in cold-stressed coconut seedlings, where accumulation of β-nicotinamide mononucleotide (β-NMN) reflected increased NAD cycling for oxidative stress defense (Lu et al., 2023). In B.9, these changes likely sustain NADPH supply for the Foyer–Halliwell–Asada cycle, regenerating reduced glutathione and ascorbate for ROS scavenging (Foyer & Kunert, 2024).

NADPH also powers respiratory burst oxidase homologs (RBOHs) that generate controlled ROS bursts—key second messengers for cold signaling, including CBF–COR pathway activation. Additionally, NAD^+ availability modulates ABA-responsive signaling via PARP enzymes, which degrade NAD^+ to regulate gene expression under stress (Feitosa-Araujo et al., 2022). Given B.9's higher ABA baseline (Saini et al., 2025), a synergistic feedback loop may exist: ABA enhances RBOH-mediated ROS, while NAD pathway activity maintains redox balance and signaling continuity. Beyond defense, NADPH also supports cold-responsive lipid remodeling. NADPH-dependent biosynthesis of carotenoids and unsaturated fatty acids preserves membrane fluidity and structural stability during freezing (Hong et al., 2020). Thus, NAD metabolism in B.9 appears to underpin a multifaceted frost adaptation strategy—supporting antioxidant defense, membrane remodeling, and ABA-ROS crosstalk to stabilize cellular function under cold stress.

3.2 Comprehensive Tissue-Level Metabolomics of Gala on M.26 Under Frost Stress

3.2.1 Shifts in Primary Carbon and Amino-Acid Pools

Cold exposure in M.26 floral buds induced significant increases in upstream phenylpropanoid intermediates, including phenylalanine, cinnamic acid (CA), and serine. Elevated CA, produced via phenylalanine ammonia-lyase (PAL), suggests a breakdown in normal metabolic coordination despite PAL enrichment, stalling full phenylpropanoid flux (Liu et al., 2021). CA, a known autotoxic compound (Wu et al., 2008; Huang et al., 2013), can promote membrane peroxidation, increase reactive oxygen species (ROS), and compromise cell integrity (Ye et al., 2006; Wu et al., 2015). Its frost-induced accumulation in M.26 may contribute to oxidative stress and impaired cellular function in this cold-susceptible genotype. Furthermore, CA interferes with photosynthetic pigment synthesis, PSII integrity, and inhibits Calvin cycle enzymes, thereby suppressing CO_2 assimilation (Lyu et al., 2022; Raines 2003; Maghsoudi et al., 2013; Yang et al., 2019). CA also elevates oxidative stress markers (lipid peroxidation, ion leakage) and triggers antioxidant enzymes, which in M.26 could indicate maladaptive ROS buildup and compromised antioxidant homeostasis (Singh et al., 2013). Serine enrichment in M.26 floral buds further highlights disrupted stress physiology. Beyond its proteinogenic role, serine is central to one-carbon metabolism, membrane lipid biosynthesis (Kishor et al., 2020) and acts as a metabolic signal influencing gene expression via photorespiratory flux regulation (Timm et al., 2013). Cold disrupts photorespiration, and post-frost serine accumulation in M.26 suggests compromised photorespiratory balance and inefficient nitrogen recycling, failing to route serine into protective metabolites or engage stress mitigation pathways (Fu et al., 2023). Elevated serine also affects RNA splicing by modulating serine/arginine-rich (SR) proteins (Palusa et al., 2010), potentially contributing to faulty splicing of stress-responsive transcripts and compromising cold tolerance pathway activation.

3.2.2 Perturbation of Indole- and Phenylpropanoid-Derived Pathways

In our study, indoline was significantly enriched in M.26 floral buds following natural frost exposure. Indoline belongs to a broader class of indole compounds that serve as metabolic precursors to various indole derivatives, including indole-3-acetic acid (IAA), which is a key hormone regulating plant growth and development and is involved in stress responses (Tang et al., 2023). The accumulation of indoline in M.26 flowers suggests an upstream activation of indole biosynthesis pathways, likely driven by frost-induced stress cues. This metabolic bottleneck implies impaired activity in IAA biosynthetic branches such as the indole-3-pyruvic acid (IPA), indole-3-acetamide (IAM), or indole-3-acetonitrile (IAN) pathways, possibly due to suppressed expression of key enzymes like Yucca family (YUC) flavin monooxygenases (Figueredo et al., 2023). Moreover, indole metabolism is linked with cold-responsive signaling and defense priming. Indole-derived compounds such as glucosinolates and melatonin activate MAPK cascades, enhance ROS scavenging via enzymes like SOD, CAT, and APX, and contribute to systemic acquired resistance (Sun et al., 2023). The accumulation of indoline, without downstream conversion into these effectors, may indicate a failed attempt at biochemical fortification, leaving M.26 buds metabolically active but insufficiently defended—a scenario consistent with its high bud mortality phenotype.

3.2.3 Depletion of Structural Phospholipids and Derived Signallers

The pronounced downregulation of key phosphatidylcholine (PC) species—PC(p-16:0), PC(20:0) and dilinoleoylphosphatidylcholine—in M.26 floral buds after frost likely reflects a breakdown in membrane integrity and impaired lipid signaling capacity. While moderate reductions in PC content can be part of adaptive membrane remodeling, especially during cold acclimation, the steep decline observed in M.26 may instead reflect a stress-induced depletion, unaccompanied by compensatory increases in downstream lipid signaling products such as lysophospholipids (LPC, LPA) or phosphatidic acid (PA). Phosphatidylcholines (PCs) are not only structural components of membranes but also precursors for stress signaling lipids produced via phospholipase D (PLD) and phospholipase C (PLC)-mediated hydrolysis pathways, which generate Phosphatidic acid (PA) and diacylglycerol (DAG), respectively—central players in ABA, ROS, and calcium-mediated stress signaling (Hou et al., 2016). In contrast to tolerant rootstocks like B.9, where coordinated lipid remodeling may support membrane stabilization and signaling under stress, M.26 may lack the necessary metabolic buffering or compensatory activation of protective lipid cascades. For example, the loss of PC, which is rich in linoleic acid residues, may reduce the pool of esterified fatty acid substrates available for lipoxygenase (LOX)-mediated oxidation—thereby impairing the initiation of jasmonate biosynthesis and oxidative signaling cascades (Welti et al., 2002; Scherer et al., 2002; Savchenko et al., 2014). Similarly, reduced PC pools could impair the generation of lysophospholipids such as lysophosphatidylcholine (LPC), which have been shown to modulate plasma membrane H^+-ATPase activity, influence auxin responses, and induce cytosolic pH shifts—processes relevant under freezing stress conditions (Viehweger et al., 2002; Scherer, 2002; Wi et al., 2014). Without these lipid intermediates, M.26 buds may struggle to maintain membrane repair, vesicle trafficking, or intracellular signaling during frost stress.

A parallel disruption was observed in the ‘Gala’ scion leaves grafted on M.26, where frost exposure triggered the upregulation of monoacylglycerol MG (20:4-2-OH/0:0/0:0) and lysophosphatidic acid [Lyso(PA)], alongside the downregulation of the hydroxy fatty acid 10-hydroxy-10-methyloctadecanoic acid. Notably, Lyso(PA) increased significantly, signaling the onset of lipid turnover processes. However, rather than indicating effective remodeling, this pattern could suggest uncoordinated membrane disassembly— could be as a passive consequence of frost-induced damage. The apparent failure to convert Lyso(PA) into downstream phospholipids or integrate it into stable membrane restructuring may reflect a bottleneck in lipid utilization.

Building on these phospholipid-related disruptions observed in ‘Gala’ grafted on M.26 floral buds, further evidence of a disjointed stress response was found in the scion leaves of ‘Gala’ on the same rootstock following frost exposure. These scion leaves exhibited a markedly different metabolic reprogramming profile, characterized by the prominent enrichment of antioxidant and redox-regulating pathways. Most notably, glutathione metabolism emerged as the most significantly enriched pathway, displaying the highest enrichment ratio among all detected metabolic sets. However, rather than indicating an efficient or protective adaptation, this pattern more plausibly reflects a dysregulated or maladaptive stress response specific to M.26. Glutathione (GSH), a tripeptide composed of glutamate, cysteine, and glycine, functions as a redox buffer, detoxifying hydrogen peroxide and other ROS via the ascorbate–glutathione cycle (Noctor et al., 2024). This hyperaccumulation may interrupt redox-sensitive signaling cascades required for cold-induced gene expression. Imbalanced ROS/GSH may result from a direct increase of ROS, consumption of GSH, intracellular oxidoreductase interference, or thioredoxin activity reduction (Liu et al., 2022). By damping the amplitude of ROS signal, the scion may fail to activate the CBF–COR regulon or engage hormonal cross-talks needed for acclimation.

In tandem with this redox imbalance, syringic acid, a phenylpropanoid-derived hydroxybenzoic acid (4-hydroxy-3,5-dimethoxybenzoic acid), was also significantly upregulated in M.26 scion leaves after frost, with strong support from both *t*-test and enrichment plots. Syringic acid, a hydroxybenzoic acid derivative (4-hydroxy-3,5-dimethoxybenzoic acid), is biosynthesized via the phenylpropanoid pathway from phenylalanine through sinapic acid, followed by methylation steps (Vo et al., 2020; Shimsa et al., 2024). Its post-frost enrichment in ‘Gala’ scion leaves on M.26 suggests a metabolically triggered attempt to buffer oxidative stress, likely due to ROS overaccumulation caused by frost-induced disruption of chloroplasts and cellular membranes.

4 Conclusion

Following frost exposure, the cold-tolerant rootstock B.9 showed strong tissue-specific metabolic responses that are consistent with known cold-protective strategies. In floral buds of Gala on B.9, we observed activation of antioxidant defense pathways such as ascorbate and aldarate metabolism, which are important for reducing oxidative stress. In Gala scion leaves on B.9, several protective sugars like trehalose and melibiose increased after frost, alongside enrichment of arginine biosynthesis pathways, which may help stabilize proteins and support osmotic balance. In B.9 sucker leaves, there was clear upregulation of starch and sucrose metabolism, nicotinate and nicotinamide metabolism, and arginine-related compounds, suggesting roles in energy supply, redox buffering, and stress signaling. In contrast, the cold-susceptible rootstock M.26 followed a different pattern in each tissue. Gala floral buds on M.26 showed increased levels of phenylpropanoid compounds and membrane-associated lipids, pointing to stress-related cell wall or membrane changes. Gala scion leaves had strong enrichment of glutathione metabolism, indicating a redox imbalance and possible oxidative stress. Sucker leaves in M.26 showed signs of disrupted sugar metabolism that might have reduced lipid stability. While each tissue and rootstock responded independently, these patterns together suggest that B.9 maintains a more balanced and protective metabolite profile after frost, while M.26 displays stress-associated changes that may reflect lower cold tolerance.

Supplementary Data

https://github.com/Amolpreet1/Supplementary/blob/acb22a60edc6e16b013c3d8d6fb91b8df203ca76/Supplementary%20Link.docx

https://github.com/Amolpreet1/Supplementary/blob/acb22a60edc6e16b013c3d8d6fb91b8df203ca76/Active%2CRepressB9Flowers.xlsx

https://github.com/Amolpreet1/Supplementary/blob/acb22a60edc6e16b013c3d8d6fb91b8df203ca76/Active%2CRepressM26Flowers.xlsx

https://github.com/Amolpreet1/Supplementary/blob/acb22a60edc6e16b013c3d8d6fb91b8df203ca76/ActiveRepressScionLeafB9.xlsx

https://github.com/Amolpreet1/Supplementary/blob/acb22a60edc6e16b013c3d8d6fb91b8df203ca76/ActiveRepressScionLeafM26.xlsx

https://github.com/Amolpreet1/Supplementary/blob/acb22a60edc6e16b013c3d8d6fb91b8df203ca76/ActiveRepressSuckerB9.xlsx

https://github.com/Amolpreet1/Supplementary/blob/acb22a60edc6e16b013c3d8d6fb91b8df203ca76/ActiveRepressSuckerM26.xlsx

References

Adolf, A., Liu, L., Ackah, M., Li, Y., Du, Q., Zheng, D., Guo, P., Shi, Y., Lin, Q., Qiu, C., & Zhao, W. (2021). Transcriptome profiling reveals candidate genes associated with cold stress in mulberry. *Brazilian Journal of Botany*, *44*(1), 125–137. https://doi.org/10.1007/s40415-020-00680-x

Akram, N. A., Shafiq, F., & Ashraf, M. (2017). Ascorbic Acid-A Potential Oxidant Scavenger and Its Role in Plant Development and Abiotic Stress Tolerance. *Frontiers in Plant Science*, *8*. https://doi.org/10.3389/fpls.2017.00613

An, J.-P., Li, R., Qu, F.-J., You, C.-X., Wang, X.-F., & Hao, Y.-J. (2018). R2R3-MYB transcription factor MdMYB23 is involved in the cold tolerance and proanthocyanidin accumulation in apple. *The Plant Journal*, *96*(3), 562–577. https://doi.org/10.1111/tpj.14050

An, J.-P., Wang, X.-F., Zhang, X.-W., You, C.-X., & Hao, Y.-J. (2021). Apple B-box protein BBX37 regulates jasmonic acid mediated cold tolerance through the JAZ-BBX37-ICE1-CBF pathway and undergoes MIEL1-mediated ubiquitination and degradation. *New Phytologist*, *229*(5), 2707–2729. https://doi.org/10.1111/nph.17050

Bai, C., Fang, M., Zhai, B., Ma, L., Fu, A., Gao, L., Kou, X., Meng, D., Wang, Q., Zheng, S., & Zuo, J. (2021). Regulations of m6A methylation on tomato fruit chilling injury. *Horticultural Plant Journal*, *7*(5), 434–442. https://doi.org/10.1016/j.hpj.2021.05.005

Barding, G. A. Jr., Fukao, T., Béni, S., Bailey-Serres, J., & Larive, C. K. (2012). Differential Metabolic Regulation Governed by the Rice SUB1A Gene during Submergence Stress and Identification of Alanylglycine by 1H NMR Spectroscopy. *Journal of Proteome Research*, *11*(1), 320–330. https://doi.org/10.1021/pr200919b

Barzegar, T., Najafi, R., Razavi, F., & Ghahremani, Z. (2021). Hydrogen sulfide and phenylalanine alleviate chilling injury in eggplant fruits during cold storage by enhancing antioxidant activities and membrane stability. *Journal of Food Processing and Preservation*, *45*(11), e15933. https://doi.org/10.1111/jfpp.15933

Becker, J. van W. (n.d.). *Evaluation of the role of PGIPs in plant defense responses*.

Benina, M., Obata, T., Mehterov, N., Ivanov, I., Petrov, V., Toneva, V., Fernie, A., & Gechev, T. S. (2013). Comparative metabolic profiling of Haberlea rhodopensis, Thellungiella halophyla, and Arabidopsis thaliana exposed to low temperature. *Frontiers in Plant Science*, *4*. https://doi.org/10.3389/fpls.2013.00499

Berg-Falloure, K. M., & Kolomiets, M. V. (2023). Ketols Emerge as Potent Oxylipin Signals Regulating Diverse Physiological Processes in Plants. *Plants*, *12*(11), Article 11. https://doi.org/10.3390/plants12112088

Bernard, A., Domergue, F., Pascal, S., Jetter, R., Renne, C., Faure, J.-D., Haslam, R. P., Napier, J. A., Lessire, R., & Joubès, J. (2012). Reconstitution of plant alkane biosynthesis in yeast demonstrates that Arabidopsis ECERIFERUM1 and ECERIFERUM3 are core components of a very-long-chain alkane synthesis complex. *The Plant Cell*, *24*(7), 3106–3118. https://doi.org/10.1105/tpc.112.099796

Brizzolara, S., Hertog, M., Tosetti, R., Nicolai, B., & Tonutti, P. (2018). Metabolic Responses to Low Temperature of Three Peach Fruit Cultivars Differently Sensitive to Cold Storage. *Frontiers in Plant Science*, *9*. https://doi.org/10.3389/fpls.2018.00706

Brunetti, C., George, R. M., Tattini, M., Field, K., & Davey, M. P. (2013). Metabolomics in plant environmental physiology. *Journal of Experimental Botany*, *64*(13), 4011–4020. https://doi.org/10.1093/jxb/ert244

Castro-Camba, R., Sánchez, C., Vidal, N., & Vielba, J. M. (2022). Interactions of Gibberellins with Phytohormones and Their Role in Stress Responses. *Horticulturae*, *8*(3), Article 3. https://doi.org/10.3390/horticulturae8030241

Chai, F., Liu, W., Xiang, Y., Meng, X., Sun, X., Cheng, C., Liu, G., Duan, L., Xin, H., & Li, S. (2019). Comparative metabolic profiling of Vitis amurensis and Vitis vinifera during cold acclimation. *Horticulture Research*, *6*(1), 1–12. https://doi.org/10.1038/s41438-018-0083-5

Chaudhuri, S., Banerjee, A., Basu, K., Sengupta, B., & Sengupta, P. K. (2007). Interaction of flavonoids with red blood cell membrane lipids and proteins: Antioxidant and antihemolytic effects. *International Journal of Biological Macromolecules*, *41*(1), 42–48. https://doi.org/10.1016/j.ijbiomac.2006.12.003

Cheng, H., Chen, X., Fang, J., An, Z., Hu, Y., & Huang, H. (2018). Comparative transcriptome analysis reveals an early gene expression profile that contributes to cold resistance in Hevea brasiliensis (the Para rubber tree). *Tree Physiology*, *38*(9), 1409–1423. https://doi.org/10.1093/treephys/tpy014

Cheng, Y., Ban, Q., Mao, J., Lin, M., Zhu, X., Xia, Y., Cao, X., Zhang, X., & Li, Y. (2023). Integrated Metabolomic and Transcriptomic Analysis Reveals That Amino Acid Biosynthesis May Determine Differences in Cold-Tolerant and Cold-Sensitive Tea Cultivars. *International Journal of Molecular Sciences*, *24*(3), Article 3. https://doi.org/10.3390/ijms24031907

Chitarra, W., Perrone, I., Avanzato, C. G., Minio, A., Boccacci, P., Santini, D., Gilardi, G., Siciliano, I., Gullino, M. L., Delledonne, M., Mannini, F., & Gambino, G. (2017). Grapevine Grafting: Scion Transcript Profiling and Defense-Related Metabolites Induced by Rootstocks. *Frontiers in Plant Science*, *8*. https://doi.org/10.3389/fpls.2017.00654

Cook, D., Fowler, S., Fiehn, O., & Thomashow, M. F. (2004). A prominent role for the CBF cold response pathway in configuring the low-temperature metabolome of Arabidopsis. *Proceedings of the National Academy of Sciences*, *101*(42), 15243–15248. https://doi.org/10.1073/pnas.0406069101

Crosatti, C., Rizza, F., Badeck, F. W., Mazzucotelli, E., & Cattivelli, L. (2013). Harden the chloroplast to protect the plant. *Physiologia Plantarum*, *147*(1), 55–63. https://doi.org/10.1111/j.1399-3054.2012.01689.x

Dahlin, J., Holkenbrink, C., Marella, E. R., Wang, G., Liebal, U., Lieven, C., Weber, D., McCloskey, D., Wang, H.-L., Ebert, B. E., Herrgård, M. J., Blank, L. M., & Borodina, I. (2019). Multi-Omics Analysis of Fatty Alcohol Production in Engineered Yeasts Saccharomyces cerevisiae and Yarrowia lipolytica. *Frontiers in Genetics*, *10*, 747. https://doi.org/10.3389/fgene.2019.00747

Demarque, D. P., Dusi, R. G., de Sousa, F. D. M., Grossi, S. M., Silvério, M. R. S., Lopes, N. P., & Espindola, L. S. (2020). Mass spectrometry-based metabolomics approach in the isolation of bioactive natural products. *Scientific Reports*, *10*(1), 1051. https://doi.org/10.1038/s41598-020-58046-y

Dong, S., & Beckles, D. M. (2019). Dynamic changes in the starch-sugar interconversion within plant source and sink tissues promote a better abiotic stress response. *Journal of Plant Physiology*, *234–235*, 80–93. https://doi.org/10.1016/j.jplph.2019.01.007

Effendi, Y., Radatz, K., Labusch, C., Rietz, S., Wimalasekera, R., Helizon, H., Zeidler, M., & Scherer, G. F. E. (2014). Mutants of phospholipase A (pPLA-I) have a red light and auxin phenotype. *Plant, Cell & Environment*, *37*(7), 1626–1640. https://doi.org/10.1111/pce.12278

Feitosa-Araujo, E., da Fonseca-Pereira, P., Knorr, L. S., Schwarzländer, M., & Nunes-Nesi, A. (2022). NAD meets ABA: Connecting cellular metabolism and hormone signaling. *Trends in Plant Science*, *27*(1), 16–28. https://doi.org/10.1016/j.tplants.2021.07.011

Figueredo, E. F., Cruz, T. A. da, Almeida, J. R. de, Batista, B. D., Marcon, J., Andrade, P. A. M. de, Hayashibara, C. A. de A., Rosa, M. S., Azevedo, J. L., & Quecine, M. C. (2023). The key role of indole-3-acetic acid biosynthesis by *Bacillus thuringiensis* RZ2MS9 in promoting maize growth revealed by the *ipd*C gene knockout mediated by the CRISPR-Cas9 system. *Microbiological Research*, *266*, 127218. https://doi.org/10.1016/j.micres.2022.127218

Foyer, C. H., & Kunert, K. (2024). The ascorbate–glutathione cycle coming of age. *Journal of Experimental Botany*, *75*(9), 2682–2699. https://doi.org/10.1093/jxb/erae023

Fu, X., Gregory, L. M., Weise, S. E., & Walker, B. J. (2023). Integrated flux and pool size analysis in plant central metabolism reveals unique roles of glycine and serine during photorespiration. *Nature Plants*, *9*(1), 169–178. https://doi.org/10.1038/s41477-022-01294-9

Fürtauer, L., Weiszmann, J., Weckwerth, W., & Nägele, T. (2019). Dynamics of Plant Metabolism during Cold Acclimation. *International Journal of Molecular Sciences*, *20*(21), Article 21. https://doi.org/10.3390/ijms20215411

Gainza, F., Opazo, I., & Muñoz, C. (2015). Graft incompatibility in plants: Metabolic changes during formation and establishment of the rootstock/scion union with emphasis on Prunus species. *Chilean Journal of Agricultural Research*, *75*, 28–34. https://doi.org/10.4067/S0718-58392015000300004

Gao, C., Mumtaz, M. A., Zhou, Y., Yang, Z., Shu, H., Zhu, J., Bao, W., Cheng, S., Yin, L., Huang, J., & Wang, Z. (2022). Integrated Transcriptomic and Metabolomic Analyses of Cold-Tolerant and Cold-Sensitive Pepper Species Reveal Key Genes and Essential Metabolic Pathways Involved in Response to Cold Stress. *International Journal of Molecular Sciences*, *23*(12), Article 12. https://doi.org/10.3390/ijms23126683

Gao, C., Sheteiwy ,Mohamed S., Han ,Jiajun, Dong ,Zhaorong, Pan ,Ronghui, Guan ,Yajing, Alhaj Hamoud ,Yousef, & and Hu, J. (2020). Polyamine biosynthetic pathways and their relation with the cold tolerance of maize (Zea mays L.) seedlings. *Plant Signaling & Behavior*, *15*(11), 1807722. https://doi.org/10.1080/15592324.2020.1807722

Gong, Z., Xiong, L., Shi, H., Yang, S., Herrera-Estrella, L. R., Xu, G., Chao, D.-Y., Li, J., Wang, P.-Y., Qin, F., Li, J., Ding, Y., Shi, Y., Wang, Y., Yang, Y., Guo, Y., & Zhu, J.-K. (2020). Plant abiotic stress response and nutrient use efficiency. *Science China Life Sciences*, *63*(5), 635–674. https://doi.org/10.1007/s11427-020-1683-x

Grechkin, A. N. (2002). Hydroperoxide lyase and divinyl ether synthase. *Prostaglandins & Other Lipid Mediators*, *68–69*, 457–470. https://doi.org/10.1016/S0090-6980(02)00048-5

Gu, S., Huang, X., Xu, X., Liu, Y., Khoong, Y., Zhang, Z., Li, H., Gao, Y., & Zan, T. (2021). Inhibition of CUB and sushi multiple domains 1 (CSMD1) expression by miRNA-190a-3p enhances hypertrophic scar-derived fibroblast migration in vitro. *BMC Genomics*, *22*(1), 613. https://doi.org/10.1186/s12864-021-07920-8

Guerra, D., Lamontanara, A., Bagnaresi, P., Orrù, L., Rizza, F., Zelasco, S., Beghè, D., Ganino, T., Pagani, D., Cattivelli, L., & Mazzucotelli, E. (2015). Transcriptome changes associated with cold acclimation in leaves of olive tree (Olea europaea L.). *Tree Genetics & Genomes*, *11*(6), 113. https://doi.org/10.1007/s11295-015-0939-x

Hannah, M. A., Wiese, D., Freund, S., Fiehn, O., Heyer, A. G., & Hincha, D. K. (2006). Natural Genetic Variation of Freezing Tolerance in Arabidopsis. *Plant Physiology*, *142*(1), 98–112. https://doi.org/10.1104/pp.106.081141

Harris, Z. N., Pratt, J. E., Kovacs, L. G., Klein, L. L., Kwasniewski, M. T., Londo, J. P., Wu, A. S., & Miller, A. J. (2023). Grapevine scion gene expression is driven by rootstock and environment interaction. *BMC Plant Biology*, *23*, 211. https://doi.org/10.1186/s12870-023-04223-w

Hong, Y., Wang, Z., Shi, H., Yao, J., Liu, X., Wang, F., Zeng, L., Xie, Z., & Zhu, J.-K. (2020). Reciprocal regulation between nicotinamide adenine dinucleotide metabolism and abscisic acid and stress response pathways in Arabidopsis. *PLOS Genetics*, *16*(6), e1008892. https://doi.org/10.1371/journal.pgen.1008892

Hou, Q., Ufer, G., & Bartels, D. (2016). Lipid signalling in plant responses to abiotic stress. *Plant, Cell & Environment*, *39*(5), 1029–1048. https://doi.org/10.1111/pce.12666

Huang, L. S., Kim, M. R., & Sok, D.-E. (2006). Linoleoyl lysophosphatidylcholine is an efficient substrate for soybean lipoxygenase-1. *Archives of Biochemistry and Biophysics*, *455*(2), 119–126. https://doi.org/10.1016/j.abb.2006.09.015

Huang, L.-F., Song, L.-X., Xia, X.-J., Mao, W.-H., Shi, K., Zhou, Y.-H., & Yu, J.-Q. (2013). Plant-soil feedbacks and soil sickness: From mechanisms to application in agriculture. *Journal of Chemical Ecology*, *39*(2), 232–242. https://doi.org/10.1007/s10886-013-0244-9

Huang, X., Cao, L., Fan, J., Ma, G., & Chen, L. (2022). CdWRKY2-mediated sucrose biosynthesis and CBF-signalling pathways coordinately contribute to cold tolerance in bermudagrass. *Plant Biotechnology Journal*, *20*(4), 660–675. https://doi.org/10.1111/pbi.13745

Huang, Y., Sun, L., Wang, J., Chen, Y., He, J., & Lyu, D. (2023). Rootstock–scion interaction affects Malus transcriptome profiles in response to cadmium. *Scientific Data*, *10*(1), 312. https://doi.org/10.1038/s41597-023-02239-3

Hudina, M., Orazem, P., Jakopic, J., & Stampar, F. (2014). The phenolic content and its involvement in the graft incompatibility process of various pear rootstocks (*Pyrus communis* L.). *Journal of Plant Physiology*, *171*(5), 76–84. https://doi.org/10.1016/j.jplph.2013.10.022

Human Metabolome Database: Showing metabocard for 1,1'-[1,11-Undecanediylbis(oxy)]bisbenzene (HMDB0039762). (n.d.). Retrieved June 20, 2025, from https://hmdb.ca/metabolites/HMDB0039762

Hwarari, D., Guan, Y., Ahmad, B., Movahedi, A., Min, T., Hao, Z., Lu, Y., Chen, J., & Yang, L. (2022). ICE-CBF-COR Signaling Cascade and Its Regulation in Plants Responding to Cold Stress. *International Journal of Molecular Sciences*, *23*(3), Article 3. https://doi.org/10.3390/ijms23031549

Ivanov, B. N. (2014). Role of ascorbic acid in photosynthesis. *Biochemistry. Biokhimiia*, *79*(3), 282–289. https://doi.org/10.1134/S0006297914030146

Jahed, K. R., Saini, A. K., & Sherif, S. M. (2023). Coping with the cold: Unveiling cryoprotectants, molecular signaling pathways, and strategies for cold stress resilience. *Frontiers in Plant Science*, *14*. https://doi.org/10.3389/fpls.2023.1246093

Jin, C., Li, K.-Q., Xu, X.-Y., Zhang, H.-P., Chen, H.-X., Chen, Y.-H., Hao, J., Wang, Y., Huang, X.-S., & Zhang, S.-L. (2017). A Novel NAC Transcription Factor, PbeNAC1, of Pyrus betulifolia Confers Cold and Drought Tolerance via Interacting with PbeDREBs and Activating the Expression of Stress-Responsive Genes. *Frontiers in Plant Science*, *8*. https://doi.org/10.3389/fpls.2017.01049

Kaplan, F., & Guy, C. L. (2004). β-Amylase Induction and the Protective Role of Maltose during Temperature Shock. *Plant Physiology*, *135*(3), 1674–1684. https://doi.org/10.1104/pp.104.040808

Kavi Kishor, P. B., Suravajhala, R., Guddimalli, R., Marka, N., Kavya Shridhar, K., Divya, D., Scinthia, K. P., Divya, K., Doma, M., Edupuganti, S., Suravajhala, P. N., & Polavarapu, R. (2020). Lysine, Lysine-Rich, Serine, and Serine-Rich Proteins: Link Between Metabolism, Development, and Abiotic Stress Tolerance and the Role of ncRNAs in Their Regulation. *Frontiers in Plant Science*, *11*. https://doi.org/10.3389/fpls.2020.546213

Khan, M., Hu, J., Dahro, B., Ming, R., Zhang, Y., Wang, Y., Alhag, A., Li, C., & Liu, J.-H. (2021). ERF108 from Poncirus trifoliata (L.) Raf. Functions in cold tolerance by modulating raffinose synthesis through transcriptional regulation of PtrRafS. *The Plant Journal*, *108*(3), 705–724. https://doi.org/10.1111/tpj.15465

Kolesnikov, Y. S., Kretynin, S. V., Filepova, R., Dobrev, P. I., Martinec, J., & Kravets, V. S. (2024). Polyamines metabolism and their biological role in plant cells: What do we really know? *Phytochemistry Reviews*, *23*(4), 997–1026. https://doi.org/10.1007/s11101-024-09913-3

Kou, S., Chen, L., Tu, W., Scossa, F., Wang, Y., Liu, J., Fernie, A. R., Song, B., & Xie, C. (2018). The arginine decarboxylase gene ADC1, associated to the putrescine pathway, plays an important role in potato cold-acclimated freezing tolerance as revealed by transcriptome and metabolome analyses. *The Plant Journal: For Cell and Molecular Biology*, *96*(6), 1283–1298. https://doi.org/10.1111/tpj.14126

Krasensky, J., & Jonak, C. (2012). Drought, salt, and temperature stress-induced metabolic rearrangements and regulatory networks. *Journal of Experimental Botany*, *63*(4), 1593–1608. https://doi.org/10.1093/jxb/err460

Lee, S. B., & Suh, M. C. (2013). Recent Advances in Cuticular Wax Biosynthesis and Its Regulation in Arabidopsis. *Molecular Plant*, *6*(2), 246–249. https://doi.org/10.1093/mp/sss159

Lee, S. B., & Suh, M. C. (2022). Regulatory mechanisms underlying cuticular wax biosynthesis. *Journal of Experimental Botany*, *73*(9), 2799–2816. https://doi.org/10.1093/jxb/erab509

Lee, Y., Hoang, N. V., Do, V. G., Foster, T. M., McGhie, T. K., Kim, S., Yang, S. J., Park, J.-H., Park, J., & Lee, J.-Y. (2023). Identification of genes associated with the regulation of cold tolerance and the RNA movement in the grafted apple. *Scientific Reports*, *13*(1), 11583. https://doi.org/10.1038/s41598-023-38571-2

Lemtiri-Chlieh, F., MacRobbie, E. A. C., Webb, A. A. R., Manison, N. F., Brownlee, C., Skepper, J. N., Chen, J., Prestwich, G. D., & Brearley, C. A. (2003). Inositol hexakisphosphate mobilizes an endomembrane store of calcium in guard cells. *Proceedings of the National Academy of Sciences of the United States of America*, *100*(17), 10091–10095. https://doi.org/10.1073/pnas.1133289100

Li, F., Lu, X., Duan, P., Liang, Y., & Cui, J. (2021). Integrating transcriptome and metabolome analyses of the response to cold stress in pumpkin (Cucurbita maxima). *PLOS ONE*, *16*(5), e0249108. https://doi.org/10.1371/journal.pone.0249108

Li, H., Ding, Y., Shi, Y., Zhang, X., Zhang, S., Gong, Z., & Yang, S. (2017). MPK3- and MPK6-Mediated ICE1 Phosphorylation Negatively Regulates ICE1 Stability and Freezing Tolerance in Arabidopsis. *Developmental Cell*, *43*(5), 630-642.e4. https://doi.org/10.1016/j.devcel.2017.09.025

Li, J., Yu, Q., Liu, C., Zhang, N., & Xu, W. (2025). Flavonoids as key players in cold tolerance: Molecular insights and applications in horticultural crops. *Horticulture Research*, *12*(4), uhae366. https://doi.org/10.1093/hr/uhae366

Li, W., Li, M., Zhang, W., Welti, R., & Wang, X. (2004). The plasma membrane-bound phospholipase Ddelta enhances freezing tolerance in Arabidopsis thaliana. *Nature Biotechnology*, *22*(4), 427–433. https://doi.org/10.1038/nbt949

Li, Y., Tian, Q., Wang, Z., Li, J., Liu, S., Chang, R., Chen, H., & Liu, G. (2023). Integrated analysis of transcriptomics and metabolomics of peach under cold stress. *Frontiers in Plant Science*, *14*. https://doi.org/10.3389/fpls.2023.1153902

Liang, C., Lü, J., Jin, M., Li, H., & Rao, J. (2017). Effects of oxalic acid treatment on chilling injury, antioxidant capacity and energy status in harvested kiwifruits under low temperature stress. *Acta Horticulturae Sinica*, *44*(2), 279–287. Scopus. https://doi.org/10.16420/j.issn.0513-353x.2016-0451

Lin, S.-T., Chiou, C.-W., Chu, Y.-L., Hsiao, Y., Tseng, Y.-F., Chen, Y.-C., Chen, H.-J., Chang, H.-Y., & Lee, T.-M. (2016). Enhanced Ascorbate Regeneration Via Dehydroascorbate Reductase Confers Tolerance to Photo-Oxidative Stress in Chlamydomonas reinhardtii. *Plant & Cell Physiology*, *57*(10), 2104–2121. https://doi.org/10.1093/pcp/pcw129

Lingner, U., Münch, S., Sode, B., Deising, H. B., & Sauer, N. (n.d.). *Functional Characterization of a Eukaryotic Melibiose Transporter*. Retrieved June 8, 2025, from https://dx.doi.org/10.1104/pp.111.178624

Liu, B., Wang, X.-Y., Cao, Y., Arora, R., Zhou, H., & Xia, Y.-P. (2020). Factors affecting freezing tolerance: A comparative transcriptomics study between field and artificial cold acclimations in overwintering evergreens. *The Plant Journal*, *103*(6), 2279–2300. https://doi.org/10.1111/tpj.14899

Liu, G., Zhang, Z., Tian, Y., Yang, J., Xu, X., & Liu, X. (2025). VvbZIP22 regulates quercetin synthesis to enhances cold resistance in grape. *Plant Science*, *350*, 112293. https://doi.org/10.1016/j.plantsci.2024.112293

Liu, H., Wang, F., Liu, B., Kong, F., & Fang, C. (2024). Significance of Raffinose Family Oligosaccharides (RFOs) metabolism in plants. *Advanced Biotechnology*, *2*(2), 13. https://doi.org/10.1007/s44307-024-00022-y

Liu, J.-H., Kitashiba, H., Wang, J., Ban, Y., & Moriguchi, T. (2007). Polyamines and their ability to provide environmental stress tolerance to plants. *Plant Biotechnology*, *24*(1), 117–126. https://doi.org/10.5511/plantbiotechnology.24.117

Liu, T., Sun, L., Zhang, Y., Wang, Y., & Zheng, J. (2022). Imbalanced GSH/ROS and sequential cell death. *Journal of Biochemical and Molecular Toxicology*, *36*(1), e22942. https://doi.org/10.1002/jbt.22942

Liu, T., Ye, X., Li, M., Li, J., Qi, H., & Hu, X. (2020). H2O2 and NO are involved in trehalose-regulated oxidative stress tolerance in cold-stressed tomato plants. *Environmental and Experimental Botany*, *171*, 103961. https://doi.org/10.1016/j.envexpbot.2019.103961

Liu, W., Feng, Y., Yu, S., Fan, Z., Li, X., Li, J., & Yin, H. (2021). The Flavonoid Biosynthesis Network in Plants. *International Journal of Molecular Sciences*, *22*(23), Article 23. https://doi.org/10.3390/ijms222312824

Liu, Y., Dang, P., Liu, L., & He, C. (2019). Cold acclimation by the CBF–COR pathway in a changing climate: Lessons from Arabidopsis thaliana. *Plant Cell Reports*, *38*(5), 511–519. https://doi.org/10.1007/s00299-019-02376-3

Lu, L., Yang, W., Dong, Z., Tang, L., Liu, Y., Xie, S., & Yang, Y. (2023). Integrated Transcriptomic and Metabolomics Analyses Reveal Molecular Responses to Cold Stress in Coconut (Cocos nucifera L.) Seedlings. *International Journal of Molecular Sciences*, *24*(19), Article 19. https://doi.org/10.3390/ijms241914563

Lyu, J., Jin, L., Meng, X., Jin, N., Wang, S., Hu, L., Zhang, G., Wu, Y., Luo, S., & Yu, J. (2022). Exogenous Si Mitigates the Effects of Cinnamic-Acid-Induced Stress by Regulating Carbon Metabolism and Photosynthetic Pigments in Cucumber Seedlings. *Agronomy*, *12*(7), Article 7. https://doi.org/10.3390/agronomy12071569

Ma, S., Sun, L., Sui, X., Li, Y., Chang, Y., Fan, J., & Zhang, Z. (2019). Phloem loading in cucumber: Combined symplastic and apoplastic strategies. *The Plant Journal: For Cell and Molecular Biology*, *98*(3), 391–404. https://doi.org/10.1111/tpj.14224

Maccarrone, M., van Aarle, P. G. M., Veldink, G. A., & Vliegenthart, J. F. G. (1994). In vitro oxygenation of soybean biomembranes by lipoxygenase-2. *Biochimica et Biophysica Acta (BBA) - Biomembranes*, *1190*(1), 164–169. https://doi.org/10.1016/0005-2736(94)90046-9

Maghsoudi, K., Emam ,Yahya, & and Pessarakli, M. (2016). Effect of silicon on photosynthetic gas exchange, photosynthetic pigments, cell membrane stability and relative water content of different wheat cultivars under drought stress conditions. *Journal of Plant Nutrition*, *39*(7), 1001–1015. https://doi.org/10.1080/01904167.2015.1109108

Marè, C., Aprile ,Alessio, Roncaglia ,Enrica, Tocci ,Emanuele, Corino ,Lorenzo Giuseppe, De Bellis ,Luigi, & and Cattivelli, L. (2013). Rootstock and soil induce transcriptome modulation of phenylpropanoid pathway in grape leaves. *Journal of Plant Interactions*, *8*(4), 334–349. https://doi.org/10.1080/17429145.2012.754958

Marguerit, E., Brendel, O., Lebon, E., Van Leeuwen, C., & Ollat, N. (2012). Rootstock control of scion transpiration and its acclimation to water deficit are controlled by different genes. *New Phytologist*, *194*(2), 416–429. https://doi.org/10.1111/j.1469-8137.2012.04059.x

Meijer, H. J. G., & Munnik, T. (2003). Phospholipid-based signaling in plants. *Annual Review of Plant Biology*, *54*, 265–306. https://doi.org/10.1146/annurev.arplant.54.031902.134748

Monroe, J. D., Storm, A. R., Badley, E. M., Lehman, M. D., Platt, S. M., Saunders, L. K., Schmitz, J. M., & Torres, C. E. (2014). β-Amylase1 and β-amylase3 are plastidic starch hydrolases in Arabidopsis That Seem to Be Adapted for Different Thermal, pH, and stress conditions. *Plant Physiology*, *166*(4), 1748–1763. https://doi.org/10.1104/pp.114.246421

Nakashima, K., & Yamaguchi-Shinozaki, K. (2006). Regulons involved in osmotic stress-responsive and cold stress-responsive gene expression in plants. *Physiologia Plantarum*, *126*(1), 62–71. https://doi.org/10.1111/j.1399-3054.2005.00592.x

Nievola, C. C., Carvalho ,Camila P., Carvalho ,Victória, & and Rodrigues, E. (2017). Rapid responses of plants to temperature changes. *Temperature*, *4*(4), 371–405. https://doi.org/10.1080/23328940.2017.1377812

Noctor, G., Cohen, M., Trémulot, L., Châtel-Innocenti, G., Van Breusegem, F., & Mhamdi, A. (2024). Glutathione: A key modulator of plant defence and metabolism through multiple mechanisms. *Journal of Experimental Botany*, *75*(15), 4549–4572. https://doi.org/10.1093/jxb/erae194

Owusu Adjei, M., Ma ,Jun, Luo ,Ruixiong, Huang ,Jianfeng, Zhao ,Zhichang, Wang ,Yingying, & and Gao, A. (2023). Transcriptome analyses revealed chilling response genes in mango (Mangifera indica L. cv. Keitt) leaf. *Journal of Plant Interactions*, *18*(1), 2172226. https://doi.org/10.1080/17429145.2023.2172226

Palusa, S. G., Ali, G. S., & Reddy, A. S. N. (2007). Alternative splicing of pre-mRNAs of Arabidopsis serine/arginine-rich proteins: Regulation by hormones and stresses. *The Plant Journal*, *49*(6), 1091–1107. https://doi.org/10.1111/j.1365-313X.2006.03020.x

Peng, T., Zhu, X., Duan, N., & Liu, J.-H. (2014). PtrBAM1, a β-amylase-coding gene of Poncirus trifoliata, is a CBF regulon member with function in cold tolerance by modulating soluble sugar levels. *Plant, Cell & Environment*, *37*(12), 2754–2767. https://doi.org/10.1111/pce.12384

Prodhomme, D., Valls Fonayet, J., Hévin, C., Franc, C., Hilbert, G., de Revel, G., Richard, T., Ollat, N., & Cookson, S. J. (2019). Metabolite profiling during graft union formation reveals the reprogramming of primary metabolism and the induction of stilbene synthesis at the graft interface in grapevine. *BMC Plant Biology*, *19*(1), 599. https://doi.org/10.1186/s12870-019-2055-9

Qian, Z., He, L., & Li, F. (2024). Understanding cold stress response mechanisms in plants: An overview. *Frontiers in Plant Science*, *15*, 1443317. https://doi.org/10.3389/fpls.2024.1443317

Raines, C. A. (2003). The Calvin cycle revisited. *Photosynthesis Research*, *75*(1), 1–10. https://doi.org/10.1023/A:1022421515027

Rani Das, P., Islam, M. T., Liu, J., Liu, Z., Dardick, C., & Sherif, S. M. (2024). Temporal changes in the proanthocyanidins to anthocyanins ratio during dormancy associate with bloom time variations in peach. *Current Plant Biology*, *40*, 100393. https://doi.org/10.1016/j.cpb.2024.100393

Ritonga, F. N., & Chen, S. (2020). Physiological and Molecular Mechanism Involved in Cold Stress Tolerance in Plants. *Plants*, *9*(5), Article 5. https://doi.org/10.3390/plants9050560

Rogowska, A., & Szakiel, A. (2020). The role of sterols in plant response to abiotic stress. *Phytochemistry Reviews*, *19*(6), 1525–1538. https://doi.org/10.1007/s11101-020-09708-2

Rohde, P., Hincha, D. K., & Heyer, A. G. (2004). Heterosis in the freezing tolerance of crosses between two Arabidopsis thaliana accessions (Columbia-0 and C24) that show differences in non-acclimated and acclimated freezing tolerance. *The Plant Journal*, *38*(5), 790–799. https://doi.org/10.1111/j.1365-313X.2004.02080.x

Roy, A., Dutta, R., Kundu, N., Banik, D., & Sarkar, N. (2016). A Comparative Study of the Influence of Sugars Sucrose, Trehalose, and Maltose on the Hydration and Diffusion of DMPC Lipid Bilayer at Complete Hydration: Investigation of Structural and Spectroscopic Aspect of Lipid–Sugar Interaction. *Langmuir*, *32*(20), 5124–5134. https://doi.org/10.1021/acs.langmuir.6b01115

Saini, A. K., Jahed, K. R., Neres, D. F., Wright, R. C., & Sherif, S. M. (2025). Investigating Frost Response, Rootstock-Dependent Cold Tolerance, and Floral Bud Mortality in Apple Cultivars through Transcriptomic Insights. *Plant Stress*, 100829. https://doi.org/10.1016/j.stress.2025.100829

Savchenko, T., Kolla, V. A., Wang, C.-Q., Nasafi, Z., Hicks, D. R., Phadungchob, B., Chehab, W. E., Brandizzi, F., Froehlich, J., & Dehesh, K. (2014). Functional convergence of oxylipin and abscisic acid pathways controls stomatal closure in response to drought. *Plant Physiology*, *164*(3), 1151–1160. https://doi.org/10.1104/pp.113.234310

Scherer, G. F. E. (2002). Secondary messengers and phospholipase A2 in auxin signal transduction. *Plant Molecular Biology*, *49*(3–4), 357–372.

Scherer, G. F. E., Paul, R. U., Holk, A., & Martinec, J. (2002). Down-regulation by elicitors of phosphatidylcholine-hydrolyzing phospholipase C and up-regulation of phospholipase A in plant cells. *Biochemical and Biophysical Research Communications*, *293*(2), 766–770. https://doi.org/10.1016/S0006-291X(02)00292-9

Schulz, E., Tohge, T., Winkler, J. B., Albert, A., Schäffner, A. R., Fernie, A. R., Zuther, E., & Hincha, D. K. (2021). Natural Variation among Arabidopsis Accessions in the Regulation of Flavonoid Metabolism and Stress Gene Expression by Combined UV Radiation and Cold. *Plant and Cell Physiology*, *62*(3), 502–514. https://doi.org/10.1093/pcp/pcab013

Schulz, E., Tohge, T., Zuther, E., Fernie, A. R., & Hincha, D. K. (2016). Flavonoids are determinants of freezing tolerance and cold acclimation in Arabidopsis thaliana. *Scientific Reports*, *6*(1), 34027. https://doi.org/10.1038/srep34027

Sheard, L. B., Tan, X., Mao, H., Withers, J., Ben-Nissan, G., Hinds, T. R., Kobayashi, Y., Hsu, F.-F., Sharon, M., Browse, J., He, S. Y., Rizo, J., Howe, G. A., & Zheng, N. (2010). Jasmonate perception by inositol-phosphate-potentiated COI1-JAZ co-receptor. *Nature*, *468*(7322), 400–405. https://doi.org/10.1038/nature09430

Shi, Y., Ding, Y., & Yang, S. (2018). Molecular Regulation of CBF Signaling in Cold Acclimation. *Trends in Plant Science*, *23*(7), 623–637. https://doi.org/10.1016/j.tplants.2018.04.002

Shimsa, S., Mondal, S., & Mini, S. (2024). Syringic acid: A promising phenolic phytochemical with extensive therapeutic applications. *R&D of Functional Food Products*, *1*(5), 1–14.

Singh, P. K., Singh, R., & Singh, S. (2013). Cinnamic acid induced changes in reactive oxygen species scavenging enzymes and protein profile in maize (Zea mays L.) plants grown under salt stress. *Physiology and Molecular Biology of Plants*, *19*(1), 53–59. https://doi.org/10.1007/s12298-012-0126-6

Smith, E. N., Schwarzländer, M., Ratcliffe, R. G., & Kruger, N. J. (2021). Shining a light on NAD- and NADP-based metabolism in plants. *Trends in Plant Science*, *26*(10), 1072–1086. https://doi.org/10.1016/j.tplants.2021.06.010

Smith, W. L., & Lands, W. E. M. (1972). Oxygenation of Unsaturated Fatty Acids by Soybean Lipoxygenase. *Journal of Biological Chemistry*, *247*(4), 1038–1047. https://doi.org/10.1016/S0021-9258(19)45612-3

Song, X., Wang, H., Wang, Y., Zeng, Q., & Zheng, X. (2024). Metabolomics combined with physiology and transcriptomics reveal how *Nicotiana tabacum* leaves respond to cold stress. *Plant Physiology and Biochemistry*, *208*, 108464. https://doi.org/10.1016/j.plaphy.2024.108464

Stillwell, W., Yu Fong Cheng, & Wassall, S. R. (1990). Plant sterol inhibition of abscisic acid-induced perturbations in phospholipid bilayers. *Biochimica et Biophysica Acta (BBA) - Biomembranes*, *1024*(2), 345–351. https://doi.org/10.1016/0005-2736(90)90364-T

Sun, P., Huang, Y., Yang, X., Liao, A., & Wu, J. (2023). The role of indole derivative in the growth of plants: A review. *Frontiers in Plant Science*, *13*. https://doi.org/10.3389/fpls.2022.1120613

Sun, S., Fang, J., Lin, M., Hu, C., Qi, X., Chen, J., Zhong, Y., Muhammad, A., Li, Z., & Li, Y. (2021). Comparative Metabolomic and Transcriptomic Studies Reveal Key Metabolism Pathways Contributing to Freezing Tolerance Under Cold Stress in Kiwifruit. *Frontiers in Plant Science*, *12*. https://doi.org/10.3389/fpls.2021.628969

Sun, X., Zhang, L., Wong, D. C. J., Wang, Y., Zhu, Z., Xu, G., Wang, Q., Li, S., Liang, Z., & Xin, H. (2019). The ethylene response factor VaERF092 from Amur grape regulates the transcription factor VaWRKY33, improving cold tolerance. *The Plant Journal*, *99*(5), 988–1002. https://doi.org/10.1111/tpj.14378

Szalay, L., György, Z., & Tóth, M. (2019). Frost hardiness of apple (*Malus X domestica*) flowers in different phenological phases. *Scientia Horticulturae*, *253*, 309–315. https://doi.org/10.1016/j.scienta.2019.04.055

Takahashi, D., Imai, H., Kawamura, Y., & Uemura, M. (2016). Lipid profiles of detergent resistant fractions of the plasma membrane in oat and rye in association with cold acclimation and freezing tolerance. *Cryobiology*, *72*(2), 123–134. https://doi.org/10.1016/j.cryobiol.2016.02.003

Takahashi, H., Morimoto, T., Ogasawara, N., & Kanaya, S. (2011). AMDORAP: Non-targeted metabolic profiling based on high-resolution LC-MS. *BMC Bioinformatics*, *12*(1), 259. https://doi.org/10.1186/1471-2105-12-259

Talla, S., Riazunnisa, K., Padmavathi, L., Sunil, B., Rajsheel, P., & Raghavendra, A. S. (2011). Ascorbic acid is a key participant during the interactions between chloroplasts and mitochondria to optimize photosynthesis and protect against photoinhibition. *Journal of Biosciences*, *36*(1), 163–173. https://doi.org/10.1007/s12038-011-9000-x

Tan, X., Calderon-Villalobos, L. I. A., Sharon, M., Zheng, C., Robinson, C. V., Estelle, M., & Zheng, N. (2007). Mechanism of auxin perception by the TIR1 ubiquitin ligase. *Nature*, *446*(7136), 640–645. https://doi.org/10.1038/nature05731

Tang, J., Li, Y., Zhang, L., Mu, J., Jiang, Y., Fu, H., Zhang, Y., Cui, H., Yu, X., & Ye, Z. (2023). Biosynthetic Pathways and Functions of Indole-3-Acetic Acid in Microorganisms. *Microorganisms*, *11*(8), Article 8. https://doi.org/10.3390/microorganisms11082077

Testerink, C., & Munnik, T. (2005). Phosphatidic acid: A multifunctional stress signaling lipid in plants. *Trends in Plant Science*, *10*(8), 368–375. https://doi.org/10.1016/j.tplants.2005.06.002

Testerink, C., & Munnik, T. (2011). Molecular, cellular, and physiological responses to phosphatidic acid formation in plants. *Journal of Experimental Botany*, *62*(7), 2349–2361. https://doi.org/10.1093/jxb/err079

Thalmann, M., & Santelia, D. (2017). Starch as a determinant of plant fitness under abiotic stress. *New Phytologist*, *214*(3), 943–951. https://doi.org/10.1111/nph.14491

Timm, S., Florian, A., Wittmiß, M., Jahnke, K., Hagemann, M., Fernie, A. R., & Bauwe, H. (2013). Serine Acts as a Metabolic Signal for the Transcriptional Control of Photorespiration-Related Genes in Arabidopsis1[W]. *Plant Physiology*, *162*(1), 379–389. https://doi.org/10.1104/pp.113.215970

Turgeon, R., & Gowan, E. (1990). Phloem Loading in Coleus blumei in the Absence of Carrier-Mediated Uptake of Export Sugar from the Apoplast. *Plant Physiology*, *94*(3), 1244–1249. https://doi.org/10.1104/pp.94.3.1244

Unterberger, C., Brunner, L., Nabernegg, S., Steininger, K. W., Steiner, A. K., Stabentheiner, E., Monschein, S., & Truhetz, H. (2018). Spring frost risk for regional apple production under a warmer climate. *PLOS ONE*, *13*(7), e0200201. https://doi.org/10.1371/journal.pone.0200201

Vaultier, M.-N., Cantrel, C., Vergnolle, C., Justin, A.-M., Demandre, C., Benhassaine-Kesri, G., Ciçek, D., Zachowski, A., & Ruelland, E. (2006). Desaturase mutants reveal that membrane rigidification acts as a cold perception mechanism upstream of the diacylglycerol kinase pathway in Arabidopsis cells. *FEBS Letters*, *580*(17), 4218–4223. https://doi.org/10.1016/j.febslet.2006.06.083

Vellosillo, T., Martínez, M., López, M. A., Vicente, J., Cascón, T., Dolan, L., Hamberg, M., & Castresana, C. (2007). Oxylipins Produced by the 9-Lipoxygenase Pathway in Arabidopsis Regulate Lateral Root Development and Defense Responses through a Specific Signaling Cascade. *The Plant Cell*, *19*(3), 831–846. https://doi.org/10.1105/tpc.106.046052

Viehweger, K., Dordschbal, B., & Roos, W. (2002). Elicitor-activated phospholipase A(2) generates lysophosphatidylcholines that mobilize the vacuolar H(+) pool for pH signaling via the activation of Na(+)-dependent proton fluxes. *The Plant Cell*, *14*(7), 1509–1525. https://doi.org/10.1105/tpc.002329

Vinson, C. C., Mota, A. P. Z., Porto, B. N., Oliveira, T. N., Sampaio, I., Lacerda, A. L., Danchin, E. G. J., Guimaraes, P. M., Williams, T. C. R., & Brasileiro, A. C. M. (2020). Characterization of raffinose metabolism genes uncovers a wild Arachis galactinol synthase conferring tolerance to abiotic stresses. *Scientific Reports*, *10*(1), 15258. https://doi.org/10.1038/s41598-020-72191-4

Vo, Q. V., Bay, M. V., Nam, P. C., Quang, D. T., Flavel, M., Hoa, N. T., & Mechler, A. (2020). Theoretical and Experimental Studies of the Antioxidant and Antinitrosant Activity of Syringic Acid. *The Journal of Organic Chemistry*, *85*(23), 15514–15520. https://doi.org/10.1021/acs.joc.0c02258

Waadt, R., Seller, C. A., Hsu, P.-K., Takahashi, Y., Munemasa, S., & Schroeder, J. I. (2022). Publisher Correction: Plant hormone regulation of abiotic stress responses. *Nature Reviews Molecular Cell Biology*, *23*(7), 516–516. https://doi.org/10.1038/s41580-022-00501-x

Wang, D.-Z., Jin, Y.-N., Ding, X.-H., Wang, W.-J., Zhai, S.-S., Bai, L.-P., & Guo, Z.-F. (2017). Gene Regulation and Signal Transduction in the ICE-CBF-COR Signaling Pathway during Cold Stress in Plants. *Biochemistry. Biokhimiia*, *82*(10), 1103–1117. https://doi.org/10.1134/S0006297917100030

Wang, H., Guo, L., Zha, R., Gao, Z., Yu, F., & Wei, Q. (2022). Histological, metabolomic and transcriptomic analyses reveal mechanisms of cold acclimation of the Moso bamboo (Phyllostachys edulis) leaf. *Tree Physiology*, *42*(11), 2336–2352. https://doi.org/10.1093/treephys/tpac064

Wang, X. (2004). Lipid signaling. *Current Opinion in Plant Biology*, *7*(3), 329–336. https://doi.org/10.1016/j.pbi.2004.03.012

Wang, Y., Li, S., Shi, Y., Lv, S., Zhu, C., Xu, C., Zhang, B., Allan, A. C., Grierson, D., & Chen, K. (2024). The R2R3 MYB Ruby1 is activated by two cold responsive ethylene response factors, via the retrotransposon in its promoter, to positively regulate anthocyanin biosynthesis in citrus. *The Plant Journal*, *119*(3), 1433–1448. https://doi.org/10.1111/tpj.16866

Wang, Y., Sun, Z., Wang, Q., Xie, J., & Yu, L. (2023). Transcriptomics and metabolomics revealed that phosphate improves the cold tolerance of alfalfa. *Frontiers in Plant Science*, *14*. https://doi.org/10.3389/fpls.2023.1100601

Welti, R., Li, W., Li, M., Sang, Y., Biesiada, H., Zhou, H.-E., Rajashekar, C. B., Williams, T. D., & Wang, X. (2002). Profiling membrane lipids in plant stress responses. Role of phospholipase D alpha in freezing-induced lipid changes in Arabidopsis. *The Journal of Biological Chemistry*, *277*(35), 31994–32002. https://doi.org/10.1074/jbc.M205375200

Wen, Y.-Q., Zhong, G.-Y., Gao, Y., Lan, Y.-B., Duan, C.-Q., & Pan, Q.-H. (2015). Using the combined analysis of transcripts and metabolites to propose key genes for differential terpene accumulation across two regions. *BMC Plant Biology*, *15*(1), 240. https://doi.org/10.1186/s12870-015-0631-1

Wi, S. J., Seo, S. yeon, Cho, K., Nam, M. H., & Park, K. Y. (2014). Lysophosphatidylcholine enhances susceptibility in signaling pathway against pathogen infection through biphasic production of reactive oxygen species and ethylene in tobacco plants. *Phytochemistry*, *104*, 48–59. https://doi.org/10.1016/j.phytochem.2014.04.009

Wielandt, A. G., Pedersen, J. T., Falhof, J., Kemmer, G. C., Lund, A., Ekberg, K., Fuglsang, A. T., Pomorski, T. G., Buch-Pedersen, M. J., & Palmgren, M. (2015). Specific Activation of the Plant P-type Plasma Membrane H+-ATPase by Lysophospholipids Depends on the Autoinhibitory N- and C-terminal Domains *. *Journal of Biological Chemistry*, *290*(26), 16281–16291. https://doi.org/10.1074/jbc.M114.617746

Winter, G., Todd, C. D., Trovato, M., Forlani, G., & Funck, D. (2015). Physiological implications of arginine metabolism in plants. *Frontiers in Plant Science*, *6*, 534. https://doi.org/10.3389/fpls.2015.00534

Wisniewski, M., Norelli, J., & Artlip, T. (2015). Overexpression of a peach CBF gene in apple: A model for understanding the integration of growth, dormancy, and cold hardiness in woody plants. *Frontiers in Plant Science*, *6*. https://doi.org/10.3389/fpls.2015.00085

Wu, Y., Zhu, H., Ling, Z., Lu, E., Peng, X., & Zheng, Y. (2023). The metabolism of nonstructural carbohydrates, lipids, and energy in two Cycas species with differential tolerance to unexpected freezing stress. *Frontiers in Plant Science*, *14*. https://doi.org/10.3389/fpls.2023.1301560

Wu, Z., Yang, L., Wang, R., Zhang, Y., Shang, Q., Wang, L., Ren, Q., & Xie, Z. (2015). In vitro study of the growth, development and pathogenicity responses of Fusarium oxysporum to phthalic acid, an autotoxin from Lanzhou lily. *World Journal of Microbiology & Biotechnology*, *31*(8), 1227–1234. https://doi.org/10.1007/s11274-015-1872-8

Xie, Y., Chen, P., Yan, Y., Bao, C., Li, X., Wang, L., Shen, X., Li, H., Liu, X., Niu, C., Zhu, C., Fang, N., Shao, Y., Zhao, T., Yu, J., Zhu, J., Xu, L., van Nocker, S., Ma, F., & Guan, Q. (2018). An atypical R2R3 MYB transcription factor increases cold hardiness by CBF-dependent and CBF-independent pathways in apple. *New Phytologist*, *218*(1), 201–218. https://doi.org/10.1111/nph.14952

Xing, J., Ye, X., Huo, K., Ding, Z., Tie, W., Xie, Z., Li, C., Meng, F., & Hu, W. (2025). Integrated metabolomic and transcriptomic analyses revealed the overlapping response mechanisms of banana to cold and drought stress. *Plant Physiology and Biochemistry*, *222*, 109766. https://doi.org/10.1016/j.plaphy.2025.109766

Xu, A., Cheng, F., Zhou, S., Hu, H., & Bie, Z. (2022). Chilling-induced H2O2 signaling activates the antioxidant enzymes in alleviating the photooxidative damage caused by loss of function of 2-Cys peroxiredoxin in watermelon. *Plant Stress*, *6*, 100108. https://doi.org/10.1016/j.stress.2022.100108

Xu, G., Li, L., Zhou, J., He, M., Lyu, D., Zhao, D., & Qin, S. (2023a). Integrated transcriptomics and metabolomics analyses reveal key genes and essential metabolic pathways for the acquisition of cold tolerance during dormancy in apple. *Environmental and Experimental Botany*, *213*, 105413. https://doi.org/10.1016/j.envexpbot.2023.105413

Xu, H., Li, J., Wang, L., Li, X., Liu, Y., Wang, X., Gao, T., & Ma, Y. (2023b). Integrated transcriptomic and metabolomics analysis reveals abscisic acid signal transduction and sugar metabolism pathways as defense responses to cold stress in *Argyranthemum frutescens*. *Environmental and Experimental Botany*, *205*, 105115. https://doi.org/10.1016/j.envexpbot.2022.105115

Yamamoto, S. (1992). Mammalian lipoxygenases: Molecular structures and functions. *Biochimica et Biophysica Acta (BBA) - Lipids and Lipid Metabolism*, *1128*(2), 117–131. https://doi.org/10.1016/0005-2760(92)90297-9

Yang, C., Yang, H., Xu, Q., Wang, Y., Sang, Z., & Yuan, H. (2020). Comparative metabolomics analysis of the response to cold stress of resistant and susceptible Tibetan hulless barley (*Hordeum distichon*). *Phytochemistry*, *174*, 112346. https://doi.org/10.1016/j.phytochem.2020.112346

Yang, P., Azher Nawaz, M., Li, F., Bai, L., & Li, J. (2019). Brassinosteroids Regulate Antioxidant System and Protect Chloroplast Ultrastructure of Autotoxicity-Stressed Cucumber (Cucumis sativus L.) Seedlings. *Agronomy*, *9*(5), Article 5. https://doi.org/10.3390/agronomy9050265

Yazdanpanah, P., Jonoubi, P., Zeinalabedini, M., Rajaei, H., Ghaffari, M. R., Vazifeshenas, M. R., & Abdirad, S. (2021). Seasonal Metabolic Investigation in Pomegranate (Punica granatum L.) Highlights the Role of Amino Acids in Genotype- and Organ-Specific Adaptive Responses to Freezing Stress. *Frontiers in Plant Science*, *12*. https://doi.org/10.3389/fpls.2021.699139

Ye, S. F., Zhou, Y. H., Sun, Y., Zou, L. Y., & Yu, J. Q. (2006). Cinnamic acid causes oxidative stress in cucumber roots, and promotes incidence of *Fusarium* wilt. *Environmental and Experimental Botany*, *56*(3), 255–262. https://doi.org/10.1016/j.envexpbot.2005.02.010

Yoshikawa, H., Honda, C., & Kondo, S. (2007). Effect of low-temperature stress on abscisic acid, jasmonates, and polyamines in apples. *Plant Growth Regulation*, *52*(3), 199–206. https://doi.org/10.1007/s10725-007-9190-2

Zhang, C., & Turgeon, R. (2018). Mechanisms of phloem loading. *Current Opinion in Plant Biology*, *43*, 71–75. https://doi.org/10.1016/j.pbi.2018.01.009

Zhang, C., Zhen, Y., Weng, Y., Lin, J., Xu, X., Ma, J., Zhong, Y., & Wang, M. (2025). Research progress on the microbial metabolism and transport of polyamines and their roles in animal gut homeostasis. *Journal of Animal Science and Biotechnology*, *16*(1), 57. https://doi.org/10.1186/s40104-025-01193-x

Zhang, J., Liang, L., Xie, Y., Zhao, Z., Su, L., Tang, Y., Sun, B., Lai, Y., & Li, H. (2022). Transcriptome and Metabolome Analyses Reveal Molecular Responses of Two Pepper (Capsicum annuum L.) Cultivars to Cold Stress. *Frontiers in Plant Science*, *13*. https://doi.org/10.3389/fpls.2022.819630

Zhang, W., Jiang, B., Li, W., Song, H., Yu, Y., & Chen, J. (2009). Polyamines enhance chilling tolerance of cucumber (*Cucumis sativus* L.) through modulating antioxidative system. *Scientia Horticulturae*, *122*(2), 200–208. https://doi.org/10.1016/j.scienta.2009.05.013

Zhang, X. D., Wang, R. P., Zhang, F. J., Tao, F. Q., & Li, W. Q. (2013). Lipid profiling and tolerance to low-temperature stress in Thellungiella salsuginea in comparison with Arabidopsis thaliana. *Biologia Plantarum*, *57*(1), 149–153. https://doi.org/10.1007/s10535-012-0137-8

Zhang, Z., Liu, Y., Dai, H., & Miao, M. (2021). Characteristics and expression patterns of six α-galactosidases in cucumber (Cucumis sativus L.). *PLOS ONE*, *16*(1), e0244714. https://doi.org/10.1371/journal.pone.0244714

Zhao, J., Quan, P., Liu, H., Li, L., Qi, S., Zhang, M., Zhang, B., Li, H., Zhao, Y., Ma, B., Han, M., Zhang, H., & Xing, L. (2020). Transcriptomic and Metabolic Analyses Provide New Insights into the Apple Fruit Quality Decline during Long-Term Cold Storage. *Journal of Agricultural and Food Chemistry*, *68*(16), 4699–4716. https://doi.org/10.1021/acs.jafc.9b07107

Zhao, L., Yang, T., Xing, C., Dong, H., Qi, K., Gao, J., Tao, S., Wu, J., Wu, J., Zhang, S., & Huang, X. (2019). The *β*-amylase *PbrBAM3* from pear (*Pyrus betulaefolia*) regulates soluble sugar accumulation and ROS homeostasis in response to cold stress. *Plant Science*, *287*, 110184. https://doi.org/10.1016/j.plantsci.2019.110184

Zhao, Y., Song, C., Brummell, D. A., Qi, S., Lin, Q., Bi, J., & Duan, Y. (2021). Salicylic acid treatment mitigates chilling injury in peach fruit by regulation of sucrose metabolism and soluble sugar content. *Food Chemistry*, *358*, 129867. https://doi.org/10.1016/j.foodchem.2021.129867

Zhu, K., Liu, J., Lyu, A., Luo, T., Chen, X., Peng, L., & Hu, L. (2024). Analysis of the Mechanism of Wood Vinegar and Butyrolactone Promoting Rapeseed Growth and Improving Low-Temperature Stress Resistance Based on Transcriptome and Metabolomics. *International Journal of Molecular Sciences*, *25*(17), 9757. https://doi.org/10.3390/ijms25179757